NTIA Report TR-06-444

Effects of RF Interference on Radar Receivers

Frank H. Sanders
Robert L. Sole
Brent L. Bedford
David Franc
Timothy Pawlowitz

U.S. DEPARTMENT OF COMMERCE
Carlos M. Gutierrez, Secretary

John M. R. Kneuer, Acting Assistant Secretary
for Communications and Information

September 2006

ACKNOWLEDGEMENT

The body of work presented in this report is the result of a long-term, dedicated, and cooperative work effort. It would have been impossible to accomplish without critical contributions from the following governments, organizations, and individuals: the Administration of the United Kingdom (including critically important guidance and assistance from Mr. Peter Griffith; Mr. Kim Fisher of Maritime and Coast Guard Agency; and the staff of the Fraser Range facility at Portsmouth); the Sperry Marine radar company; the Kelvin Hughes radar company; the Federal Aviation Administration (including critical assistance from Mr. Greg Barker and Mr. Mitch Hughes and the rest of the staff of the long range radars of the FAA Technical Center in Oklahoma City, OK; the staff of the airport surveillance radars at that facility; Mr. Michael Biggs; and the FAA radar staff at Kirksville, MO); the U.S. Coast Guard radar staff at Curtis Bay, MD, who assisted us well beyond ordinary limits in their already-busy schedule; the National Weather Service (including Mr. Dan Friedman and the radar staff at Norman, OK); the US Air Force, including especially Darrell McFarland and Ricardo Medilavilla of the 84th Radar Evaluation Squadron (RADES) from Hill AFB, UT; staff of the NTIA Office of Spectrum Management (OSM), especially Mr. Robert Hinkle and Mr. Mike Doolan, and also Matt Barlow and Larry Brunson; and finally Ms. Kristen Novik of the NTIA/ITS laboratory, who drafted the technical drawings in this report. All photographic images in this report were taken by one of the authors (Sanders).

DISCLAIMER

Certain commercial equipment, instruments, or materials are identified in this report to specify the technical aspects of the reported results. In no case does such identification imply recommendation or endorsement by the National Telecommunications and Information Administration, nor does it imply that the material or equipment identified is necessarily the best available for the purpose.

CONTENTS

FIGURES

TABLES

ABBREVIATIONS/ACRONYMS

A-D	analog-to-digital (information conversion) in a radar receiver
AGC	automatic gain control radar receiver processing
AIS	automatic identification systems (for ships)
AWG	arbitrary waveform generator
BPSK	binary phase-shift keyed signal modulation
CDMA	code division multiple access signal modulation
CFAR	constant false alarm rate radar receiver processing
CRT	cathode ray tube
COHO	coherent oscillator (for MTI, or Doppler, processing)
CW	carrier wave (sine wave) signal modulation
DTE	digital target extractor
DVB	digital video broadcast
EESS	earth exploration satellite service
EIRP	effective isotropic radiated power
ENG-OB	electronic news gathering-outdoor broadcast (video data) signal modulation
FAA	Federal Aviation Administration (of the United States of America)
FTC	fast time constant (or logarithmic FTC, log-FTC) radar receiver processing
HF	high frequency
I	interference power level (in a bandwidth in a radar receiver)
I/N	interference-to-noise power ratio (in a radar receiver)
IF	intermediate frequency (of a radar receiver) stage
IAGC	instantaneous automatic gain control (also simply AGC)
IMO	International Maritime Organization
IMT-2000	International mobile telecommunications (year 2000) signal modulation defined by ITU-R (also known as wireless 2.5 G, wireless 3G, next-generation (NG) wireless mobile, and IMT-Advanced)
I-Q	in-phase and quadrature components of a signal, differing by a phase shift of $\pi/2$
IR	interference rejection (feature in a radar receiver used against pulsed interference)
IS-95	interim standard 95, also known as TIA-EIA-95 and by a trade name, cdmaOne
ISM	industrial, scientific, and medical (spectrum bands)
ITS	Institute for Telecommunication Sciences (of NTIA, U.S. Dept. of Commerce)
ITU-R	International Telecommunication Union, Radiocommunication Sector
LNA	low noise amplifier
Log FTC	logarithmic fast time constant (also simply FTC) radar receiver processing
MCA	Maritime and Coast Guard Agency (of the United Kingdom)
MDS	minimum detectable signal level (in a radar receiver)
MTI	moving target indicator (radar target processing feature)
N	noise power level (in a bandwidth in a radar receiver)
NTIA	National Telecommunications and Information Administration (of the U.S. Department of Commerce)

NWS	National Weather Service (of the United States of America)
OFDM	orthogonal frequency division multiplexing signal modulation
OS CFAR	ordered statistic constant false alarm rate
OSM	Office of Spectrum Management, NTIA, U.S. Department of Commerce
OTR	on-tuned rejection factor (for bandwidth mismatches)
P_d	probability of detection (of radar target(s))
PPI	plan position indicator radar display
prf	pulse repetition frequency (of radar pulses)
pri	pulse repetition interval (between radar pulses)
prt	pulse repetition train
pw	pulse width (of a radar)
QAM	quadrature amplitude modulation (phase-coded signals, with a numeric prefix indicating the available number of phase states, e.g. 64 QAM is QAM with 64 possible phase states)
QPSK	quadrature phase-shift keyed signal modulation
R_{max}	maximum range of a radar
Radar	radio detection and ranging, paired receiver and transmitter
RBW	resolution bandwidth (or IF bandwidth) of a spectrum analyzer
RCS	radar cross section (often simply called cross section in radar-specific contexts)
RF	radio frequency
RMS	root mean square (average power detection)
S	signal power in a radar receiver
S_{min}	minimum detectable signal level
SOLAS	safety of life at sea (international regulations)
STC	sensitivity time control (or swept gain) radar receiver processing
TBM	threshold bias map
TDMA	time division multiple access signal modulation
Tx/Rx	transmitter-receiver combination
UHF	ultrahigh frequency
USCG	United States Coast Guard
UWB	ultrawideband
VHF	very high frequency
W-CDMA	wideband code division multiple access signal modulation

EXECUTIVE SUMMARY

Radars play critical roles in national security, air traffic control, weather observation and warning, scientific applications, mapping, search and rescue operations, and other safety-of-life missions. Radar transmitter and receiver characteristics are engineered to successfully accomplish their missions in these areas. The technical characteristics of radars (such as high transmitter peak power levels and very sensitive designs for the receivers) have typically resulted in exclusive or primary spectrum allocations for radar operations in selected radio bands.

In recent years, spectrum crowding has led to proposals for reduction of available spectrum for exclusive or primary radar operations, as well as for co-channel (or nearly co-channel) spectrum sharing between radars and non-radar (communication-type) signals. It has been proposed in various forums, for example, that communication signals can (and should) share spectrum bands with radar systems. Such proposals typically presume that radar receivers will not suffer undue loss of performance due to such sharing as long as the interference levels are relatively low. Some sharing analyses assume that radar receivers are relatively robust against radio frequency (RF) interference effects from communication signals at low levels.

Such proposals raise critical questions regarding the robustness of radar receiver performance in the presence of RF interference, especially at low levels. These include: At what power levels do interfering signals cause adverse effects on the performance of radar receivers? How are interference effects manifested in radar receivers? What are the interference levels at which radar receivers lose desired targets? What if any low-level interference effects occur on radar receiver displays? Are radar targets only lost at the edge of radar coverage?

To answer these questions this report's authors have performed extensive tests and measurements on many radar receivers performing a variety of critically important missions in several spectrum bands. Radar types that have been examined include: short-range and long-range air traffic control; fixed ground-based weather surveillance; airborne weather surveillance; and maritime navigation and surface search. The radars that have been tested operate in the spectrum bands: 1215-1400 MHz; 2700-2900 MHz; 2900-3700 MHz; and 8500-10500 MHz.

The most important results of this work can be summarized in four major findings:

1) Interference with communication-type signals degrades radar performance at interference-to-noise (*I/N*) levels between -9 dB and -2 dB (well *below* the internal noise of the radar receivers). One radar lost targets at an *I/N* level of -10 dB, and *I/N* = -6 dB caused all but one of the radars to lose targets. Future improvements to weather radars are predicted to render them vulnerable at *I/N* levels as low as -14 dB.

2) In contrast to the effects of interference from communication signal modulations, pulsed interference at low duty cycles (less than about 1-3%) is tolerated at *I/N* ratios as high as +30 dB to +63 dB. In other words, the radar receivers that were tested performed very robustly in the presence of the type of signals that are transmitted by other radars. Radars tend to share spectrum well with other radars.

3) When radar targets are lost due to low-level interference, those losses are insidious. There are no overt indications to radar operators or even to sophisticated radar software that losses are occurring. No dramatic indications such as flashing strobes on radar screens are observed. This insidiousness can make low-level interference more dangerous than higher levels that will generate strobes and other obvious warning indications for operators or processing software.

Even when radars experience serious performance degradation due to low-level interference, it is very unlikely that such interference will be identifiable as such. It is therefore unlikely that such interference will ever result in reports to spectrum management authorities even when it causes loss of desired targets. Since low-level interference is not expected to be identified or to generate reports when it occurs, lack of such reports *cannot* be taken to mean that such interference does not occur.

4) Interference can (and will) cause loss of targets at any distance from any radar station; loss of targets due to radio interference is not directly related to distance of targets from radar stations. When radar performance is reduced by some number of decibels, *X*, then all targets that were within *X* decibels of disappearing from coverage will be lost. Range from the radar is not a factor in this relationship. Interference can cause loss of desired, large targets (such as commercial airliners, oil tankers, and cargo ships) at long distances, as well as small targets at close distances. Low-observable targets that could be lost include, for example, light aircraft; business jets; incoming missiles; missile warheads; floating debris including partially submerged (and therefore dangerous) shipping containers; life boats; kayaks, canoes, dinghies; periscopes; and swimmers in life jackets.

Because any marginal radar target can potentially be lost at any distance in the presence of radio interference, radio interference does not translate directly into an equivalent radar range reduction. While "range reduction" due to interference can be used as a metric, its use must be qualified with the (unrealistic) condition of a fixed, constant cross section for all desired targets.

Taken together, the technical results in this report show that radar receivers are not generally robust against low-level interference from non-radar (communication-type) radio signals. The low thresholds at which interference effects occur, the insidious characteristics of such interference, and the wide range of distances over which radar receivers can experience interference effects are critical technical indications that, to avoid impairment of radar operations, care must be taken to ensure that radar receivers are not subjected to unnecessary interference from non-radar signals above identified thresholds. Conversely, radars have now been shown to operate robustly when they share spectrum with other radar signals having low duty cycles (i.e., when the interference duty cycles are less than about 1-3%).

EFFECTS OF RF INTERFERENCE ON RADAR RECEIVERS

Frank H. Sanders,[1] Robert Sole,[2] Brent L. Bedford,[1] David Franc,[3] and Timothy Pawlowitz[4]

This report describes the results of interference tests and measurements that have been performed on radar receivers that have various missions in several spectrum bands. Radar target losses have been measured under controlled conditions in the presence of radio frequency (RF) interference. Radar types that have been examined include short range and long range air traffic control; weather surveillance; and maritime navigation and surface search. Radar receivers experience loss of desired targets when interference from high duty cycle (more than about 1-3%) communication-type signals is as low as -10 dB to -6 dB relative to radar receiver inherent noise levels. Conversely, radars perform robustly in the presence of low duty cycle (less than 1-3%) signals such as those emitted by other radars. Target losses at low levels are insidious because they do not cause overt indications such as strobes on displays. Therefore operators are usually unaware that they are losing targets due to low-level interference. Interference can cause the loss of targets at any range. Low interference thresholds for communication-type signals, insidious behavior of target losses, and potential loss of targets at any range all combine to make low-level interference to radar receivers a very serious problem.

Key words: radar interference; radar interference vulnerability; radar performance degradation; radar target loss; radar target detection; RF interference; UWB interference effects

1 RADAR FUNDAMENTALS RELATED TO INTERFERENCE TESTING AND MEASUREMENTS

1.1 Introduction

Radars play critical roles in national security, air traffic control, weather observation and warning, scientific applications, mapping, search and rescue operations, and other safety-of-life missions. Radar transmitter and receiver characteristics are engineered to successfully accomplish their missions in these areas. The technical characteristics of radars (such as high peak power levels emitted by the transmitters and very sensitive designs for the receivers) have usually resulted in exclusive, or at least primary, spectrum allocations for their operations.

In recent years, spectrum crowding has led to proposals for reduction of available spectrum for exclusive or primary radar operations, as well as for co-channel (or nearly co-channel) spectrum

[1] Institute for Telecommunication Sciences, National Telecommunications and Information Administration (NTIA), U.S. Department of Commerce, Boulder, CO.
[2] Office of Spectrum Management (OSM), NTIA, Washington, DC.
[3] National Oceanic and Atmospheric Administration (NOAA), formerly with the National Weather Service (NWS), Washington, DC.
[4] Federal Aviation Administration (FAA), Washington, DC.

sharing between radars and non-radar radio signals. It has been proposed in various forums, for example, that communication signals can (and should) sometimes share spectrum bands with radar systems. Such proposals typically presume that radar receivers will not suffer undue loss of technical performance due to such sharing so long as the interference levels are relatively low. Some sharing analyses assume that radar receivers are relatively robust against radio frequency (RF) interference effects from low levels of non-radar signals.

These proposals raise critical technical questions. These include: At what power levels do interfering signals cause adverse effects on the performance of these receivers? How are interference effects manifested in these radar receivers? Specifically, what are the interference levels at which radar receivers lose desired targets, and do low-level interference effects create observable manifestations on radar receiver displays?

NTIA, in cooperation with other US Government agencies and the United Kingdom (UK),[5] has performed a series of tests and measurements of the response of microwave radars to low levels of RF interference from a variety of communication and non-communication signals. This report describes the results of interference tests and measurements on several representative radar receivers. Interference data have been collected on radars performing various missions in several different spectrum bands. Radar types that have been examined include short range air traffic control; long range air traffic control; fixed weather surveillance; airborne weather surveillance; and maritime navigation and surface search. These radars have been operational in the spectrum bands 1200-1400 MHz; 2700-2900 MHz; 2900-3700 MHz; and 8500-10500 MHz.

1.2 Noise Versus Interference

Radars operate by directing transmitted radio energy through space toward remote objects that need to be observed and subsequently receiving and processing reflections of small portions of the transmitted energy returned as echoes from the desired objects (called targets). The time delay between transmission and reception of the energy is used to determine the distances between the radar and the targets, while the direction in which the energy is initially directed and then returned as reflections informs the direction of the targets from the radar. Ultimately, the key to successful radar design is the solution of two technical problems: generation and direction of an adequate amount of radio energy from the transmitter in sufficiently localized directions through space; and the reception, detection, and discrimination of the small fraction of energy that has been reflected from both desired targets and undesired reflecting objects (collectively called clutter) in the presence of natural (and sometimes manmade) noise in the radar receiver.

This report addresses the general question of how, and to what extent, RF interference causes degradation to the performance of radar receivers. Before interference effects are discussed, it is necessary to define interference, describe how it differs from other environmental degradation effects, and explain why it is considered separately from those effects. It is also necessary to describe the normal processes of target reception, detection, and discrimination in radar receivers. Those topics are addressed in the following parts of this report section.

[5] Including the National Oceanic and Atmospheric Administration (NOAA), U.S. Coast Guard (USCG), Federal Aviation Administration (FAA), and the United Kingdom's (UK) Fraser Test Range at Portsmouth.

1.2.1 Definition and Distinction of Noise Versus Interference

Unwanted energy coupled into radar receivers from natural sources and from manmade devices that are not intentional radio transmitters is called *noise*. Noise degrades radar receiver performance and is generated by many sources. A natural source is the energy produced by thermal electrons within radar receiver circuitry; it is one of the most fundamental limiting factors in radar receiver performance. Other noise is coupled into radar receivers from naturally occurring, distant sources. In the high frequency (HF) spectrum these prominently include noise from lightning strokes reflected from our planet's ionosphere and (as a smaller effect) Jupiter, while at higher frequencies (very high frequency (VHF), ultrahigh frequency (UHF), and lower microwave), important noise sources are the Sun and to a lesser extent our galactic center and a variety of other astronomical objects. Manmade noise across the spectrum from HF to lower microwave frequencies (around 1.5 GHz) is coupled into radar receivers from unintentional emission sources such as electric motors, above-ground power lines, and automotive ignition systems. Spectrum survey data [1-4] indicate that manmade noise levels tend to decrease below receiver thermal noise at higher microwave frequencies (above about 1.5 GHz), although some sources (e.g., microwave ovens) can produce significant background microwave emissions in industrial, scientific, and medical (ISM) radio bands such as at 2.5 GHz [5-8].

Randomly distributed radio energy from all sources, both natural and manmade, combines to generate overall environmental background noise against which radar receivers must always perform. Noise sources are unavoidable and generally uncontrollable. However, they do produce known background levels, their emissions obey well-understood patterns in time and space, and they are generally predictable in both their location and their timing (e.g., the diurnal location and movement of astronomical sources across the celestial sphere and the diurnal power levels, cycles, and spectrum ranges of manmade noise near cities, highways, and industrial zones).

In contrast to noise, *interference* is unwanted radio energy[6] coupled into radar receivers from manmade, intentional radio transmitter sources such as communication devices. Like noise, interference degrades radar receiver performance. Interference, however, generally has statistical and spectrum characteristics that are different from noise. Another important contrast between noise and interference is that, while noise may be unavoidable and largely uncontrollable, interference is both avoidable and controllable through sound spectrum engineering and management procedures.

Although both noise and interference cause degradation in radar receiver performance, the existence of noise does not logically imply that radar receivers should therefore be expected to operate in the presence of interference. If any connection is to be drawn between the two phenomena, it is that the existence of noise as a source of uncontrollable and unavoidable degradation in radar environments implies that interference (which in contrast, and by definition, is both controllable and avoidable) must be restricted all the more carefully in order not to add to the inevitable performance degradation caused by environmental noise.

Noise phenomena and their effects on radar receiver performance have been treated extensively in existing technical literature [9-12, for example]. Noise effects are typically taken into account

[6] Interference is sometimes defined as the *effect* of unwanted energy in a receiver, rather than the energy itself.

in radar receiver design and are distinct and separable in both their origins and their behavior from interference effects. For these reasons, and because interference is a controllable phenomenon, this report does not address noise effects in radar receivers other than as an inherent limiting factor generated by thermal electron activity in receiver circuitry. Only interference degradation effects on radar receivers are addressed in this report.

1.3 Detection of Radar Targets

Radar targets are detected by transmitting radio energy into space, receiving a portion of the transmitted energy that is reflected as echoes from targets, and processing it inside receiver circuitry to separate the echo energy from whatever noise and interference are present in the receiver. A radar will always have a maximum range that is a function of the transmitter power, the degree to which the transmitted energy is confined directionally in space, the effective area of the receiving antenna, the efficiency with which targets reflect radio energy at the radar frequency, and the minimum threshold within the receiver for detection of echo energy.

1.3.1 The Radar Equation

Assuming theoretically perfect free-space radio signal propagation conditions, the maximum range of a radar, R_{max}, is given by the so-called radar equation (modified from [9, pg. 15]):

$$R_{\max} = \left[\frac{P_t G_t A_e \sigma_0}{(4\pi)^2 L_s S_{\min}} \right]^{1/4} \tag{1}$$

where:

P_t = transmitted power, watts;
G_t = gain of the transmitter antenna, linear term;
A_e = effective aperture of the receiving antenna, m^2;
σ_0 = nominal (specified) target cross section, m^2;
L_s = system loss between transmitter/receiver and antenna, linear dimensionless quantity;
S_{min} = minimum detectable signal, watts.

With the exception of the target cross section term, σ_0, all of the variables in (Eq. 1) are in principle controllable by radar designers (although there are practical limits on all of the variables). R_{max} is a theoretical maximum that is never realized due to practical engineering and design limitations of field-deployed equipment and unanticipated losses within radar systems. Actual values of R_{max} are typically half of the theoretical value [9]. A variety of environmental factors tend to decrease radar range. These include propagation losses that exceed the free-space assumption of the radar equation as well as fluctuations in the radar cross sections of targets.

1.3.2 Radar Target Detection Probability

The peak values of transmitted power, P_t, that are required for effective observation and tracking of radar targets are so high that they often can only be generated for short intervals. Furthermore, most radar designs require that the radar transmitters be periodically turned off so that the receivers can listen for the target echoes. Therefore most radars transmit radio energy in pulses.[7]

Detection of radar targets is a probabilistic process; for any given target, there is a probability that it will be detected as an echo from any individual pulse of transmitted energy. But the probability of detection on a per-pulse basis is usually too low for effective radar operations. The per-pulse detection probability can be increased by raising the values of the parameters in (Eq. 1), but in well-engineered radars the values of the (Eq. 1) parameters have already reached the limits of available technology and practicality. The only way to obtain high probabilities of target detection is to illuminate a target with more than one pulse, so that the cumulative probability of detection becomes adequate for effective operations. In the most simplistic approach, it is established that the probability of detection per pulse is x (where $x<1$). The probability of not detecting a target with a single pulse is thus $(1-x)$. Assuming independence of detection probability from pulse to pulse, the probability of *not* detecting a target with any of n pulses is $(1-x)^n$. The probability of detection of a target, P_d, with at least one of n pulses is unity minus that value:

$$P_d(x,n) = 1-(1-x)^n. \tag{2}$$

Figure 1 illustrates the principle of variation of P_d as a function of n for a variety of values of x. For typical operational radar designs, n is often between 10 and 20. When fewer than 10 pulses illuminate a target, detection probability is low and detection probability increases rapidly with the use of additional pulses. But detection probability only increases slowly after more than about 20 pulses are used on a target; diminishing returns in radar performance relative to longer dwell times on each target tend to preclude the use of many more pulses for illumination.[8] The need for targets to be illuminated with 10 to 20 pulses leads in turn to the selection of a variety of additional radar parameter values, such as the maximum rate that the radar beam may be scanned through space.[9]

Explained another way, the low per-pulse probability of detection must be somehow overcome to make radars work effectively. Since the parameters in (Eq. 1) (such as transmitter power and antenna gain) have already been optimized in good radar designs, the only remaining method for reliably observing targets is through receiver processing of multiple pulses reflected from each target. This is receiver processing gain. Although processing gain enhances target detection, and may tend to mitigate some special types of interference (such as from pulsed sources that

[7] Some radars, especially those used for certain types of target tracking, do transmit continuously.

[8] There are some exceptions. For example, some meteorological radars examine the very weakly reflecting phenomena of high-altitude winds. These radars, called wind profilers, may need to integrate echo energy from tens of thousands of pulses over a period of a few minutes in order to generate a single data point.

[9] For example, if a radar must have a 200 nm range and at least 15 pulses must illuminate each target within a 1-degree wide beamwidth, then the radar must scan at a rate that is not faster than one revolution every 13.4 sec. This of course becomes the lower bound for the time interval between updates on target locations.

transmit energy at a low (less than 1 per cent) duty cycle), it is not an interference rejection technique per se.

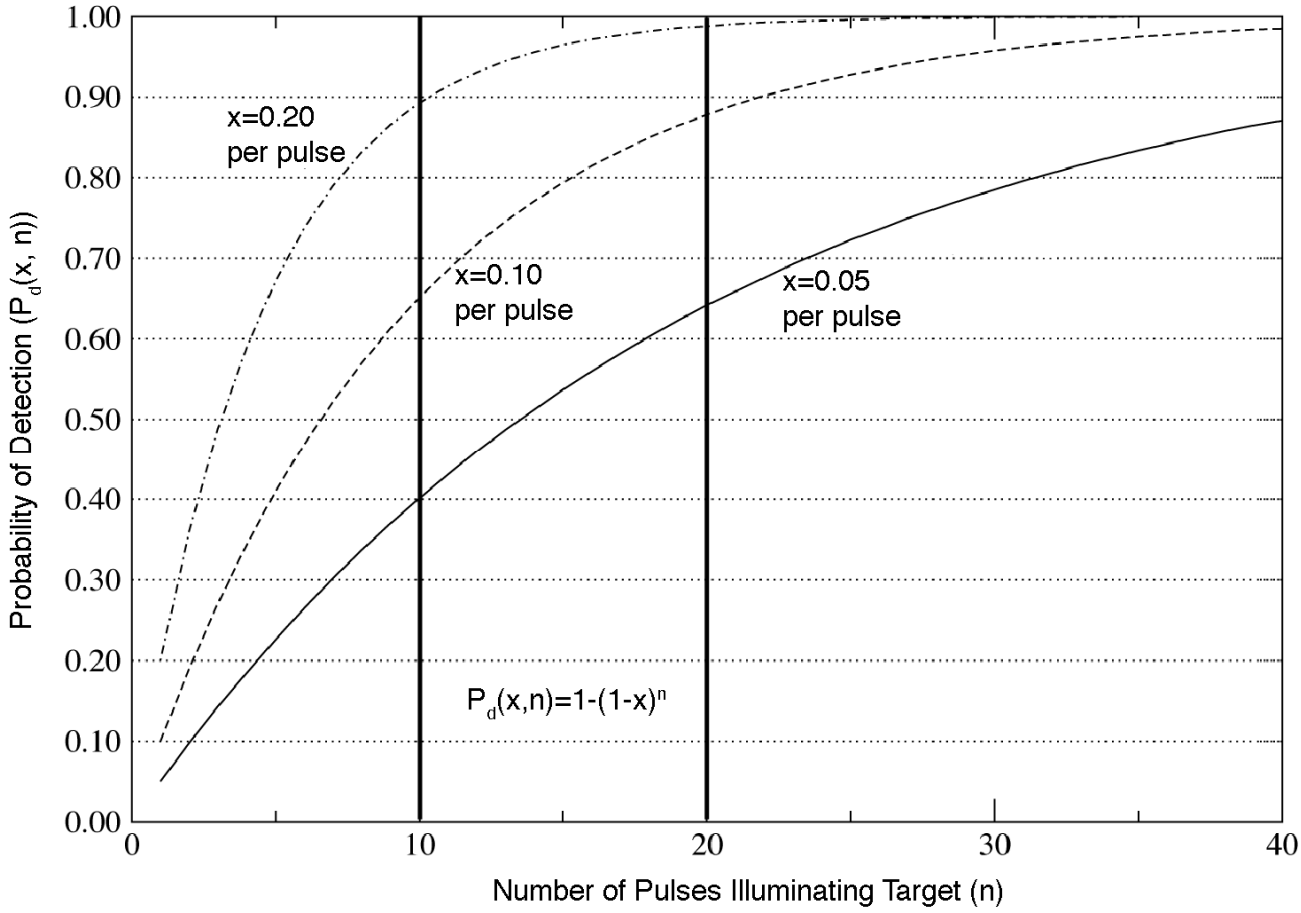

Figure 1. Probability of detection versus number of radar pulses illuminating a target for three probabilities per pulse, from (Eq. 2): x=0.05, x=0.10, and x=0.20. Many radars balance the need to detect targets with high probability against the need to update scans in a timely manner by using between 10 to 20 pulses per target (indicated with solid vertical lines).

1.4 Radar Receiver Inherent Noise

As noted in Section 1.2, one of the most fundamental limitations on microwave radar receiver performance is inherent, internal noise generated by thermal electrons in receiver circuitry. The average power level in watts, *P*, of this noise is:

$$P = kTB \tag{3}$$

where:

k = Boltzmann's constant ($1.38 \cdot 10^{-23}$ J/(K·Hz));
T = temperature of the circuitry (K);
B = bandwidth of the circuitry (Hz).

For example, a circuit at room temperature (about 290 K) operating in a bandwidth of 1 MHz (10^6 Hz), will have an inherent noise level of $4 \cdot 10^{-15}$ W, or -144 dBW, or -114 dBm.

The *noise factor*, f_n, of a receiver is defined as:

$$f_n = \frac{N_{out}}{kTB} = \left(1 + \frac{\Delta N}{kTB}\right) \tag{4}$$

where:

N_{out} = total available output noise power from the circuit;
ΔN = noise power in addition to kTB generated by the circuit.

The *noise figure*, F_n, of the circuit, a decibel quantity, is defined as:

$$F_n = 10\log(f_n). \tag{5}$$

Ideally, $N_{out} = kTB$, or, equivalently, $\Delta N = 0$. If this performance could be achieved, then the noise factor of the receiver would be unity and the noise figure of the receiver would be zero decibels. The sensitivity of such a receiver would be theoretically optimal.

Realistically, such performance is impossible; the values of N_{out} and ΔN will be somewhat larger than kTB and zero, respectively. In a well-designed receiver in which the noise figure and gain characteristics of the first low-noise amplifier (LNA) are properly cascaded with all of the circuitry after the LNA, the LNA noise figure will nearly determine the overall noise figure of the entire receiver. A high-performance LNA noise figure in a radar receiver is a few decibels higher than kTB. Insertion loss of components in the radar receiver ahead of the LNA (such as RF band-limiting filtering) will add directly to the overall noise figure of the receiver. Such losses can add up to another decibel or more.

In practice, an overall noise figure of 10 dB is an easily achievable value for radar receivers, while a value of 5 dB or less is usually considered to be nominal. To continue with the example given above, if kTB is -114 dBm and the noise figure of the receiver is 5 dB, then the radar receiver overall noise level will be effectively -109 dBm. Ultimately, all desired targets must somehow be detected against receiver noise.

1.5 Minimum Detectable Signal

Figure 1 illustrates the importance of obtaining the highest possible probability of detection on a per-pulse basis for the overall problem of detecting targets with *n* pulses. Each pulse is detected relative to radar receiver noise. The total signal power available to the receiver from all pulse echoes is *S*. There is a minimum *S* value, S_{min} (Eq. 1), which determines the maximum radar range, R_{max}, for a given target cross section. (It can also be used to determine the minimum target cross section that may be detected at any range.) This critical (S_{min}) itself is limited by the radar receiver inherent noise.

If a radar is barely able to detect a target at maximum range, R_{max}, then the corresponding minimum signal-to-noise ratio, $(S/N)_{min}$, must be related to S_{min} as follows:

$$S_{\min} = kTBF_n\left(\frac{S}{N}\right)_{\min} . \tag{6}$$

For a false-alarm probability of 10^{-6}, a detection probability of 0.8, and a standard echo-power variation model (Swerling case 1, see Section 1.7 below), the required signal-to-noise ratio is about 17 dB [12, pg. 24], which is a linear factor of 50:1. With a nominal noise figure of 5 dB (a linear factor of 3.16), the value of (Eq. 6) in a (nominal) 1-MHz bandwidth is $S_{min}=6.3\cdot10^{-13}$ W.

The value of S_{min} is further reduced by the effect of integrating n pulses, where typically n=20. This effect results in a value of S_{min} that is about 10^{-13} W [12, pg. 25].

Although (Eq. 6) is obtained by inverting (Eq. 1) for the maximum detection range of a target with a nominal cross section σ_0, it is important to note that the value of S_{min} of 10^{-13} W is itself independent of range. Any target, at any range, that returns less than this much energy to the radar receiver will probably not be observed on a radar display. If all targets had the nominal cross section σ_0 of (Eq. 1), then S_{min} would be returned only by targets at the edge of the coverage range and all targets within that range would be detected. But in reality, cross sections vary widely and many targets will have cross sections that are less than σ_0. Such targets will be lost at distances less than R_{max}.

1.6 Increase in Receiver Noise Figure as a Function of Interference Power Level

If interference is introduced into a radar receiver, the average power contribution from the interference, *I*, will sum with the radar inherent noise power, *N*, and that summed power will tend to mask the detection of desired targets. The ratio of the summed noise-plus-interference to inherent noise is *(I+N)/N*, and its behavior relative to the ratio of *I/N* is portrayed graphically in Figure 2.

As shown in Figure 2, the receiver noise figure is increased by 0.5 dB when the average interference power is 9.5 dB below the nominal receiver noise level, and the receiver noise figure is increased by 1 dB when the average interference power is 6 dB below the nominal receiver noise level. *These effective noise figure increases would represent equal increases in the minimum detectable signal level of radar receivers that are subjected to interference.*

1.7 Detection of Radar Targets When Their Levels Fluctuate

The power level of echoes from radar targets will normally vary in time. Such variations may occur due to time-dependent changes in the range, the aspect angle of the target, and the propagation and multi-path characteristics between the radar and the target. The result is that the variable of cross section in (Eq. 1), σ_0, is really a time-varying effective cross section, $\sigma_{eff}(t)$.

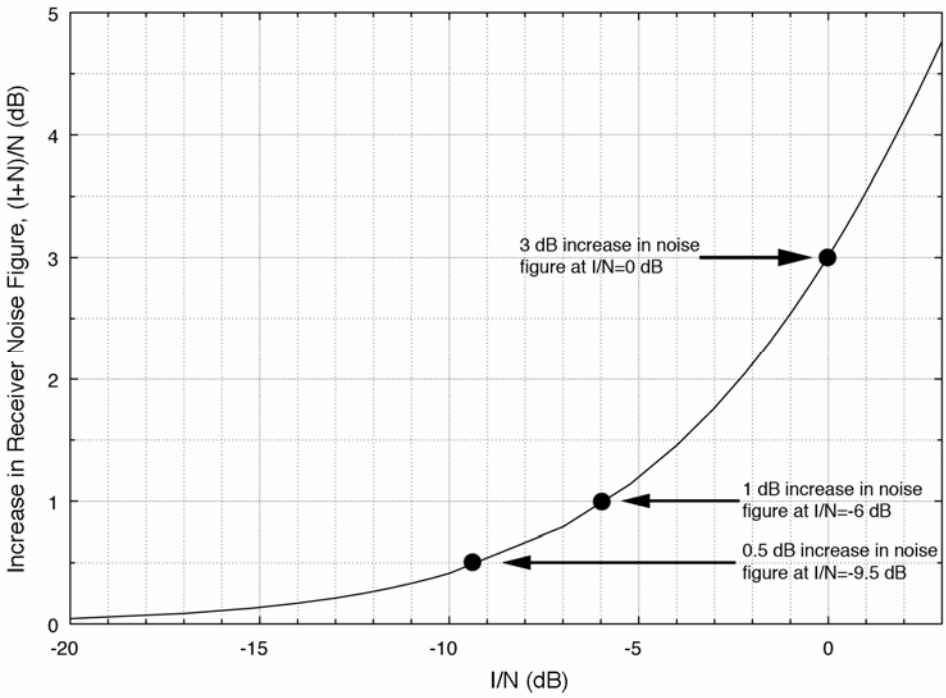

Figure 2. Receiver noise figure increases as the sum of interference power, *I*, and inherent internal noise, *N*, divided by the same noise power: *(I+N)/N*. This is the relation between *(I+N)/N* and *I/N*.

How do radar designers take these fluctuations in effective target cross sections into account when they design the systems? A naïve approach would be to increase radar transmitter power to accommodate the deeper power dips in such fluctuations. But this is not practical because the capacity for high peak power generation in radar transmitters is very expensive. Furthermore, most radar transmitters are designed to produce the highest possible peak power levels that technology can create and that budgets can afford. Thus it is not generally possible to increase the transmitter peak power, and another way must be found to compensate for target power fluctuations.

The compensation method that is actually implemented is to transmit *more pulses* at fluctuating targets than would have been needed if the targets had constant echo amplitudes, and to integrate the resulting multiple echoes to detect targets even when they are weaker than the nominal cross section. The approach is explained in standard radar design references [9-15, for example]. In this approach, standard mathematical models are used to describe the statistical characteristics of radar echo amplitudes. But however useful such models are when applied to radar design, they

ironically do not reproduce the behavior of real radar targets [9, pg. 52]. "The uncertainty regarding fluctuating target models makes the use of the constant (non-fluctuating) cross section in the radar equation an attractive alternative when a priori information about the target is minimal," [9, pg. 52].

1.8 Criteria for Radar Receiver Interference Thresholds

A recent, comprehensive compilation of currently accepted interference criteria from the existing literature indicates that currently accepted limits on *I/N* for carrier wave (CW) and noise-like interference in radar receivers are currently between -6 dB to -10 dB [16, pp. 5-2 and 5-3]. No standards currently exist for any other categories of interference (e.g., digital signal modulations) in radar receivers.

Based on the existing literature on this subject [16], limits on *I/N* in radar receivers are understood to mean the maximum allowable ratio of interference power to radar receiver noise power in the IF stages of radar receivers. The protection criteria that have been identified *do not* ensure that interference effects will not occur at (or below) those *I/N* levels; rather, it has simply been generally understood that these values should not be exceeded unless additional compatibility studies are performed which show that higher *I/N* levels would be acceptable under any given set of circumstances for any given type of radar receiver. The state of the existing literature on this subject begs several questions:

1) Is a limit on the *I/N* ratio in a radar receiver IF stage necessarily the best (or most appropriate) criterion for interference protection?

2) How reliable is the range of existing *I/N* protection criteria of -6 dB to -10 dB for protection of radar receivers from CW and noise-like interference?

3) For types of interference other than CW and noise-like (e.g., digital signal modulations), what should be the *I/N* protection criteria for radar receivers?

4) Can tighter bounds be placed on interference protection criteria for radar receivers?

In answer to the first question, alternative proposals have been variously problematic because they do not address some types of radar, or because they invoke protection criteria that cannot be analyzed or verified in any practical sense for operational, deployed systems. For example, it has been proposed that interference might be allowed to occur in some types of radar receiver in some spectrum bands on a statistical basis, with more interference allowed for shorter amounts of time and lower interference allowed for longer periods, according to some sort of predetermined 'interference budget.' But one of the problems with this approach is that no practical method has been identified for monitoring such interference in radar receivers, determining the sources, computing the current state of the interference budget from the interfering sources, and then somehow communicating from the radars to the interference sources that those sources must modify (in some unspecified way) their operations so as to mitigate the interference they are generating. In contrast, the approach of analyzing worst-case interference levels in radar receiver IF stages from the known characteristics of the radars and potential interference sources, while conservative, is nevertheless practical and verifiable (both theoretically and through

measurements), while providing assurance that critical radar missions (including safety-of-life) are not adversely impacted by interference sources. As documented in this report, degradation of radar receiver performance can be closely correlated with *I/N* levels in radar receivers for high-duty-cycle interference such as CW, noise, and digital signal modulations.

As for the remaining questions above, until now very little information has been available in the technical literature regarding the effects of low-level interference in radar receivers. It has therefore been debatable as to whether *I/N* interference protection limits of -6 dB to -10 dB *I/N* are necessarily appropriate for radar receivers in general, and whether those bounds might be determined more closely for various types of radar systems. These questions have been the impetus for the tests and measurements that are documented in this report.

1.9 Radar Detector Characteristics

The detector in a radar receiver is the device that extracts modulation information from the received carrier signal of the target echoes. The "detector" usually comprises the parts of the radar receiver between the output of the last IF amplifier and the input of the data processor (or other data display indicator). Detectors operate on both signal and noise inputs. The most widely used types are described below.

1.9.1 Envelope (Square-Law, Optimum-Law, or Quadratic) Detectors[10]

An envelope detector produces an output that is a function of the amplitude of the input waveform modulation envelope; phase information in the waveform is lost. The output of the detector is usually either a linear function of the input envelope[11] or, more commonly, is proportional to the square of the input envelope level. The response of an associated radar video integrator, if any exists, is normally included as part of the detector response for purposes of analysis. Empirical work [15, pp. 58-62] revealed that the optimum response function for a radar detector (when the signal-to-noise ratio of targets is small) is:

$$\psi(v) = Av^2 = y \tag{7}$$

where:

ψ = the output of the detector;
v = the amplitude of the modulation envelope of the input;
A = a scaling constant, often 1/2;
Y = the value of a single, discrete output from the detector.

The scaling constant, A, is only a multiplier of a bias level; it does not ultimately affect the P_d for a radar target. The square-law detector output usually feeds a linear-law video integrator. The integrator accumulates the results of n samples (such as from n pulses) [15, pg. 58]:

[10] The terms square-law, optimum-law, and quadratic detector are all used interchangeably.
[11] Noting that even so-called linear detectors are non-linear devices, by definition of detectors.

$$Y = \sum_{i=1}^{n} y_i = A \sum_{i=1}^{n} v_i^2 \tag{8}$$

where:

Y = the output of the integrator;
y_i = the amplitude of the i-th sample from the square-law part of the detector, from (Eq. 7).

The square-law detector-integrator is a simple and widely used device in radar receiver designs; as a default it is usually assumed to be the type of detector that is used in radar receivers. Linear-law detectors are not unknown, but their performance is generally similar to square-law detectors [15, pg. 62].

1.9.2 Logarithmic Amplifier Detectors

Some types of radar, such as maritime navigation units, experience a very wide range of echo amplitudes. This wide dynamic range of target echoes may span orders of magnitude, and will tend to exceed the response range of a single, linear receiver IF amplifier. To cope with this problem, *logarithmic amplifier* detectors are used. In logarithmic amplifier detectors, a cascaded chain of amplifier stages operates in parallel with a chain of envelope detectors to generate a receiver output that is proportional to the logarithm of the input envelope. Each stage in the cascade must have fixed, identical gain. A conceptual block diagram of a logarithmic amplifier detector is shown in Figure 3.

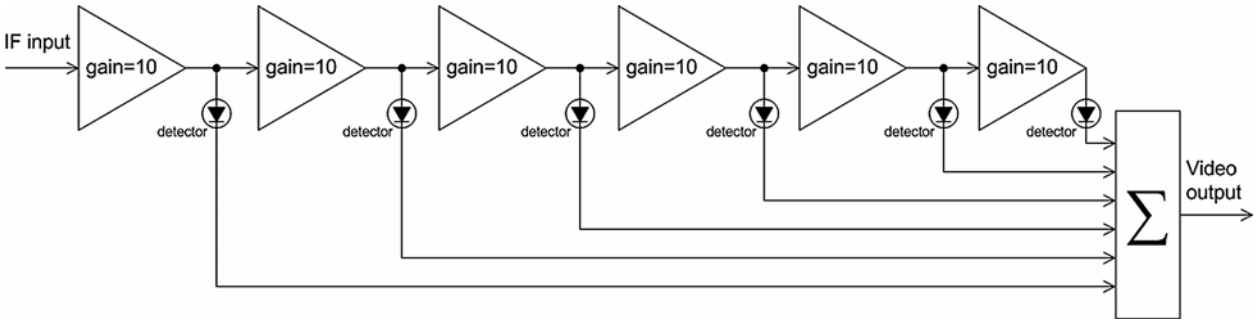

Figure 3. Block diagram of a logarithmic amplifier detector. The gain value of 10 is for example only.

The key principle of the design is that each detector is able to operate on the output of a graduating accumulation of gain. Thus the first detector operates on a small amount of gain that is suitable for very strong target echoes. Conversely, the last detector operates on perhaps 60 dB of gain, which will have been totally saturated for strong echoes but which is still adequate to provide a linear response to extremely weak target echoes. Thus strong target echoes produce outputs from all detector stages, extremely weak echoes produce an output from only the last detector stage, and all other echoes produce intermediate numbers of detector responses. The fact that the detector responses are finally summed means that a logarithmically varying range of output levels occurs across a very wide dynamic range of target inputs. Along with avoiding

saturation problems, logarithmic detectors also reduce the effects of unwanted clutter targets in radar receivers that do not have moving target indicator (MTI, or Doppler) processing (see below).

Logarithmic detectors cause a penalty in the probability of target detection that is manifested as a receiver gain reduction factor [9]. The reduction in the P_d as a function of the number of integrated pulse-echoes can be characterized as follows [9]: For 10 pulses integrated, logarithmic receiver loss is about 0.5 dB; for 100 pulses integrated, the loss is about 1.0 dB; and for an indefinitely large number of pulses integrated, effective reduction due to the use of a logarithmic detector maximizes at about 1.1 dB.

1.9.3 Zero-Crossings Detectors

Zero-crossings detectors work on the principle that signals can be identified in noise by extracting information about the zero-crossings of the desired energy. The operative principle is that the average number of zero-crossings will decrease as signal-to-noise ratio increases. Put another way, the principle is that signal-plus-noise voltage will tend to exceed the voltage of noise alone. In a zero-crossings detector, a device is constructed that counts the average number of zero-crossings per unit time, n_{ave}, compares n_{ave} to a predetermined threshold value, T, and then declares that a target is present if ($n_{ave} < T$). Whereas envelope detectors discard phase information in target echoes, zero-crossings detectors eliminate amplitude information about target echoes.

1.9.4 Coherent Detectors

A coherent detector is a balanced mixer with a low-pass filtered output. One of the balanced mixer inputs is a reference signal, generated by an internal reference oscillator, which provides a signal with some specified frequency and phase. The other input of the mixer is from the last radar receiver IF amplifier. The detector works on the assumption that the frequency and phase of the target echo from the IF amplifier output matches the reference signal. The low-pass output filter allows only the dc and low-frequency modulation components to pass, rejecting higher frequencies near the carrier. In effect, the carrier frequency is translated to direct current.

Coherent detectors preserve both amplitude and phase information in target echoes, and are theoretically more efficient than envelope detectors (by about 1-3 dB), especially at low signal-to-noise ratios [9]. Coherent detectors are seldom used in radar receivers, however, because the phase of the received signal usually cannot be known or controlled relative to the phase of the transmitted pulse.

1.9.5 Moving Target Indicator (MTI) or Doppler Processing

In many radar applications it is desirable and even necessary to distinguish moving targets from all other echo returns. This feature, called moving target indicator (MTI) or Doppler return processing, is ubiquitously implemented in air search radars. Although MTI processing is not

strictly a type of detection, its close integration with radar detection functions makes it worthwhile to mention in this context.

MTI works on the principle that electromagnetic echo energy emitted by a target that is moving with respect to the receiver platform will experience a Doppler shift in wavelength (and, consequently, frequency) compared to the wavelength of the radiation emitted by the radar transmitter. If echo energy is blocked in the receiver if it has the same frequency as the transmitted pulses, but is passed through the receiver otherwise, then only targets that are moving relative to the receiver will be displayed.

One low-cost method for implementing MTI is to lock a coherent oscillator (COHO) to the frequency of a set of individual transmitted pulses, use the COHO to beat against frequency of the echo returns from the same pulses, and filter the output with a DC block. This allows only non-zero beat frequency outputs to pass through the filter and be displayed. More costly MTI implementations may rely on high-precision frequency references for the generation of transmitted pulses.

Although MTI processing offers a number of advantages in terms of target discrimination, especially against clutter, it also has drawbacks. Some radars cannot use it because their PPI displays must show non-moving targets (e.g., floating debris and shorelines). Because MTI processing will be impaired by targets that are moving at speeds that cause the Doppler shift of the return echoes to be an integral multiple of the prf of the radar (e.g., a Doppler shift of 1 kHz or 2 kHz or 3 kHz, etc., in a radar that is transmitting a 1-kHz prf), radars that are designed for MTI must normally stagger the intervals between transmitted pulses by intervals that do not divide evenly into one another. Typically three or more such intervals must be generated between successive pulses to eliminate these so-called “blind speeds.” Staggering the transmitted pulses, providing for a precision frequency reference and/or COHO-mixer hardware in the transmitter, and incorporating MTI filters and software into the receiver adds to the cost and complexity of a radar. Furthermore, like all target-return processing, implementation of MTI will cause an effective increase in noise figure and the consequent loss of some desired targets from the PPI display under various circumstances. MTI processing does not reject interference.

1.10 Radar Features for Detection of Targets in Clutter and Interference

Unwanted radar echoes are called clutter [9, pg. 470] because the output of the undesired echoes tends to clutter the radar display. Sources of clutter include terrain features and structures, ocean-surface features, precipitation, flocks of birds, and insect swarms. Small pieces of metal foil (chaff) intentionally ejected in the atmosphere cause degradation of radar performance by intentionally creating clutter effects. Regardless of the origin, clutter always tends to degrade radar performance. An example of clutter is shown in Figure 4.

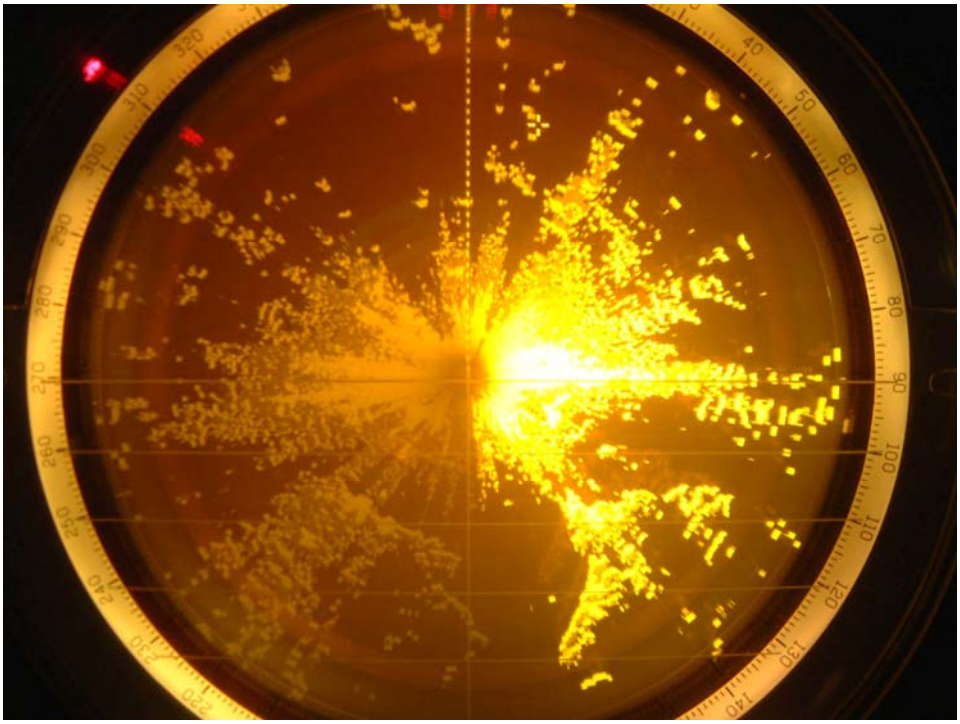

Figure 4. An example of clutter on a 9-GHz maritime radionavigation radar plan position indicator (PPI) display. The clutter includes local buildings, terrain, and vegetation. No intentional interference or test targets are present on this display.

Clutter effects may be mitigated by some radar design features. Since clutter sources tend to be either stationary or slow-moving, they may be somewhat reduced by the use of Doppler filtering (MTI) that eliminates the effects of echo energy with less than a minimum amount of frequency-shift relative to the transmitted frequency. However, motion characteristics of birds and insects do not always allow their echoes to be eliminated by such processing.

If fixed, ground-based clutter due to terrain is severe in the vicinity of a fixed-sited radar (an example being large hills or mountain ranges that protrude into the radar beam coverage), a clutter fence that is electromagnetically opaque may be built around part of the radar site. The fence attenuation may reduce the clutter effects, but will tend to adversely affect the radar performance in other respects [9, pg. 498].

Otherwise, clutter effects may be reduced generally by the use of the feature of sensitivity time control, as described below. None of the techniques that reduce clutter will mitigate the effects of radio interference in radar receivers.

1.10.1 Sensitivity Time Control (STC), or Swept Gain

Sensitivity time control (STC) suppresses the effects of clutter-producing objects that are located near the radar. STC reduces the dynamic range requirements of radar receivers by reducing receiver gain just after each pulse is transmitted. This sensitivity reduction, also called *swept gain*, is gradually recovered in a controlled manner, often as a fourth-power function of time [12,

pg. 13]. The receiver gain, in other words, is reduced for echoes that originate near the radar, and is increased to a nominal level for echoes that originate at large distances from the radar. Figure 5 shows an example of an STC curve for an air surveillance radar. Although some interference energy might fall below the STC noise threshold for close-in targets, STC is not, per se, a radio interference suppression mechanism.

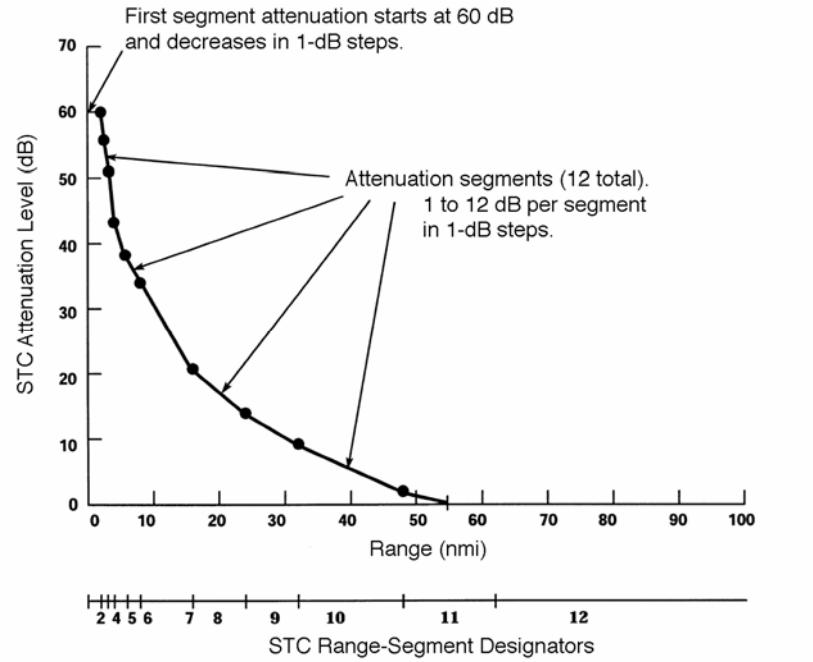

Figure 5. Example STC curve for an air surveillance radar.

1.10.2 Log Fast Time Constant (Log-FTC or FTC) and Comparison with STC

Another important method for reducing the effect of clutter echoes is *log fast time constant* (log-FTC, or simply FTC). FTC log-compresses the dynamic range of clutter energy [12, pg. 77] and therefore reduces the variation in clutter levels at the receiver output. This effect, in turn, results in a relatively constant false alarm rate (CFAR) with a somewhat inexpensive implementation in the radar design. CFAR is described in more detail below.

FTC works if the input clutter (or noise) is described by a Rayleigh probability density function. Sea clutter and land clutter are non-Rayleigh, and thus log-FTC is not so effective against them. But FTC works well against precipitation clutter, and is sometimes called a *weather fix* [9, pg. 506-507].

The effect of FTC is somewhat like automatic STC, but unlike STC it does not suppress clutter entering the radar receiver through the antenna sidelobes. (Because STC reduces gain when the transmitted radar pulse energy is still at close distances, it does work against echoes entering through the sidelobes.) If clutter is strong enough to be received through the sidelobes it may not be adequately reduced by the log effect of FTC. Therefore, STC and logarithmic receivers are sometimes used together, with the STC working in the RF part of the receiver and the logarithmic amplifier working in the radar IF section.

STC is range-dependent, while log-FTC is range-independent. Neither technique improves the ratio of target-to-clutter power. The benefits of FTC are traded against some loss in the probability of detection of targets. FTC is not a radio interference-suppression feature.

1.10.3 Instantaneous Automatic Gain Control (IAGC, or AGC)

Instantaneous automatic gain control (IAGC, or simply AGC) is yet another technique for avoiding overload of radar displays by strong clutter blocks. AGC works through a negative-feedback loop between the IF amplifier output and the gain control of that circuit [12, pg. 78]. The time constant of the AGC is set to a long interval, so that extended clutter effects are reduced, while the short-response time responses due to echoes from discrete targets are not affected. AGC is commonly implemented in aircraft-tracking radars that implement conical beam-scanning and monopulse tracking techniques [9, 11]. The AGC filter loop is a low-pass design that passes frequencies from dc to just below the antenna beam-scan rate, thus assisting tracking capabilities.

AGC causes reduction in receiver sensitivity in the presence of strong signals and thus mitigates radar display overload, but it also decreases the probability of detection of undesired targets. It is therefore not an interference mitigation technique.

1.10.4 Constant False Alarm Rate (CFAR)

A simple form of analog constant false alarm rate (CFAR) processing was discussed in Section 1.10.2 in connection with log-FTC circuitry. CFAR is often an optional feature for many simple, analog radar displays, but its implementation is often essential for digitally processed radar signals [12, pg. 98]. The reason for the discrepancy is the intelligence that human operators bring to the problem of interpreting radar plan position indicator (PPI) displays, versus the inherent limitations of digital processing algorithms relative to human intelligence. Human operators can become skilful at distinguishing true targets from noise and clutter artifacts on such displays, and if too many false targets (false alarms) are occurring, then the operator can reduce the gain setting of the PPI display—in effect providing an approximation of automatic CFAR, albeit with a relatively slow response time [12, pg. 99].

But in automated detection and tracking systems, where the design goal is to automatically designate targets and display them, the processing algorithm can be overwhelmed by too many false targets. (A change of only 1–dB in the threshold-to-noise or threshold-to-clutter ratio can change the false alarm rate by 2 orders of magnitude [12, pg. 99]. Thus an automatically adaptive CFAR technique is therefore essential for such radars.

In a typical CFAR implementation, a test cell is designated. Around that cell, a group of tapped digital delay lines are used to estimate the average level of noise or clutter. The tap outputs (usually 16 to 20) are summed, the sum is multiplied by an appropriate constant, and the result is used to set the detection threshold for the test cell [12, pg 99, and 9, pp. 392-395]. The output of the test cell is the radar output. This approach is called *adaptive video thresholding*.

Additional variations of CFAR exist [9, pg. 394]. One of these is a post-detection integrator (a low-pass filter) that is used to estimate average noise, the output then being fed forward to control the detection threshold. Another technique, called the *Dicke fix*, is to use a broadband IF filter followed by a hard limiter and a narrow matched filter. The hard limiter is set low enough to limit receiver noise. But signal energy causes the output of the matched filter to increase by a factor that is equal to the ratio of the bandwidths of the wideband and narrowband filters. A variant of this approach uses limiters to discriminate between desired target echoes and interference by observing the change in time of the phase pattern at the limiter output [17, pg. 3.49]. The limiter output is correlated with phase-coded information in the transmitted waveform; the better the correlation, the more likely the energy is a target echo. This approach, called *phase-discrimination CFAR* or *coded-pulse anticlutter system* (CPACS), destroys all amplitude information in the echo returns.

CFAR processing has a number of drawbacks. It causes losses relative to optimum detection, and the number of pulses that are required for processing must be large to minimize this loss. CFAR inevitably reduces the overall probability of detection of desired targets, and thus will cause some targets to be lost. These losses can be insidious because operators will often be unaware that CFAR-controlled detection thresholds are gradually creeping upward as noise, clutter, or interference increase in some environment [9, pg 395; 12, pg. 99]. In CFAR radars, anti-interference measures should therefore be implemented (if any are available) ahead of the stage where CFAR processing occurs.

In summary, CFAR processing is a necessary evil that suppresses clutter and noise effects at the cost of losing some desired targets. CFAR will suppress interference from low duty-cycle (less than a few percent), asynchronously pulsed sources (i.e., other radar transmitters). But CFAR does not function as an anti-interference technique for higher duty-cycle (i.e., non-radar) signals. In fact CFAR can make the effects of high duty-cycle interference worse by insidiously suppressing desired targets in the presence of such interference without any awareness of the problem on the part of radar operators.

1.10.5 Interference Rejection (IR)

As described in [18], many radar designs include an operator-selectable feature called *interference rejection* (IR). The purpose of IR is to reject or suppress interference into a radar receiver from co-channel transmissions from *other radars*. For reasons that will presently become clear, IR is not effective against non-radar (communication-type) signals. IR is especially useful in radar bands in which large numbers of radars are tuned to the same frequency; two of these cases are 3050 MHz, a popular frequency for S-band maritime radionavigation radars, and 9400 to 9410 MHz, a popular range for the tuning of X-band maritime radionavigation radars. Without the IR feature activated, the effect of interference from multiple, co-channel radars is shown in Figure 6.

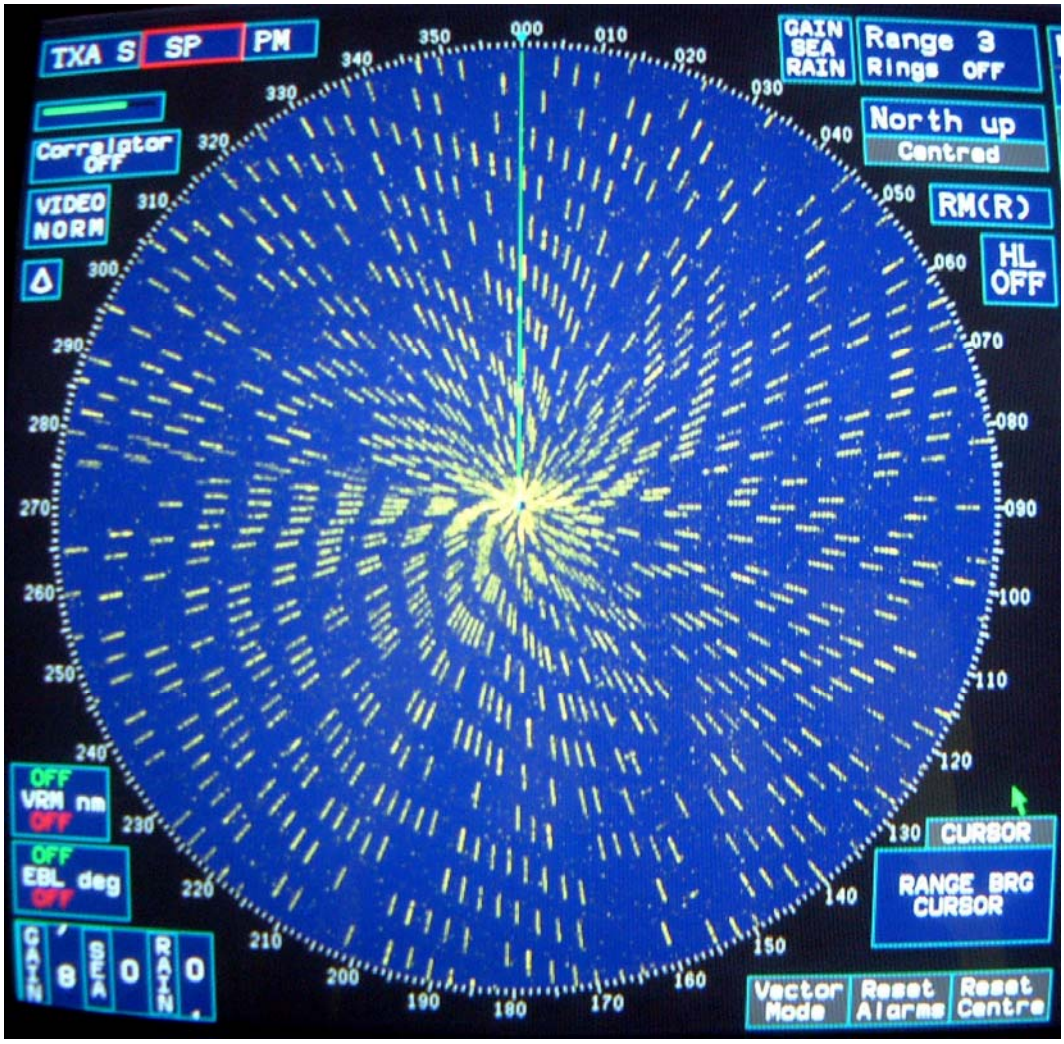

Figure 6. An example of continuous severe co-channel radar interference on a PPI display. The average *I/N* level of the interference is 0 dB and the IR and STC features are switched off.

IR circuit designs are often protected as trade secrets, but there are at least two broad approaches that work on two different principles of pulse-to-pulse correlation: Pulse repetition interval (pri) discrimination, and pulse width (pw) discrimination [18].

A block-diagram for the pri discrimination IR design is shown in Figure 7. In this approach, echo pulses in the radar video section are passed through a threshold comparator and then through two channels via a splitter. In one channel the pulses are delayed by the pulse repetition interval and in the other channel there is no net delay relative to the first channel. The two resulting outputs are then ANDed. If the echo intervals match the radar transmitter pri, then the AND gate output goes high; otherwise the AND output goes low; the AND gate condition is used to pass video data. The result is that radar pulse sequences that do not match the transmitter pri are suppressed at the video output. Note that one of the input pulses is lost, and that low-amplitude echoes are discriminated against. Also, this technique does not enhance desired signals, but only suppresses undesired signals.

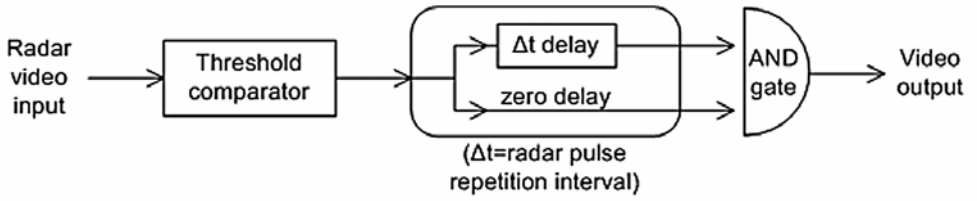

Figure 7. Pulse repetition interval (pri) interference rejection circuit block diagram.

A somewhat similar conceptual approach is used for pw discrimination IR. In this design, the input pulses are differentiated and split into two channels. In one channel the differentiated pulses are delayed an interval corresponding to desired pulse width, τ, while in the other channel the differentiated pulses are inverted. If an input pulse is of width τ, the differentiated trailing edge inverted pulse will coincide in time with the leading edge pulse delayed in time τ. The coincidence circuit passes signals in the two channels only if they are in time coincidence; if an input pulse is not of width τ, the two spikes will not be coincident in time and the pulse is rejected. This technique results in reduced receiver sensitivity and probability of target detection. Figure 8 shows a radar display (with radar interference present) when IR is deactivated versus activated.

In addition to pulse-to-pulse IR techniques, some radars also incorporate IR that works on a scan-to-scan basis. This feature operates by using a memory of apparent targets that is either reinforced (or not) from one scan to the next. Since false targets generated by stray pulses from other radar systems will not be expected to occur at the same location on the PPI display from one scan to the next, such targets may be dropped from the display if no reinforcement occurs on a scan-to-scan basis. Targets that do continue to occur at the same location on the PPI display (or at nearly the same location, within some specified bounds of translational movement) are remembered from previous scans and continue to be displayed.

The IR feature in radar receivers only works against low duty cycle, pulsed, asynchronous interference. The use of IR is a necessary evil for radar operations, because it causes some targets, especially ones that are weak, to be lost. For pulse-to-pulse IR techniques, losses occur due to the comparator threshold setting (in the pri IR design) and because of the reduced number of pulses that are available for data processing and overall reduced receiver sensitivity with these circuits. For scan-to-scan IR processing, weak targets that tend to fade out normally in a high percentage of scans will be lost because of their intermittent behavior. IR is not effective against communication-signal interference because such interference is normally of much higher duty cycle than radars. Appendix A expands on the results of IR performance studies that were performed in conjunction with the test effort described in this report.

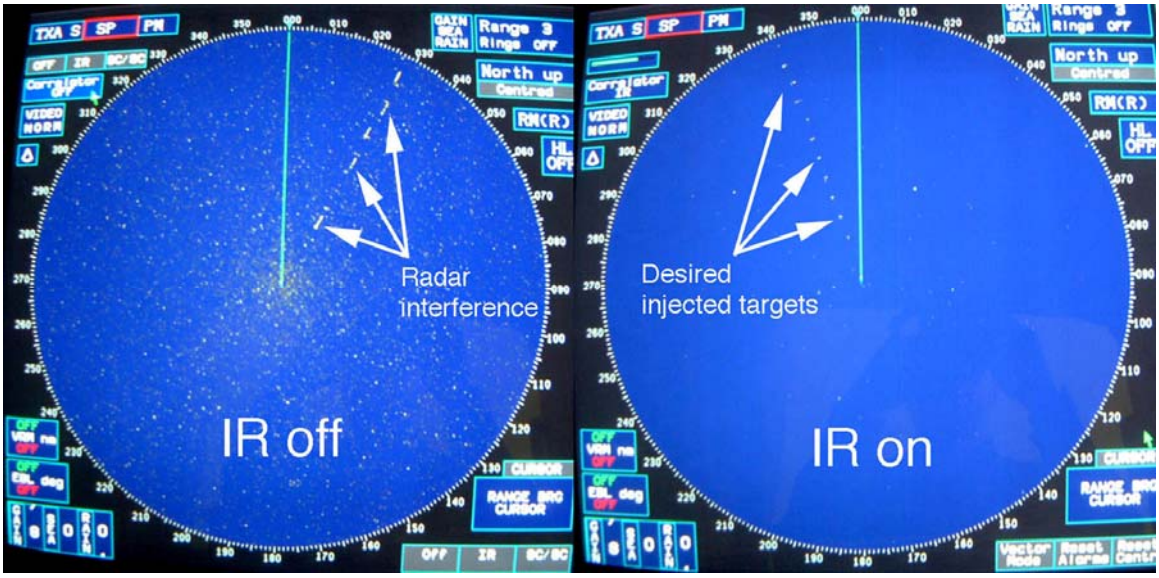

Figure 8. Radar display with IR turned ‘off’ versus ‘on’ in the presence of interference from other, gated radar-like pulses. A set of ten desired targets has been injected in both images, at 30 degrees azimuth at the left and at 340 degrees azimuth on the right. The targets are obscured by coincident radar interference when the IR is turned off (left), but are easily visible through the same interference when the IR feature is activated (right). IR has been found to be effective only for low duty-cycle (less than about 1-3 percent) interference, such as generated by radar transmitters.

2 SETTING CONDITIONS FOR INTERFERENCE MEASUREMENTS ON RADAR RECEIVERS

For tests and measurements of radar receiver performance in the presence of RF interference, it has proven crucial to establish baseline conditions for the operation of the radars and the injection of interference into the receivers. The basic baseline conditions and parameters are described here. Additional and more detailed descriptions of the test conditions are provided in later sections of this report, in connection with the discussion of tests and measurements on the individual radars in this study. Figure 9 shows the typical appearance and conditions of a radar station control console and PPI display.

Figure 9. Typical conditions inside an air-search radar station, showing the main console for display and control.

2.1 Interference Coupling Technique

It was essential that the levels of interference in each radar receiver be quantified as precisely as possible. Such quantification is difficult or impossible if interference is coupled radiatively into the radar receivers. Radiative coupling also introduces problems with spectrum coordination with other agencies. There is also always a chance that other signals in the vicinity of the radar might cause some sort of additional interference in the receiver. Taking all of these factors into

consideration, interference signals were injected into all of the radars in this study via hardline couplings, with desired targets likewise injected at the RF front end via a combiner. The typical test configuration is shown in Figure 10.

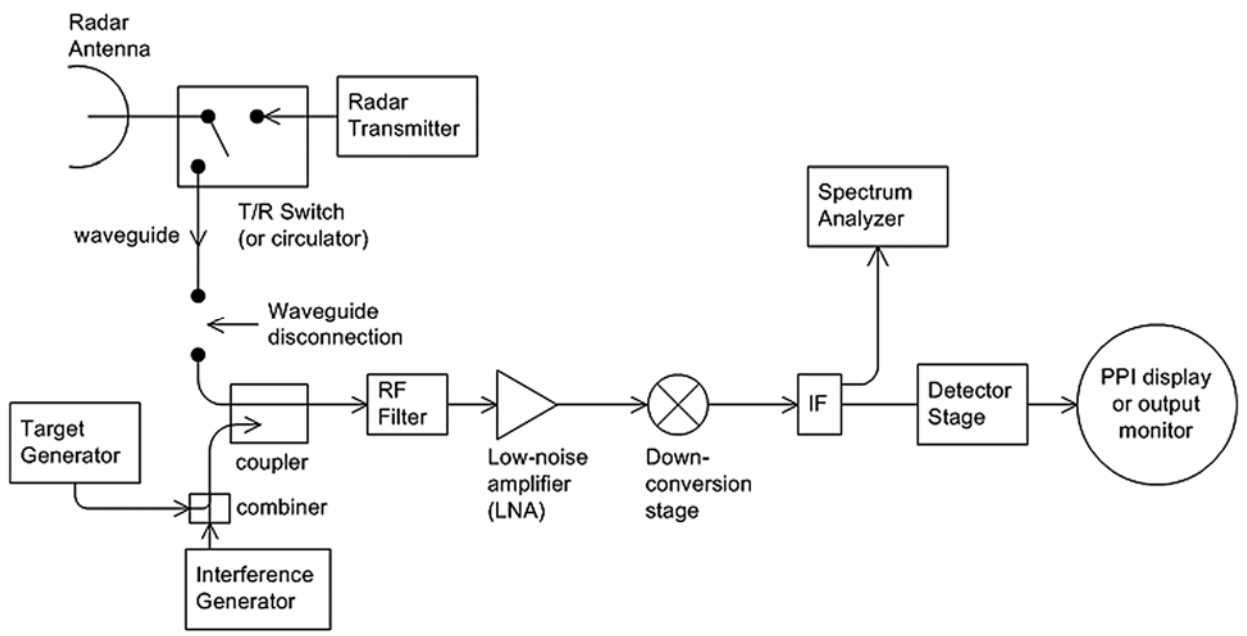

Figure 10. Block diagram of a typical test configuration in this interference study. Interference and desired targets were generated at radio frequencies and were injected at the radar receiver RF front-end ahead of the first RF filter and LNA. The spectrum analyzer is an external, diagnostic test and measurement accessory that is tapped from the IF via a directional coupler.

The hardline connections for interference were always made at the radar RF front end, as close as possible to the radar antenna, with the radar running in a receive-only mode. In particular, the RF interference was fed into the radars *ahead* of the first RF low noise amplifier (LNA). Thus the receivers were subjected to RF interference that replicated energy that would have otherwise been fed into the receivers via the radar antennas. This approach ensured that all sections within the radars behaved normally, the same way that they would have if the interference had been radiated normally into the radar units.

For the second model of long range air route surveillance radar, as described in Section 3, the first RF low-noise amplification section consisted of a distributed array of LNAs built on a feed platform in front of the antenna reflector; it was mechanically impossible to couple the RF interference into this array in such a way as to feed all of the LNAs. Instead, a hardline connection was made to the input of the first RF stage ahead of a selected LNA on a selected element row of the array.

2.2 Calibration of Interference Levels

Whenever possible, the relative levels of interference, *I*, and receiver noise, *N*, were directly measured as *I/N* ratios within the IF section of each radar. Figure 11 shows NTIA and FAA engineers assessing such an IF tap point. When no access was available to a radar's IF section, then the radar receiver noise figure was measured and the *I/N* levels were computed. Procedures for both the direct observation method and the indirect computation method are provided here.

Figure 11. NTIA and FAA engineers determining the locations on a radar IF-stage circuit card where the *I/N* level could be monitored.

In all of these *I/N* calibration procedures, it is critical to distinguish between cases in which the interference bandwidth exceeds the radar IF bandwidth (wideband) versus cases in which the interference bandwidth is less than or equal to the radar IF bandwidth (narrowband). The critical difference between these two cases is that all of the power generated for narrowband interference will be coupled into the radar IF, whereas only a fraction of wideband interference power will contribute to the *I/N* ratio, and account must be taken of that offset (called on-tuned rejection, or OTR) in the effective value of *I* in the receiver IF stage.

2.2.1 *I/N* Calibration with Access to the Radar IF for Non-Pulsed Signals

In cases where access to the radar IF was available, the technique for determining *I/N* levels was to first connect a spectrum analyzer with average detection to the radar IF output and observe the radar noise power level in a resolution bandwidth (RBW) matched as closely as possible to the radar IF bandwidth. Then the interference generator output was fed into the radar RF front end input and the interference power was adjusted until it caused an increase of 3 dB on the spectrum analyzer display. Since the spectrum analyzer display showed the quantity [*I/(I+N)*], this meant that [*I/(I+N)*]=3 dB, implying that *I=N* and therefore *I/N*=0 dB. With this method, all *I/N* levels were referenced to the indicated *I=N* level. Figure 12 shows an example of the IF output for this approach.

Because the interference level was directly monitored in the radar IF bandwidth, no special account needed to be taken of the *I* power level if the interference bandwidth exceeded the bandwidth of the radar IF. Whatever the amount of OTR that might occur due to the bandwidth difference, the direct observation of a 3-dB increase in the IF at some interference power generator setting provided assurance that the corresponding setting of the generator output panel was in fact creating a 0-dB value for *I/N* in the radar IF bandwidth.

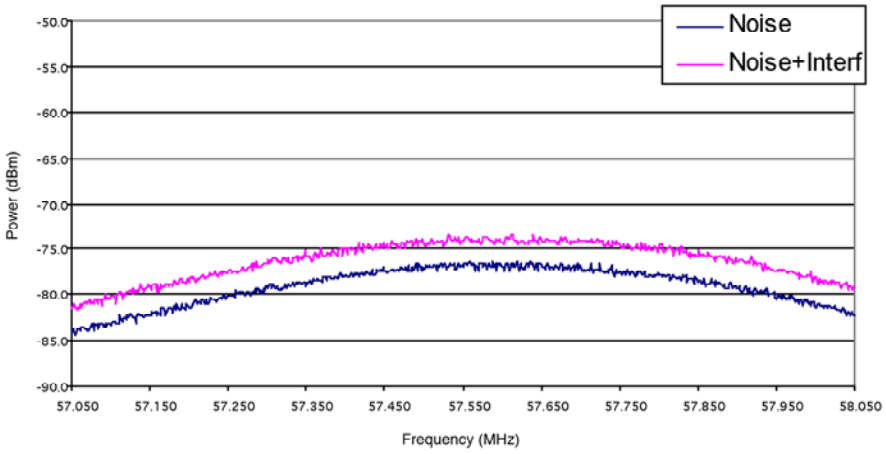

Figure 12. Example of a 0-dB *I/N* calibration noise spectrum (57.55 MHz IF frequency). Interference is wideband CDMA (W-CDMA). The noise-plus-interference curve is 3-dB higher than noise-only curve.

2.2.2 *I/N* Calibration with Access to the Radar IF for Pulsed Signals

For tests in which pulsed interference was injected, the level of the pulsed interference was adjusted until the peak power from the pulses was observed 20 dB above the receiver IF level. In that case, [*I/(I+N)*]=20 dB, implying that *I/N* was virtually 20 dB. (Care was always taken to be sure that the pulse peak power level was measured in a bandwidth that was wider than (1/pulse width) to ensure that all pulse power was convolved into the measurement.) This approach is depicted in Figure 13. With this method, all interference *I/N* levels were simply referenced directly to the level that gave an indicated *I/N* of 20 dB in the receiver IF stage.

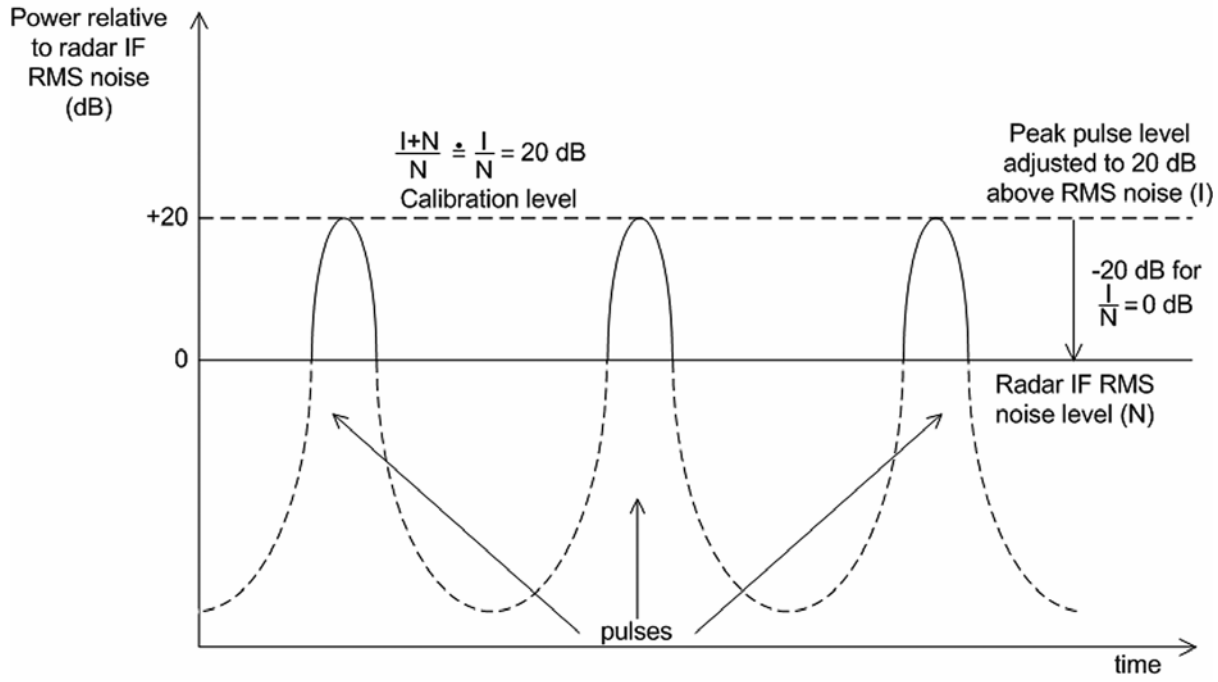

Figure 13. Calibration technique for pulsed interference. Peak pulse power is measured in a bandwidth exceeding (1/pulse width), and peak power for all subsequent testing is referenced to the injected level where [*(I+N)/N*]=20 dB, which differs from *I/N*=20 dB by only 0.04 dB, well within the uncertainty of the measurement itself.

Although pulsed signals would generally produce emission bandwidths that would be wider than the radar IF bandwidth, the OTR factor due to the bandwidth offset was physically incorporated into the observation of effective interference power in the radar IF stage. Thus the direct observation of the effective *I/N* level in the radar IF stage obviated any need to compute an OTR factor for such interference; the signal generator setting that produced a 20-dB increase relative to the radar IF noise floor was in fact the setting that produced a true *I/N* level of 20 dB.

The analysis above only applies if it is possible to match the spectrum analyzer resolution bandwidth (RBW) to the radar IF bandwidth. If it is impossible to make the spectrum analyzer IF bandwidth match the radar IF bandwidth, then the *I/N* at the radar IF output is determined by taking into account the OTR:

$$\left(\frac{I}{N}\right)_{IF} = \left(\frac{I}{N}\right)_{T} - OTR \qquad (9)$$

where:

$(I/N)_{IF}$ = interference to noise ratio in the bandwidth of the radar IF stage;
$(I/N)_{T}$ = interference to noise ratio that would occur if the radar IF bandwidth were equal to or wider than the bandwidth of the RF interference produced by the transmitter;
OTR = on-tuned rejection factor.

For CW-like signals, the OTR factor is given by:

$$OTR = 0 \text{ for } B_{IF} \geq B_T \quad (10a)$$

$$OTR = 10\log(B_T/B_{IF}) \text{ for } B_{IF} < B_T \quad (10b)$$

where:

B_{IF} = radar receiver IF 3-dB bandwidth (Hz);

B_T = transmitter 3-dB bandwidth of the interference signal (Hz).

During the measurements described in this report, the *I/N* ratio calculated above (taken into consideration with the OTR) was noted where applicable, along with any associated attenuation settings. The interference generator power output level and associated attenuation settings that produced an *I/N* ratio of 0 dB at the radar IF output was recorded, and other *I/N* values were obtained by adjusting the interference attenuator setting.

2.2.3 *I/N* Calibration without Access to the Radar IF

Almost all radars used in this study were accessible at their IF stages. But in the rare cases in which no access to the radar IF stage was available, an indirect *I/N* calibration method based on the specified radar noise figure and 3 dB IF bandwidth was used; radar noise figure and radar IF bandwidth were taken from documentation.[12]

Thermal noise at room temperature (about 290 K) is kTB = -114 dBm/MHz. The receiver inherent noise level (in dBm) N, at the receiver IF output referred to the receiver RF input is given by:

$$N = -114 \text{ dBm/MHz} + 10\log(B_{IF}) + NF \quad (11a)$$

or

$$N = -168.6 \text{ dBm} + 10\log(B_{IF}) + 10\log(T) \quad (11b)$$

where:

B_{IF} = receiver IF bandwidth (MHz);

NF = radar receiver noise figure (dB);

T = radar receiver effective noise temperature (K).

For example, suppose that a radar operated with a 100-ns pulse width. Then a typical IF bandwidth matching that pulse would be (1/100 ns) = 10 MHz. A good radar receiver noise figure would be 5 dB. In this case the radar noise power in the IF would be (-114 dBm +

[12] Radar IF bandwidth would normally be nearly equal to (1/pulse width) of the radar, and this knowledge was used to help verify that the specified IF bandwidth was sensible.

10log(10 MHz) + 5 dB) = -99 dBm (that would be measured in a 10 MHz RBW). In other values of RBW, the measured noise power in the radar IF would vary as 10log of this value.

The OTR complication (already described above) arises for interference signals with bandwidths that are wider than the radar IF bandwidth. Extending the example above, suppose that an interference signal that has noise-like characteristics (such as code division multiple access (CDMA)), and which thus varies in power as 10log(RBW) is to be injected into the radar RF front end. The complication arises because the radar IF is too narrow to convolve all of the power in the interference signal; in effect, the radar sees only a fraction of the interference power, that fraction being given by an OTR ratio $10\log(B_{interference}/B_{IF})$.

Suppose, for example, that the CDMA signal bandwidth were 20 MHz and the goal is to inject this signal into the radar with a 10 MHz IF bandwidth at an *I/N* ratio of 0 dB. The nominal 0–dB signal generator power output level would in this case have to be increased by the OTR amount of 10log(20 MHz/10 MHz) = +3 dB. Account would also have to be taken of all losses between the signal generator and the RF injection input point, which would typically be on the order of 15 dB loss. The resulting 0-dB *I/N* is calculated by the equation:

$$P_{gen} = P_{noise} + OTR + P_L \tag{12}$$

where:

P_{gen} = power output (panel display level) from the interference generator, dBm;
P_{noise} = radar IF noise power level in the bandwidth of the radar IF (dB);
OTR = on-tune rejection factor $10\log(B_{interference}/B_{IF})$ dB;
P_L = loss between the signal generator output and the radar RF front end input, dB.

Suppose for example that P_{noise} = -99 dBm in 10 MHz; OTR = 10log(20 MHz/10 MHz) = +3 dB; and P_L = 15 dB. Then P_{gen} = -99 + 3 + 15 dB = -81 dBm displayed power output from the interference generator for an *I/N* level of 0 dB. All other values would follow from this, as shown in Table 1. It should be noted that, in this method, *all* losses and gains between the interference generator output and the radar RF front end input must be carefully measured.

Table 1. Example of Interference Power Levels When Interference Bandwidth Exceeded Radar IF Bandwidth

***I/N* (dB)**	**Path Loss (dB)**	**Radar IF Bandwidth (MHz)**	**Interference Signal Bandwidth**	**OTR (dB)**	**Interference Signal Generator Panel Display (dBm)**
-6	15	10	20	+3	-87
-3	15	10	20	+3	-84
0	15	10	20	+3	-81
+3	15	10	20	+3	-78
+6	15	10	20	+3	-75

2.2.4 Setting *I/N* Levels from Calibration Data

For all calibration techniques, the various levels of interference were subsequently adjusted to particular values by attenuating the input relative to the calibrated level. For example, suppose that the panel display power value that gives *(I+N)/N* = 3 dB is -84 dBm. This becomes the 0-dB *I/N* point. Then a 3-dB reduction in the interference level relative to that point would be an *I/N* level of -3 dB, which would occur at -87 dBm output power from the generator. An example of a complete conversion table as used for typical radar interference measurements is shown in Table 2.

Table 2. Example of Interference Power Levels When Interference Bandwidth was Less Than or Equal to Radar IF Bandwidth

***I/N* (dB)**	**Interference Signal Generator Panel Display (dBm)**
-10	-94
-9	-93
-6	-90
-3	-87
0	-84
+3	-81
+6	-78

2.3 Injection of Desired Targets

All of the radars that were tested were designed to detect and display discrete targets, with the exception of a meteorological (weather surveillance) radar. Degradation effects needed to be assessed based on target detection effects (loss of targets versus false targets). Therefore it was critical to ensure that a useful set of baseline targets were provided at all stages of testing on each radar receiver. For most testing, the need for a good set of baseline targets was met by injecting a hardline-coupled set of n_{target} fixed-amplitude pulses, the number of pulses being:

$$n_{target} = \left(\frac{\theta}{360}\right)\left(\frac{T_{scan}}{pri}\right) \tag{13}$$

where:

n_{target} = number of pulses injected for each target;
θ = 3-dB radar antenna azimuthal beamwidth (degrees);
T_{scan} = time required for a 360-degree radar antenna scan;
Pri = pulse repetition interval (sec).

For example, if a radar with a 1-degree beamwidth generated 1000 pulses per second (for a pri of 0.001 sec) and had a scan interval of 4.75 sec, then n_{target} = 13 (rounded to the nearest integer).

The injection was done at the radar IF frequency. Usually a set of ten targets were injected in this way. Figure 14 shows the target and interference injection equipment typically transported by NTIA engineers to a radar station. Figure 15 shows a block diagram of the target-generation hardware developed for the study; additional hardware was used to synchronize target injection with radar PPI scan triggering.

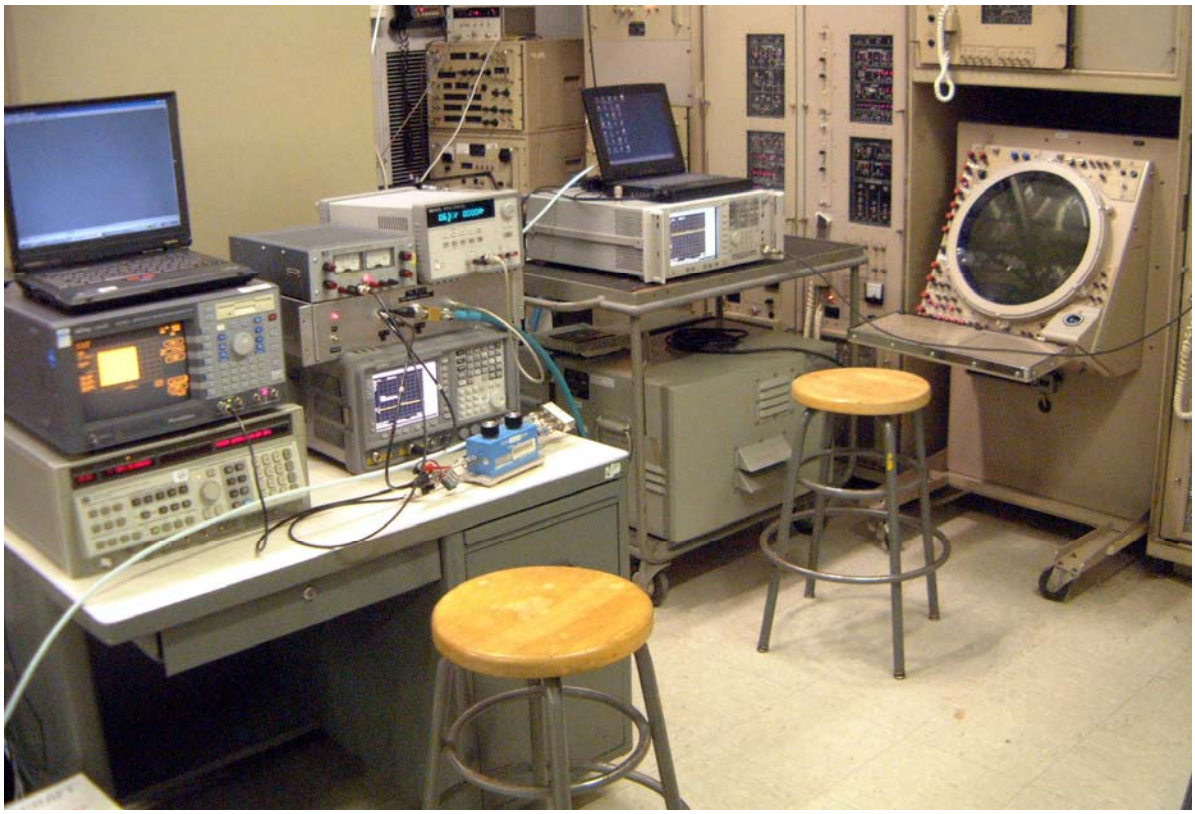

Figure 14. Typical arrangement of NTIA interference and target generators at an air search radar station. The NTIA equipment is spread across the table in the foreground and the cart in the background, with the radar PPI display at right.

The set of desired targets was injected on every radar scan.[13] In most tests the targets were injected synchronously with a scan trigger from the radar set, thus keeping the targets at fixed locations on the radar PPI displays from scan to scan.[14] In tests in which scan synchronicity was not possible to achieve, target positions shifted a few degrees in azimuth from one scan to the next.

On each scan, at least ten equally spaced test targets were usually injected at equal power levels in a sequence that placed them radially on the radar PPI display, as shown in Figure 16.[15] For real targets, this radial distribution would imply a change in distance between the radar site and the

[13] In this report, "scan" means a single, 360-degree rotation of the radar beam.
[14] For a few radars, no such trigger was available and operator-adjusted synchronous timing was used instead.
[15] In some tests, a set of four such radials were injected during each scan at angular intervals of ninety degrees, providing forty targets per scan.

targets, with a concomitantly increasing cross section with distance. But for the purpose of the NTIA test and measurement series, this arrangement was *not* meant to replicate effects due to changes in distance. Instead, it was simply an expedient to ease the difficult process of counting targets during interference runs; radially distributed targets were found to be easier to count than equal-radius, sector-distributed targets.

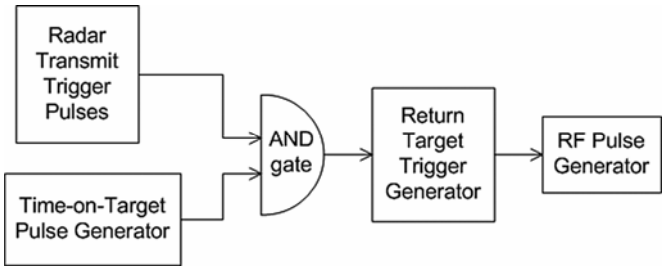

Figure 15. Block diagram of the radar target-generation hardware developed and used for the study.

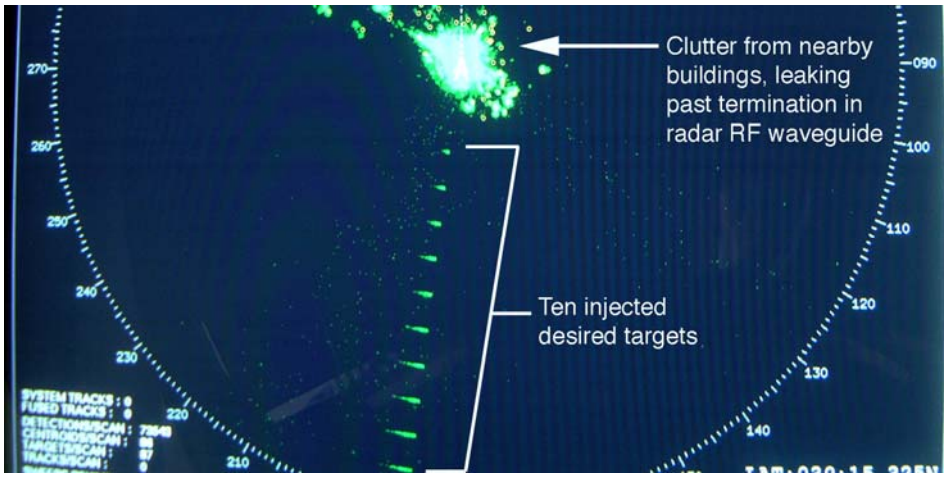

Figure 16. Example of a maritime radar PPI display during interference testing with ten injected targets on a single radial. Clutter condition was used diagnostically to verify proper radar operation.

One radar, a long-range air surveillance system, incorporated a built-in target generator and an automated target counter; NTIA engineers took advantage of those features during the testing. Those targets were displayed throughout sector wedges on the PPI display as shown in Figure 17, but again the target cross sections were constant; no distance effects were incorporated. As was the case for the NTIA-generated targets, the radar PPI display arrangement in sector wedges was simply a convenient way for the system software to arrange the targets on the screen.

Figure 17. Sector-wedge distribution of desired targets on a PPI display during testing on a long-range air search radar. Targets are shown as "+" signs, and are generated at the radar RF stage.

Some live-target testing was done within range of a busy airway with a long-range air surveillance radar in the Midwestern area of the US. Although a test phase at that radar included the use of standard NTIA-generated desired targets, the live-target phase of the testing allowed the observation of interference effects against actual aircraft in flight, ranging from commercial airliners to small airframes.

For meteorological radar tests and measurements, discrete targets could not be used because those radars are designed to monitor extended atmospheric phenomena. For those tests, actual weather echoes and radar internal noise were used in the course of the test program, as described more fully in Sections 5 and 7.

2.4 Use of Fluctuating Versus Non-Fluctuating Targets in Radar Testing

The question naturally arises whether tests of the effects of low-level interference in radar receivers should be performed with constant amplitudes for the desired targets, versus against desired targets with fluctuating levels. It can be argued that fluctuating targets might resemble real-world targets most closely, and thus should be used. But this argument has been found to be incorrect. The reasons are as follows:

1) Real targets do not fluctuate in accordance with the mathematical models (called Swerling models or cases [9, pp. 46-52]) that are used to design microwave radars. There is no general-purpose mathematical description of target fluctuation that works for a general class of radar targets under all operational conditions. The Swerling models are used because they are analytically tractable and provide some resemblance to the range and rate of variation that might be seen in some real targets.

2) Although radars are designed to use a sufficient number of pulses per target per scan to accommodate some amount of target-power fluctuation, this does not necessitate the use of power fluctuations during testing of radar performance. Rather, testing can be just as well performed against a fixed, *nominal* target power level. Such a level would represent the behavior of many real targets, which have been observed by the authors to fluctuate little or not at all from one scan to the next in many cases.

3) During testing, radar receiver performance must be compared in two conditions: interference being present versus no interference being present. A meaningful comparison of these two conditions means that a baseline target detection performance level must be established when no interference is present. Experience of NTIA engineers has shown that such a baseline is easy to establish if target power level in the receiver is held constant, but is difficult to achieve if target power levels fluctuate about that nominal value in accord with the Swerling models. The problem is that, if the target power fluctuates according to, for example, Swerling case 1 [9, pp. 46-47], then (roughly) half of the targets nearly burn the phosphor on the PPI display, while the other half (roughly) are simply absent. Therefore the baseline level of detection becomes approximately 50% for such targets. But meaningful performance tests need to be performed with a target probability of detection that is closer to 90%. To achieve 90% performance with Swerling case 1 fluctuating target distributions, as shown in Figure 18, the *mean value of the fluctuating targets must be increased by perhaps 10 dB or more*. This approach would be problematic because it would be equivalent to compensating for target fluctuations by turning up the radar transmitter power by 10 dB, which is exactly what operational radars *cannot* do to enhance target returns. Furthermore, if this step is taken with a target generator in actual testing, then most of the target returns nearly burn the phosphor on the PPI, which again is not a realistic scenario.

4) Observation of genuine targets, both aircraft and boats, by NTIA engineers indicates that non-fluctuating test targets more nearly resemble the behavior of real targets on radar PPI displays. Furthermore, non-fluctuating test targets can be adjusted to a 90% probability of detection and that level can be used as a reliable baseline through all testing on a radar unit.

For all the reasons above (maintenance of a constant non-interference performance baseline, replication of the behavior of genuine airborne and maritime radar targets, and overall practicality of testing), NTIA testing has mostly used constant-amplitude test targets that are held at a power level at which they are detected 90% of the time on the radar PPI display when no interference is present. An exception has been made for meteorological radars, which do not detect discrete targets, and in which actual atmospheric echo returns have been used.

It is worth noting that by setting the probability of detection of the test targets to 90%, NTIA engineers provided substantially stronger target levels for the radar receivers than might have been justified by the 80% probability of detection criteria that many reference sources [9-14 and 19] quote for purposes of adequate radar design. The two probabilities might not be comparable because setting a design criterion is not the same as setting an interference-test performance criterion. The purpose of the NTIA tests and measurements was to determine upper limits for interference levels that produce deleterious effects in radar receivers. In other words, the purpose was to test interference effects against targets that were undoubtedly high-quality, but still within the range of credibility for real radar echoes. If an interference level with some modulation was found to affect the detection of targets that had a 90% probability of detection in the absence of interference, then the detection of almost any real targets by the same radar receiver would be expected to be adversely affected by the same interference level of that modulation. Put another way, with 90% probability of target detection in the absence of interference, the tests were structured in the direction of accepting higher rather than lower levels of interference before radar receiver performance was adversely affected.

2.4.1 Overview of Fluctuating Target Level Generation

Even considering all of the arguments above, some interference tests were performed on a maritime radar with fluctuating targets. Those test procedures and their results are specifically described in Section 6, but an overview of the fluctuating target approach is as follows.

As seen in Figure 18, the behavior of logarithms causes the values in each distribution to naturally be below 0 dB (and further below 0 dB) more often than they are above 0 dB. This is consistent with the physical reality that reflected power levels from radar targets may increase only a finite amount *above* an average, but may be reduced by an infinite amount *below* an average.

A baseline P_d curve needs to be determined without any interference being present and with the target power levels fluctuating. To assess the effects of interfering signals when the targets are fluctuating, the P_d is determined when the I/N level is set to an array of values such as: -9 dB, -6 dB, -3 dB, 0 dB, +3 dB, +6 dB, and so on. This approach allows the fluctuating target baseline P_d to be compared with the steady target power P_d and just as importantly allows comparison between the P_d when the targets are at a fixed power level at some I/N level to the P_d when targets are fluctuating under the same I/N condition. A key element is to use the same fluctuating target power levels with and without the presence of interference signals.

In choosing target fluctuation values for the tests, the lower part of Figure 18 can be used to select the decibel power values relative to the median target power level, which is 1.6 dB below the mean value. The rationale for this offset can be gleaned from standard texts [e.g., 17, pg. 46-52]. The set of test values are then selected from the curve. For example, the -5.5 dB value has a cumulative probability of about 0.175. So if the target power that gave P_d=0.90 was -75 dBm from the testing signal generator, then the value for that cumulative probability would be -80.5 dBm. Twenty fluctuating target values from the curve will be selected from the figure, an example group being listed in Table 3. One value will be selected for each scan. On each scan, all of the injected targets (usually ten) will thus have a common value.

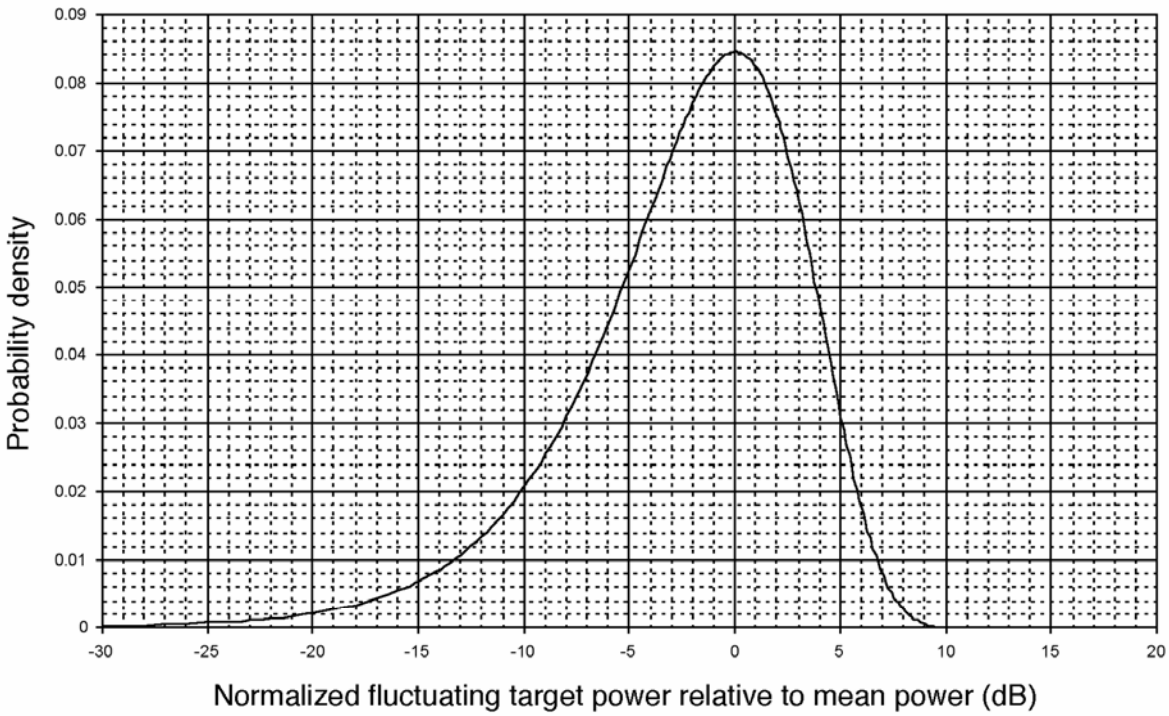

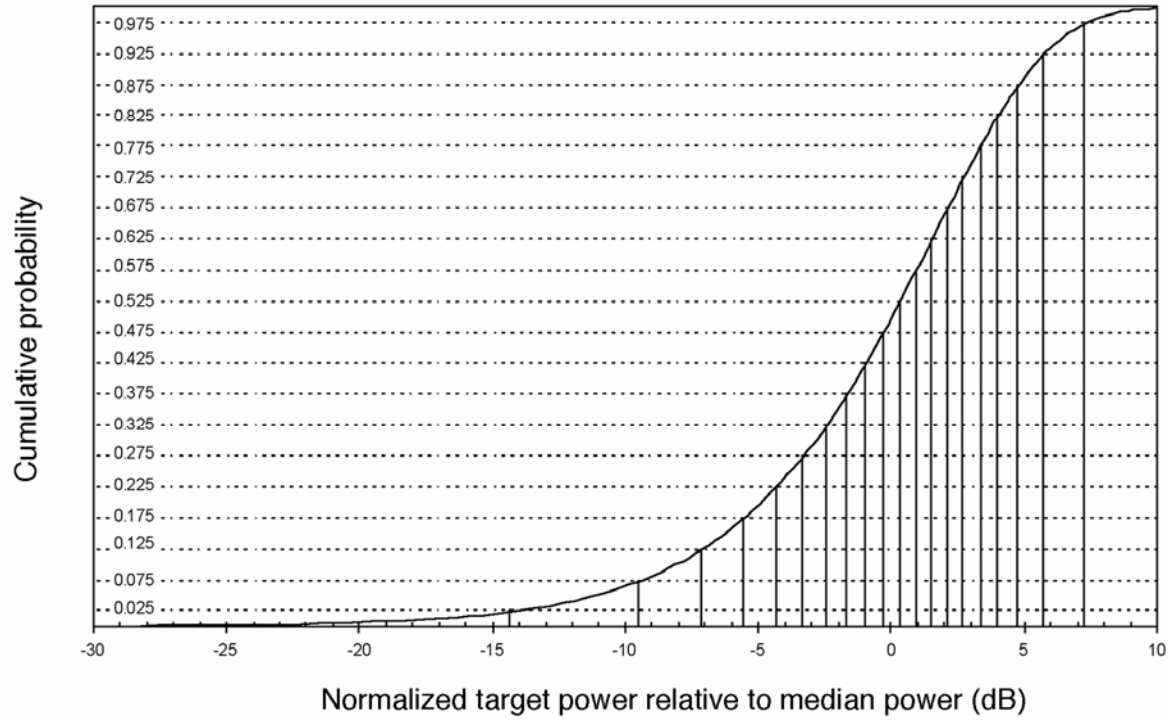

Figure 18. Statistical distributions for Swerling case 1 fluctuating radar target power. If the average level is set to the same value as required for 90% probability of detection of non-fluctuating targets, then most of the targets are not visible on the radar display.

Table 3. Fluctuating Target Power Levels Derived from the Curves of Figure 18

Signal levels (dB) Relative to median power level	
-14.4	0.30
-9.5	0.91
-7.2	1.5
-5.6	2.1
-4.3	2.7
-3.3	3.3
-2.5	4.0
-1.7	4.8
-0.90	5.7
-0.30	7.3

At the end of a test run at a given *I*/N level, (usually twenty scans altogether), the total number of observed targets would be divided by the total number of injected targets (say 200) to obtain a single data point for the P_d of fluctuating targets under the interference condition being tested. Then the interference *I/N* level would be changed (its value would be either raised or lowered, or the modulation would be changed), and the entire sequence of fluctuating target levels would be used again for another set of (usually twenty) scans at the new interference level.

2.4.2 Test Methods with Fluctuating Targets

Specifically, the procedure for interference testing with Swerling Case 1 targets was as follows:

First, the zero mean power level for the targets was set to the value that produced a target P_d of 0.90 without interference present and steady target power levels. Then the variation of the target power level from the value that gave the 90 percent P_d was chosen from Table 3. The target power was set to that level and the targets were counted. The power of the groups of pulses that defined a target was set to cycle through the twenty entries in the list of power values (relative to the mean value) contained within Table 3. A P_d count was made by observing the PPI through twenty scans.

Next, the *I/N* level was set to one of the following values (-9, -6, -3, 0, 3, 6, 9, 12, 20, or 40 dB) using one of the undesired waveforms and the target generator was cycled through the same varying set of power levels for the chosen sigma; the P_d was computed for those twenty scans, and so forth.

2.5 Target Identification and Counting During Tests and Measurements

Although many radars, including those used in the NTIA test and measurement series, provide automatic target identification and tracking features, NTIA engineers determined during the tests that a human operator (one of the authors, Sanders) was more skilled at identifying and discriminating radar targets than the automated routines built into the radar processors. Many

marginal targets that would be rejected by automated radar processing algorithms were easily identifiable by the human operator, and false alarms were more easily rejected. Most of the tests were therefore run without automated target detection, and the targets that were observed were counted, scan by scan, by the human operator. An additional benefit of using the human operator to identify targets and reject false alarms was that the operator brought the same acceptance criteria to bear on all of the target displays of all the radars in the tests. Figure 16 shows the typical appearance of radar PPI displays under test conditions.

The result was that uniform criteria were applied to target identification on all of the radars (except meteorological, where discrete targets were not used), and the effects of interference were more flexibly allowed to occur before targets were declared to be degraded than would have been the case if automated target identification features had been used. That is, thresholds for the effects of interference were documented at *higher* interference levels than would have probably been allowed if automated processing of targets had been performed. As was the case with 90% probability of detection for targets in the absence of interference, this structured the test results in favor of the occurrence of higher, rather than lower, interference levels before performance degradation was documented.

2.6 Radar Receiver Parameter Settings

Every radar used in the NTIA tests and measurements had to be configured for some sort of nominal operation throughout every test series. The most critical settings that had to be considered for all of the discrete-target radars were STC, AGC, and CFAR. (For the meteorological radar, these features were not applicable, and the configuration was adjusted by site personnel who were intimately familiar with the radar behavior, and who adjusted the radar to function nominally in the presence of the local atmospheric and weather conditions.)

Since STC is used to suppress close-in clutter, and since no such clutter could occur due to the hardline-coupled nature of both the RF interference and the injected test targets, the STC feature was normally disabled during radar interference measurements unless otherwise noted in the descriptions of individual tests.

As for AGC, this feature was normally activated during tests in which interference was gated on momentarily during each radar scan, but AGC was deactivated during tests in which interference was continually present during every radar scan. (The first case corresponds to desired target displays on one radial or a few radials, and the latter case corresponds to situations in which the desired targets were displayed in broad sectors throughout radar PPI displays.) AGC was activated for the momentary-interference testing because such interference behavior is expected to replicate ordinary coupling into a radar antenna mainbeam, and AGC could be expected to respond normally (which is to say minimally) to such momentary interference. But in the case of continually-present interference (which would not be expected in the real world except in extreme cases, where the interference would couple strongly into the radar antenna sidelobes), the AGC had to be deactivated because otherwise the AGC feature would decrease the radar gain to a very low value, thereby effectively desensitizing the radar and resulting in the loss of most or all of the desired targets. Such a condition would become a test of AGC behavior rather than of radar receiver performance; the goal of the tests was to determine more inherent system

responses, rather than the response of the AGC feature to interference. (Note, too, that AGC, like STC, is *not* an interference-suppression feature.)

Regarding CFAR, this feature is most useful when automated target identification routines are invoked. It was usually activated during testing because it is used so ubiquitously in the operational modes of most radar receivers. In some cases, CFAR processing can be controlled by manipulating the number of guard cells, but the settings for this feature are usually not changed much during the operational life of most radars.

Considering IR functionality, this feature was sometimes toggled on and off during testing (for radars that incorporated this feature, such as the maritime units) to demonstrate the effectiveness of the IR features in the radar system. Because testing revealed that IR was not effective at high duty cycles, some tests were performed to determine the threshold at which IR functionality was impaired. The behavior of IR in radar receivers is further described in Appendix A.

3 INTERFERENCE MEASUREMENTS ON LONG-RANGE AIR SEARCH RADARS

3.1 Introduction

Long-range air surveillance radars routinely search for, and track, airborne targets at distances exceeding 200 nmi. They sometimes incorporate meteorological (weather) surveillance capabilities as well. These radars perform critical missions for air traffic control and national security. Although their designs vary, they tend to be similar in some vital receiver characteristics such as noise figure. For this study, NTIA engineers worked closely with personnel from other US Government agencies[16] to determine the susceptibility of two differently designed types of long-range air surveillance radars. Both of these radars operated in the so-called L-band, on individual frequencies assigned between 1250-1350 MHz. In this report these radars are referred to as Long Range Radars 1 and 2.[17]

3.2 Description of Long Range Radar 1

3.2.1 General Description

Long Range Radar 1 detects weather and aircraft within a radius of about 200 nautical miles (370 km) for the FAA and other Federal agencies. It provides data concerning the location and strength of weather as well as range, azimuth, and altitude of aircraft within its search volume. A separate beacon interrogator system that is incorporated into the radar design provides additional information on aircraft beacon codes, aircraft-encoded altitudes, and emergency status[18] of aircraft.

The radar has two channels, denoted as F1 and F2, which require at least 25 MHz of frequency separation.[19] Two frequencies are provided for the purpose of compensating for atmospheric fading, distortion, and other effects on any one frequency; effects that degrade one frequency are not expected to affect the other channel. *Two-frequency capability is not provided for the purpose of using one frequency to compensate for interference effects on the other frequency.* This study did not address radar performance on two channels when one is affected by interference.

Two receiver processing channels, designated A and B and corresponding to each of the two operational frequencies, are provided. Each channel consists of a synchronizer, a frequency generator, a transmitter, weather and target receivers, a receiver processor, and a digital target extractor (DTE). The radar uses frequency separation and orthogonal polarization for the two channels so that they can transmit and receive via the same antenna for the diplex mode of operation. The radar transmits RF energy on a low beam, and receives reflected RF energy on

[16] Including the Federal Aviation Administration and the US Air Force.
[17] Long Range Radar 1 is the air route surveillance radar model 3 (ARSR-3), and Long Range Radar 2 is the ARSR-4.
[18] Beacon code, altitude, and emergency status are provided via an associated secondary surveillance radar operating at 1030 MHz and 1090 MHz. Interference to that out-of-band system was not considered in this study.
[19] The tested radar installation operates at 1292.08 and 1330.20 MHz.

both the low beam and a high beam. The high beam is used to detect aircraft at short ranges and the low beam is used to detect aircraft at longer ranges and also weather.

3.2.2 Receiver Processing

Each channel in the radar receiver has both normal and moving target indicator (MTI)[20] video available. The normal and MTI video both have identical constant false alarm rate (CFAR) processing. Both channels contain independent CFAR circuitry. The CFAR samples the input signal at 1/8 mile intervals, from 5/8 mile before the target to 5/8 mile after the target, to determine the mean noise level from the appropriately delayed main target signal.

Long Range Radar 1 also contains integrator-adder circuitry that functions on the normal and MTI video. The integrator-adder contains a digital video integrator. The integrator digitally sums, into a single output, all of the target-hit video occurring within the 1.1-degree (3 dB points) azimuth beamwidth of the radar antenna. Because there are about 12 transmitted pulses within that beamwidth, there can be approximately 12 consecutive target hits or echo returns at the same range and azimuth. Also, since the integrator operates synchronously with the radar's transmitter, asynchronous pulses (from other nearby radars) are automatically eliminated from the video output.

Independent receiver processors in channels A and B are electrically identical. Each receiver processor contains a target processor function. After detection the target information is digitally processed into suitable form for identification by the DTE. When the radar is operating in a two-frequency (called diplex) mode, processed target video data in each radar channel are digitally summed with the adjacent channel target video data before distribution to the DTE. This cross-channel target video summation feature enhances target detection. Cross-channel video summation during dual channel operation improves the probability of target detection since a fluctuating target fade in one channel should not be experienced in the opposite channel due to frequency-polarization diversity between the two channels.

3.2.3 Antenna Characteristics

Long Range Radar 1 uses a dual horn fed parabolic reflector enclosed in a radome and mounted on a dual drive pedestal. The antenna forms two cosecant-squared beams shaped for additional high elevation gain. The two beams are almost identical. The azimuth beamwidth of both beams is 1.1 degrees at the 3 dB points. The upper beam has coverage from 3.6 to 44 degrees in elevation while the lower beam covers 2 to 42 degrees in elevation. The antenna rotates at 5 revolutions per minute (rpm). A complete list of the relevant radar technical parameters is contained in Table 4.

[20] Moving target indicator is a Doppler processing output with a velocity threshold. It reduces clutter by eliminating the display of target returns that are moving at less than a critical threshold velocity.

Table 4. Technical Characteristics of Long Range Radar 1

Parameter	Value
Frequency range	1250-1350 MHz
Range	200 nmi
Altitude coverage	Up to 18,300 m (60,000 ft)
Distance resolution	0.25 nmi
Azimuth resolution	2 degrees
Receiver IF bandwidth	420 kHz
Pulse width	2 μs
Noise figure	2 dB
Pulse repetition frequency	310 – 364 (8 discrete prf values)
Receiver noise (calculated) level in receiver bandwidth	-115 dBm
Sensitivity with normal processing	-115 dBm
Sensitivity with moving target indicator	-112 dBm
False alarm rate	10^{-4} for a 2-m^2 cross section
Antenna type	Dual horn reflector
Antenna mainbeam gain	Low beam: 34.5 dBi High beam: 33.5 dBi
Antenna elevation beamwidth	$cosecant^2$ 3.6º to 44º degrees
Antenna azimuth beamwidth	1.1 degrees
Antenna scan rate	5 rpm (12 sec/rev)
Antenna polarization	Linear and circular available

3.3 Test Approach for Long Range Radar 1

3.3.1 General

The radar's performance was monitored by observing targets on the radar's PPI display and through the use of the radar's built-in target counting software. Desired targets were generated using RF signal generators and additional testing was accomplished using live traffic. In addition to the desired target signals, signal generators were used to inject CW and binary phase-shift keyed (BPSK) interference into the radar receiver. Radar P_d performance was evaluated as a function of the calibrated *I/N* ratio at the IF output of the radar receiver.

As noted above, the radar could operate on either of channels A and B singly, or on both channels simultaneously. Target power was adjusted to achieve a P_d value of 0.9 in the absence of interference on a single channel. The same target power was maintained during both single-channel and dual-channel testing on the radar. As a result, the P_d value was close to 1 when the two channels were used simultaneously. Interference tests were performed in both single-channel and dual-channel operational modes.

3.3.2 Injected Targets

In order to speed testing, a total of forty injected test targets (ten targets on each of four separate radials) were separated in range to allow for easy determination of missed targets. They were monitored for five consecutive antenna rotations for a total of 200 injected, desired targets examined for each data point. Each target, regardless of range, was set to the same power at the receiver input, making each target equivalent in terms of receiver P_d. The target power was adjusted to a level that provided an average target P_d in the absence of interference of about 90 percent.

The target P_d, based upon 200 attempted target scans, was based on manual counting from the radar PPI display by one of the authors (Sanders). Although information about target P_d on a per-pulse basis was collected by the radar's internal data collection software, that information was not used in this study because the radar's overall performance in the presence of interference was the topic of study. (Any one target or "blip" on the radar screen also has an intrinsic P_d for each individual pulse within the group of pulses that defines that target.) The target generator produced about 12-13 pulses per target. Whenever the radar integrated enough of those pulses to define a target and produce a "blip" on the display, it was counted as a good target. As a result, the actual P_d per pulse in the group of pulses that defines the target could have been lower than 90 percent.

In order to determine the equivalent radar cross section (RCS) represented by injected test targets, a measurement was made at the end of the test cable connecting the signal generator and the waveguide. Accounting for the waveguide coupler and other losses between the injection point and the receiver, the target signal level into the receiver IF was -107.2dBm.

The radar requirement[21] is for detection at main beam gain of a 2 m^2 target out to at least 195 nmi. One form of the basic radar equation (Eq. 1) is:

$$R = 0.282 \cdot \left[\frac{P_t G_t A_e \sigma_0}{P_r} \right]^{1/4} \tag{14}$$

where:

P_t = peak transmit power, watts;
G_t = transmitter low beam gain, linear term;
σ_o = test target cross section, m^2;
A_e = effective antenna aperture, m^2;
P_r = received target signal level, watts;
R = target range, m.

In addition, the Long Range Radar 1 specification allows for a total of 4.1 dB loss in the receiver-to-antenna path. This same loss is also present on the transmitter-to-antenna signal path. For the tested configuration, then:

[21] FAA-E-2483b, paragraph 3.4, of the radar System Performance Requirements document.

P_t = 5 MW – 4.1 dB loss = 1.945x10^6 W;
G_t = alog(34.5dB/10) = 2818.38;
A_e = $G_t\lambda^2/4\pi$ = 12.07;
P_r = -107.2 dBm + 4.1 dB = -103.1 dBm = 4.898x10^{-14} W;
R = 195 nmi = 361235 m.

Rearranging the equation to solve for the test target cross section for a received power of -107.2 dBm, (Eq. 14) becomes:

$$\sigma_0 = \left(\frac{R}{0.282}\right)^4 \cdot \left(\frac{P_r}{P_t G_t A_e}\right) \tag{15}$$

σ_0 = (361235/0.282)^4 /[(1.945x10^6)(2818.38)(12.07)/(4.898x10^{-14})]

σ_0 = 1.99 m^2.

3.3.3 Live Targets

A limited amount of data were also collected using live 'targets of opportunity,' For that testing, the radar was placed into its normal operational mode and the PPI screen was monitored for detected aircraft in the radar coverage area. Though the level of these targets was uncontrolled (being dependent on the interaction geometry between the radar and the aircraft itself), the local FAA air traffic control center was contacted to determine the aircraft type for specific targets of interest on the PPI display.

3.4 Undesired Signals in Long Range Radar 1

3.4.1 General

RF signal generators and arbitrary waveform generators (AWGs) were used to generate CW interference and also the following BPSK signals:

1) BPSK at 0.511 MBit/s,
2) BPSK at 1.023 MBit/s,
3) BPSK at 5.11 MBit/s,
4) BPSK at 10.23 MBit/s.

Spectra of the injected signals are shown in Appendix B. BPSK signals contain data bits that are encoded into symbols that a spreading pseudorandom code further breaks into chips. However, the radar receiver does not discriminate between phase changes representing either a chip or a bit for this type of interfering waveform. The radar receiver processes the BPSK signals as band-limited constant amplitude noise sources, which fall into all of the range cells. Since the noise-like BPSK signal falls into all of the range bins, the CFAR processing cannot eliminate it and the CFAR raises the target detection threshold.

The emission spectrum for each BPSK interference signal was measured and recorded, and tuned to the frequency of the radar channel(s) under test. The BPSK signal generator had the capability to generate *I/N* ratios of -12 dB to +30 dB at the receiver RF input; however testing was usually accomplished only over the subset of that range where meaningful P_d data could be collected. For each signal type, calibrations were performed to allow for conversion between signal generator settings and the resultant *I/N* level using the process described in Appendix C.

3.4.2 Duration of Interference Signals with Injected Targets

For the injected desired signal tests, the undesired signals were also injected into the radar at the RF input path to the receiver with durations equal to the main beam dwell time and overlaying them on the desired targets at the same azimuth. As shown below, the dwell time for the main beam of the radar's antenna is 0.04 seconds through a stationary object. This dwell time was used as the duration of the BPSK interference source for the simulated target tests. For any live target, this interval may be different due to the motion of the target.

$$dwell\_time = \frac{antenna\_beamwidth}{360\,\mathrm{deg}} \cdot 12\,\mathrm{sec} = 0.04\,\mathrm{sec}. \tag{16}$$

3.4.3 Live Target Tests

For the live target tests, as for the injected target tests, the undesired signals were injected into the radar at the RF input path to the receiver (see Figure 10). Because of the mobile characteristics of the live targets however, the injected targets maintained their positions for longer intervals. In particular, the injected targets were controlled so as to cover approximately a 40-degree sector of the radar scan. In addition, for a given set of live targets only a single level of *I/N* could be tested. These tests did not attempt to simulate a potential interference source's exact behavior as it might move through the radar's antenna beam at any particular azimuth. The actual dwell time of such an event (and its possible periodicity) would depend upon both the proper motion of the source and the characteristics of the radar antenna beam scanning through space.

3.5 Test Procedures on Long Range Radar 1

3.5.1 Injected Target Tests

For the injected target tests, the desired signal targets were overlaid with BPSK interference signal at a given *I/N* and observed for 5 complete scans. This resulted in a total of 200 possible targets (5 scans x 10 targets/radial x 4 radials/scan), and probability of detection was calculated as the number of observed targets divided by 200. The test was then repeated at a different *I/N* level. For these tests the transmitter was turned off and though the antenna was still rotating and receiving external signals, a spectrum analyzer measurement showed that none were present in the IF stage (see Figure 10). When testing was completed for a given BPSK signal type, a different BPSK interference modulation was used and the testing was repeated. For each *I/N* level and BPSK modulation, testing was performed with:

- interference and targets on one channel and the other channel disabled;
- interference and targets on both channels;
- baseline "no interference" measurements were performed before and after each "interference" data set.

3.5.2 Live Target Tests

For these tests, since the target amplitude was largely uncontrolled, the procedure followed was to operate the radar without injected interference for 15 scans, then turn on the injected BPSK interference at a fixed *I/N* for 15 scans, and finally turn off the injected interference for another 15 scans. This allowed for examination of live targets within the BPSK-interfered sector to determine whether there was any discernable impact to the target due to the BPSK interference. The targets were recorded from the PPI display to a radar data file for all 45 scans. Upon replay of the data file to a laptop computer, it was observed that the BPSK interference manifested itself as a reduction of a 'reinforced target' (i.e., a primary, skin-track target that had a secondary surveillance radar (SSR) beacon reply superimposed upon it). The skin track part of the reinforced target would fade, but the SSR part, which operates at 1030 MHz/1090 MHz, was not affected.

For targets of interest where a skin-track was lost but the beacon reply was still present, the type of aircraft that was being tracked was determined by contacting the local FAA air traffic control center (ATC) in Kansas City and providing them with the associated beacon code. The ATC was then able to use the beacon code to provide the flight number and type of aircraft to the authors.

3.6 Results from Interference Tests on Long Range Radar 1

3.6.1 Injected Targets with Single Channel Operation

A plot of the target P_d versus the *I/N* ratio for the radar operating in single channel mode with injected targets and BPSK interference is shown in Figure 19. The figure shows that as the *I/N* ratio increases, the target P_d decreases. At an *I/N* level of -9 dB the P_d curves are beginning to drop perceptibly. At -6 dB *I/N* the target P_d has dropped substantially below the baseline value of 0.9. Detection probability of simulated radar targets (of the minimal acceptable cross section) for single channel operation was degraded by about 0.15 (from 0.90 to 0.75) at the *I/N* level of -6 dB.

3.6.2 Injected Targets with Dual Channel Operation

A plot of the target P_d versus the *I/N* ratio for the radar operating in dual channel mode with injected targets and BPSK interference on both channels is shown in Figure 20. The figure shows that as the *I/N* ratio increases, the target P_d drops. Figure 20 shows that though the baseline target P_d per channel was set to the 90 percent value, the overall baseline target P_d is reinforced (improved) with dual channel operation. But dual channel operation only makes the radar

perform better to a point; at *I/N* levels of -6 dB, the target P_d has dropped below the baseline value. Detection of simulated radar targets (of the minimal acceptable cross section) for dual channel operation was degraded by about 0.10 (from 0.9 to 0.80) from the improved dual-channel baseline at *I/N* = -6 dB.

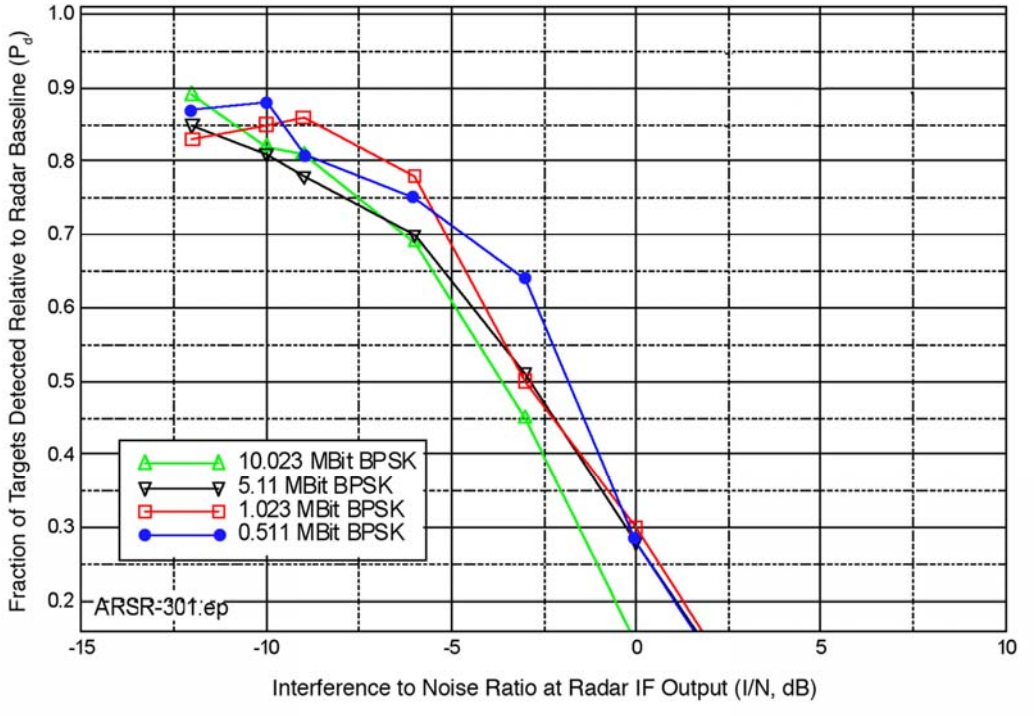

Figure 19. Long Range Radar 1 single channel operation P_d with BPSK interference.

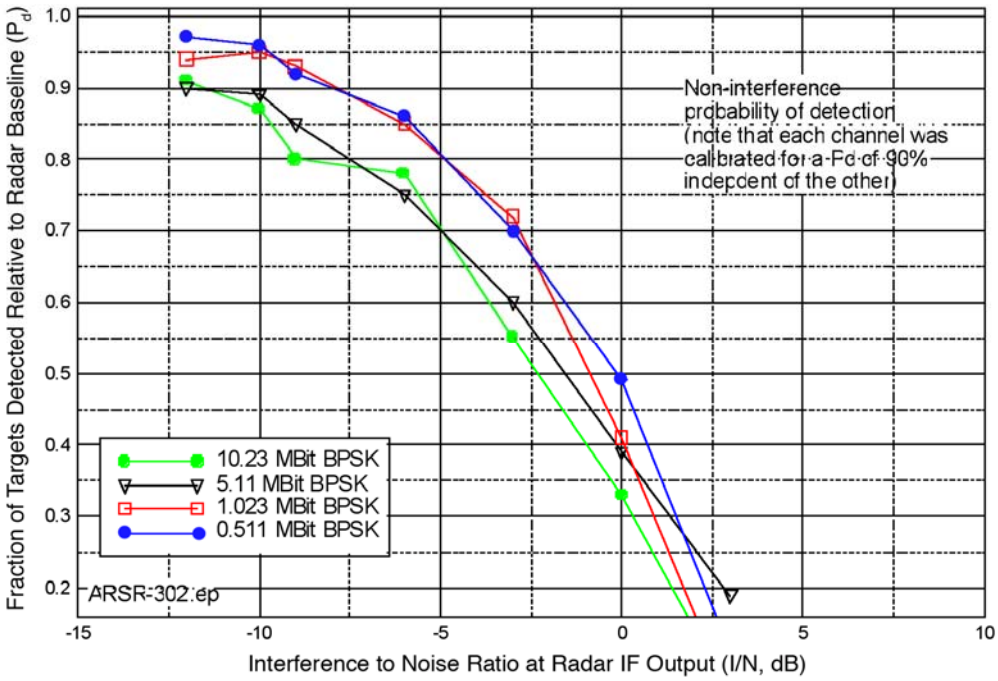

Figure 20. Long Range Radar 1 dual channel operation P_d with BPSK interference.

3.6.3 Results of Live Sky Tests

The 10 MBit/s BPSK waveform was injected into the radar's RF circuitry between the antenna and the receiver (as shown in Figure 10, but with the waveguide connected to the antenna). The *I/N* ratio was set to +20 dB for a 40 degree wide azimuth wedge between 160-200 degrees. Figure 21 shows a recording of the aircraft traffic for a full 360 degree view of the PPI display for 45 antenna rotations (scans). Figure 21 represents a 9-minute recording of both skin tracks and beacon tracks from aircraft within the vicinity of the radar. Interference was present during scans 16-30. The figure shows aircraft that were tracked with the radar and beacon. Tracks that are dark represent targets that have both radar track and beacon data. Track segments that are light represent targets with only beacon data.

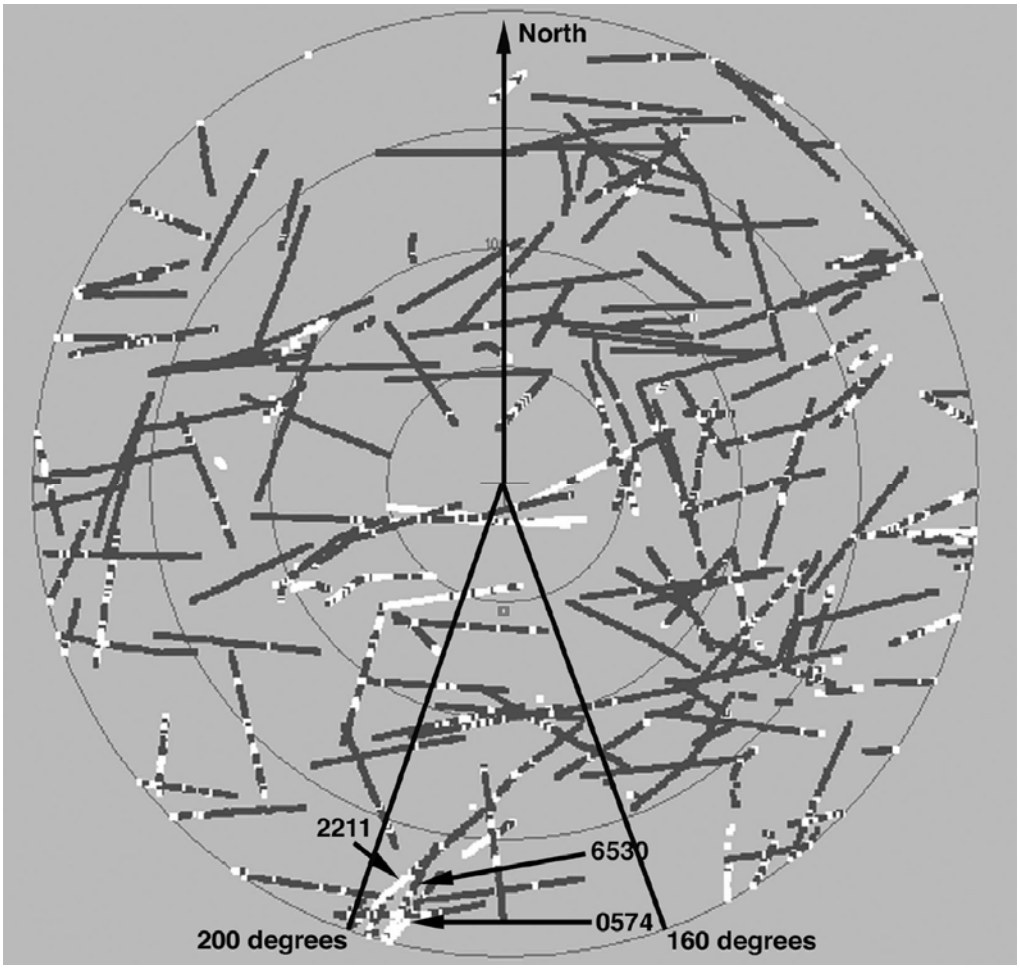

Figure 21. Cumulative PPI display of Long Range Radar 1 for 45 scans during interference in the indicated sector.

Figure 21 shows one aircraft (identified by flight number via the beacon data) within the 160-200 degree wedge of interest that had radar and beacon data for the initial 15 scans (no interference), then only beacon data for the next 15 scans (10 MBit/s BPSK interference), and finally radar and beacon data for the final 15 scans (no interference). The maximum range on the PPI display is 200 nmi. The figure shows that the simulated BPSK interference caused the radar to lose track of this target. The radar also dropped other targets, but the aircraft flew outside of the ATC area before the aircraft type could be identified. Figure 21 also shows that other parts of the PPI output (without known interference) display some aircraft that have intermittent radar data along with their beacon tracks. These are aircraft that may not be fully in the radar's antenna beamwidth due to their altitude and range.

Figure 22 shows the details for the three aircraft of interest. Flight 2211 was an MD-80 observed before, during, and after the interference was injected. The aircraft's initial track is dark, then it goes light, and then it goes dark again. The points where the tracks transitioned from dark represent the circumstance in which interference was turned on. There was a two-scan lag between the moment that interference was switched on or off and the moment at which the resulting effect was observed on the display. Flights 6530 (DC-8 Type 7) and 0574 (TLF-04) entered the interference wedge when the interference was already on. Their tracks begin light (which indicates beacon-only returns being received during interference) and then went dark when the interference was removed (indicating that skin tracking had been restored at that point). The aircraft in question tended to be flying toward or away from the radar station during these episodes. Returns from small aircraft tended to be affected at shorter ranges from the radar than those from larger aircraft, as shown in Figure 22.

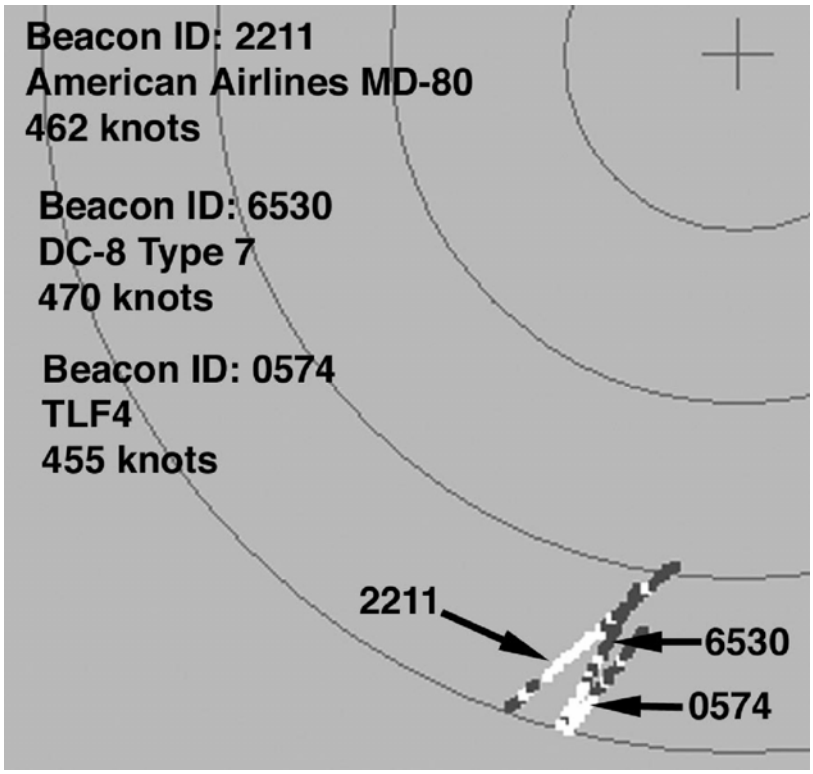

Figure 22. Details of Long Range Radar 1 PPI display during live target interference tests.

3.6.4 Test Results from a Second Installation of Long Range Radar 1

Interference tests with injected, desired targets were performed on a second installation of the Long Range Radar 1 model that was at a second location in the U.S. The test protocols were the same as described above, although due to time constraints fewer interference levels were tested on that radar. The results of those tests are shown in Figure 23. Performance was decreased markedly at *I/N*=-6 dB. The individual channel P_d's had been adjusted to 0.9, and therefore the cumulative, dual-channel P_d values in Figure 23 (which are normalized to the single-channel P_d values) are higher than 0.9.

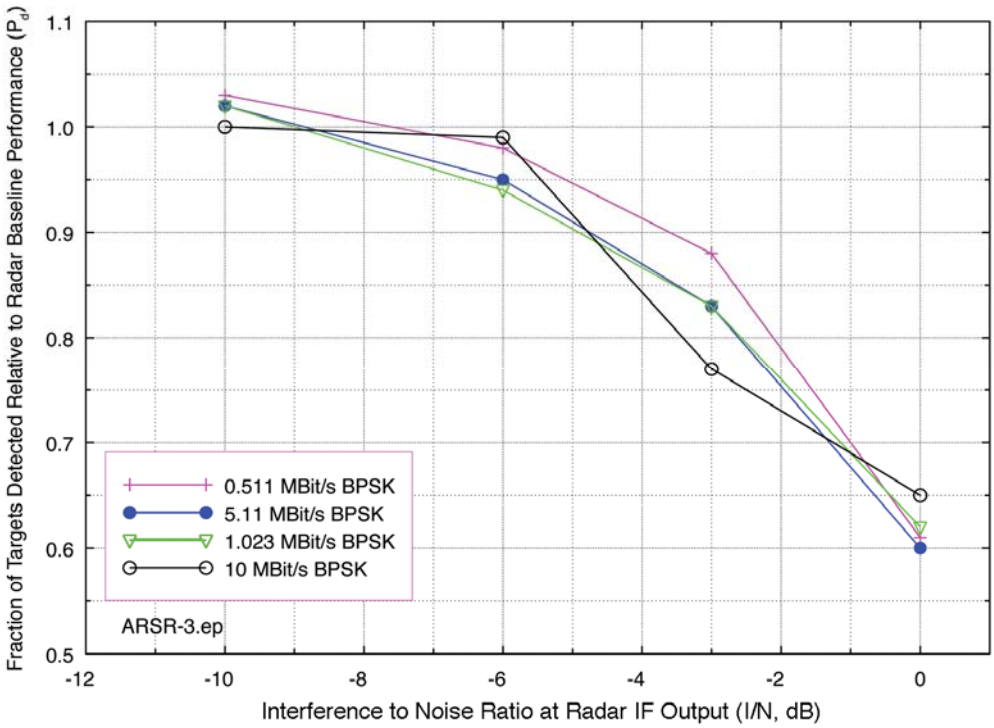

Figure 23. Test results with injected targets at a second installation of the Long Range Radar 1 type.

3.7 Description of Long Range Radar 2

3.7.1 General Description

Long Range Radar 2 is a coherent, non-linear FM-pulsed system that uses a parabolic reflector, a phased-array feed horn, and all solid-state electronics to meet the needs of both defense and air traffic control. It detects targets at up to 250 nmi (400 km) at an altitude of 100,000 feet. The air traffic control requirement for target detection is P_d=0.8 or more in clear air for a target cross section of 2.2 m^2 at a range of 200 nmi. To satisfy the defense requirement, the radar was designed for very high reliability (e.g., designed for 1500 hours of mean time between critical failures that would interrupt service) and high sensitivity (including the capability to detect 0.1 m^2 targets at a distance of 92 nmi against a Sea State 5 clutter-background). The solid-state transmitter power amplifiers are located below the antenna rotary joint to minimize out-of-

service time for maintenance, as the amplifiers can be maintained without halting antenna rotation. The designs of the antenna, the transmitter, and the receiver signal processing hardware and software have all been integrated to optimize the radar's functionality for both defence and air traffic control requirements. A separate beacon interrogator system that is incorporated into the radar design provides additional information on aircraft beacon codes, aircraft-encoded altitudes, and emergency status of aircraft. General characteristics are summarized in Table 5.

The radar is normally operated in a diplexed (two RF channels) mode, denoted as F1 and F2. Unlike Long Range Radar 1, this radar's CFAR is *not* independent between the two channels. Two frequencies are provided for the purpose of compensating for atmospheric fading, distortion, and other effects on any one frequency; effects that degrade one frequency are not expected to affect the other channel. *Two-frequency capability is not provided for the purpose of using one frequency to compensate for interference effects on the other frequency.*

Table 5. Technical Characteristics of Long Range Radar 2

Parameter	Value
Tuning range	1215-1400 MHz
Channelization	44 frequency pairs
Uncompressed pulse widths	88.8 μs and 58.8 μs
Pulse repetition rates	291.5 or 312.5 pps
Pulse modulation	Non-linear FM
3 dB RF bandwidth	58 MHz
3 dB IF bandwidth	690 kHz
Noise figure	3.6 dB
Receiver noise power (in 690 kHz bandwidth)	-112 dBm
Antenna type	Parabolic reflector with phased array feed array
Polarizations available	Vertical, horizontal, RHCP, LHCP
Horizontal scan rate (scan interval)	5 rpm (12 sec/revolution)
Mainbeam gain	41.8 dBi
Beam number one 3-dB beamwidth	Vertical 2.0 degrees, horizontal 1.4 degrees

3.7.2 Receiver Processing

Low-noise amplifiers (LNAs) for the RF front-end are located on the flat, phased-array feed array of the antenna. LNAs are installed for row assemblies in the array. LNA outputs are fed from the phased array to the receiver via the antenna rotary joint.

Two receiver processing channels, designated A and B and corresponding to each of the two operational frequencies F1 and F2, are provided. Each channel has a receiver processor and a modular DTE. A built-in tracker can process 800 aircraft plus 200 non-aircraft reports per scan. The radar uses frequency separation and orthogonal polarization for the two channels so that they can transmit and receive via the same antenna in the diplex mode of operation. Figure C-3 shows the radar IF inherent noise spectrum. The receiver's adaptive threshold algorithm establishes a CFAR level by taking the average signal level over several range bins.

Processed target video data in each radar channel are digitally summed with the adjacent channel target video data before distribution to the DTE. Cross-channel target video summation enhances the probability of target detection since a fluctuating target fade in one channel should not be experienced in the opposite channel due to frequency-polarization diversity between the two channels.

3.7.3 Antenna Characteristics

The antenna is normally located inside a dome and mechanically rotates. The antenna design provides some three-dimensional search capabilities using nine vertically stacked beams that operate up to 30 degrees above the horizon. (The total range of elevation coverage is -7 to +30 degrees.) To obtain accurate data for targets at long range (which will occur at low elevation angles) the low beams are narrower in the vertical dimension than the higher-elevation beams. An interleaving arrangement enables the upper stack of vertical beams to receive nearby target echoes during the inter-pulse intervals of more widely spaced pulses from the lower-elevation beams.

The phased array antenna feed has a flat configuration, is located at the base level of the reflector, and contains approximately 600 radiators that can operate with either linear or circular polarization. Linear polarization is normally used, but circular polarization provides better penetration in rain conditions. As azimuth scans advance, the radar automatically selects the optimum polarization for each of 32 azimuth sectors, depending upon whether each sector contains rain. A significant feature of the radar is side lobes with low gain, which help to reduce clutter and jamming effects.

3.8 Test Approach for Long Range Radar 2

3.8.1 General

The radar's performance was monitored primarily using the built-in target generation and target counting software. Desired signal targets were generated using a built-in, diagnostic RF signal generator. In addition to the desired targets, signal generators were used to inject interference into the radar receive path. The interference was coupled into the radar's RF front end Beam 2 coupler via a fitting that was below the rotary joint. The interference energy and the target energy were both fed through the rotary joint to a built-in coupler on the phased array feed, so that both the desired targets and the interference entered the radar system *ahead* of one of the antenna assembly RF front-end LNAs. Radar P_d performance was evaluated as a function of the calibrated *I/N* level at the IF output of the radar receiver.

3.8.2 Injected Targets

Because the built-in target generator was used to create desired targets for Long Range Radar 2, the test team performed extensive observations of the desired targets to thoroughly understand them and demonstrate their adequacy for the tests. The radar target generator produced simulated

echo pulses that matched the time characteristics of the radar's stagger[22] pattern and, to some extent, the antenna radiation pattern. Figure 24 shows a time-domain scan in the radar receiver IF stage of the pulses comprising a target. The varying amplitudes of successive pulses are a replication of the radar antenna beam shape, and the pulse intervals have the stagger sequence of the radar.

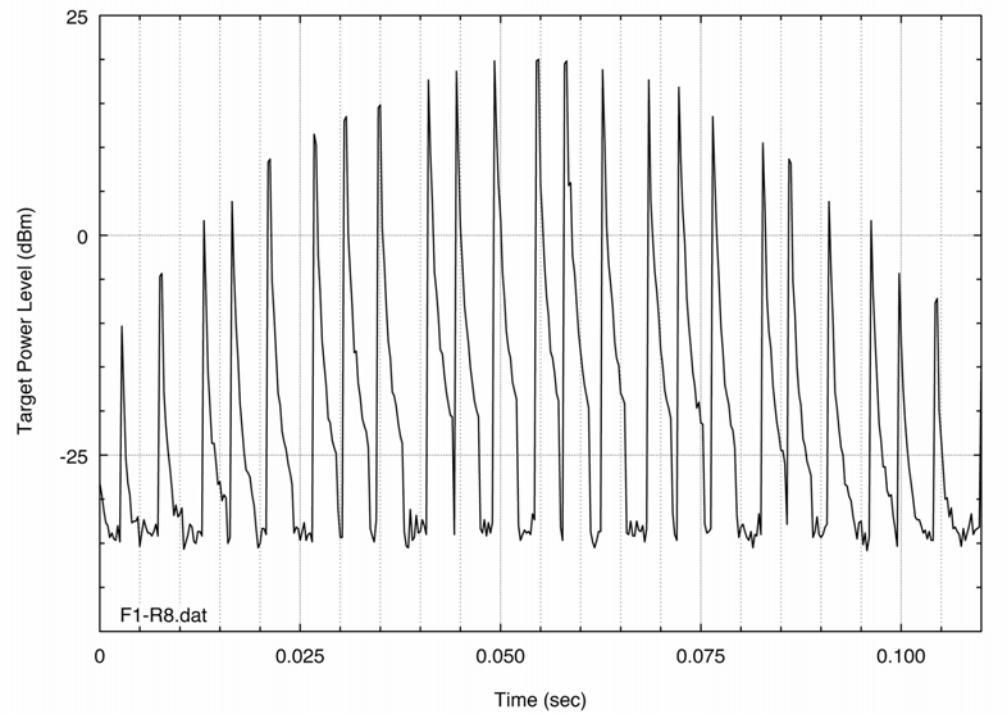

Figure 24. Sequence of desired-target pulses in the IF stage of Long Range Radar 2.

In order to speed testing, a total of 202 injected test targets (distributed in sector wedges on the PPI display) were monitored for 17 consecutive antenna rotations for a total of 3434 injected, desired targets examined for each data point. Each target, regardless of displayed range, was set to the same power at the receiver input, making each target equivalent in terms of receiver P_d. The target power was adjusted to a level that provided an average target P_d in the absence of interference of about 90 percent.

The target P_d, based upon 3434 attempted target scans, was based on automated counting by radar validation software. Whenever the radar integrated enough target pulses to validate a target, it was counted. As was the case for Long Range Radar 1, the actual P_d *per pulse* in the group of pulses that defined each target would have been lower than 90 percent.

[22] Stagger is a non-constant pulse repetition interval. It eliminates Doppler-processing 'blind-speeds' that occur at the pulse repetition frequency of fixed-pulse interval radars.

3.9 Undesired Signals in Long Range Radar 2

3.9.1 General

RF signal generators and AWGs were used to simulate the following interference signals in Long Range Radar 2:

1) BPSK at 0.511 MBit/s,
2) BPSK at 1.023 MBit/s,
3) BPSK at 5.11 MBit/s,
4) BPSK at 10.23 MBit/s,
5) Carrier wave (CW),
6) QPSK at 2 MBit/sec,
7) Ultrawideband (UWB) pulses at 10 MHz prf (dithered pulse sequence),
8) UWB pulses at 10 MHz prf (undithered pulse sequence),
9) BPSK 10 MHz, radiated from a remotely located transmitter.

Spectra of the injected signals are very similar to those shown in Appendix B; with the exception of the CW interference, the interference spectra are lobed $(\text{sinc})^2$ forms. BPSK and QPSK signals contain data bits that are encoded into symbols that a spreading pseudorandom code further breaks into chips. However, the radar receiver does not discriminate between phase changes representing either a chip or a bit for these types of interfering waveforms. The radar receiver will process the BPSK, QPSK, and UWB signals as band-limited constant amplitude noise sources, which fall into all of the range cells. Since the noise-like BPSK and QPSK signals fall into all of the range bins, the CFAR processing cannot eliminate them and the CFAR raises the target detection threshold.

UWB signals consisted of pulsed emissions of 10^7 pulses per second at a pulse width of 0.511 ns. The BPSK signal was radiated from the van through an external antenna mounted on a mast towards the radar.

The emission spectra for the interference signals were measured and recorded, and tuned to the frequency of the radar channel(s) under test. (The tuned frequencies for Long Range Radar 2 were 1228 MHz and 1311 MHz.) The loss between the interference signal injection point and the LNA input on the radar feed array was about 74 dB (depending upon the exact path that was used), so that a signal level of about -38 dBm from the interference generator produced about 0 dB *I/N* in the radar receiver. The interference signal simulator had the capability to generate *I/N* ratios of up to +30 dB at the receiver RF input, but testing was usually accomplished only over the subset of that range where meaningful P_d data could be collected. For each signal type, calibrations were performed to allow for conversion between signal generator settings and the resultant *I/N* level using the process described in Appendix C.

3.9.2 Duration of Interference Signals with Injected Targets

Because the injected targets were produced in sector wedges, the interference signals were kept on continuously for about three minutes at a time, which was the duration of each interference

test run at each level for each modulation. To prevent the radar AGC from responding, its value was frozen (at about 80 (arbitrary units)) during the runs. Test results were not affected by the STC state.

Some radiated interference tests were performed with 10 MBit/sec BPSK signals. In these tests, the duration of the interference was only as long as the interval for the radar beam to sweep across the location of a remotely located vehicle that was the interference source, on the order of 0.4 sec per radar scan (Eq. 16). Because the interference was intermittent, AGC was allowed to float for those tests.

3.10 Test Procedures on Long Range Radar 2

3.10.1 Hardline Coupled Interference Testing

The desired signal targets were overlaid with any one of the interference signals at a given *I/N* and observed for 17 complete scans. This resulted in a total of 3434 possible targets (17 scans x 202 targets/scan), and probability of detection was calculated as the number of observed targets divided by 3434. (During UWB interference testing the nominal number of 3434 targets was increased to 4579.)

The interference test runs normally began with a given modulation at a low level (an initial *I/N* level of -18 dB or -12 dB). The level was then gradually increased through each run, with 3434 (or 4579 for UWB interference) targets tested at each intermediate *I/N* level in increments of about 3 dB, up to *I/N* values that sometimes reached +21 dB, but that usually stopped at *I/N*=+5 or +15 dB. The same interference modulation was always maintained throughout an entire amplitude run. Interference runs were normally performed with:

- interference and targets on one channel and the other channel disabled;
- interference and targets on both channels;
- baseline “no interference” measurements were performed before and after each “interference” data set.

As noted above, AGC was frozen at a fixed level during these runs to prevent adverse effects due to the continuous presence of the interference. This expedient would replicate the behavior of a radar if interference were momentarily encountered in its beam pattern (for about 0.04 sec, as shown in Eq. 16), because in that circumstance the radar would be exposed to interference for such a short period that the AGC would not respond.

The condition of STC (on versus off) was tested to determine whether it would affect the test results. It did not matter, as it turned out, whether STC was activated or not. This was presumably because the targets were displayed at distances that exceeded the STC turn-on interval (which confines the effect to areas that are very close to the radar site).

3.11 Results of Tests on Long Range Radar 2

3.11.1 Single-Channel Interference Test Results

A plot of the target P_d versus the *I/N* ratio for Long Range Radar 2 operating in single channel mode with injected targets and interference is shown in Figure 25, with a smoothed-curve fit between the data points. The figure shows that as the *I/N* ratio increases, the target P_d decreases. At -6 dB *I/N* the target P_d has dropped several percentage points below the baseline value of 0.95.

3.11.2 Dual-Channel Interference Test Results

A plot of the target P_d versus the *I/N* ratio for the radar operating in dual channel mode with injected targets and interference on both channels is shown in Figure 26. The figure shows that as the *I/N* ratio increases, the target P_d drops. The figure shows that although the baseline target P_d per channel was set to 0.95, the overall baseline target P_d is reinforced (improved) with dual channel operation to about 0.98. But dual channel operation only helps the radar perform better to a point; at an *I/N* level of -6 dB, the target P_d has dropped several percent.

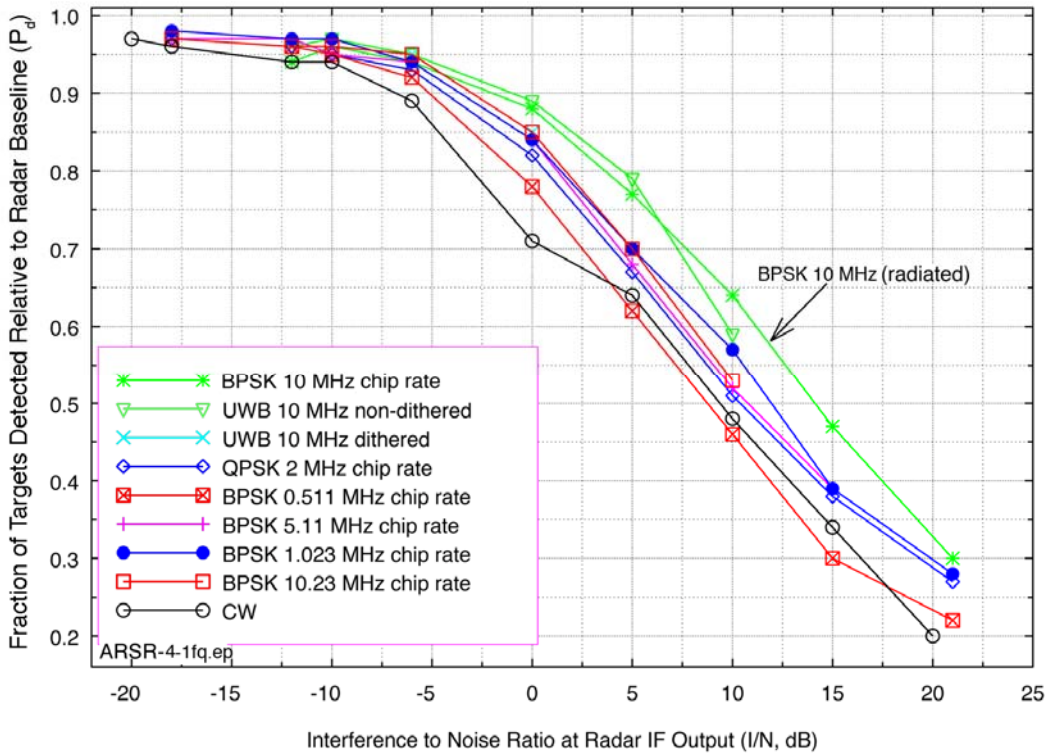

Figure 25. Long Range Radar 2 single channel operation variation in P_d with interference.

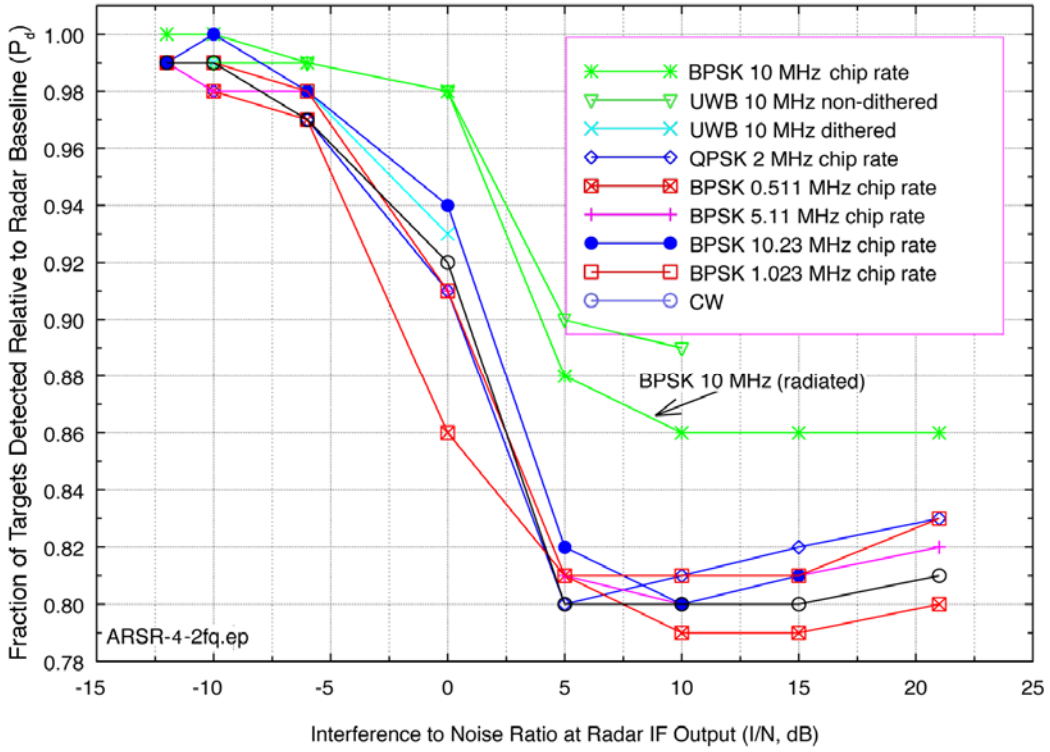

Figure 26. Long Range Radar 2 dual channel operation variation in P_d with interference.

3.12 Summary of Interference Effects on Long Range Radars

From the data obtained, the following general conclusions can be drawn regarding the performance of Long Range Radars in the presence of low-level interference signals:

- The P_d of simulated radar targets (of the minimal acceptable cross section) for single channel operation showed degradation at interference levels as low as *I/N*= -9 dB.

- The P_d of simulated radar targets (of the minimal acceptable cross section) for single channel operation was always measurably degraded, by as much as 0.15 (with P_d dropping to 0.75 from a nominal 0.90), at *I/N*= -6 dB.

- The P_d of simulated radar targets (of the minimal acceptable cross section) for dual channel operation with interference on both channels was degraded by as much as 0.10 (from 0.90 to 0.80) at *I/N*= -6 dB.

- The beginning of degradation appears to be independent of the interference modulation type. This may be because all modulations that were tested were wider than the radar IF bandwidths. However, this is a realistic condition, in that it is expected that the bandwidth of most interference signals will exceed the bandwidths of most radar receivers.

- Radar dual frequency operation with interference on both channels did not significantly improve performance in the presence of low-level interference, but did seem to keep the P_d value at 0.8 at *I/N* levels of +5 dB and above.

- Live sky tests showed that with an *I/N* of +20 dB and a 10 MBit/s BPSK interfering signal, the radar lost track of some targets near the edge of its coverage range.

- While the effects of strong interference in radar receivers can be very dramatic, as shown in Figure 27, *the damaging effects of low-level interference in radar receivers are insidious because there is no overt indication that interference is occurring*, as shown in Figure 28. For low levels of interference (typically less than *I/N*=+3 dB), target losses were not accompanied by any other indications that interference was occurring. Were such losses to occur during normal radar operations, the operators would probably not be aware that targets that should otherwise have been detected were missing, nor that any interference was occurring. It is suggested that one reason that low-level interference effects are rarely reported by radar operators is the subtle, insidious nature of such interference in radar receivers.

- Loss of desired targets in the presence of interference is purely a function of the target echo level relative to the radar receiver noise limit; target range from the radar is not a factor, as illustrated, for example, in Figure 28. It is true that, all other factors being equal, targets at long ranges will return weaker echoes than closer targets. But all other factors are *never* equal; target cross sections vary. Therefore, *any target at any distance from a radar can be lost due to interference when its return echoes are weak*. This means that *low-level interference will not just result in loss of targets at the edge of radar coverage*. Weak targets that are close to radar sites will be lost as well. Weak targets, at any range, are just as critical in national defense and safety considerations as larger cross section targets at the edge of radar coverage; small cross section targets at short ranges may be *more* critical in some situations.

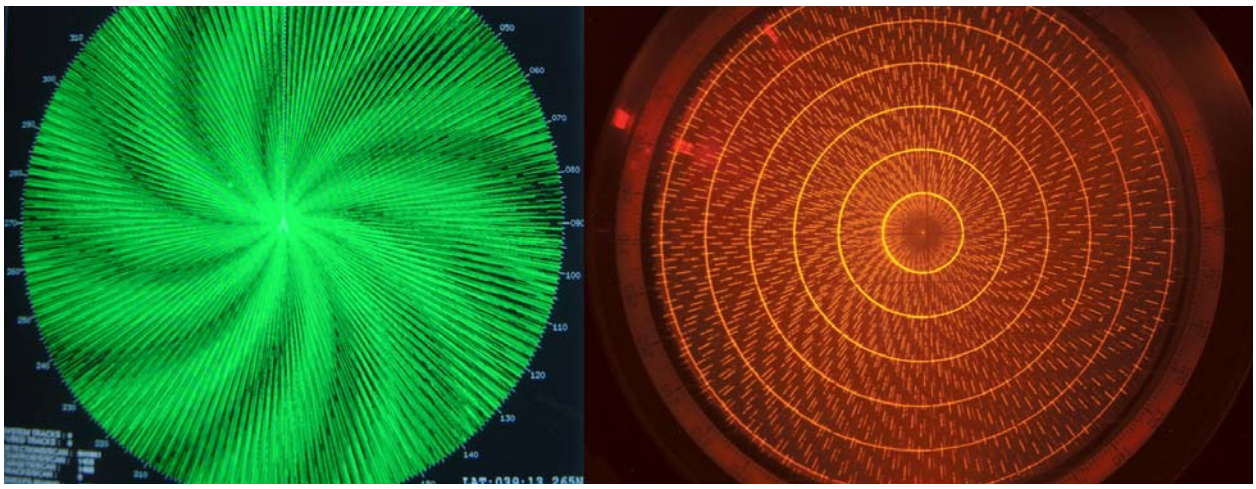

Figure 27. The effects of strong interference in two radar receivers, such as these examples where *I/N* is on the order of +20 dB, will normally be obvious to operators. (When such effects occur on single azimuths they are visible as bright lines called strobes.)

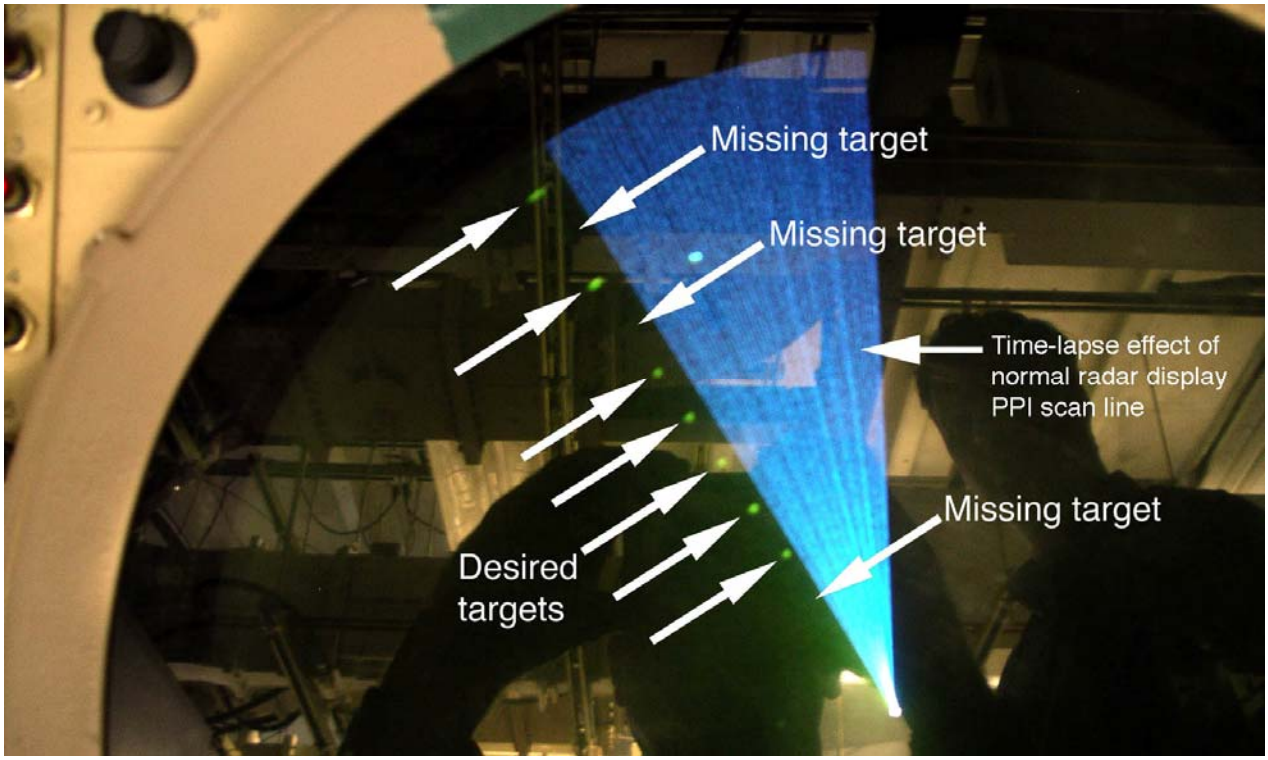

Figure 28. In contrast to the effects of strong interference in Figure 27, target losses due to low-level interference effects (occurring here at an *I/N* level of about -3 dB in Long Range Radar 1) are insidious; *there is no indication on the PPI display that interference is occurring*. The insidiousness of the phenomenon of low-level interference in radar receivers is of considerable concern because of its implications for adverse impacts on radar missions without even the possibility of warning indications for operators.

4 INTERFERENCE MEASUREMENTS ON A SHORT-RANGE AIR SEARCH RADAR

4.1 Introduction

Interference measurements and tests were performed to determine the effects of emissions from digital communication signals on a short-range air search (radionavigation) radar operating within the primary allocation for airport surveillance radars (ASRs) in the 2700-2900 MHz band. Such radars are operated at shorter ranges than the radars examined in the previous section, typically on the order of 100 nmi.

The radar that was tested employs pulse widths, prfs, IF bandwidth, noise figure, and antenna beamwidths typical of those identified in an ITU-R Recommendation for radars in this band [20]. Those radars typically employ interference mitigation techniques/processing methods identified in another ITU-R Recommendation [18] to allow them to operate in the presence of other radionavigation and radiolocation radars. As noted in Section 1, those techniques are effective in reducing pulsed interference between radars but not high duty cycle interference from communication signals.

The tests described here investigated the effectiveness of the radar's interference suppression circuitry and software to reduce or eliminate interference due to the emissions from communication signals employing a digital modulation scheme.

4.1.1 Objectives

The objectives of the testing were to:

- quantify the capability of a short-range air search (radionavigation) radar's interference-rejection processing to mitigate unwanted emissions from digital communication systems as a function of their power level;

- develop *I/N* protection criteria for unwanted digital communication systems emissions received by such a radar;

- observe and quantify the effectiveness of the short-range air search radar's interference rejection techniques to reduce the number of false targets, bright radial lines on the PPI display (strobes), and background noise.

4.2 Short Range Air Search Radar Technical Characteristics

4.2.1 General Characteristics

The short-range air search radar that was tested is used for monitoring air traffic near airports, and is also referred to as a terminal radar. Nominal values for the principal parameters of this radar are presented in Table 6.

Table 6. Technical Characteristics of the Short-Range Air Surveillance Radar

Parameter	Value
Frequency	2700-2900 MHz
Maximum range	60 nmi
Pulse width	1.08 μs
Pulse repetition frequency	928 and 1193 Hz; 1027 and 1321 Hz
IF bandwidth	653 kHz
Spurious response rejection	60 dB
System noise figure	4 dB
RF bandwidth	10 MHz
Antenna scan rate (scan time)	12.5 rpm (4.8 sec/revolution)
Antenna horizontal beamwidth	1.4 degrees
Antenna vertical beamwidth	4.8 degrees
Polarization	Right-hand circular or linear

The radar divides its 60-nmi operational range into 1/16-nmi intervals and azimuths, and each of those by 256 intervals of approximately 1.4 degrees each, for a total of 245,760 range-azimuth cells. In each 1.4-degree azimuth interval the transmitter sends ten pulses at a single prf and then sends eight pulses at a lower prf. The receiver processes each set of 18 pulses to form 18 Doppler filters. Alternating prfs within every 1.4-degree wedge helps to eliminate blind speeds, unmasks moving targets hidden by weather, eliminates second-time-around clutter returns, and divides the radar output into approximately 4,483,584 range-azimuth-Doppler cells.

4.2.2 Antenna Characteristics

The radar employs a parabolic reflector with two horns, for high and low beams, in the antenna feed array. Target echo pulses received by the high and low beam horns in the antenna array are amplified by RF front-end low noise amplifiers and are sent via toggle-switched paths to their respective receivers. The high-beam horn receives returns from high elevation-angle targets close to the antenna, while the low-beam horn receives returns from low elevation-angle targets at greater distances. The high beam receiver reduces clutter strength at short ranges in order to improve sub-clutter visibility.

For these tests, the low beam receiver was selected because the radar would be most likely to receive interference from local ground-based emitters through this path. The low beam is used for observation of targets at ranges exceeding about 15-20 nmi. The beams are not used simultaneously; the radar receiver toggles sequentially between them. The coverage patterns for the high and low beams for a 1 m^2 target cross section with P_d=0.80 are shown in Figure 29.

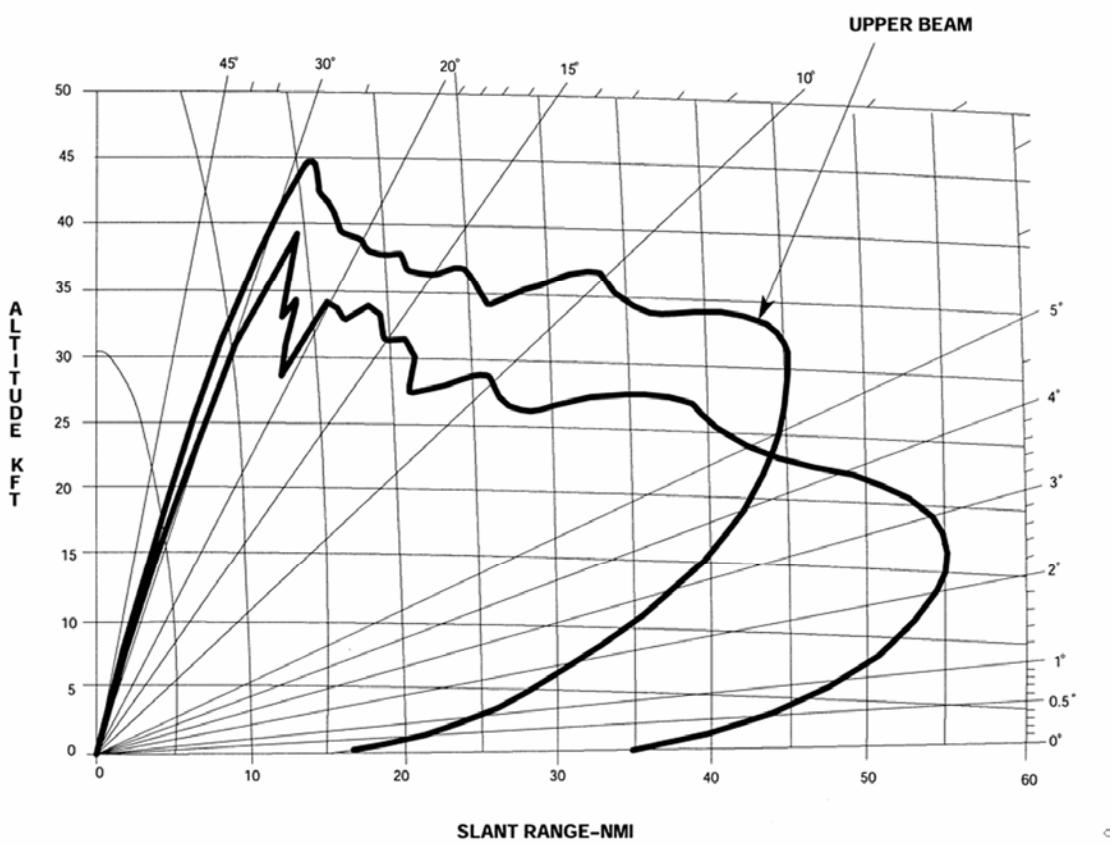

Figure 29. Beam coverage patterns for the short-range air surveillance radar.

4.2.3 Target Receiver

The target receiver/processor employs STC and Moving Target Detection (MTD), which includes Doppler filtering and CFAR processing, to detect and separate target returns from noise, ground clutter, and weather. The target receiver/processor sorts the target returns according to range, detects their Doppler shifts, and sends them to the radar system post processor.

4.2.4 STC

The radar uses STC in its receiver to provide attenuation immediately after the start of the transmitted pulse to decrease its sensitivity at close range, as described in Section 1 of this report. The radar STC curve is shown in Figure 5. The STC was disabled during the tests, but the target amplitudes were set at values that would not have been affected by STC even if it had been active.

4.2.5 IF Circuitry

The IF receiver amplifies the outputs of the RF receiver and detects their phase shifts. The IF circuitry consists of a three-stage logarithmic video detector/amplifier with a wide dynamic range

and I and Q phase detectors. The output of the IF amplifier receiver is at 31.07 MHz. A CW signal swept at RF frequencies was applied as an input stimulus to the radar receiver to obtain the receiver's 3-dB bandwidth, which was measured to be about 680 kHz at the input to the phase detectors. The receiver's response to the swept CW signal is shown in Figure C-4. The dynamic range of the radar receiver was measured by varying the power level of a fixed frequency CW signal and monitoring the output of the IF circuitry at the same test point. Figure 30 shows the gain characteristics of the radar receiver. Measurable compression occurs with an input signal power level of about -43 dBm.

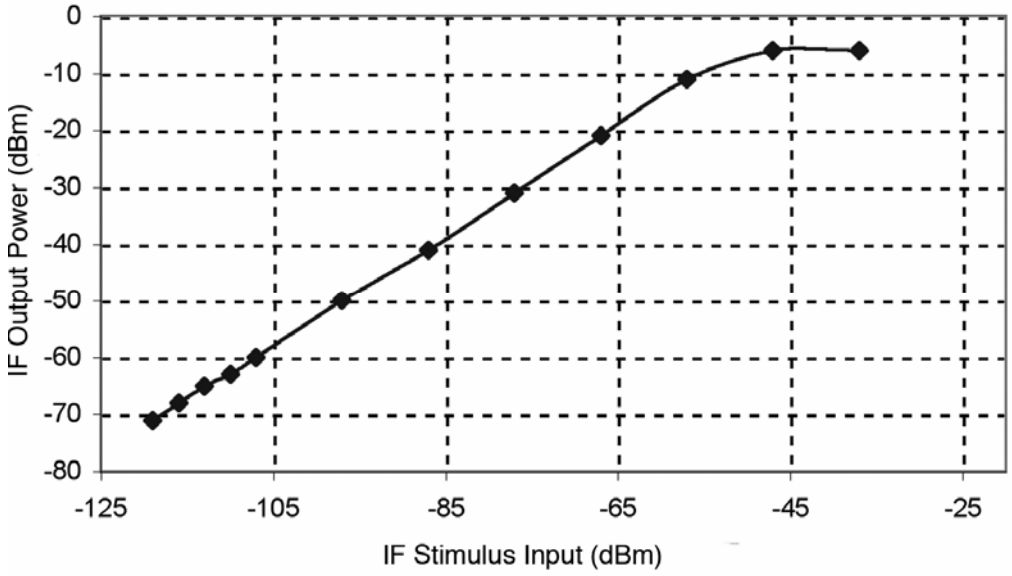

Figure 30. Short-range air surveillance radar input/output gain curve.

The phase detectors at the output of the IF amplifier determine the change in phase between the returns and the transmit pulses that produced them, using the coherent oscillator (COHO) from the frequency generator as a transmit-pulse phase reference. The phase detectors each have sinusoidal responses, and produce in-phase (I) and quadrature (Q) outputs with a sine-cosine (90 degree) phase relationship to each other. Because the I and Q phase detector responses are sine and cosine functions, their outputs can be vector-summed to determine the actual magnitude of the target returns. Software-implemented servo loops set the DC offsets, gain balance, and phase balance of the I and Q outputs based on the state of the phase detectors. They also set the AGC level of the RF and IF amplifiers to limit the noise level within one quantum (the change in RF level represented by the least significant bit (LSB) output of the analog-to-digital (A/D) converter) of the radar internal noise level.

The I and Q outputs of the IF circuitry are sampled and digitized by A/D converters during each 0.77 μs (equal to 0.75 percent of the transmitted pulse width), covering a 1/16-nmi range cell, at a clock rate of 2.6-MHz. The results are then interleaved. The A/D converter produces 12-bit digital words that represent the samples of the I and Q signals to the filter and magnitude processor.

4.2.6 Doppler Filtering

In each 1/16-nmi range cell, coherent processing intervals (CPIs), consisting of returns from alternately 10 and 8 successive pulse repetition intervals, are formed. In the 10-pulse case, the batches associated with each successive 1/16-nmi range increment are sequentially applied to the same set of 10 Doppler filters. The radar random access memory (RAM) stores digital representations of the returns over several pulse-repetition trains (PRTs) and the Doppler filters process them together so that pulse-to-pulse changes in target-return amplitudes (representing apparent Doppler frequencies) can be calculated. For the 10-pulse CPI, five of the filters are used to detect targets moving towards the radar antenna and the other five are used to detect receding targets. A similar process is used for the 8-pulse CPI, except that eight filters are used. The Doppler filters improve the receiver's signal-to-noise ratio because the Doppler filters add or integrate a series of target returns at their frequency. This causes return signals to progressively accumulate at the output of the filter, while random-frequency noise accumulates at the filter outputs at a much slower rate.

4.2.7 CFAR Processing

The radar uses a 27-cell sliding-window averaging (or range averaging) CFAR technique to calculate the mean level threshold (MLT). (CFAR processing automatically varies a detection threshold to maintain false target declarations, based on the return signal plus noise outputs of the Doppler filters at a constant rate, as described in Section 1 of this report.) Each Doppler filter sums the energy contained in the stream of returns received as the antenna sweeps over a target. The energy combines with the noise energy that accumulates in the filter during the same time interval. If the integrated signal plus noise at the output of a filter exceeds the MLT, the detector concludes that a target is present.

Thresholds for the non-zero velocity resolution cells are established by summing the detected outputs of the signals in the same velocity filter in a 27-cell window centered about the cell of interest. Thus, each filter output is averaged to establish the mean level of non-zero velocity clutter. Filter thresholds are determined by multiplying the mean levels by an appropriate constant to obtain the desired false-alarm probability.

Random noise will occasionally exceed the MLT and the detector will falsely indicate that a target is present. The higher the detection threshold to the mean level of the noise energy the lower the probability of a false alarm will be, and vice versa. If the detection threshold is too high, valid targets may go undetected. The outputs of the Doppler filters are continuously monitored to maintain an optimum threshold setting. The CFAR sets the detection thresholds to maintain the false alarm rate for each Doppler filter at an optimum value. A QPSK-type waveform covering the band of the radar receiver will appear simultaneously in all the Doppler filters as noise and cause the CFAR to raise the detection threshold, causing all targets to have a correspondingly lower probability of detection.

4.3 Interference Procedures and Methods for the Short Range Air Search Radar

4.3.1 Interference Signals

Three types of interference signals were injected into the radar as unwanted emissions through a 20 dB coupler port in the receiver's waveguide path, as shown in Figure 31. The signals were an un-modulated continuous wave (CW), a continuous 2-MBit/s QPSK waveform, and a 2-MBit/s QPSK waveform with a 1/8 time slot duty factor. All three signals were co-channel with the radar's operating frequency and occurred within the full 360 degrees of the antenna's rotation. The continuous and pulsed QPSK waveforms represent the type of signals that would be expected to be used by digital communication systems such as IMT-2000 in CDMA and TDMA

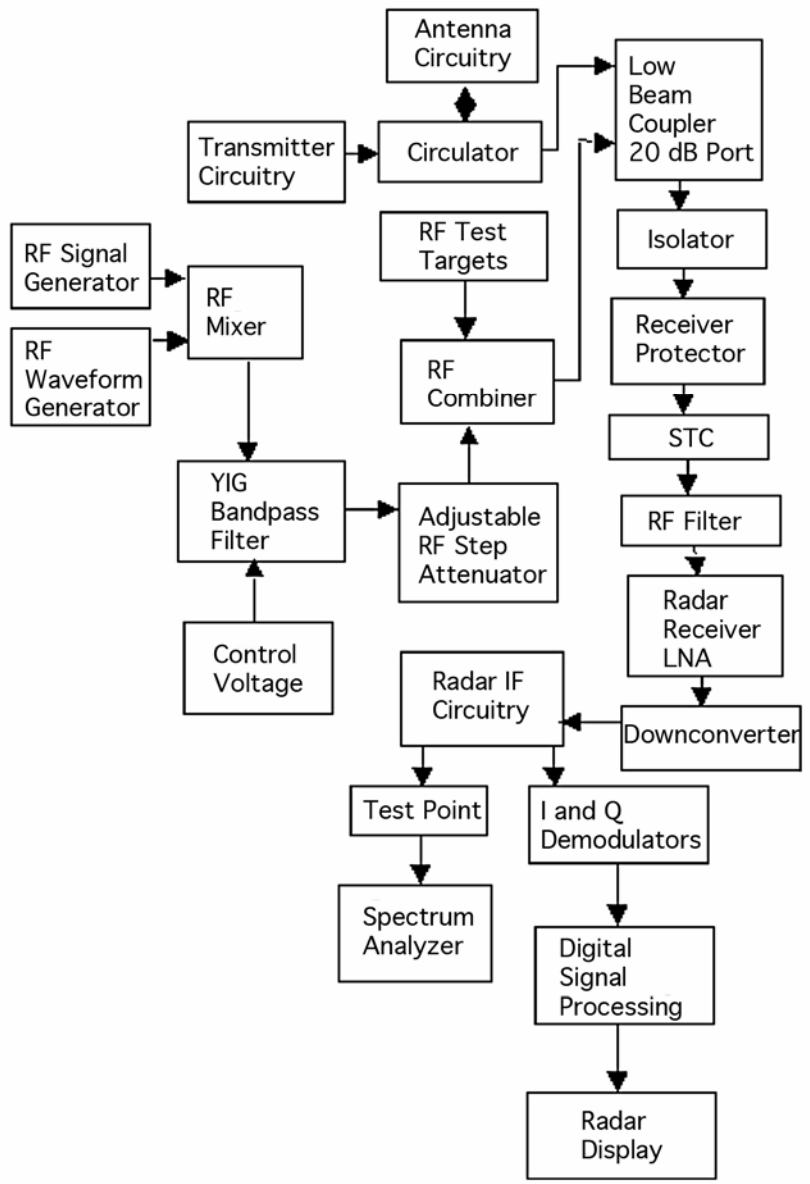

Figure 31. Test set-up for interference injection into short-range air search radar.

systems, respectively. The measured emission spectrum of the continuous QPSK signal is shown in Figure B-5. The QPSK signal was generated and injected into the short-range air search radar using the test set-up shown in Figure 31.

The CW signal was simulated using an RF signal generator. For the CDMA type QPSK waveform, an AWG was programmed to output a QPSK waveform at a data rate of 2 MBit/s. The program simulated a uniform distribution of random bits containing no repetitions with a code length long enough to ensure that no spectral lines occurred within the bandwidth of the radar receiver. For the TDMA (time-sliced) type QPSK waveform, another AWG was used to pulse the QPSK waveform for a 1/8 time slot duty factor. The on-time of the pulses was 577 μs and the repetition period was 4.6 ms.

The output of the AWG was fed to a mixer whose other input was connected to an RF signal generator. The RF signal generator functioned as a local oscillator and its frequency was adjusted so that the carrier of the QPSK waveform was co-tuned with the radar receiver. A YIG bandpass filter was used to suppress any spurious emissions that resulted from the mixing process. An RF step attenuator immediately after the YIG filter was used to control the power level of the QPSK emissions.

4.3.2 Target Generation and Counting

Ten simulated, equally-spaced targets were generated along a radial using the radar's built in test target generator (consisting of a combination of hardware and software). The targets on the radial had a constant power envelope. Each target count P_d was made with 20 rotations of the radar; in 20 rotations, 200 targets were generated. The value of P_d was determined by dividing the number of counted targets by 200. For example, if 180 targets were counted the P_d was 0.90. The targets were counted manually, by observing the correlated video output on the radar's PPI display.

4.3.3 Test conditions

The tests were performed with the parameters shown in Table 7 set on the short-range air search radionavigation radar.

Table 7. Control Settings for the Short Range Air Surveillance Radar

Receiver Parameter	Value
Sensitivity time control (STC)	Off
Interference rejection (IR)	On
Automatic gain control (AGC)	On
PPI image selected for target counting	Processed video
Radar range mode	60 nmi

4.3.4 Test Procedures

The RF power output of the target generator system was adjusted so that the target P_d was as close as possible to 0.90 (given that the target levels could only be adjusted in 1-dB increments) without interference being present (for correlated video targets). As noted above, targets were counted in twenty scans to set the baseline P_d. The radar was observed to have a sort of memory of target conditions, as the target P_d was slow to change when the target power level was adjusted using the target control software. Due to the CFAR processing, the radar took 8-10 scans before it would reach a new steady state after the target power was adjusted.

After the radar was set to its baseline condition, the CW and QPSK interference was injected into the radar receiver. The power of the CW and QPSK signals that were injected into the radar receiver was set to different levels while the power level of the targets was held constant.

The power levels of the CW and QPSK signals were set to values that produced *I/N* levels of -12 dB, -10 dB, -9 dB, -6 dB, -3 dB, 0 dB, +3 dB, and +6 dB in the IF circuitry of the radar receiver, as described in Appendix C. To account for the radar's target memory, the targets were not counted until 10 scans had occurred after the interference had been enabled. After 20 scans with the interference enabled and the targets counted, the interference was disabled and an additional 10 scans were allowed to occur before the next *I/N* level was tested. Waiting 10 scans to occur *between* each change in target and interference conditions ensured that each measurement was not affected by the previous one.

As the CW and QPSK power levels were varied, the display of the radar was observed for any increase in the number of false targets, bright radial streaks or lines (strobes), or any increase in background speckling.

4.4 Test Results for the Short Range Air Search Radar

Curves showing the target P_d versus the *I/N* levels were produced for the CW, CDMA-QPSK, and TDMA-QPSK interference are shown in Figure 32. The data in Figure 32 show that all three emissions caused a reduction in the target P_d ranging from 9 to 25 percent for *I/N* levels equal to -6 dB. The TDMA type emission did not cause as much of a reduction in the target P_d at the higher *I/N* levels as the other waveforms. This is believed to be because the radar's CFAR was able to treat it as pulsed interference and reduce its effects to some degree. However, the radar's operation was still adversely impacted. Furthermore, higher time-slot duty factors would increase the effects from the TDMA waveform, until at some point they would equal the effects from the CDMA type signal.

4.5 Summary of Interference Effects on a Short-Range Air Search Radar

The P_d interference curves show that the short range air search radar's target detection capability was adversely impacted at an *I/N* level of -6 dB. This result is consistent with the observations of the behavior of the long range air search radars.

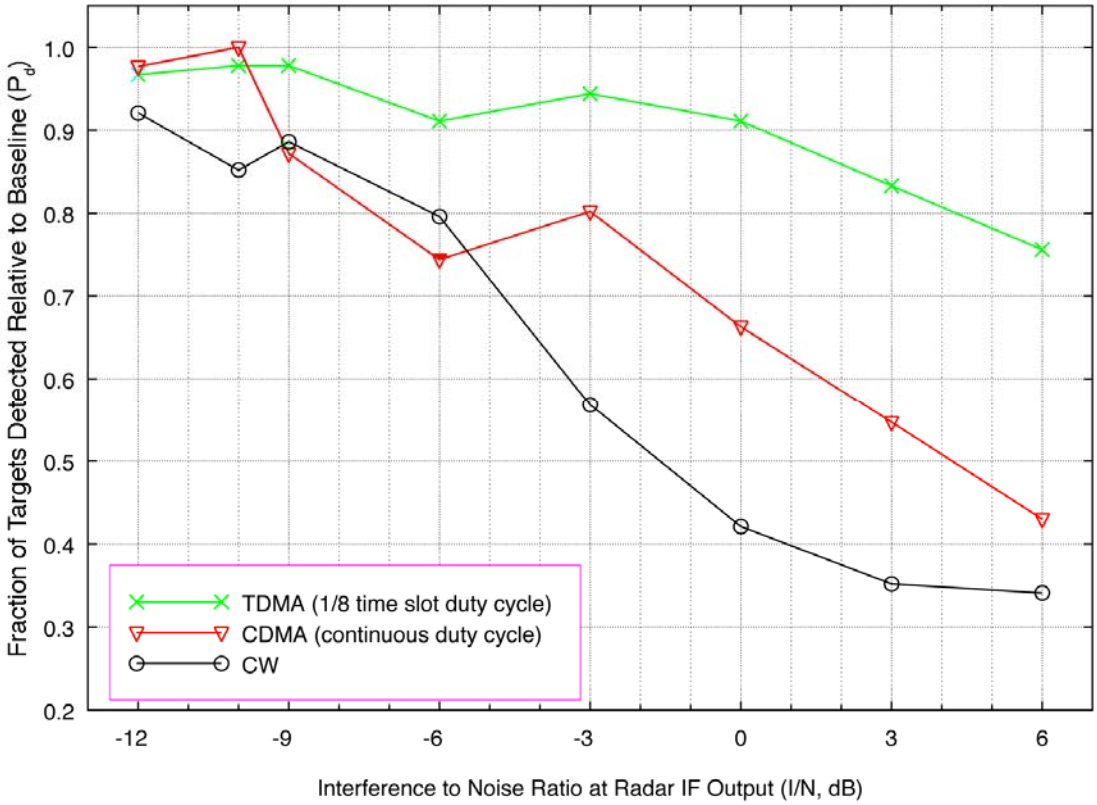

Figure 32. Interference response curves for the short-range air search radar. CDMA-2000 mobile terminal modulation was used for these tests.

5 INTERFERENCE MEASUREMENTS ON A FIXED GROUND-BASED METEOROLOGICAL RADAR

5.1 Introduction

The key objective of the work described in this section was to establish the maximum interference level that a representative meteorological radar, deployed on a worldwide basis, could withstand before its forecasting capability was compromised; the interference being based on typical communication signal modulations. Based upon the radar's technical specifications, mathematical models were developed for its key outputs, or 'products' (called base reflectivity, mean radial velocity, and spectrum width), that indicate what these expected levels should be. In order to physically validate this analysis, a test and data analysis methodology was defined through which data were collected and analyzed.

The data analysis supported the calculated value required for protection of the reflectivity measurements. Limitations in the radar calibration and noise removal process performed by the system's low-level data processor at the time the tests were run tended to limit the measurement accuracy of the necessary protection criteria for the spectrum width measurements. However, correction of the data for the limitations of this processing did result in values that supported the calculated protection values.

Field tests were run on the meteorological radar to determine the appropriate criteria necessary for protection from CW and CDMA signals in the 2700-2900 MHz band. The tests were performed by injecting a CW signal and six different CDMA modulation schemes into the radar receiver while it was scanning the atmosphere. Low-level (called base) meteorological products (base reflectivity, mean radial velocity, and spectrum width) were recorded while conducting a series of radar antenna rotations at a single antenna elevation. Interference signals were injected with *I/N* levels ranging from -15 dB to +6 dB.

5.2 Theoretical Calculation of Necessary Protection Criteria

The radar generated three base products that are used by the signal processing system to derive meteorological products. These base products are:

- Volume reflectivity, Z, in mm^6/m^3, which for rain is a measure of total water in the radar sample volume;
- Mean radial velocity, V, in m/s, which is the power-weighted mean radial motion of the targets in the sample volume;
- Spectrum width, W, in m/s, which is a measure of the radial velocity dispersion of the targets in the sample volume.

5.2.1 Minimum Signal Level

Radar signal processing normally removes the radar system noise effects from the reflectivity and spectrum width products so that the system can provide these products when the signal level

is below the receiver noise level. The signal to noise ratio (SNR) threshold, i.e., the lowest level for which the return signal is processed, is selectable by the radar operator between the limits of -12 dB SNR and +6 dB SNR. With the present version of signal processing, the lower values are generally not used due to limitations with noise removal but the system does provide useful products down to -3 dB SNR. The interference level that compromises the system is related to the minimum signal level of -3 dB SNR and the product characteristics themselves, as described below. Excessive interference will adversely impact data quality, degrade the meteorological products, and compromise the system's ability to accomplish its mission of providing data necessary for public weather forecasting, severe weather warning, and rainfall measurement for flash flood prediction and water management.

5.2.2 Reflectivity

Reflectivity is used in multiple applications; the most important of these is rainfall rate estimation. Reflectivity is calculated from a linear average of return power and is subject to contamination by interference as an unknown increase in the measured reflectivity. Reflectivity is seriously contaminated if the bias exceeds 1 dB. A 1-dB bias is twice the radar calibration accuracy and equal to the standard deviation of the reflectivity estimate specified in the radar technical requirements. Bias in terms of interference to signal ratio is given by [21]:

$$dBbias = 10\log\left(\frac{S+I}{S}\right), \tag{17}$$

and a 1-dB bias occurs at:

$$I/S = 0.26$$

$$10 \log I/S = -6 \text{ dB}.$$

Therefore, reflectivity is biased 1 dB at an interference level 6 dB below the signal. Since the minimum signal level has an SNR of -3 dB and the maximum I/S level for the reflectivity product is -6 dB, the maximum *I/N* is:

$$(-3 \text{ dB}) + (-6 \text{ dB}) = -9 \text{ dB } I/N.$$

5.2.3 Mean Radial Velocity

Mean radial velocity is calculated from the argument of the single lag complex covariance. The complex covariance argument provides an estimate of the Doppler signal vector angular displacement from pulse to pulse. The displacement divided by the time interval between the pulses is the Doppler vector angular velocity.

If it has the characteristics of broadband noise, an interference signal vector has uniform probability over the complex plane and thus does not introduce a systematic rotation nor a bias in

the estimate. However, the randomness of the composite signals plus interference vector due to the interference increases the variance of the Doppler signal estimate.

The Doppler frequency variance, retaining all terms except those inversely proportional to the number of samples squared can be calculated as [21]:

$$\mathrm{var}\left(\hat{f}\right) = \frac{2\pi^{3/2}WT}{8\pi^2 M\beta^2(T)T^2} + \frac{\left(\frac{N}{S}\right)^2 + 2\left(\frac{N}{S}\right)\left[1-\beta(2T)\right]}{8\pi^2 M\beta^2(T)T^2}, \quad (18)$$

where:

$\hat{f}$ = frequency estimate, Hz;
W = standard deviation of frequency spectrum, Hz;
W = 4 m/s for NTR benchmark = 80 Hz at f_c = 2995 MHz;
T = sampling interval, sec;
T = 10^{-3} sec for NTR benchmark;
M = number of samples in estimate;
N = noise power;
S = signal power;
β = signal correlation at lag T;
β = exp [$-2\pi^2 W^2 T^2$] for the assumed Gaussian spectra.

The first term is the variance contribution due to the signal characteristics and the second term is the variance contribution due to the noise.

The frequency variances are severely compromised if the interference increases the variance by more than 50%. The uncertainty in the data degrades all velocity based products and the velocity shear measurements in particular. (Velocity shear is a velocity difference over some distance.) A 50% increase in variance increases the reliably detected shear value approximately 25% above the severe weather event formative stage value.

An expression for the interference to noise ratio resulting in a 50% variance increase of the technical requirements benchmark parameters and SNR = -3 dB is given by [21]:

$$2\pi^{3/2}WT + \left(\frac{I+N}{S}\right)^2 + 2\left(\frac{I+N}{S}\right)\left[1-\beta(2T)\right] = \frac{3}{2}\left(2\pi^{3/2}WT\right) + \frac{3}{2}\left(\frac{N}{S}\right)^2 + \frac{3}{2}(2)\left(\frac{N}{S}\right)\left[1-\beta(2T)\right], \quad (19)$$

where:

W = 80 Hz;
T = 10^{-3} sec;
$2\pi^{3/2}WT$ = 0.89;
$[1 - \beta(2T)]$ = 0.4;
S = 0.5 N.

Substituting and solving for I/N yields the quadratic expression:

$$(I/N)^2 + 2(I/N) - 1.21 = 0$$
$$I/N = 0.49 .$$

Therefore, the interference must not exceed the minimum signal value.

5.2.4 Spectrum Width

The spectrum width is calculated from the single lag correlation assuming a Gaussian spectral density. The algorithm is expressed as [21]:

$$W = \frac{Va}{\pi}\left|\ln\frac{R^2}{S^2}\right|^{1/2}, \tag{20}$$

where:

W = Spectrum width (standard deviation);
Va = Nyquist velocity, 25m/s from the radar technical requirements document;
R = single lag covariance power;
S = signal power.

Interference causes both a bias and a variance increase in spectrum width estimation but the bias is more detrimental. Spectrum width is compromised when the interference-induced bias exceeds the radar technical requirement width accuracy of 1 m/s. The interference to noise ratio at which this bias level occurs can be calculated by solving for the covariance at 4 m/s and signal power of *N/2*, then solving for the *(S+I)* level producing a 5 m/s spectrum width. 4 m/s is the base value given in the radar technical requirements document. To calculate *I/N*, the equation above is solved for the 4 m/s and 5 m/s cases.

For W = 4 m/s:		For W = 5 m/s:	
$25 / \pi \left\| \ln (R^2/S^2) \right\|^{(1/2)} = 4$		$25 / \pi \left\| \ln (R^2 / (S + I)^2) \right\|^{(1/2)} = 5$	
$ln\ (R^2/S^2)$	= -0.25	$ln\ (R^2 / (S + I)^2)$	= -0.39
R/S	= 0.88	$R/(S+I)$	= 0.82
R	= 0.88 S		

$$R = 0.88(N/2)$$

Substitute: $R = 0.88(N/2)$, $S = N/2$:

$$[0.88\ (N/2)] / [(N/2) + I] = 0.82$$
$$0.82\ [(N/2) + I] = 0.88\ (N/2)$$
$$I/N = 0.0366$$
$$10\log(I/N) = -14.4 \text{ dB}.$$

So in this example, an *I/N* ratio of -14.4 dB will cause a spectrum width error of 1 m/s.

5.3 System Operation, Output Products, and Interference Sensitivity

5.3.1 System Operational Mode for Testing

The radar that was used for the tests and measurements has multiple modes of operation that utilize different antenna rotation rates, antenna elevations and prfs. The operational mode selected for the tests was one that is commonly used, and is optimized for system sensitivity, leading to high susceptibility of interference. Table 8 provides the characteristics of the radar mode used in testing.

Table 8. Technical Characteristics of the Meteorological Radar

Parameter	Value
Frequency	2995 MHz
Pulse power (peak)	750 kW
Pulse width	4.7 μs
Pulse repetition frequency	322 Hz (first cut) 446 Hz (second cut)
Maximum coverage range	290 mi.
RF bandwidth (at 3-dB points)	13 MHz
IF bandwidth (at 3-dB points)	630 kHz
System noise figure	4.9 dB
System noise floor (in receiver bandwidth of 630 kHz)	-111 dBm
Main beam antenna gain	[45 dBi]
Antenna pattern type	pencil
Antenna scan interval (scan period)	0.84 rpm (71.4 sec)
Antenna height above ground	30 m
Antenna beamwidth (vertical and horizontal)	0.90 deg
Polarization	linear horizontal

In the mode used, the antenna rotation starts at an elevation of 0.5 deg., the radar transmits a 4.7-μs pulse every 3.1 ms for the first rotation, and then transmits a pulse every 2.24 ms for the second rotation. These correspond to prfs of 322 Hz and 446 Hz, respectively. Each revolution covers 360 deg. in azimuth. In normal operation, the radar also performs antenna rotations at several higher elevation angles before returning to 0.5 deg. For the purposes of this test, the two elevation cuts at the single antenna elevation provided sufficient data for analysis and the cuts at higher elevations were not performed. The first antenna rotation is used to measure reflectivity and the second rotation is used to measure mean radial velocity and spectrum width (see below). For each location in the atmosphere, multiple pulses are transmitted and received. Due to the duration of the transmit pulses compared to the time between pulses, the system is in receive mode more than 99.5% of the time. The magnitude of the received pulses is approximately

200 dB lower than the transmitted pulses because the pulses are scattered by small airborne objects (on the order of millimeters in diameter or smaller) at distances up to hundreds of kilometers from the radar. The received signal is downconverted from 2,995 MHz to the IF frequency of 57 MHz where it is then applied to a synchronous detector. The detected *I-Q* baseband signals are digitized to a 16-bit level for use in the processing subsystems.

5.3.2 Output Products

The returned pulses from each location are used by the processing subsystems to derive the three meteorological base moments of base reflectivity, mean radial velocity, and spectrum width. The base moments are displayed as products to users and are used to develop other meteorological products representing rainfall accumulation, tornadoes, wind shear, etc. Reflectivity is derived from the amplitude (or power) of the received signal. Mean radial velocity is the mean radial speed and is derived from the differences in the I and Q vectors caused by the Doppler shift. Spectrum width is the variance between pulses of the velocities received from the same location.

5.3.3 Interference Sensitivity

Base products are affected by interference in two different ways. First, values can be biased which decreases the accuracy of the system, and second, the variance of the outputs can be affected. In the presence of interference, reflectivity is sensitive to bias, mean radial velocity is sensitive to variance errors, and spectrum width is affected by both bias and variance errors. For spectrum width, the errors due to biasing are more significant than the errors due to variance because the bias, or offset, represents a velocity measurement error while the variance represents the uncertainty of the velocities measured. Table 9 shows which interference-induced errors, bias and variance affect the base products.

Table 9. Sensitivity of Meteorological Products to Interference Induced Error

	Interference Induced Errors	
Meteorological Product	**Bias**	**Variance**
Reflectivity	X	
Velocity		X
Spectrum Width	X	X

To calibrate the test set-up for a known interference level at the radar receiver input, the receiver noise floor was measured, without interference, at the 57.55 MHz IF output of the receiver. When the noise floor was recorded at the IF output, the interference signal was activated and its level was increased until the radar IF output noise floor increased by 3 dB. The point at which the noise increased by 3 dB corresponded to the interference level within the radar passband being equal to the radar receiver noise within the passband, and an *I/N* ratio of 0 dB. The signal source output was recorded for the 0-dB *I/N* ratio and the actual level being injected into the radar

receive path was also measured and recorded. Knowing the signal source setting for the 0 dB *I/N*, the signal source could be set for any other desired *I/N* by adjusting the signal source output level. Testing was conducted at interference level points corresponding to the following *I/N* levels: -15 dB, -12 dB, -10 dB, -6 dB, -3 dB, 0 dB, +3 dB and +6 dB. Figure 12 shows an example result of the receiver noise level measurement with and without the presence of interference for the W-CDMA signal testing; Figures B-6 and B-7 show spectra of CDMA interference signals used for this testing.

The radar was set to scan the atmosphere (hereafter called a "volume scan") at one antenna elevation without interference followed by a volume scan with interference. For each volume scan, with or without interference, the antenna made two complete rotations allowing elevation cuts at the same elevation using two different prfs. The prf used on the first rotation was a low value optimized for collecting the base reflectivity product. The prf used on the second rotation was a high value and was used for collecting the mean radial velocity and spectrum width data. This alternating pattern of volume scans, with and without interference, was continued for interference levels ranging from -15 dB to +6 dB. This test approach provided a volume scan immediately before and after each interference volume scan that could be used as baseline references for determining the statistical effects of the interference. During the entire test, base product radar data was recorded for analysis.

Figure 33 shows the test setup, which consisted of a signal generator feeding an RF coupler where the interference signal is combined with the received radar return signal at input to the receiver. The receiver amplified and downconverted the signal to IF where it was monitored on a spectrum analyzer. The I and Q outputs were digitized and processed to provide the meteorological base products of base reflectivity, mean velocity and spectrum width. The base products were recorded for statistical analysis. Testing with each of the CDMA signal types, at all data rates and modulation schemes, was not feasible due to the large number of available permutations. Representative modulations (CDMA and TDMA, for example) and a representative range of data rates were used instead.

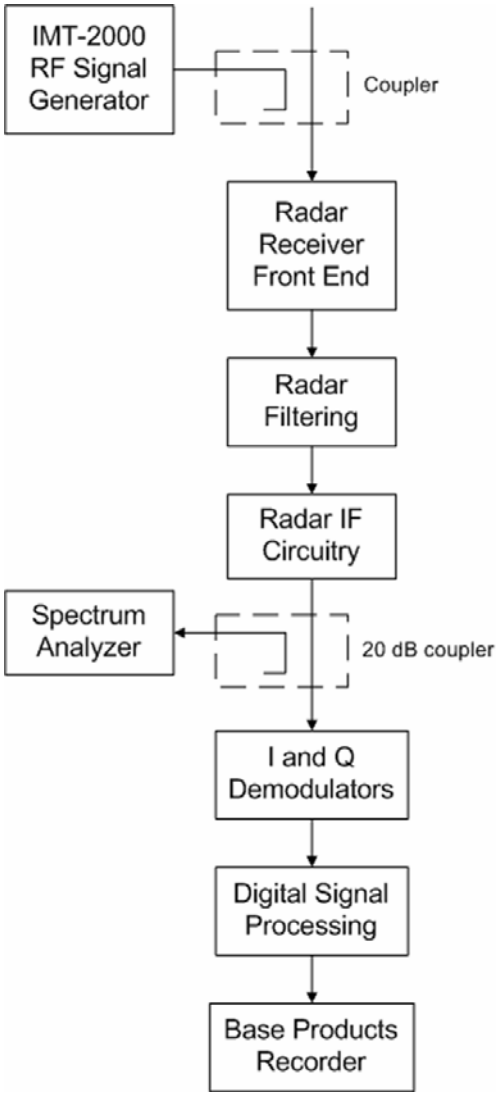

Figure 33. Meteorological radar test set-up block diagram.

5.4 Data Analysis Methodology and Results

Radar tests described in other sections of this report concern systems that locate and track discrete, point targets. Meteorological radars, in contrast, collect a completely different type of data, namely on extended, diffuse phenomena. Meteorological radars such those addressed in this section perform volume scans of the atmosphere and present data on the atmosphere for a full 360 degrees in azimuth and through elevations as high as about 60 degrees.

For discrete-target radars, analysis of the effects of interference on the probability of detection are usually sufficient, and interference effects in those types of systems will tend to mask desired targets and/or created false targets.

In meteorological radars, where data are collected and analyzed for a volume of the atmosphere, the system performance is not characterized with the use of probability of detection. Although visual inspection of the radar display can show some effects due to interference, such inspection does not provide a scientific analysis of the results on the meteorological products generated such as rain fall estimates, wind speed measurement or shear detection. The data analysis for meteorological radar outputs must take a much different approach in order to provide meaningful results, and it has been determined that in fact an extensive statistical analysis must be performed on the low level meteorological data for each range gate response that is received.

5.4.1 Assumptions

- As stated above, the test procedure used to inject interference signals into the radar receiver called for injecting a known interference level at the radar receiver's input.
- The minimum usable signal, with current technology, is 3 dB below the noise floor.
- The required maximum *I/N* ratio is equal to the interference level below the signal that resulted in a 1-dB bias plus the minimum signal level that needed to be retrieved.

The system used processing to remove the effects of noise, allowing the radar to process signals below the noise floor. In a system that would contain no residual effects, one would expect the interference that was injected at the receiver input to linearly track the interference level that was detected through the data analysis. Figure 34 compares the relative levels of the interference that was injected at the receiver input to the interference level that was detected through the data analysis. A divergence can be seen at -6 dB.

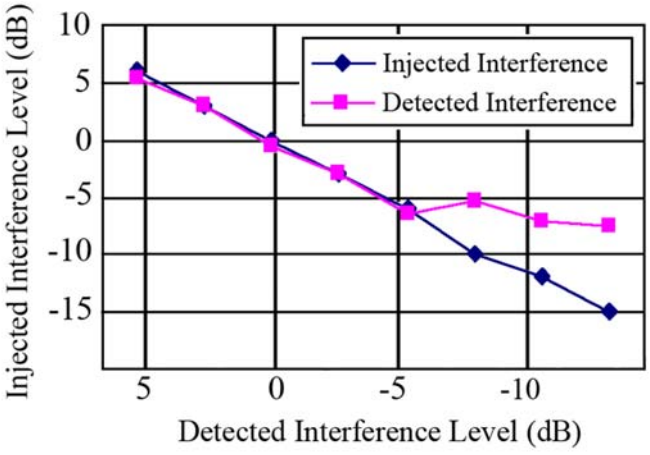

Figure 34. Injected versus detected interference level in the meteorological radar receiver.

This residual effect impacts the analysis in the following way:

- Reflectivity: No effect as the graphical technique that was used to determine the level at which a 1-dB bias in the reflectivity occurs is relative and is not impacted by this residual effect.
- Spectrum width: Residual noise (be it present because it is an artifact of the radar's calibration, inherent to the radar's performance, or as a result of graphical analysis errors) impacts the analysts' ability to graphically determine the level at which the spectrum width difference exceeds 1 m/s.

This residual effect can be characterized, and the data analysis can be compensated accordingly, using the curve shown in Figure 35. These data were used to compensate for analysis errors that were introduced by using an absolute graphical technique to determine the level at which the spectrum width difference is 1 m/s. The data were not required for the reflectivity analysis. Additional variability that adds to the data analysis errors comes into play as a function of graphically estimating the mean and associated data points. An analysis follows, based on the topics of reflectivity and spectrum width.

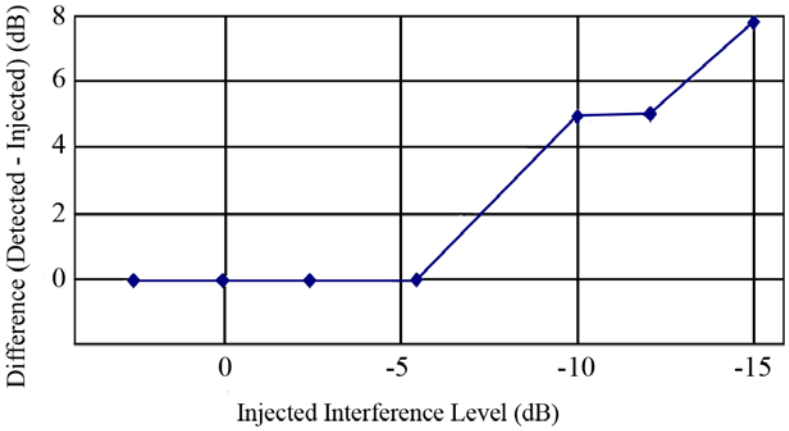

Figure 35. Detected minus injected interference levels as a function of injected level.

5.4.2 Reflectivity Analysis Methodology

Figure 36 represents the regression of the (interference+signal) level to the signal level for the TDMA-GMSK interference signal. This regression analysis has been used to graphically derive an interference level relative to the received signal level that results in a 1-dB bias in the reflectivity measurement. The interference level that results in a 1-dB bias is set equal to the difference between SNR (without interference) corresponding to the 3-dB and 1-dB SNR difference points. Adding this number to the -3-dB SNR level that was derived above results in the true *I/N* level. As an example, an average has been drawn on the data in Figure 36. The 1-dB and 3-dB points are noted on the y-axis and horizontal lines have been drawn to intersect the average. At the points of intersection, vertical lines have been drawn to intersect the x-axis (SNR without interference). The difference between these points of intersection represents the interference level below the signal level that results in a 1-dB bias.

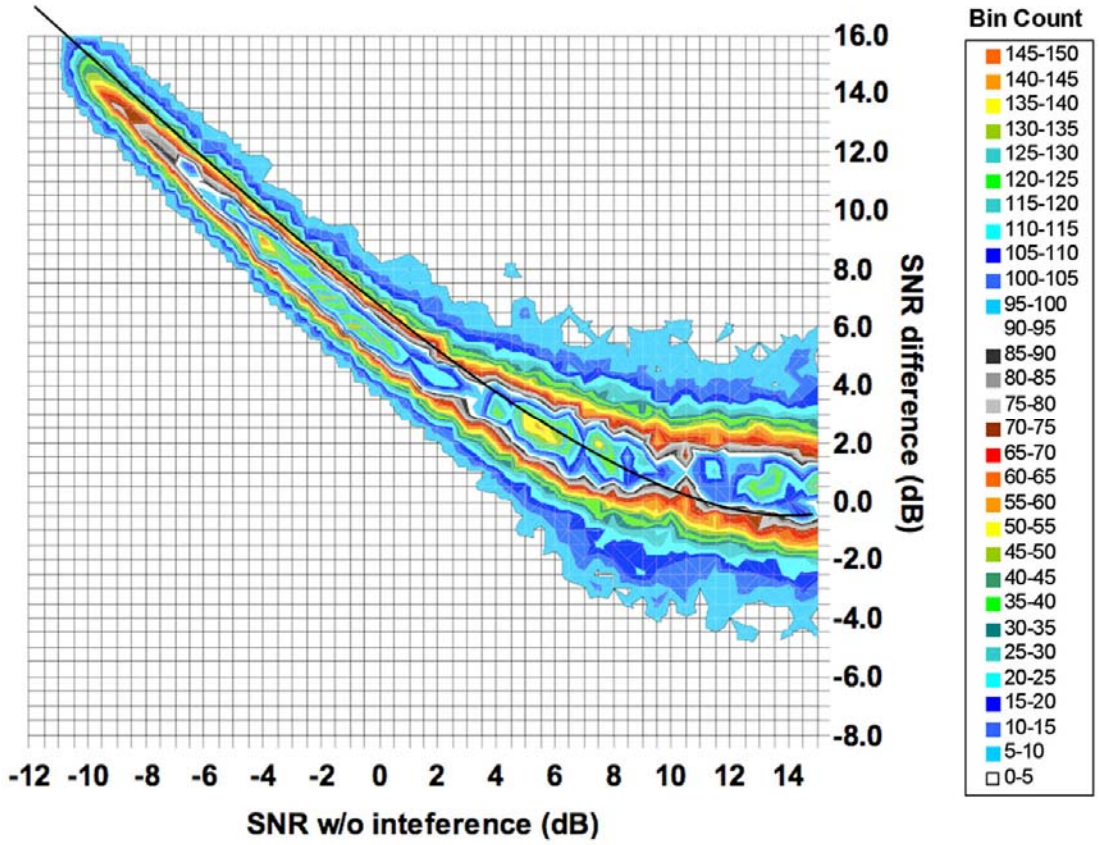

Figure 36. Reflectivity regression for interference in the meteorological radar.

For this example analysis, the *I/N* calculation yields the following results:

> *I/N* = (The interference level below the signal that results in a 1 dB bias) + (The minimum signal level that needs to be retrieved).

Table 10 illustrates the results of this analysis for one test case. The results presented in this table are consistent with the expected values as derived in Section 5.3.2.

5.4.3 Spectrum Width Analysis Methodology

A similar analysis approach was taken for determining the level at which a 1m/s bias occurred in the spectrum width product. In this case the regression that was used for graphically determining this value is shown in Figure 37.

Table 10. Reflectivity Results for Example Analysis

Interference Level Relative to Signal (dB)	***I/N* Level at which 1-dB Bias Occurs (dB)**
+6	-9.5
+3	-9.5
0	-9.5
-3	-10
-6	-7.5
-10	-9
-12	-7.5
-15	-8
Mean	-8.9
Standard Deviation	0.93

5.4.4 Spectrum Width Regression

The process for analysis of spectrum width regression is very similar to the method used to determine the level at which a 1-dB bias occurred in the reflectivity data. An absolute level is derived from the reflectivity plot at a SNR difference level of 3 dB. A visual estimate of the mean is drawn onto the spectrum width plot and a spectrum width difference of 1 m/s is identified on the y-axis. A horizontal line is drawn to intersect the mean, and the SNR without interference level at which the spectrum width difference equals 1 m/s second is identified on the x-axis. To compensate for the residual effect that was described earlier, the values from Table 11 need to be algebraically added to this number. The results of using this technique at *I/N* level of -3 dB are shown in Table 12. The data set supports the theoretical analysis results in Section 5.2.4.

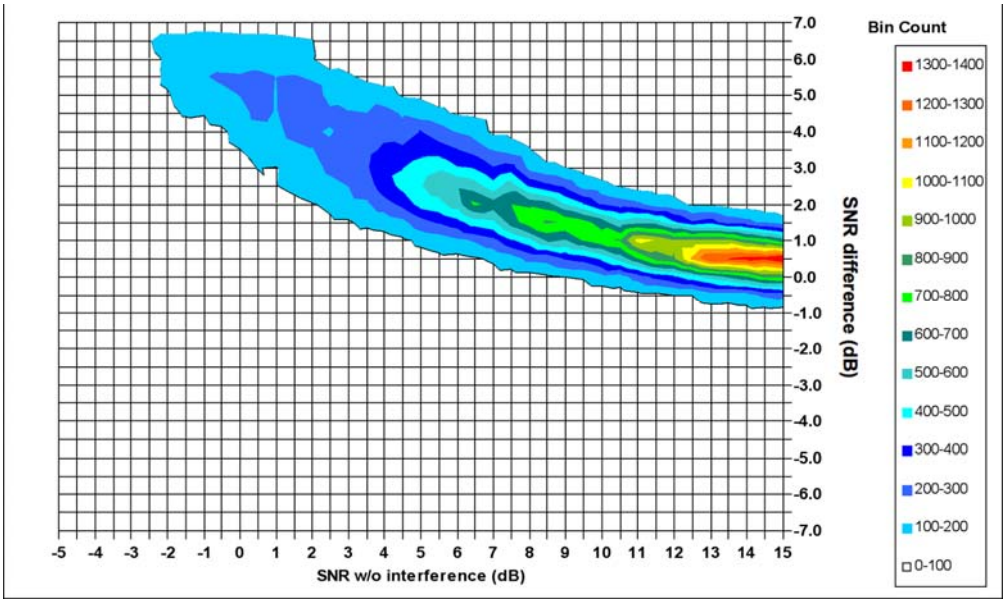

Figure 37. Spectrum width regression for the meteorological radar.

Table 11. Error Reduction Values

Interference Level Relative to Signal (dB)	SNR w/o Interference (dB)	SNR – IL (dB)
6	5.5	-.5
3	2.5	-.5
0	-.5	-.5
-3	-3.5	-.5
-6	-3.75	2.25
-10	-5.25	4.75
-12	-7	5
-15	-7.6	7.4

Table 12. Spectrum Width Results for Example Analysis

Interference Level Relative to Signal (dB)	*I/N* Level at which a 1 m/s difference occurs (dB)
6	14
3	11.5
0	7
-3	5.5

5.5 Summary of Measurement Results

The interference test results are summarized in Table 13.

Table 13. Measured *I/N* Thresholds Necessary for Protection of the Meteorological Radar

Interference Signal		Reflectivity Bias	Spectrum Width Bias
CW		-7.5 dB	-11.5 dB
W-CDMA	4.096 MS/sec	-9.5 dB	-10.75 dB
CDMA-2000-3X (fwd link)	3.686 MS/sec	-7.0 dB	-13.5 dB
CDMA-2000-3X (rev link)	3.686 MS/sec	-9.5 dB	-13.75 dB
TDMA-GMSK	384 kS/sec	-8.75 dB	-14.0 dB
TDMA–8PSK	384 kS/sec	-8.75 dB	-11.75 dB

These results support the calculated value required for protection of the reflectivity measurements. As noted above, the measurements and analysis of the mean velocity were difficult to perform because the mean radial velocity is the least sensitive to interference, and those results do not necessarily indicate the overall interference levels that the radar can tolerate. As discussed above, current limitations in the radar calibration and noise removal process performed by the low level data processor limit the measurement of the necessary protection criteria for the spectrum width measurements. However, correction of the data for the limitations of the radar processing do result in values that support the calculated protection values presented in Section 5.2.4. Improvements to the radar receiver and processor are currently underway which will allow the system to approach or exceed its originally intended design criteria. This lower value will become meaningful when those improvements are made. Section 5.6 addresses those improvements in more detail.

5.6 Meteorological Radar Improvements

The weather radar system that was used for testing is one that has been operating in the United States for approximately eleven years. Upgrades to these systems that incorporate advances in signal-processing systems are currently underway. These upgrades will enable signal detection 10 dB below the current level.

The need for these improvements is driven by several requirements: 1) improved measurement performance above the planetary boundary layer; 2) detection of small water drops and fine mist precipitation that can result in aircraft icing; and 3) with the event of dual polarization measurements, improved monitoring of meteorological growth processes. All of these requirements call for a detection performance that is about 10 dB better than what is achievable today with current weather radar systems. To meet these requirements the radar's performance can be improved by increasing the transmitter power, reducing the receiver's noise floor, or increasing the radar's computational power for better signal processing capabilities.

Among these possibilities, increasing the transmitter power is not cost effective. The alternative of noise floor reduction could be accomplished by extending the pulse width, because extension of the pulse width reduces the required bandwidth of the matched filter and thereby reduces the noise power within the receiver IF. Increasing the pulse width by a factor of 2 increases the sample volume by a factor of 3 dB. Matching the receiver bandwidth results in a reduction of the receiver noise by 3 dB. This would lead to an overall detection improvement of 6 dB. Unfortunately, design limitations on the transmitter duty cycle will not allow extension of the pulse width for the system used in these tests. The receiver noise temperature could also be reduced but a reduction of 1 to 2 dB in noise is all that can be achieved with technology that will be available in the foreseeable future.

Ultimately, the most cost-effective way to achieve these improvements is through enhanced signal processing. Increasing the radar processing power with upgraded hardware will enable implementation of data processing algorithms that were not previously available. This additional processing will utilize coherent integration and frequency domain detection. The radar currently collects all the parameters necessary for performing these functions, but limited processing power has prevented implementation. The planned improvements that are currently under way will eliminate the processing power limitation.

Coherent integration, as implemented on this radar, has demonstrated a 10 dB improvement in detection. Frequency domain detection, the upgrade that is presently underway, will provide about 10 dB of improved performance. With frequency domain detection, the spectrum is broken into discrete coefficients, where the actual number of coefficients is determined by antenna rotation rate and operating mode. In the present storm modes the number of samples ranges from 41 to 111. Processing in the frequency (spectral density calculation) domain results in the desired signal being confined to a few spectral coefficients while the noise is spread over all the coefficients at a much lower level. Although about 20 dB of improvement is anticipated through the use of these two technologies, 10 dB of degradation is expected due to other engineering changes, including a new feature in which transmitter power will be divided between two polarizations. The net change, however, is [(20 dB) - (10 dB)]=10 dB.

The improvements to the radar performance enabled by greater processing power do not reduce the actual noise floor of the receiver, but the effect is a reduction in the effective noise floor by providing the ability to recover signals of interest at much lower signal levels. The difference between the actual noise floor and the effective noise floor is the processing detection improvement. Ultimately, improvements to the radar performance will also cause the radar to be adversely affected by interference at even lower levels.

5.7 Summary of Interference Effects on a Weather Radar

Weather radars, designed to track particles in the atmosphere and hydrometeors of submillimeter size, utilize extensive processing to extract signals from received noise. Tests conducted on one radar type used worldwide have characterized this processing gain as on the order of 6 to 9 dB. In addition, meteorological radars detect more than just the presence of return pulse energy; the processing derives data on return pulse characteristics to determine factors such as wind velocity, wind shear, turbulence, and precipitation type. This processing makes them very vulnerable to interference.

The test results demonstrate that depending on the radar base product considered, the necessary protection criteria vary. Since all three products are necessary for proper operation of the radar, the most stringent values are applicable to ensuring the radar does not experience harmful interference. Though testing was conducted on a single type of meteorological radar, most modern meteorological radar systems employ equally complex processing systems that are as susceptible to interference.

The test results suggest a requirement for a protection value of -9 dB *I/N* for the base reflectivity data. The results also show that while the theory predicts a necessary protection value of -14 dB *I/N* for spectrum width, the radar is presently sensitive to interference down to an *I/N* of approximately -6 dB for that parameter. Introduction of the radar improvements discussed in Section 5.6 will provide a net improvement of about 10 dB through improved processing power, resulting in a reduction in the effective noise floor by a value equivalent to the detection improvement. The end result is that the point where the radar's actual sensitivity to interference deviates from the theoretical curve in Figure 38 will decrease by the amount equal to the processing power. Figure 38 shows the divergence between test results and theory at *I/N*= -6 dB. Near-term improvements will provide 10 dB of processing power.

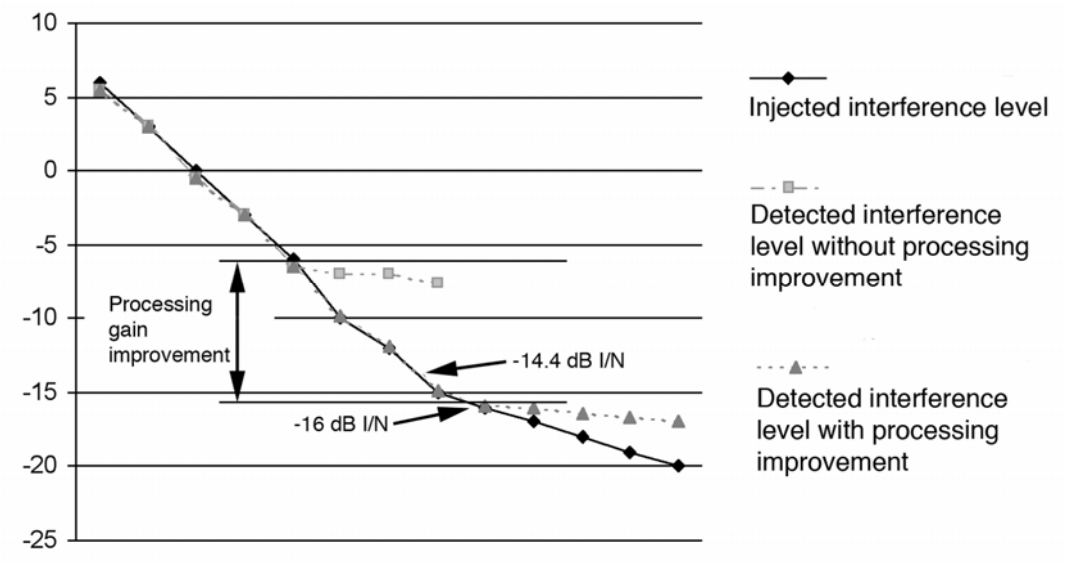

Figure 38. Impact of near-term processing improvements on the weather radar interference threshold, which is expected to ultimately be about *I/N*=-14.4 dB.

6 INTERFERENCE MEASUREMENTS ON MARITIME RADIONAVIGATION RADARS

6.1 Introduction

Maritime radionavigation radars may fail to meet their performance requirements if undesired signals inflict excessive amounts of various types of interference degradation. Dependent upon the specific interacting systems and the operational scenarios, those types of degradation may include:

- diffuse effects, e.g. desensitization or reduction of detection range, target drop-outs and reduction of update rate;
- discrete effects, e.g. detected interference, increase of false alarm rate.

Associated with these varieties of degradation, interference protection criteria may consist of threshold values of parameters, e.g., for a collision avoidance system:

- tolerable reduction of detection range and associated desensitization;
- tolerable missed-scan rate;
- tolerable maximum false-alarm rate;
- tolerable loss of real targets.

These protection criteria and the thresholds used to derive them for shipborne radionavigation systems need to be developed further. The operational requirement for maritime radars is a function of the operational scenario. This is related to the distance from shore and sea obstacles. In simplistic terms this can be described as oceanic, coastal or harbor/port scenarios.

There is as yet no international agreement on the protection criteria required for radars installed on ships for the scenarios identified above. The International Maritime Organization (IMO) is developing a revision to the operational performance standards for maritime radar that takes account of ITU-R requirements for limits on unwanted emissions from radio services. The IMO revision, for the first time, gives recognition to the possibility of interference from other radio services. Most importantly, the IMO has stated without reservation in its recent update of the IMO Safety of Life at Sea (SOLAS) Convention that *radar remains a primary sensor for the avoidance of collisions*. This statement should be viewed in the context of the mandatory fitting of Automatic Identification Systems (AIS) to some classes of ships.

AIS technology relies upon external references (e.g., GPS) for the verification of relative position indication in terms of collision avoidance scenarios. However, AIS cannot take account of many maritime objects (e.g., icebergs, floating debris, small vessels, and wrecks) that are not fitted with AIS. These objects may potentially cause collisions at sea, and must be detectable by maritime radars. Radar will therefore remain the primary system for oceanic collision avoidance for the foreseeable future.

Intensive discussion with maritime authorities, including users, has not yet created any quantitative consensus regarding the minimum required P_d level for any scenarios. Rather, the instinctive reaction by such authorities is that during any maritime voyage *no interference that can be controlled by regulation is acceptable*. In the absence of additional guidance, a P_d value of 0.9 for maritime targets (within a single scan) has been used as a nominal minimum in electromagnetic compatibility studies submitted to the ITU-R.

Tests were performed to assess the effects of pulsed emissions and emissions from digital-signal communication systems on three maritime radionavigation radars that operate with a primary allocation in the 2900-3100 MHz band and three radars that operate with primary allocation in the 9200-9500 MHz band. The systems that were tested are IMO category maritime radionavigation radars that employ scan rates, pulse widths, prfs, IF bandwidths, noise figure, and antenna beamwidths typical of those identified in a pertinent ITU-R Recommendation [22]. These radars are representative of the types being used by the United States Coast Guard (USCG) for shipboard navigation, by the commercial shipping industry, and recreational boaters as well. The radars operating in the 2900-3100 MHz band are identified as maritime radionavigation Radars A, B, and C and the 9200-9500 MHz radars are identified as maritime radionavigation Radars D, E, and F. Tests on radar F concentrated on the effects of pulsed interference.

Radars such as those identified in [22] and used in the NTIA tests typically employ interference mitigation techniques and processing methods identified in another ITU-R Recommendation [18] to allow them to operate in the presence of other radionavigation and radiolocation radars. Techniques of that kind are effective in reducing or eliminating low duty-cycle asynchronous pulsed interference between radars. All of the radars that were tested have some type of interference rejection circuitry/processing, which by default was enabled during testing.

These tests investigated the effectiveness of each of the radar's interference suppression circuitry and software to reduce or eliminate interference due to the emissions from a communication systems employing digital modulation schemes. Additional tests were also performed using low duty-cycle pulsed emissions as an interference source. The tests were performed with the assistance of the radar manufacturers and experienced mariners. Their guidance was used to properly set up and to operate the radars. This section describes the results of those studies to date.

6.1.1 Objectives

The objectives of the maritime radar testing were to:

- quantify the capability of each of the six maritime radionavigation radar's interference-rejection processing to mitigate unwanted emissions from digital communication systems as a function of their power level;
- develop *I*/*N* protection criteria that would mitigate interference from digital communication systems emissions in maritime radionavigation radars;
- observe and quantify the effectiveness of each of the maritime radionavigation radar's IR techniques to reduce the number of false targets, radial streaks (strobes), and background noise or "speckle."

6.2 Description of Maritime Radars Tested

6.2.1 Maritime Radionavigation Radar A

Maritime radionavigation Radar A, which was introduced circa 2000 and is still being refined, is designed for commercial applications and is an IMO category radar that operates in the 2900-3100 MHz band. Nominal values for the principal parameters of this radar were obtained from regulatory type-approval documents, sales brochures and technical manuals. These are presented in Table 14.

Table 14. Technical Characteristics of Maritime Radionavigation Radar A.

Parameter	Value			
Frequency (MHz)	3050 (+/-30) MHz			
Pulse power (peak) into antenna	30 kW			
Range	0.375-1.5 nmi	3-6 nmi	12 nmi	24-96 nmi
Pulse width	0.08 μs	0.30 μs	0.60 μs	1.2 μs
Pulse repetition frequency	2.2 kHz		1.028 kHz	600 Hz
IF bandwidth	28 MHz	3 MHz	3 MHz	3 MHz
Spurious response rejection	60 dB			
System noise figure	4 dB			
Receiver noise in given bandwidth	-96 dBm	-105 dBm	-105 dBm	-105 dBm
Antenna mainbeam gain	[xx]			
RF bandwidth	Unknown			
Antenna scan rate (scan period)	26 rpm (2.3 sec/rev)			
Antenna horizontal beamwidth	1.9 degrees			
Antenna vertical beamwidth	22 degrees			
Polarization	Linear horizontal			

The radar uses a multistage logarithmic IF amplifier/detector. This type of receiver design is very common in marine radionavigation radars since they have to detect targets that have very small and large returns. A logarithmic amplifier increases the range of target returns that can be handled by the radar receiver without it becoming saturated.

The noise figure of the radar was measured and was found to be 5.3 dB, which was consistent with the nominal value of 4 dB. The 3-dB IF bandwidth is about 3 MHz for the range scale used for the tests. Using those parameters the noise power of the radar receiver is calculated to be about -104 dBm.

Radar A has extensive signal processing and target tracking capabilities, including an adaptive local CFAR feature and a scan-to-scan correlation feature. The local CFAR (acting within a small fraction of one range sweep) is known as an ordered-statistic CFAR, which is a type that permits the desensitizing effect of interfering pulses to be lessened or avoided. This is done by discarding a selectable number of background signal samples that would otherwise be used in establishing the detection threshold. The process discards the samples having the greatest amplitude. As more samples are discarded which contain the higher amplitude interfering pulses, the less influence they are likely to have on the sensitivity of valid target detection.

Radar A can also perform a scan-to-scan correlation process that provides an additional means for discriminating between signals that are present consistently, such as a valid target, and signals that appear at random times, such as asynchronous pulsed interference.

6.2.2 Radars B and D

Radars B and D are maritime radionavigation IMO category type of radars produced by the same manufacturer and are designed for commercial applications. Radar B operates in the 2900-3100 MHz band while Radar D operates in the 9200-9500 MHz band. Radars B and D locate their transmitter/receiver below deck and use waveguides to send/receive signals from the antenna. They use different antennas and receiver front-ends, but have a common display along with common receiver elements, including the interference rejection processing and IF circuitry. The radars use a multistage logarithmic IF amplifier and a separate video detector. Radars B and D also use pulse jitter. The transmitted pulse prf can be jittered to prevent second time around echoes and also to reduce the interference from other transmitters in the vicinity. This function is automatically set in the transceiver and provides up to ±25μs jitter about the nominal value. Nominal values for the principal parameters of these radars were obtained from regulatory type-approval documents, sales brochures and technical manuals. They are presented in Table 15.

Table 15. Technical Characteristics of Maritime Radionavigation Radars B and D

Parameter	Value			
Frequency	3050 (± 10) MHz	9410 (± 30) MHz		
Pulse power (peak) into antenna	30 kW			
Range	0.125-1.5 nmi	3-24 nmi	48 nmi	96 nmi
Pulse width	0.070 μs	0.175 μs	0.85 μs	1.0 μs
Pulse repetition frequency	3.1 kHz	1.55 kHz	775 Hz	390 Hz
IF bandwidth	22 MHz	22 MHz	6 MHz	6 MHz
Spurious response rejection	Unknown			
System noise figure	5.5 dB			
Receiver noise in given bandwidth	-95 dBm	-95 dBm	-101 dBm	-101 dBm
RF bandwidth	Unknown			
Antenna mainbeam gain	[xx]			
Antenna scan rate (scan period)	24/48 rpm (2.5/1.25 sec/rev)			
Antenna horizontal beamwidth	2.8 degrees	1.2 degrees		
Antenna vertical beamwidth	28 degrees	25 degrees		
Polarization	Linear horizontal			

The values of pulse width and prf in Table 15 are the default settings for that particular range. The operator can, for some ranges, select pulse widths and prfs that differ from the default values.

Pulse-to-pulse and scan-to-scan correlators are used by Radars B and D to mitigate interference from other radars. For pulse-to-pulse correlation, returns from successive pulses are compared to reduce interference; a target is displayed only if it is present for consecutive pulses. This IR function is most effective if the transceiver has been set to provide prf jitter. Scan-to-scan correlation will only display targets if they are present in consecutive scans. These radars do not have CFAR processing. More discussion of these radar interference mitigation techniques can be found in Section 1 and Appendix A of this report, as well as in an ITU-R Recommendation [18].

6.2.3 Maritime Radionavigation Radars C and E

Radars C and E are maritime radionavigation IMO category type of radars produced by the same manufacturer and were designed for commercial applications. Radar C operates in the 2900-3100 MHz band while Radar E operates in the 9200-9500 MHz band. Radars C and E are a topmast design. The receiver/transmitter (R/T) is encapsulated in a metal housing located directly below the rotating antenna. The video from the R/T unit is sent to the PPI located below deck via cables. They use different antennas and receiver front-ends, but have a common display along

with common receiver elements including the interference rejection processing and IF circuitry. Both of the radars use an eight-stage successive approximation logarithmic IF amplifier/detector.

Nominal values for the principal parameters of these radars were obtained from regulatory type-approval documents, sales documentation, and technical manuals. They are presented in Table 16. The values of pulse width and prf in the table are the default settings for that particular range. The operator can, for some ranges, select pulse widths and prfs that differ from the default values.

Radars C and E use pulse-to-pulse and scan-to-scan correlators to mitigate interference from other radars, as described above. These radars do not have CFAR processing.

Table 16. Technical Characteristics of Maritime Radionavigation Radars C and E

Parameter	Value		
Frequency	3050 (+/-10) MHz	9410 (+/-30) MHz	
Pulse power into antenna	30 kW		
Range	0.125-3 nmi	6-24 nmi	48-96 nmi
Pulse width	0.050 μs	0.25 μs	0.80 μs
PRF (Hz)	1.8 kHz	785 Hz	
IF bandwidth	20 MHz	20 MHz	3 MHz
Spurious response rejection	Unknown		
System noise figure	4 dB		
Receiver noise in given bandwidth	-97 dBm	-97 dBm	-105 dBm
RF bandwidth	Unknown		
Antenna mainbeam gain	30 dBi		
Antenna scan rate (scan period)	25/48 rpm (2.4/1.25 sec/rev)		
Antenna horizontal beamwidth	2.0 degrees	1 degree	
Antenna vertical beamwidth	30 degrees	15 degrees	
Polarization	Linear horizontal		

6.2.4 Maritime Radionavigation Radar F

Maritime radionavigation Radar F is nearly identical to Radar A, except that its RF front end operates in the 9200-9500 MHz band. Nominal technical characteristics of this radar are presented in Table 17. The radar uses a summing multistage logarithmic amplifier with the IF bandwidths given in Table 17 for each pulse width and associated range. A test point was provided that is located at the output of the third IF amplifier. A CW signal was swept in frequency to determine the response of the receiver and measure the IF bandwidth. The result is shown in Figure C-5. The 3 dB IF bandwidth of the radar when set to short pulse mode 1, which

uses a pulse width of 200 ns for a maximum range of 3 nautical miles, was measured to be about 6.5 MHz. This mode was used for all of the tests.

Table 17. Technical Characteristics of Maritime Radionavigation Radar F

Parameter	Value				
Frequency	9410 (+/-30) MHz				
Pulse mode	Short pulse 1	Short pulse 2	Medium pulse 1	Medium pulse 2	Long pulse
Pulse width	80 ns	200 ns	400 ns	700 ns	1.2 μs
Range mode	0.125-1.5 nm	0.5-3 nm	1.5- 6 nm	3-24 nm	6-72 nm
Pulse repetition rate	2.2 kHz		1 kHz		600 Hz
IF bandwidth	27 MHz	4.5 MHz	3 MHz		
Spurious response rejection	60 dB				
System noise figure	4 dB				
Receiver noise in given bandwidth	-96 dBm				
Antenna mainbeam gain	31 dBi				
RF bandwidth	Unknown				
Antenna scan rate (scan period)	24 rpm (2.5 sec/rev)				
Antenna horizontal beamwidth	1.5 degrees				
Antenna vertical beamwidth	22 degrees				
Polarization	Linear horizontal				

6.2.5 Radar Video Displays

Radars A and F use the same video display unit. Their enhanced signal processing capabilities can display various types of targets in different combinations. The radars could display amorphous, raw-video "blips" (known as the image display), synthetic targets that appeared as "o" symbols, and/or tracked targets that appeared as "x" symbols. The brightness of the video image targets roughly corresponded to the power of the target echoes. Figure 39 shows an example of synthetic and raw video targets on the same PPI display.

Synthetic targets require about 2-3 dB of additional desired power compared to raw-video targets to obtain the same P_d when operating at minimum detectable signal (MDS) level but do not

change their brightness in correspondence with echo strength. That is, if the target power for the 0.9 P_d for blip display was -90 dBm, then the power level to achieve the 0.9 P_d for the synthetic targets would be about -88 dBm. Adding signal power did not change the intensity of the display of the synthetic targets. For synthetic targets the radar has a built-in target counter that shows the number of targets per scan and displays that value on the PPI display.

Radars B and D (from the same manufacturer) use a color CRT to display targets and radar information to the user, including prf, pulse width, range rings, and other parameters. These radars do not show synthetic targets and only display raw-video blips. Likewise, Radars C and E (from another manufacturer) only display raw-video blips. However, the displays used with radars C and E are monochromatic raster scan types. Besides targets, these displays also indicate various radar parameters. Like Radar A, for these radars the raw-video blips are brighter for targets that have stronger return echoes.

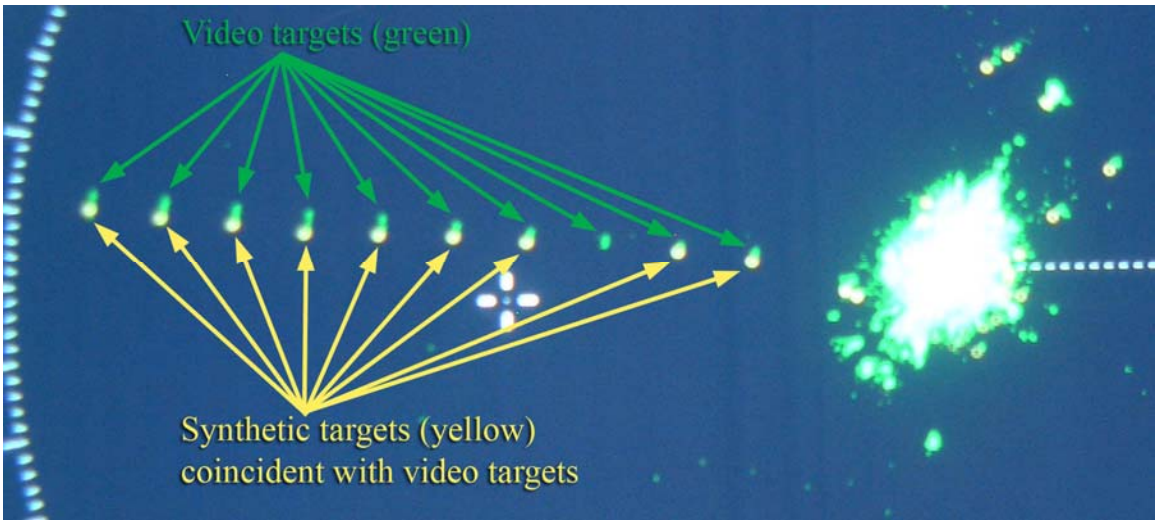

Figure 39. Example of synthetic and raw video targets on a PPI display.

6.3 Interference Signal Characteristics

6.3.1 Interference Generation for Radars A Through E

Radar A was tested with a 2 MBit/s QPSK waveform as an interference source. Radars B and C were tested with 64 quadrature amplitude modulation (QAM), 16 QAM, CDMA-2000, and W-CDMA signals as interference sources. Radars D and E were only tested with the CDMA-2000 and W-CDMA signals. All interfering signals were on-tune (co-channel) with the radars. The QPSK signal injected into Radar A was continuous, occurring for a full 360 degrees.

The unwanted CDMA signals that were injected into Radars B, C, D and E were gated to occur at the same time of the target generation within the same azimuth. The gate time was equal to the length of time that a stationary interference source would be within the radar's antenna 3-dB horizontal beamwidth as it rotates. The QAM signals were not gated. A measured emission spectrum of the continuous QPSK signal is shown in Figure B-5.

Communication test sets were used to generate the DVB-T 16 QAM, DVB-T 64 QAM, CDMA 2000 and WCDMA signals. Spectrum shots of each of the unwanted signals are shown in Figures B-8 and B-9. The CDMA-2000 signal was for the reverse link (mobile-to-base) standard according to interim standard 95 (IS-95) format for cellular mobile telephones. The W-CDMA signal was for the uplink standard according to the 3GPP 3.5 format. The 16 and 64 DVB-T QAM signals in Figure B-8 represent the type of modulation scheme that is television camera crews for electronic news gathering outdoor broadcast (ENG-OB) purposes.

6.3.2 Interference Generation for Radar F

Tests on Radar F concentrated on the effects of pulsed interference from radiolocation radars. In a departure from most of the work described in this report, and for reasons that will become clear, effects of pulsed interference were explored up to +40 dB *I/N* levels. In fact, at one point during the testing, an attenuator setting was inadvertently set to a lower value than was intended. As a result, *I/N* levels as high as +60 dB were injected. At these levels, the LNA at the radar RF front end was gain-compressed and radar performance was seriously compromised as a result. The tests were performed with radiolocation waveforms that are representative of the radar systems that operate in the 9000-9200 MHz and 9300-9500 MHz bands.

Three types of radiolocation waveforms were used for the tests. They are chirped, phase coded, and unmodulated (simple pulsed) waveforms. The waveforms were gated on for the duration of the mainbeam dwell time for the radionavigation receiver as if it were scanning past a stationary object. They were also on-tuned (co-channel) with the radar.

6.3.2.1 Linear Chirped-Pulse Interference Waveform

Table 18 shows the parameters of the chirped interference. They were developed based on the characteristics of existing 9-GHz radars. The number of pulses per beam dwell is dependent on the type of radiolocation system being simulated.

Table 18. Chirped-Pulse Interference Waveform Characteristics

Waveform	Pulse width	Prf	Pri	Duty cycle	Chirp	Chirp rate
Chirp 1	10 μs	750 Hz	1.3 ms	0.8%	10 MHz	1 μs/MHz
Chirp 2	10 μs	750 Hz	1.3 ms	0.8%	50 MHz	5 μs/MHz
Chirp 3	13.6/1.65 μs	5 kHz	0.20 ms	0.8%	660/80 MHz	48.5 μs/MHz
Chirp 4	10 μs	2 kHz	0.5 ms	0.4%	400/80 MHz	40 MHz/μs
Chirp 5	80 μs	4.5 kHz	0.22 ms	7.2%	400/80 MHz	5 MHz/μs
Chirp 6	10 μs	515 Hz	1.94 ms	0.91%	45/80 MHz	4.5 MHz/μs
Chirp 7	10 μs	5.15 kHz	1.94 ms	0.88%	460/80 MHz	46 MHz/μs

Radar F was tested with linear chirped pulsed interference waveforms. These waveforms primarily use a chirped modulation scheme as shown in Table 18. The duty cycles are calculated from the scaled pulse widths.

In some cases, the frequency sweep range of the chirp-pulse generation system used in these tests was limited by hardware to less than the full chirp range of the corresponding radar emission being modeled. In such cases, the tests were still performed to fully and accurately replicate the response of radar receivers to the specified chirp parameters. To accomplish this goal, the chirped pulses used in the tests were swept across at least twice the -20-dB frequency response range of the Radar F receiver, at the same rate as the sometimes wider-bandwidth chirp pulses from potentially interfering sources.

For example in Table 18, the 660-MHz chirp in a 13.6 μs pulse (R_c = (660 MHz/13.6 μs) = 48.5 MHz/us) was not possible to generate with available test equipment. But an equivalent interference effect was generated with an 80-MHz chirp pulse in an interval of 1.65 μs (R_c = (80 MHz/1.65 μs) = 48.5 MHz/μs), provided that the -20-dB radar IF pass-band of the Radar F victim receiver is less than 50 MHz wide.

In these tests, the value of R_c was always preserved and the Radar F receiver always saw the chirped interference across its full receiver IF passband in exactly the same way as it would have if the chirped interference had been generated across wider bandwidths. That was the key element in accessing the effects of the interference.

For Radar F, the interference signals were injected into the radar at the same azimuth as the targets for a duration time equal to the antenna beam sweeping across a stationary object. The receiver's noise power measured at the IF test point using a spectrum analyzer in zero span mode without any targets, radiolocation, or linear chirped pulsed waveforms present in the bandwidth was about -57 dBm. This indicated a nominal gain of about 40-42 dB in the receiver. The gain compression point[23] using an on-tune CW signal was found to be -25 dBm on the generator panel display, or -43 dBm at the LNA input. The radar receiver interference suppression circuitry and software *cannot* mitigate the effects of receiver saturation.

The Radar F receiver IF output response (amplitude and pulse width) to interference from chirped pulses is a function of the rate at which the chirped frequency sweeps through the victim radar receiver pass-band. This rate, called chirp rate (R_c), is given by: $R_c = (B_c/\tau)$, where R_c is the sweep rate in megahertz per microsecond, B_c is the chirp frequency range in megahertz and τ is the pulse duration in microseconds. Victim radar receivers should not respond to interference on frequencies outside the -20-dB pass-band of their IF circuitry, assuming that the interference is below the RF front-end overload threshold.

6.3.2.2 Phase Coded Pulsed Interference Waveform

Table 19 shows the parameters of the phase coded pulsed interference waveform, based on a 13-bit Barker code sequence.

[23] The gain compression point is the value where the LNA is saturated by the input signal and will no longer give a linear relationship between the input and output signals.

Table 19. Phase Coded Pulsed Interference Waveform Characteristics

Waveform	Pulse width	Prf	Sub-pulse width
Phase 1	0.64 μs	1.6 kHz	0.049 μs
Phase 2	20 μs	1.6 kHz	1.54 μs

6.3.2.3 Unmodulated Pulsed Interference Waveform

Table 20 shows the parameters of the unmodulated pulsed interference waveforms. They are based on the characteristics of existing radars along with higher duty cycles that may be used in future systems. The starred (*) waveforms did not replicate particular radar signals; they were used determine the effectiveness of radar signal processing at high duty cycles.

Table 20. Unmodulated Pulsed Interference Waveform Characteristics

Waveform	Pulse width	Prf	Pri	Duty Cycle
Unmod 1	1 μs	8 kHz	125 μs	0.8%
Unmod 2	1 μs	19 kHz	52.63 μs	1.9%
Unmod 3	1 μs	35 kHz	28.57 μs	3.5%
Unmod 4*	1 μs	50 kHz	20.0 μs	5.0%
Unmod 5*	1 μs	75 kHz	13.3 μs	7.5%
Unmod 6*	1 μs	100 kHz	10 μs	10%
Unmod 7*	1 μs	200 kHz	5 μs	20%

6.3.2.4 OFDM/BPSK Interference Waveforms

In addition to the radiolocation waveforms, Radar F was subjected to an on-tune orthogonal frequency division multiplexing (OFDM/BPSK) waveform. It was used to demonstrate the radar response to interference of a continuous nature (non-pulsed). These signals were gated for the duration of the mainbeam dwell time. The OFDM/BPSK waveforms, although not specific to any type of communication system in the 9-GHz band, are a typical modulation of those types of waveforms used by communications systems in other bands for broadband, high data rate applications. It was used to show the contrast in interference suppression capabilities between the effects of pulsed interference in the radar receiver and a digital modulation that appears noise-like.

6.4 Target Generation

6.4.1 Target Generation for Maritime Radars A Through E

Ten simulated, equally-spaced, equi-amplitude targets were generated along a radial using RF signal generators, AWGs, and other miscellaneous equipment (combiners, attenuators, etc.) for each of the radars out to a 3-nmi range as shown in Figure 40. The target generation system provided groups of RF pulses with the width and timing to appear as ten individual targets on the radar's PPI display. The targets had identical signal power in the radar receiver, simulating RCS that increased with distance. The number of pulses needed to generate each target depended on the radar's characteristics.

The train of transmitter trigger pulses (A) was used to trigger the simulated-target generator. A free-running pulse generator was used to produce gate pulses (B) representing the amplitude modulating effect on target return due to the antenna beam. Those pulses gated the train of transmitter triggers in an AND gate circuit, producing bursts (C) of trigger pulses containing from 6 to 23 pulses each. Each trigger pulse was applied to an arbitrary waveform generator, which delayed the trigger appropriately and generated a burst of ten pulses (D), each having the width of one of the radar's short pulses. All ten of these occurred within one "sweep" of the radar, i.e., within the displayed fraction of one pulse repetition interval or PRI. Each of those pulses in turn modulated an RF signal generator set to a frequency near 3050 or 9410 MHz to produce a simulated-target-return pulse train. The specific RF signal generator frequency was adjusted to maximize the radar's response.

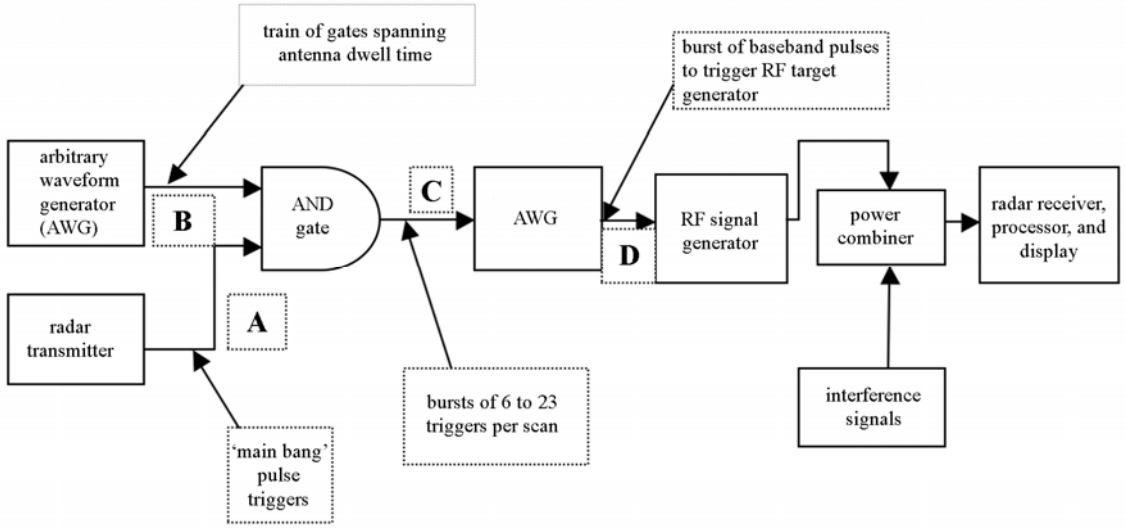

Figure 40. Target generator instrumentation for maritime radionavigation radar tests.

6.4.2 Non-Fluctuating Target Generation for Radar F

The targets for these tests were generated using the same basic hardware as for the other maritime radars, with ten equally spaced targets generated on a radial and the farthest target

being located at the maximum range of 3-nmi. Each target was comprised of 18-19 pulses with the characteristics of the short pulse 2 mode setting in Table 17. Each target on the radial had the same power level in the radar receiver.

The ten target pulses triggered by each radar trigger all occur within the return time of one of the radar's short range scales, i.e., one "sweep". Consequently, the pulses simulate ten targets along a radial, i.e., a single bearing. For adjustment of the display settings, the RF power of the target generator was set to a level so that all ten targets were visible along the radial on the PPI display with the radar's video controls set to positions representative of normal operation. The pulse repetition rate of the target generator (waveform B) was adjusted so the targets would appear at the same azimuth on consecutive scans of the PPI. The target generator timing diagram is shown in Figure 41.

A number of trials were performed to determine the target signal power that would result in a P_d of 90 percent *without* the interference radiolocation or linear chirped pulse waveforms being present. This value was found to be about -70 dBm at the panel display of the target generator. With RF losses, the target power supplied to the LNA input of the radar receiver was -88 dBm. The noise figure was measured to be about 9 dB. This results in a calculated noise power of about -97 dBm in the (approximately) 6-MHz IF bandwidth of the radar receiver. Therefore, the signal-to-noise value to achieve the P_d of 90 percent was about 8-10 dB. Note that the accuracy of this measurement is probably within ±2 dB.

While the Radar F antenna was not used for the tests, appropriate signals from the antenna positioner circuitry were supplied to the radar receiver to mimic the antenna's normal rotation.

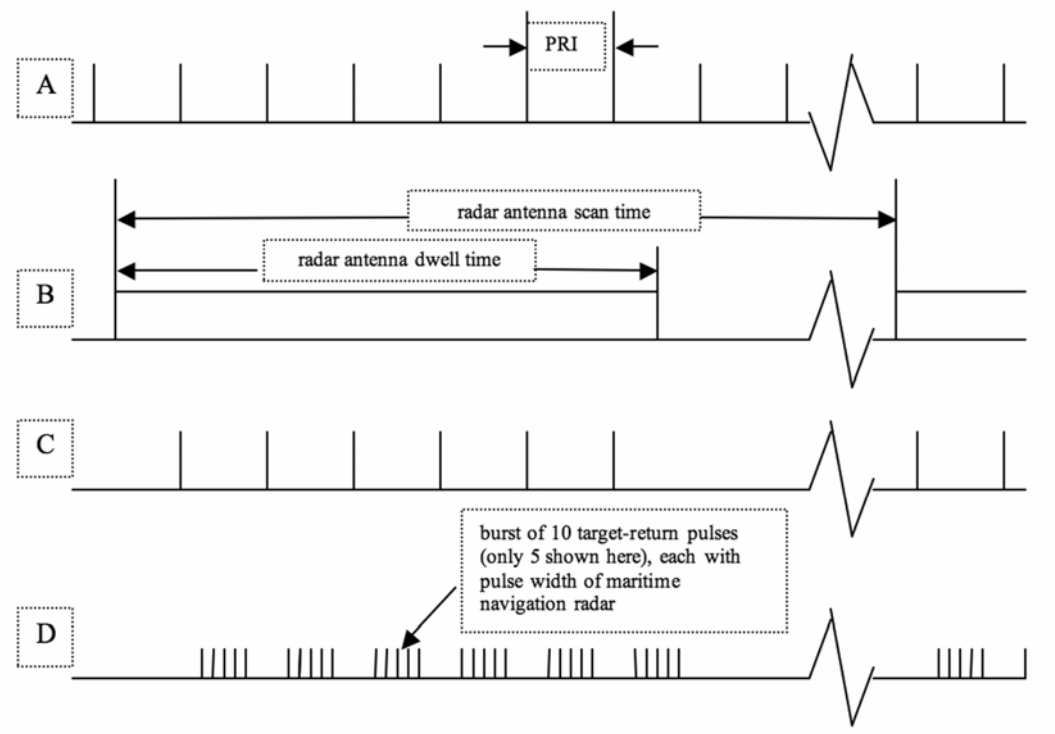

Figure 41. Target generator timing diagram for maritime radionavigation radar tests.

6.4.3 Fluctuating Target Generation for Radar F

For maritime Radar F, tests were also performed with fluctuating-power targets that changed their power levels on a scan-by-scan basis according to Swerling case 1 statistics[24] (see Section 2.3 of this report). All ten targets on the PPI radial were varied by the same amount; each Swerling level was held constant for all ten targets for a total of twenty scans, then the next Swerling level was used for all ten targets for the next twenty scans, and so forth. Thus each data point represented the counting of (10 targets per scan x 20 scans per level)=200 injected targets at each Swerling level. A total of twenty Swerling levels were used, and were programmed to run in a random order from one level to the next. The Swerling power levels were applied relative to the nominal value of RF power that gave P_d=0.9 without interference; their order and values are shown in Table 21. For example, the P_d=0.9 nominal target power value was -88 dBm and on the first scan the power was adjusted by +2.1 dB to be -85.9 dBm, on the second scan the power was -86.5 dBm, and so on.

For the tests, the signal levels of all targets were adjusted to produce stationary target detections consistent with a fixed P_d of about 0.9. This P_d value was chosen to reflect the case that the P_d can never be 100 percent due to propagation effects, interference and other factors. As of the time that this report was written, the IMO has not specified a minimum P_d for marine radionavigation radars. The IMO performance standard[25] does specify target types, RCS, and the minimum ranges to detect them. The IMO is developing a minimum P_d for these types of radars and should publish this value in the near future.

The target power level output was controlled by a computer and sequenced through the twenty Swerling values of Table 21 without interruption to accurately reproduce the true effect of a scan-to-scan scenario. Note that in other interference tests the radar was allowed about five scans to 'settle' between each data point. A number of baseline runs through the sequence were performed without interference, versus with the OFDM signal being injected. Effects of fluctuating levels on target P_d *without* any interference are noted in Table 21.

[24] Swerling case 1 target levels were generated by summing the squares of pairs of Gaussian-distributed real numbers.

[25] Extracts from IMO Resolutions A222(VII), A278(VIII), A477(XII) for radar equipment required by Regulation 12, Chapter 5 of the IMO-SOLAS Convention.

Table 21. Swerling Case 1 Target Power Levels (Relative to Nominal Value of -88 dBm)

Signal levels in dB Relative to Median Power Level and Effect on Target P_d Without Interference					
Scan number	dB	Effect	Scan number	dB	Effect
Scan 1	+2.1	P_d 100%	Scan 11	+2.7	P_d 100%
Scan 2	+1.5	Near 100%	Scan 12	+0.90	P_d higher
Scan 3	+3.3	P_d 100%	Scan 13	-5.6	No targets
Scan 4	+0.3	Baseline	Scan 14	+7.3	P_d 100%
Scan 5	+4.5	P_d 100%	Scan 15	-0.3	Reduced P_d
Scan 6	-7.2	No targets	Scan 16	-2.5	No targets
Scan 7	-1.7	Few targets	Scan 17	-3.3	No targets
Scan 8	-14.4	No targets	Scan 18	-9.5	No targets
Scan 9	+4.0	P_d 100%	Scan 19	-4.3	No targets
Scan 10	+5.7	P_d 100%	Scan 20	-1.0	Reduced P_d

6.5 Maritime Radar Test Conditions

The tests were performed with the following parameters set on the maritime radionavigation radars as shown in Table 22.

For all of the radars, the STC and FTC features could be activated at the operator's discretion. As noted in Sections 1.10.1 and 1.10.2, STC suppresses sea-clutter returns by attenuating strong echoes at short ranges, while FTC suppresses rain clutter by differentiating echo returns after envelope detection.

For each of the radars that were tested, baseline values for the software functions that controlled the target and background brilliance, hue, and contrast settings were found through experimentation by test personnel and with the assistance of the manufacturers and with professional mariners that were experienced with operating these types of radars on ships of various sizes. Once these values were determined, they were used throughout the test program for that radar.

Table 22. Maritime Radar Test Control Settings

Parameter	**Value**
Sensitivity time control (STC)	Disabled
Fast time constant (FTC)	Disabled (default)
Interference rejection (IR)	On (default)
Automatic gain control	On (default)
Radars A and F image selected	Raw video ("image") and/or synthetic targets
Radars B, C, D, E	Raw video
Range scale	3 nmi

6.5.1 Interference Suppression Features in Radars A and F

In addition to conventional STC and FTC features for clutter reduction, Radars A and F deserve special mention of the following capabilities to minimize clutter and RF interference: ordered statistic CFAR, spike suppression, clutter mapping, and scan-to-scan correlation. As shown in Table 22, STC and FTC were disabled for the tests, since they are used to discriminate sea clutter returns from target returns and to offset the effects of rain, respectively. Obviously, sea clutter and rain did not affect these measurements as they were performed on a test bench. A brief description of the other interference mitigation features follows.

The spike suppression circuitry provides a means of instantaneously filtering interference from other transmitters by detecting and eliminating spikes that occur at a given range over three adjacent sweeps based on a maximum rise and fall criteria. The circuit substitutes the spike value with the average of the amplitudes on the previous and subsequent sweeps.

The CFAR uses an ordered statistic (OS) technique. This adaptive technique minimizes clutter breakthrough in large homogeneous clutter areas. It permits target returns near or above the peak noise plus clutter level to be detected while eliminating the bulk of the noise and clutter. The OS CFAR operates by automatically adjusting the detection threshold based on an instantaneously derived estimate of the predominant noise plus clutter level in the vicinity of the test cell. A programmable guard cell region allows the OS CFAR to accommodate targets of extended range run length, such as supertankers, without loss of sensitivity while still discriminating against clutter.

The clutter mapping compensates for unique spatially distributed clutter situations, such as ones that might be caused by multi-path, grazing angle versus sea state, or a combination of such conditions. The radar operator is provided a means of biasing the OS CFAR derived threshold on an area-by-area basis through the use of a threshold bias map (TBM). The threshold offset stored in the TBM for a particular area is added to the OS CFAR computed threshold for all detections occurring in that area. There are sixteen TBM areas centered around the radar's position which permit the specification of an annulus clutter filter area, and which may be used to counter effects that are range dependent but bearing independent. The TBM area may be defined to negatively bias the OS CFAR generated threshold to increase sensitivity or completely mask returns such as those from land mass. The TBM is organized as a table of 1024 range cells by 1024 azimuth cells.

The scan-to-scan correlator takes advantage of the fact that sea clutter is correlated on a pulse-by-pulse basis, but de-correlated on a scan-by-scan basis. Clutter that is permitted to pass through all previous clutter suppression stages is processed through a temporal-spatial de-correlation filter, the retrospective processor. This processor performs scan-to-scan correlation, maintaining as many as nine scans of data.

6.6 Maritime Radar Test Procedures (Non-Fluctuating Targets)

For each radar that was tested, the RF power output of the target generator system was adjusted so that the target P_d was about 90 per cent without unwanted signals being present, with the baseline PPI target and background display settings. Table 22 lists the target power at each radar's RF input that was required to obtain a P_d of 0.90. Once these values were determined, they were used throughout the tests.

Table 23. Target Power Levels (Non-Fluctuating) Required to Achieve a P_d of 0.90

Radar	Target power at RF input for a P_d of 0.90
A	-90 dBm
B	-89 dBm
C	-77 dBm
D	-89 dBm
E	-86 dBm
F	-88 dBm

For Radars A, C and E, the appropriate levels of unwanted signal powers that were required to produce the *I*/*N* levels within the radar receivers was determined using the calculated receiver noise power calibrated to the receiver's waveguide input. The receiver noise power was calculated using the IF bandwidth and noise figure. Any differences in bandwidths between the radar receiver and the test signals were accounted for in setting the *I*/*N* levels.

The appropriate levels of unwanted signal powers that were required to produce the *I*/*N* levels within radar receivers B and D were determined by monitoring the output of the IF circuitry at a test point located at the detector input with the spectrum analyzer. The spectrum analyzer was set to zero-span mode and the value of the radar receiver noise power at the IF test point, without any unwanted signal being present, was measured and recorded. The unwanted signal was then injected into the radar RF front-end and the noise power at the IF test point was monitored for a 3-dB increase as the power level of the unwanted signal was also increased. A 3-dB increase in the receiver noise power is equal to an *I*/*N* of 0 dB. Once the value of the unwanted signal that generated the *I*/*N* of 0 dB was found, the unwanted signal power levels that generated the other *I*/*N* values were easily determined. The power levels of the unwanted signals were controlled using step attenuators or the test set panel display.

For Radars B and D, the number of targets on each radial was counted for 50 simulated rotations of the antenna for each *I*/*N* level for each type of unwanted signal. The P_d was calculated by dividing the number of counted targets by the total number of targets that were generated.

For Radars A, C and E, observations of the relative strength or brightness of the targets displayed on the PPI were performed and documented at the various *I*/*N* levels. The nature of the effect of the interference on Radars A, C, and E target displays prevented performing an actual "count" of the targets because all of the targets tended to "fade" at the same rate. These effects included a

"dimming" of the targets, an increase in the number of false targets, radial streaks ("strobes"), and an increase in background "speckle" or noise.

6.7 Test Results for Maritime Radionavigation Radars

6.7.1 Radar A (3 GHz)

Figure 42 shows a digital photograph of Radar A's PPI baseline operating state (no interference injected). Note that the raw-video targets appear along a radial at about 320 degrees. Local clutter returns from buildings and slight speckling are also visible on the radar display.

Observations of video image targets on the radar's PPI display were made with emissions from the QPSK generator applied to its receiver. The power level of the QPSK emission was adjusted until the appearance of the radar's PPI was in a baseline condition. The power level of the QPSK waveform was adjusted within a range of values to find the level where the QPSK emissions did not adversely affect the performance of the radar in displaying video targets. Figures 43 and 44 are photographs of the radar's PPI that show the effects of the QPSK waveform at power levels of -112 and -102 dBm (measured within a 3-MHz bandwidth), respectively. The radar's receiver noise power was approximately -104 dBm. The resulting I/N ratios were -8 dB and +2 dB.

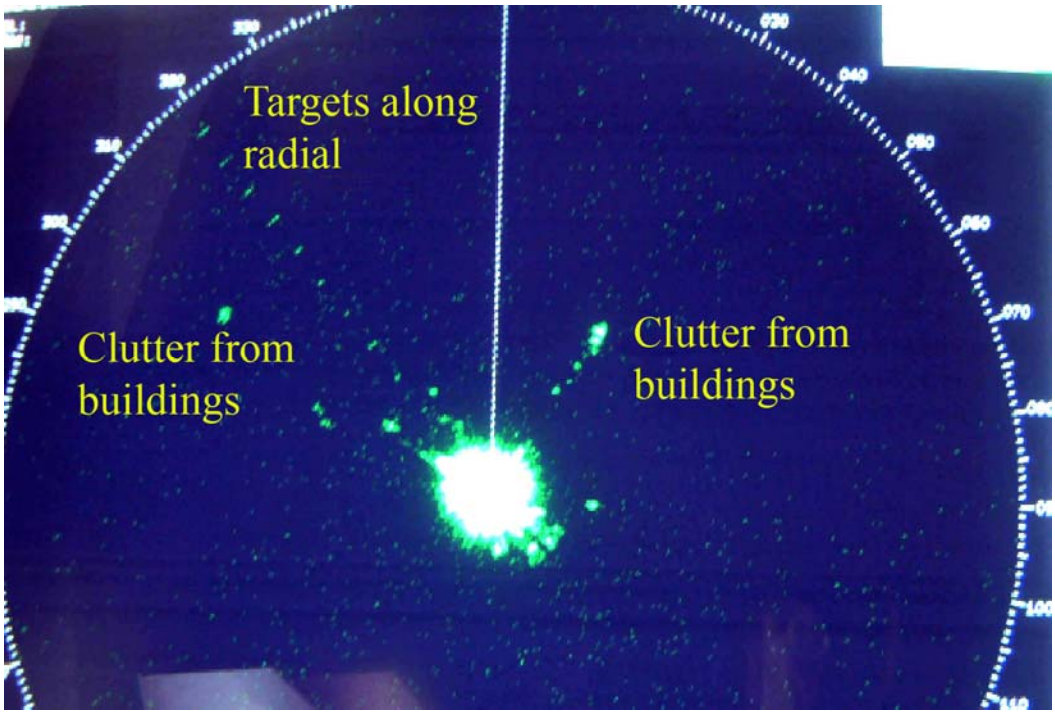

Figure 42. Radar A baseline state (no interference) with video targets.

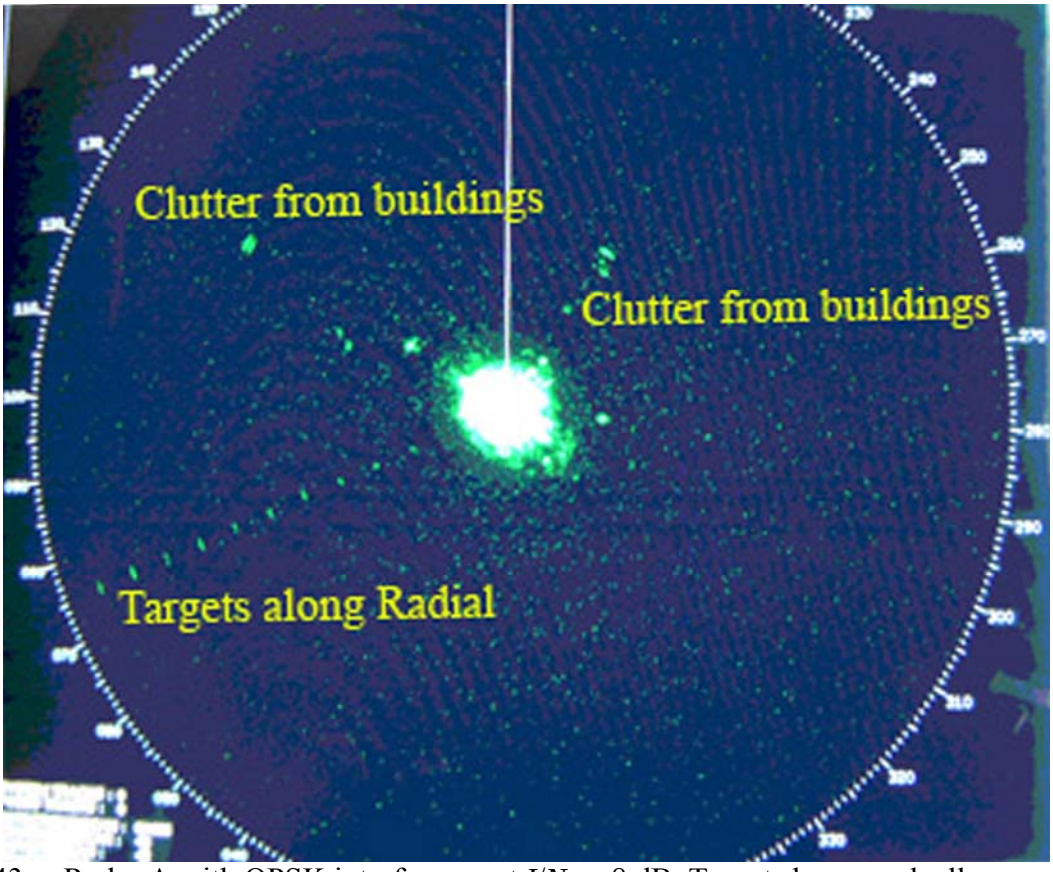

Figure 43. Radar A with QPSK interference at I/N = -8 dB. Targets have gradually precessed on the display since the time that the picture of Figure 42 was taken.

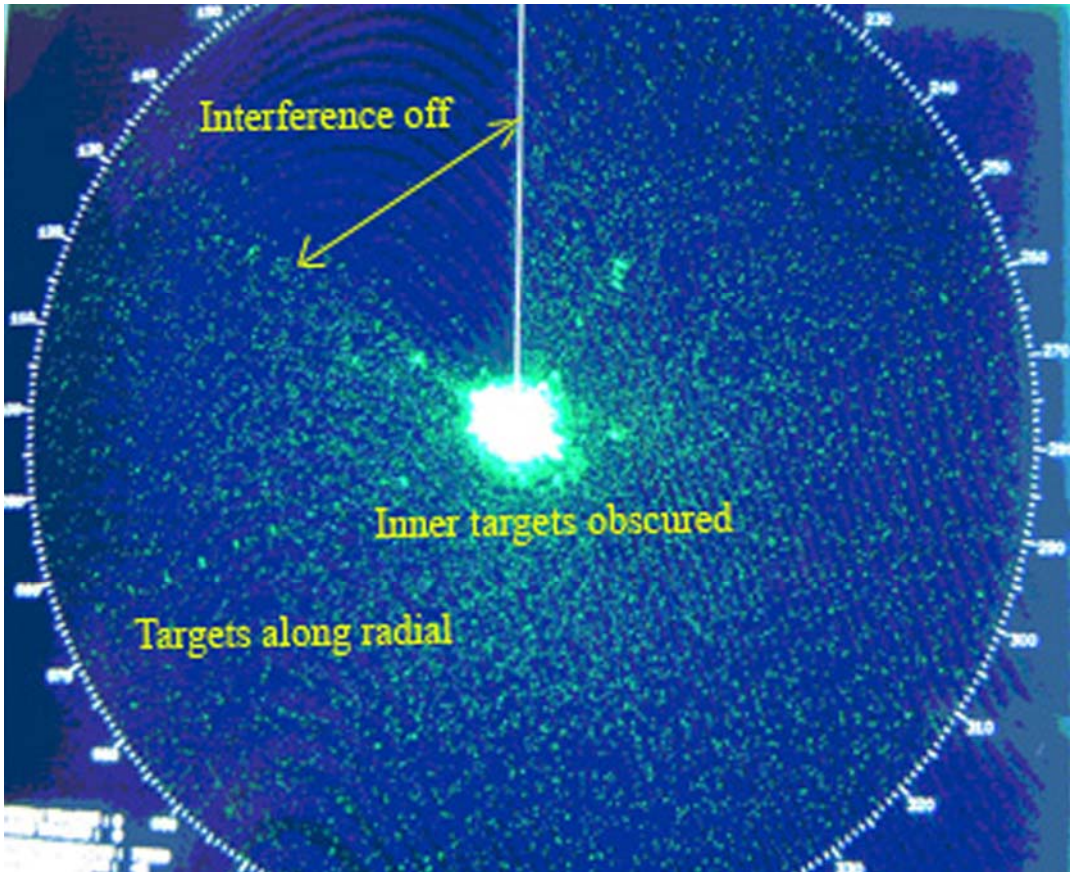

Figure 44. Radar A with QPSK interference at *I*/*N* = +2 dB. Targets are on same radial as in Figure 43. Interference was turned off during the indicated segment of the scan at upper left. The black lines (Moiré pattern) in that sector were not present on the radar screen; they are an artifact of the reproduction of this image.

Table 24 summarizes the results for Radar A. The images show that the QPSK emissions caused an increase in the background noise or speckle. In comparing Figure 41, which is the radar baseline state without interference, to Figure 42 (which has an *I*/*N* of -8 dB) the background speckle has increased but the targets are still detected and displayed. In Figure 44 the *I*/*N* is +2 dB and the QPSK emissions have increased the background noise to the extent that the targets are becoming indistinguishable from the speckle.

Table 24. Radar A Responses to QPSK Interference

***I*/*N* Ratio of Interference**	**Effect**
-8 dB	Slight increase in background speckle; targets distinguishable
-7 dB	More increase in background speckle; targets distinguishable
-6 dB	Target visibility degraded due to increasing speckle effect
+2 dB	Targets becoming indistinguishable from background speckle

The power level of the QPSK emissions was adjusted to find the point where the video targets were still clearly visible and the background speckle was similar to the baseline level. That power level was found to be about -111 dBm at the receiver input, for an *I*/*N* ratio of about -7 dB.

It is important to note that the test targets on the radial are more visible than "real world" targets that would be distributed anywhere on the radar's PPI. Therefore, care needs to be taken in interpreting radar presentations in the presence of noise. The *I*/*N* values were not based on one specific photograph *per se*. The photographs in this report are representative of the interference condition. Some of the radar's scans might show a worse state (denser speckle/false targets) while others might show a better state (clearer PPI) at the same *I*/*N* level. Approximately 20 scans were observed at each *I*/*N* level in choosing the *I*/*N* values represented in Figures 42 through 44.

6.7.2 Radar B (3 GHz)

For Radar B it was possible to observe the effect that the unwanted signals had on individual targets. For each unwanted signal, it was possible to count the decrease in the number of targets that were visible on the PPI as the *I*/*N* level was increased. Target counts were made at each *I*/*N* level for each type of interference. A baseline target P_d count was performed before the beginning of each test. The results of the tests on Radar B are shown in Figure 45, which shows the target P_d versus the *I*/*N* level for each type of interference. The baseline P_d in Figure 45 is 0.93 with the 1-sigma error bars 0.016 above and below that value. Note that each point in Figure 45 represents a total of 500 desired targets.

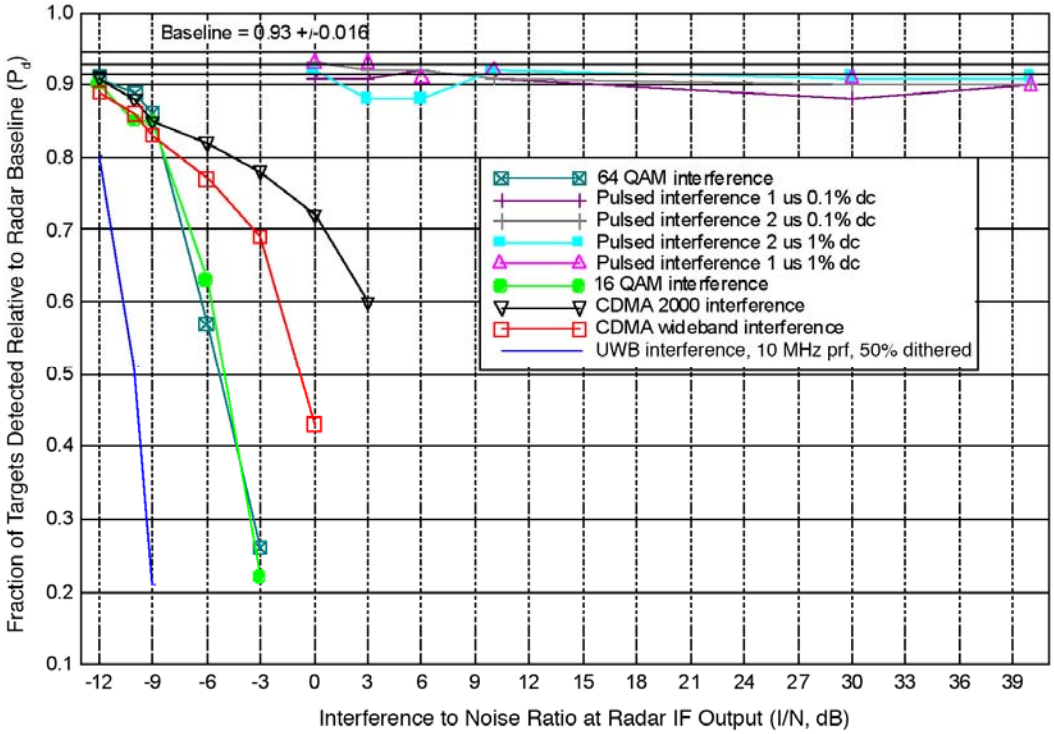

Figure 45. Radar B P_d curves.

Figure 45 shows that, except for the case of the pulsed interference, the target P_d was reduced below the baseline P_d used in these tests minus the standard deviation for *I*/*N* values above -12 dB for all of the unwanted signals that used a digital modulation. The QAM interference caused the quickest drop in the P_d as the *I*/*N* was increased. Data was not taken for higher *I*/*N* values above of -3 dB for QAM because all of the targets were gone on the PPI above that level. The CDMA 2000 had the least effect on the target P_d, but it was still causing a drop in the target P_d at *I*/*N* values above -12 dB.

The performance of Radar B was highly robust against in the presence of pulsed interference up to *I/N* levels of +39 dB. The low duty cycle of the pulsed interference allowed the radar's interference rejection mechanism (which relies on non-coherence between the desired and the undesired pulse repetition sequences) to work effectively.

6.7.3 Radar C (3 GHz)

For Radar C it was difficult to count the decrease in target P_d as the interference was injected into the radar's receiver. The interference caused all of the targets to fade at the same rate no matter where they were located in the string of targets. It was not possible to make individual targets "disappear" as the interference power was increased, and count the number of lost targets in order to calculate the P_d. Therefore, the data taken for Radar E reflects whether or not the appearance of all the targets was affected at each *I*/*N* level for each type of interference. The data for Radar C are summarized in Tables 25 and 26.

Table 25. Radar C Responses to Continuous QAM Interference

***I*/*N* Ratio**	**64 QAM**	**16 QAM**
-12 dB	No effect	No effect
-10 dB	No effect	No effect
-9 dB	Targets slightly dimmed	Targets slightly dimmed
-6 dB	Targets dimmed	Targets dimmed
-3 dB	Targets not visible	Targets not visible
0 dB	Targets not visible	Targets not visible
+3 dB	Targets not visible	Targets not visible
+6 dB	Targets not visible	Targets not visible

The data in Table 25 show that the unwanted QAM signals affected the visibility of the targets for Radar C on its PPI at an *I*/*N* level of -9 dB. At that level the brightness of the targets on the PPI was slightly dimmed from their baseline state. At *I*/*N* levels of -6 dB they were dimmed more and for *I*/*N* levels above -3 dB the targets had dimmed so much that they were no longer visible on the PPI display.

The data in Table 26 show that the unwanted CDMA signals affected the visibility of the targets for Radar C on its PPI at an *I*/*N* level of -6 dB. At that level the brightness of the targets on the

PPI was noticeably dimmed from their baseline state. At *I*/*N* levels of -3 dB and above, the targets had dimmed so much that they were no longer visible on the PPI.

For Radar C, the gated 2.0 and 1.0 μs pulsed interference with duty cycles of 0.1 and 1.0 percent did not affect the visibility of the targets on the PPI at the highest *I*/*N* level, which was 40 dB.

Table 26. Radar C Responses to Gated CDMA Interference

***I*/*N* Ratio**	**W-CDMA**	**CDMA-2000**
-12 dB	No effect	No effect
-10 dB	No effect	No effect
-9 dB	No effect	No effect
-6 dB	Targets dimmed	Targets dimmed
-3 dB	Targets not visible	Targets not visible
0 dB	Targets not visible	Targets not visible
+3 dB	Targets not visible	Targets not visible
+6 dB	Targets not visible	Targets not visible

6.7.4 Radar D (9 GHz)

For Radar D it was possible to observe the effect that the unwanted signals had on individual targets. For each unwanted signal, it was possible to count the decrease in the number of targets as the *I*/*N* level was increased. Target counts were made at each *I*/*N* level for each type of interference. A baseline target P_d count was performed before the beginning of each test. The results of the tests on Radar D are shown below in Figure 46 with the target P_d versus the *I*/*N* level for each type of interference. The baseline is shown at a P_d of 0.92 with the 1-sigma error bars 0.016 above and below. Note that each point in Figure 46 represents a total of 500 desired targets.

The performance of Radar D was highly robust against in the presence of pulsed interference up to *I/N* levels of +39 dB. The low duty cycle of the pulsed interference allowed the radar's interference rejection mechanism (which relies on non-coherence between the desired and the undesired pulse repetition sequences) to work effectively.

The data in Figure 46 show that, except for the case of the pulsed interference, the target P_d was reduced below the baseline P_d used in these tests minus the standard deviation for *I*/*N* values above -12 dB for the unwanted CDMA signal.

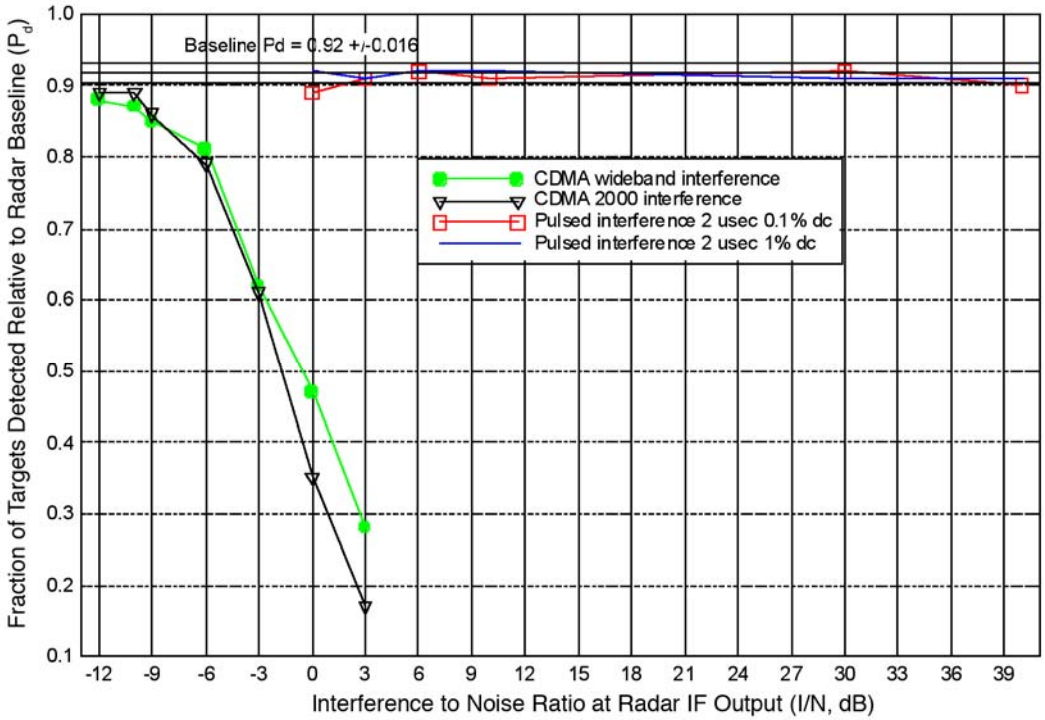

Figure 46. Radar D P_d curves.

6.7.5 Radar E (9 GHz)

As in the case of Radar C, for Radar E it was difficult to count the decrease in target P_d as the interference was injected into the radar's receiver. The interference caused all of the targets to fade at the same rate no matter where they were in the string of targets. It was not possible to make individual targets "disappear" as the interference power was increased. Therefore, the data taken for radar E reflects whether or not the appearance of all the targets was affected or not at each *I*/*N* level. The data for Radar E are summarized in Table 27.

Table 27. Radar E Responses to Gated CDMA Interference

***I*/*N* Ratio**	**WB CDMA**	**CDMA-2000**
-12 dB	No effect	No effect
-10 dB	No effect	No effect
-9 dB	No effect	No effect
-6 dB	Targets dimmed	Targets dimmed
-3 dB	Targets dimmed	Targets dimmed
0 dB	Targets not visible	Targets not visible
3 dB	Targets not visible	Targets not visible
6 dB	Targets not visible	Targets not visible

The data in Table 27 show that the unwanted CDMA signals affected the visibility of the targets for Radar E on its PPI at an *I*/*N* level of -6 dB. At that level the brightness of the targets on the PPI was noticeably dimmed from their baseline state. At *I*/*N* levels of 0 dB and above, the targets had dimmed so much that they were no longer visible on the PPI.

For Radar E, the gated 2.0 and 1.0 µs pulsed interference with duty cycles of 0.1 and 1.0 percent did not affect the visibility of the targets on the PPI at the highest *I*/*N* level, which was 40 dB.

6.7.6 Radar F (9 GHz)

The test results for the maritime radionavigation Radar F are contained in Table 28. The table shows that the radar did not suffer any degradation to its performance with any of the chirped or phase-coded waveforms up to an *I/N* of +40 dB. For the unmodulated pulses the radar did not suffer any degradation at an interference duty cycle of 5 percent and an *I/N* of +40 dB. At the higher duty cycles for the unmodulated radiolocation waveform, the radar produced a strobe on the PPI display at the target azimuth when the *I/N* exceeded +20 dB. At lower *I/N* ratios the strobe on the PPI was transformed into an increase in the amount of false targets or speckle. These effects are shown in photographs of the radar's PPI in Figures 47 and 48. These photographs are representative examples of the PPI condition; there was variation from scan-to-scan in the number of false targets.

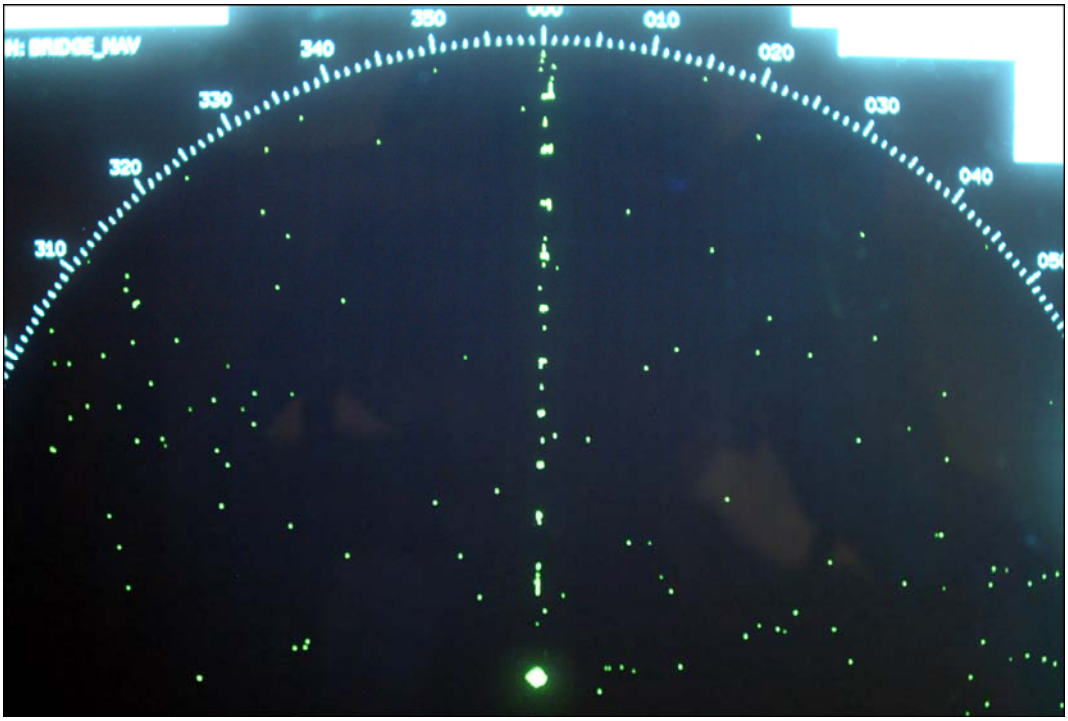

Figure 47. 1-µs pulsed interference at 7.5% duty cycle and *I/N*= +40 dB.

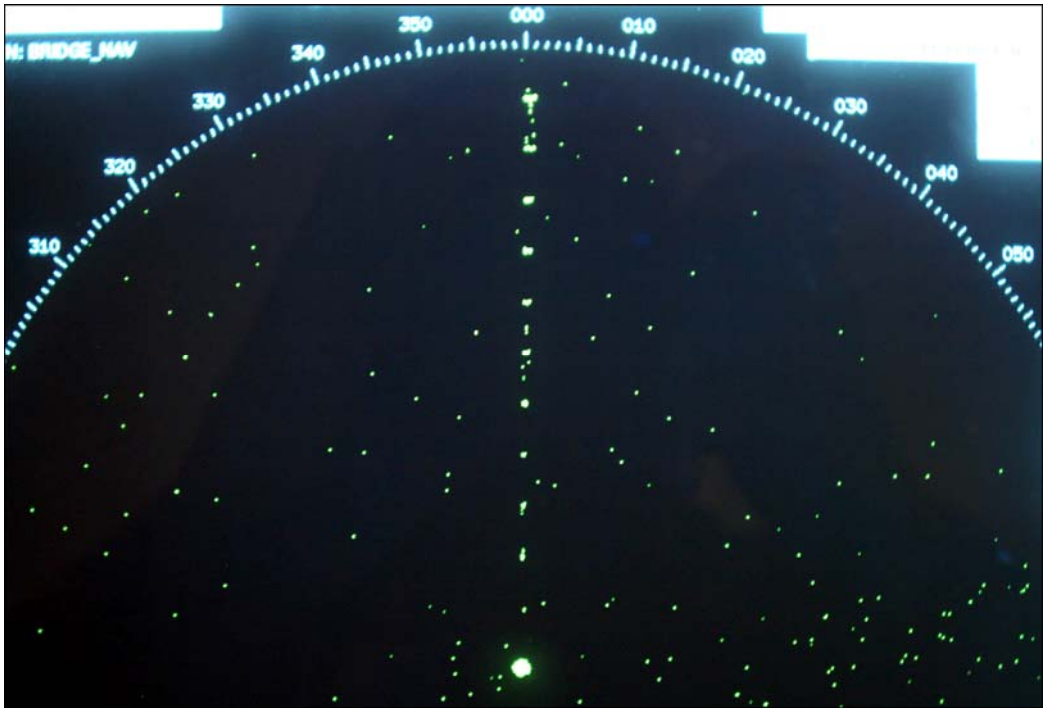

Figure 48. 1-μs pulsed interference at 7.5% duty cycle and *I/N*= +12 dB.

Regarding Figures 47-48, the observers knew in advance where the targets would be displayed and that knowledge made it easier for them to distinguish the targets from interference speckling. Radar operators viewing ordinary targets in an operational environment would not have that condition available to them, making the targets harder to distinguish from background speckle (as seen off the target radial) in these in real-world scenarios. The off-radial speckling is due to random radar receiver noise.

For the OFDM interference (Figures 49-50), the effects on the PPI were noticeable at *I/N* = +3 dB as false targets, and strobes were produced above that *I/N* value. At *I/N* values of 0 dB and -3 dB, the radar's CFAR circuitry performed exactly as it was supposed to, reducing the P_d as the overall noise level increased. (The OFDM signal would appear to the radar as broadband noise.) At *I/N* = 0 dB the P_d was 0.83 and at *I/N* = -3 dB the P_d was 0.85. At *I/N* = -6 dB the radar appeared to have recovered to its baseline state. This response demonstrates that the radar was able to reject most of the pulsed interference, but it did not effectively mitigate the OFDM interference effects.

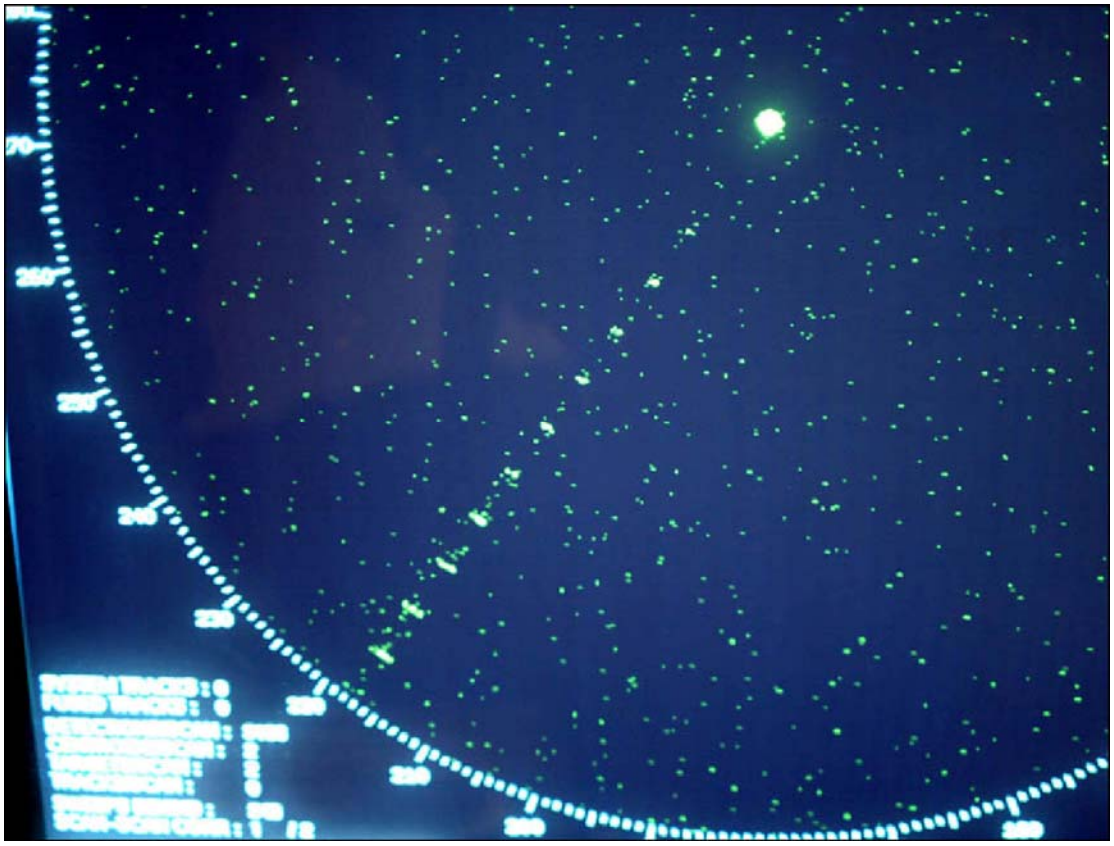

Figure 49. OFDM interference effect at *I/N*= +3 dB.

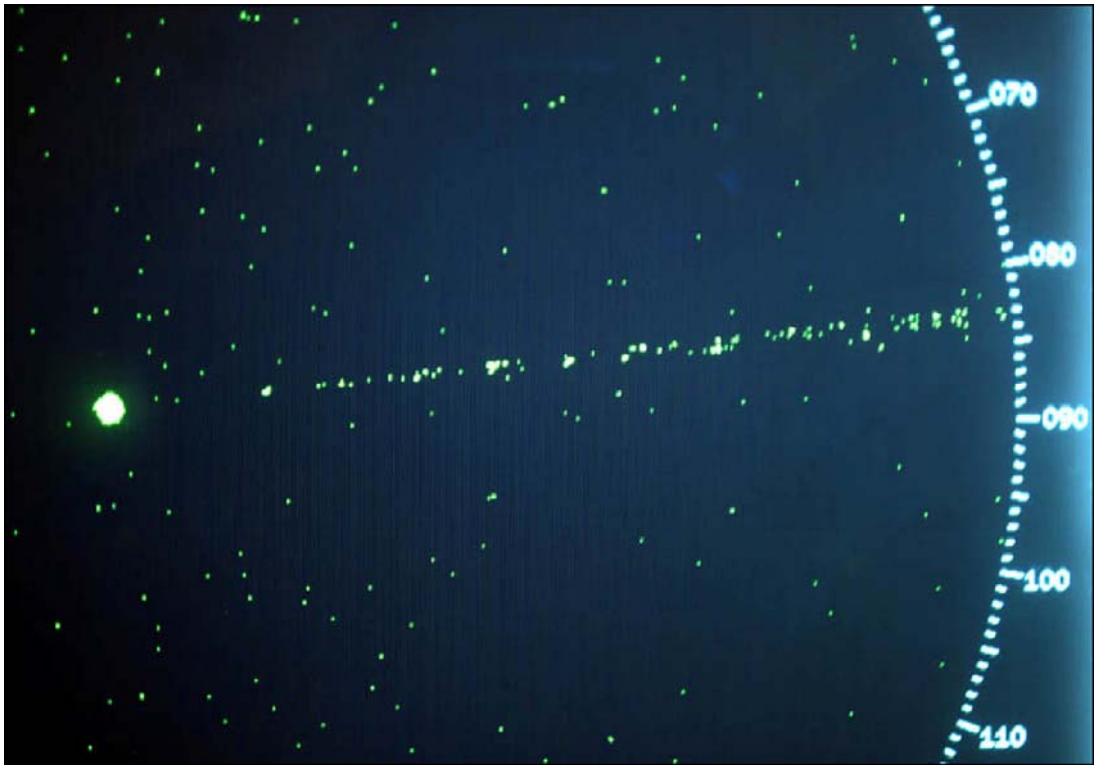

Figure 50. OFDM interference effect at *I/N*= +6 dB.

6.7.6.1 Radar F with Fluctuating Targets

Interference tests were performed with the targets fluctuating in power as described in 2.4.1 of this report using an OFDM interference source. The results showed that there was a small gain in the target P_d at low I/N levels when the target power fluctuated "upwards" (scans 1-5, 9-12, and 14 in Table 21). That is, the target P_d increased because the target power was above the level that produced the P_d of 0.90 percent. However, this effect has limits. When the *I/N* value was around 0 to 3 dB, an increase in target power *did not* further enhance the target P_d even when the target power increased to the higher values in Table 3. This was the effect even when the target power was increased to its maximum Swerling value of 7.3 dB (scan 14 in Table 21) above the baseline power level.

Conversely, when the target power fluctuated "down" from the baseline value that produced the P_d of 0.90 percent, the targets were already weak and the interference made them disappear. In fact, when the target power was only 1.7 dB (scan 7 in Table 21) below the baseline state, the targets were severely degraded without interference. When the interference was injected at low *I/N* levels, the targets disappeared.

Table 28. Radar F Responses to Interference*

Interference Waveform	Effect at Given *I/N* Ratio (dB)									
	-9	-6	-3	0	+3	+6	+9	+12	+20	+40
Chirp 1	None	none	none	none	none	none	none	none	none	none
Chirp 2	None	None	None	None	None	None	None	None	None	none
Chirp 3	None	None	None	None	None	None	None	None	None	None
Chirp 4	None	None	None	None	None	None	None	None	None	None
Chirp 5	None	None	None	None	None	None	None	None	None	None
Chirp 6	None	None	None	None	None	None	None	None	None	None
Chirp 7	None	None	None	None	None	None	None	None	None	None
Phase1	None	None	None	None	None	None	None	None	None	None
Phase2	None	None	None	None	None	None	None	None	None	None
Unmod pulsed 1	None	None	None	None	None	None	None	None	None	None
Unmod pulsed 2	None	None	None	None	None	None	None	None	None	None
Unmod pulsed 3	None	None	None	None	None	None	None	None	None	None
Unmod pulsed 4	None	None	None	None	None	None	None	None	None	None
Unmod pulsed 5	None	None	None	None	None	None	None	False targets	strobe	strobe
Unmod pulsed 6	None	None	None	None	None	None	None	False targets	strobe	strobe
Unmod pulsed 7	None	None	None	None	None	None	False targets	False targets	strobe	strobe
OFDM	P_d= 0.93	P_d= 0.90	P_d= 0.85	P_d= 0.83	False targets	strobe	strobe	strobe	strobe	strobe

* When no effect is indicated, the interference P_d was within ±3 percent of the baseline P_d, and the number of false targets or "speckle" was at the baseline state as well.

The results of these tests with fluctuating targets have demonstrated that:

- Trying to establish interference criteria using fluctuating targets is pointless because changing the *I/N* value while changing the target power only leads to an uncontrolled experiment without a baseline measure or state;

- Adding target power to the radar can only help at low values of *I/N* levels even when the target power is increased to 7.3 dB above the baseline state. Once the interference causes a high increase of false targets and strobing, the radar cannot recover the targets even when the target power increases to its maximum Swerling Case 1 value.

Both of these points are very important and the second one is a key element for radar analyses. There is currently a misconception that by merely increasing the target power, a radar can overcome any level of interference. These test results have disproved that assumption. It *would* be true if target power were adjusted along with detection levels, but that would tantamount to building a new radar with a more powerful transmitter or a bigger antenna.

6.8 UWB Interference Tests on a Maritime Radar

This section describes the results of UWB interference susceptibility tests that were performed on maritime radionavigation Radar A. The purpose of the tests was to inject impulse UWB interference into the radar's receiver and observe and document the degradation of the radar's performance as the power level of the UWB signal in the radar receiver was varied. The tests were performed closed-loop, as described above.

6.8.1 UWB Interference Test System

The test system and target generator were the same as described for Radar A in Section 6. These tests used UWB signals with prfs of 100 kHz, 1 MHz, and 10 MHz. The UWB transmitter unit that was used for these tests was supplied by the Time Domain Corporation. This UWB device had been used in previous UWB/GPS testing by NTIA. The UWB pulser was connected to an AWG that provided triggering for dithered and non-dithered UWB waveforms. The RF outputs of the target generator and the UWB pulser were combined and connected to a cable-to-waveguide adapter that was then connected to the mixer input of the radar receiver. In effect, this removed the radar antenna from the system but still allowed for normal operation of the radar. The IF output of the radar was monitored with a spectrum analyzer by connecting to a test point on the receiver circuit board.

6.8.2 UWB Interference Test Parameters

The RF power output of the target generator system was adjusted so that the target P_d was as close as possible to 0.90 without UWB interference being present. This value was approximately -90 dBm at the waveguide input of the receiver. Figure 42 shows a photograph of the baseline operating state of the radar. The targets appear along a radial, and local clutter returns from buildings are visible on the radar display.

The IR feature of the radar was activated for these tests. The STC and FTC functions were turned off and the auto gain function was selected. This configuration is a normal operating mode for the radar, as confirmed by USCG personnel who are certified to operate the radar on Coast Guard vessels.

6.8.3 UWB Test Method

The power of the target generator was held at a constant -90 dBm at the waveguide input. The UWB signal power was varied with an adjustable attenuator and was gated to coincide with the target radial. This simulated the radar's mainbeam sweeping across a UWB device. The radar display was then observed for interference effects. UWB interference effects were documented with digital photographs of the ppi. Between tests, the interference power was reduced until the radar returned to baseline operation.

6.8.4 UWB Test Results

The test results for each UWB prf are discussed below. Overall, the results showed that for moderate UWB power levels, the UWB interference caused strobes along the radial of the targets. The targets were impossible to distinguish within the strobes when the UWB interference occurred. As the UWB power was decreased, the strobes become less intense and at some point transformed into numerous false targets. So the effect of the UWB interference at low levels was an increase in the false targets, while at higher levels the desired targets were masked altogether. Figures 51-65 show the PPI display under various interference circumstances. The results showed that for dithered UWB waveforms, independent of the UWB prf, the maximum allowable UWB power in the radar receiver which would let the radar operate at the baseline performance level was about -115 dBm/MHz (root mean square (RMS) average power detected).

6.8.5 Effect of UWB Interference on Synthetic Targets

Figures 66-68 show radar PPI displays with synthetic targets in the presence of UWB interference. As shown in those figures, UWB interference was observed to suppress synthetic targets on desired targets while generating false synthetic targets at other locations on the display. Synthetic target generation did not perform well in the presence of UWB interference.

6.8.6 Comparison to *I/N* Values

The noise power of the radar receiver for an IF bandwidth of 3 MHz and noise figure of 5.3 dB is -104 dBm. In a 1-MHz bandwidth this is about -109 dBm/MHz. The maximum allowable UWB power was about -115 dBm/MHz, equating to an *I/N* of -6 dB to -7 dB. This value matches the interference threshold used in the UWB analyses in [23].

6.8.7 Additional Observations on UWB Interference Effects

Adding more power to the desired targets, i.e., making the targets "stronger," did not help the radar overcome the effects of UWB interference. When the target power was increased by 3 dB the UWB interference still caused false targets to appear. This effect is shown in Figures 66-67. The UWB interference did not resemble clutter returns.

6.9 Summary of Interference Effects on Maritime Radars

The results of interference tests on maritime radionavigation radars show that when interference with the characteristics of digital communication signal modulations is coupled into these radars at *I*/*N* levels of -6 dB, some of the radars begin to show degradation effects such as dimmed targets, lost targets, or false targets. For maritime radars with logarithmic IF amplifier/detectors (radars A, C, E, and F), these effects began to be manifested at slightly higher *I/N* levels; the targets were either not visible or dimmed at the *I*/*N* levels of -3 dB and -6 dB, as indicated in Tables 24-27 (and Table 28 for OFDM interference into Radar F). The effects of interference on Radars A, C, and E were maximized (i.e., the targets had disappeared from the PPI and no other effects were visible) at *I*/*N* levels between 0 dB and -10 dB. For Radars B and D (which use a logarithmic amplifier and separate video detector), at the *I*/*N* level of -6 dB, the target P_d values dropped below the baseline 1-sigma error. These test results show that at an *I*/*N* of -10 dB, for Radars A, C, and E, the targets were no longer dimmed and for radars B and D, the target P_d values were slightly below the baseline 1-sigma error. For Radar A the synthetic targets required about 2 dB to 3 dB of additional desired signal power compared to the raw-video targets to obtain the same P_d level when operating at a minimum detectable signal level, but the appearance of the targets was not brighter on the PPI display, as shown in Figure 66.

The test results for Radars B, D, and F show that the maritime radars can withstand low-duty cycle, asynchronous pulsed interference at extremely high (+30 dB to +40 dB) *I*/*N* levels due to the inclusion of radar-to-radar interference mitigating circuitry and/or signal processing. The radar-to-radar interference mitigation techniques of scan-to-scan and pulse-to-pulse correlators and CFAR processing [18, 19] have been shown to work well. But the test results show that the same techniques do not mitigate continuous emissions that appear noise-like or CW-like within the radar receiver.

As most maritime radionavigation radars in the 2900-3100 and 9200-9500 MHz bands are very similar in design and operation, it is expected that these test results should apply equally well to other models of marine radars in these bands.

Determining an exact boundary for acceptable levels of interference effects for these types of radars can be somewhat subjective due to such variables as the eyesight and experience of radar operators, possible fatigue due to staring at PPI displays for long periods, and grading of the brightness and distinguishability of the targets relative to the background noise on the PPI displays. But the design of these radars permits no alternative test techniques, and the tests as run do replicate actual operational conditions.

Experienced, trained radar operators may be better able to discern real targets from false targets, interference and/or clutter than inexperienced ones. But for these tests, the radar manufacturers provided radar design engineers and the UK Maritime and Coast Guard Agency (MCA) provided experienced radar operators and instructors. Those personnel all concurred with the results and conclusions of these tests.

The radar could only marginally process out UWB interference and then only at low power levels such as -115 dBm/MHz for a 1-MHz prf signal. This was probably due to the high prf of the UWB signals.[26] UWB interference did not resemble clutter returns.

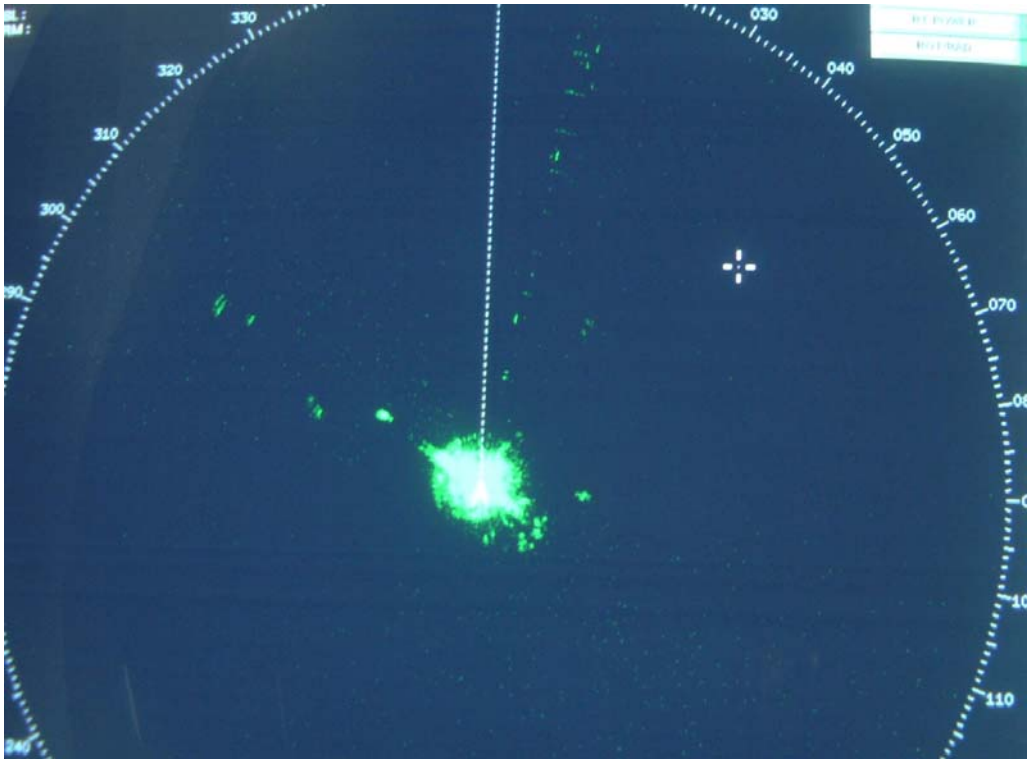

Figure 51. Radar A PPI display with 100-kHz prf gated UWB signal at -85 dBm/MHz (RMS detection).

[26] At high prf values, there is a high probability that a UWB pulse will occur at the beginning of the IR gate and that another UWB pulse will occur at the end of the IR gate.

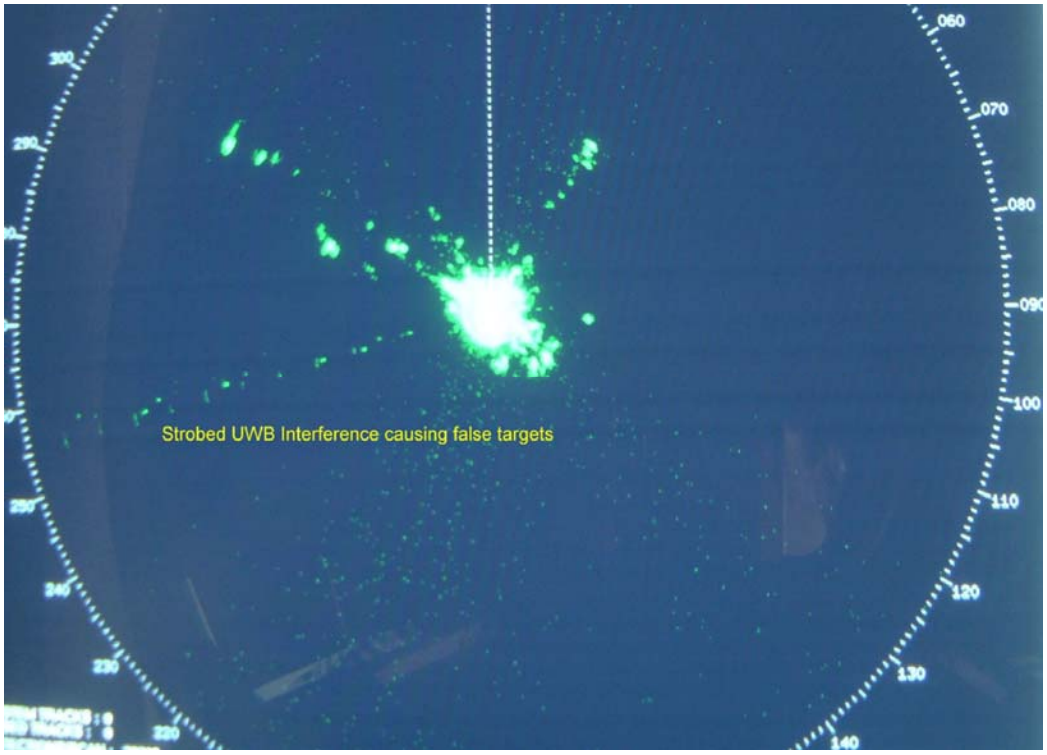

Figure 52. Radar A PPI display with 100-kHz prf gated UWB signal at -95 dBm/MHz (RMS detection).

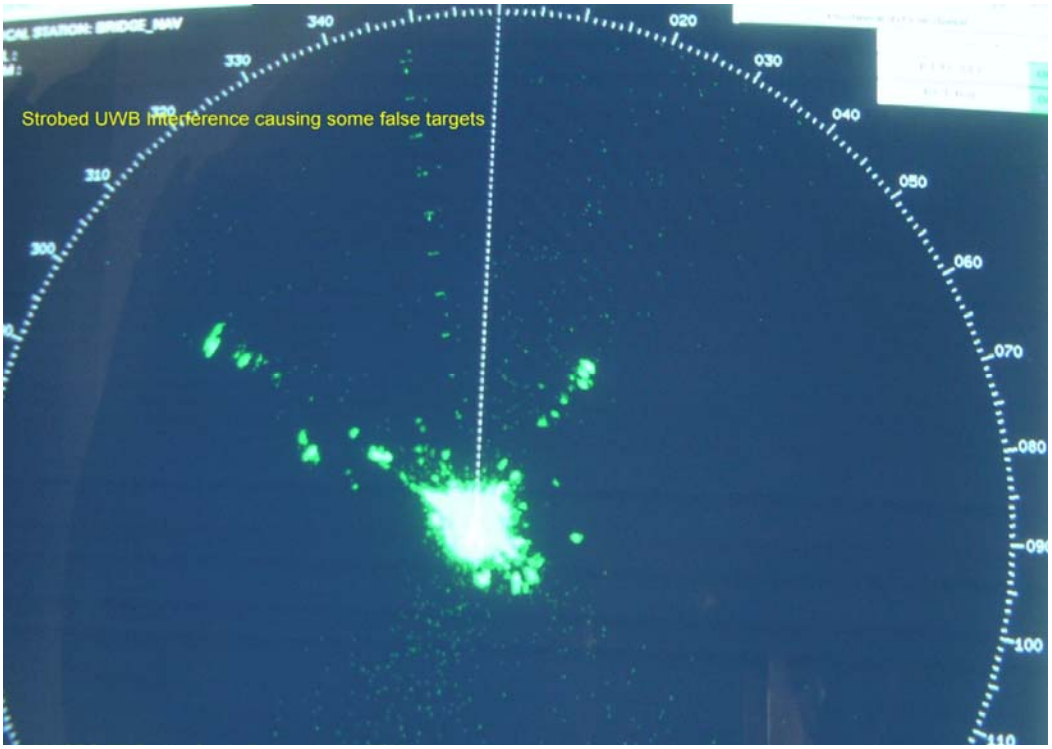

Figure 53. Radar A PPI display with 100-kHz prf UWB signal at -105 dBm/MHz (RMS detection).

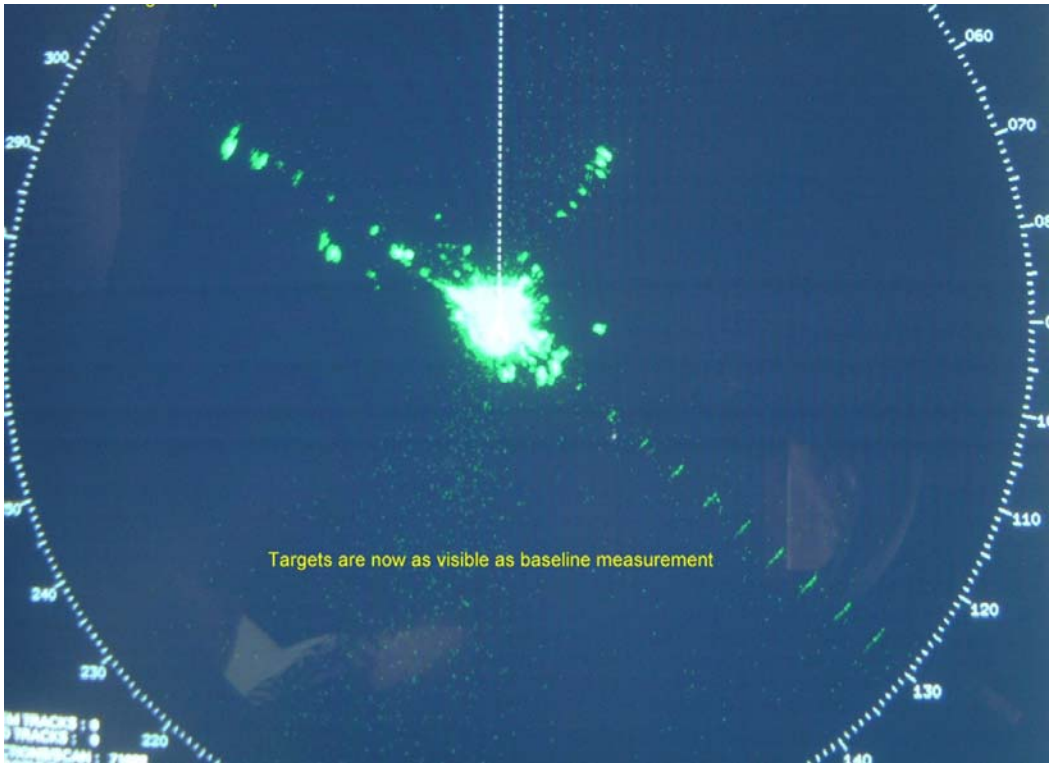

Figure 54. Radar A PPI display with 100-kHz prf UWB signal at -110 dBm/MHz (RMS detection).

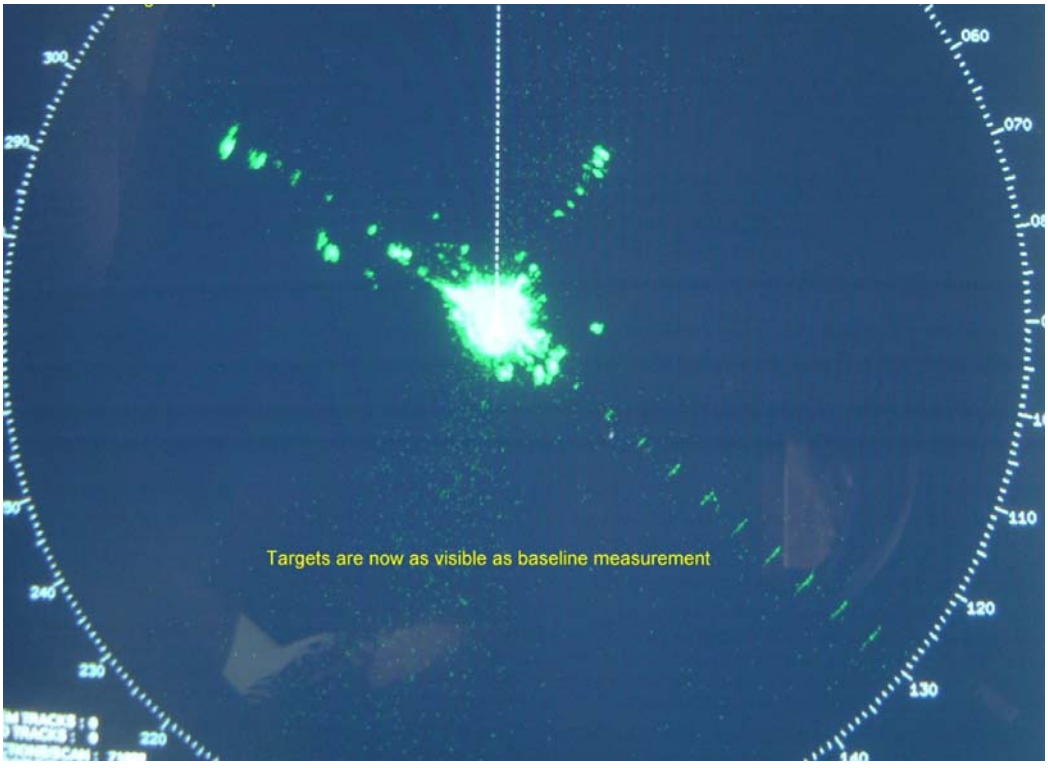

Figure 55. Radar A PPI display with 1-MHz prf UWB signal at -115 dBm/MHz (RMS detection).

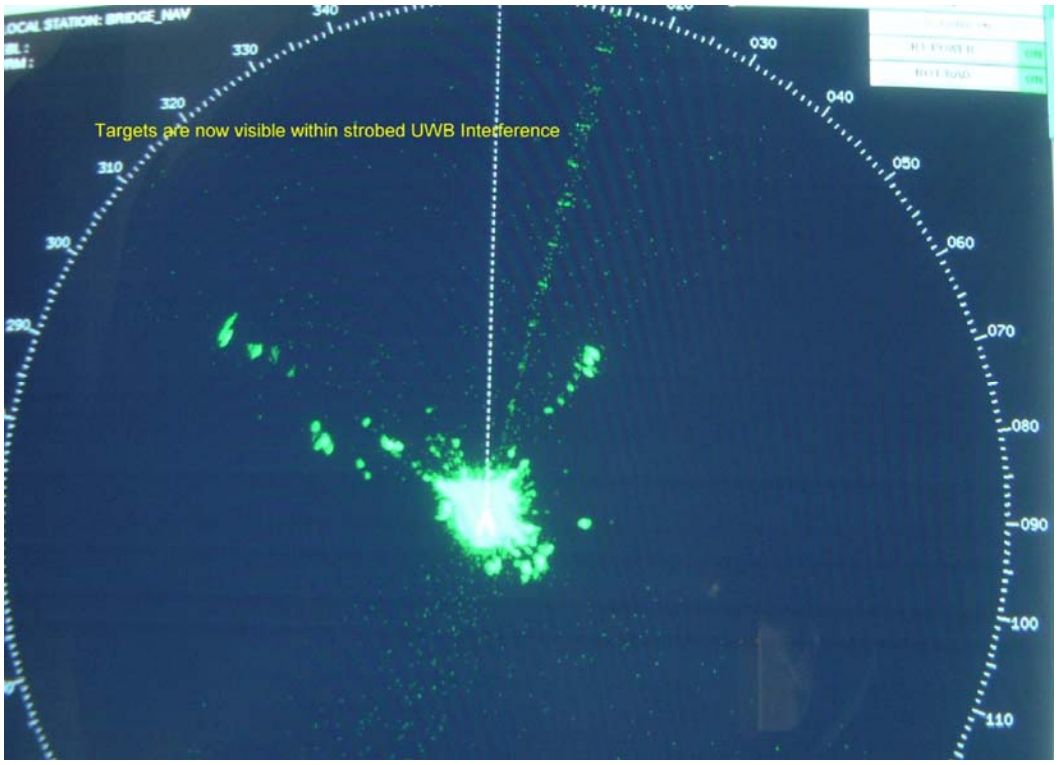

Figure 56. Radar A PPI display with 1-MHz prf UWB signal at -110 dBm/MHz (RMS detection).

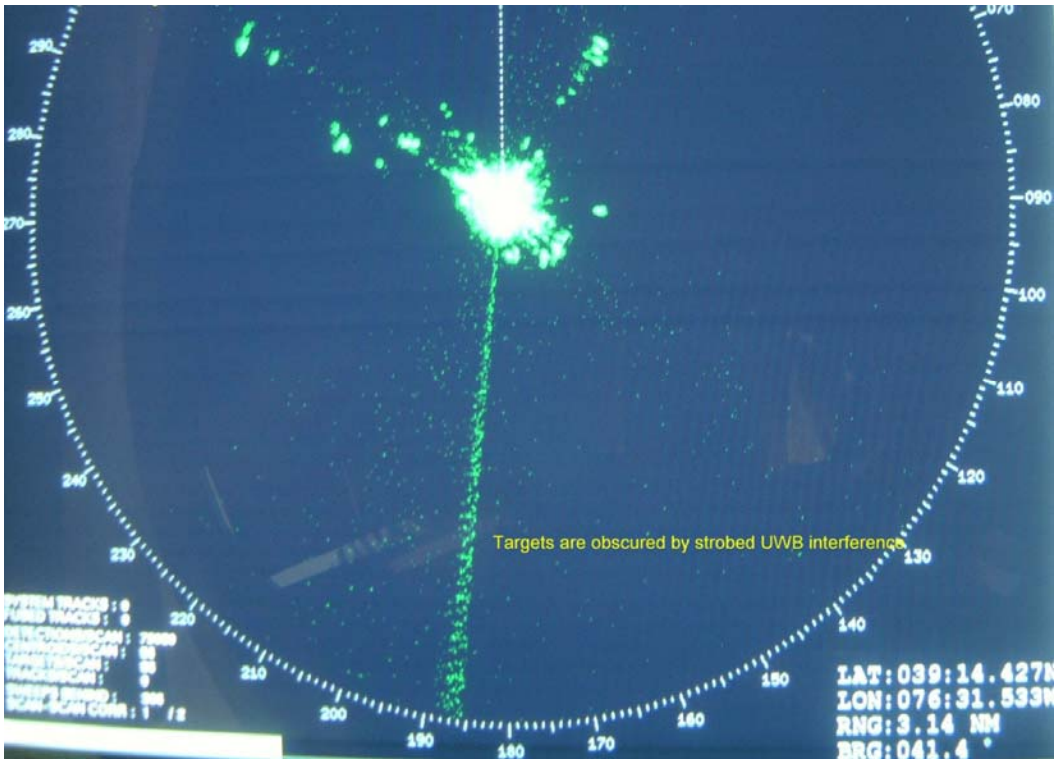

Figure 57. Radar A PPI display with 1-MHz prf UWB signal at -105 dBm/MHz (RMS detection).

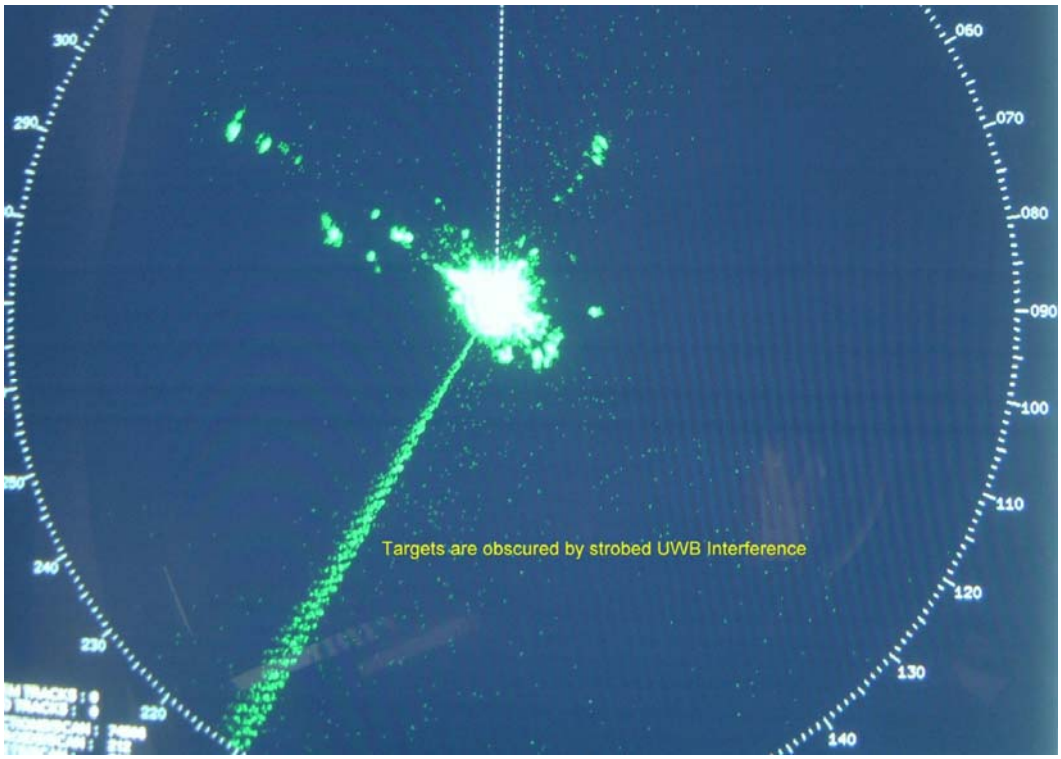

Figure 58. Radar A PPI display with 1-MHz prf UWB signal at -95 dBm/MHz (RMS detection).

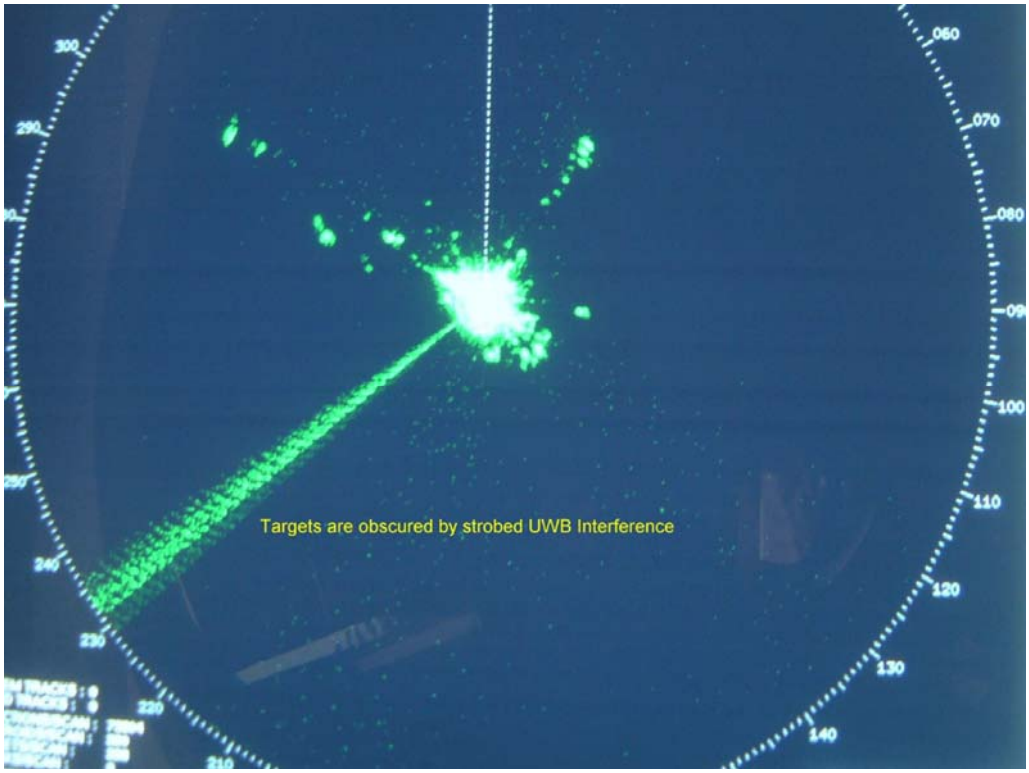

Figure 59. Radar A PPI display with 1-MHz prf UWB signal at -85 dBm/MHz (RMS detection).

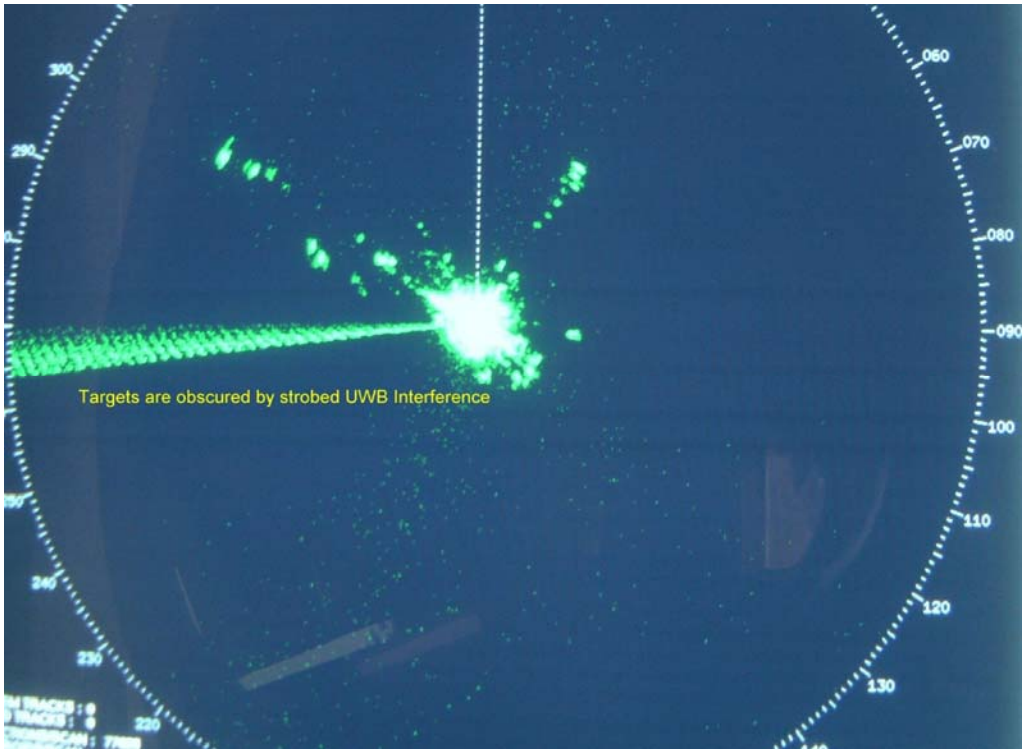

Figure 60. Radar A PPI display with 1-MHz prf UWB signal at -75 dBm/MHz (RMS detection).

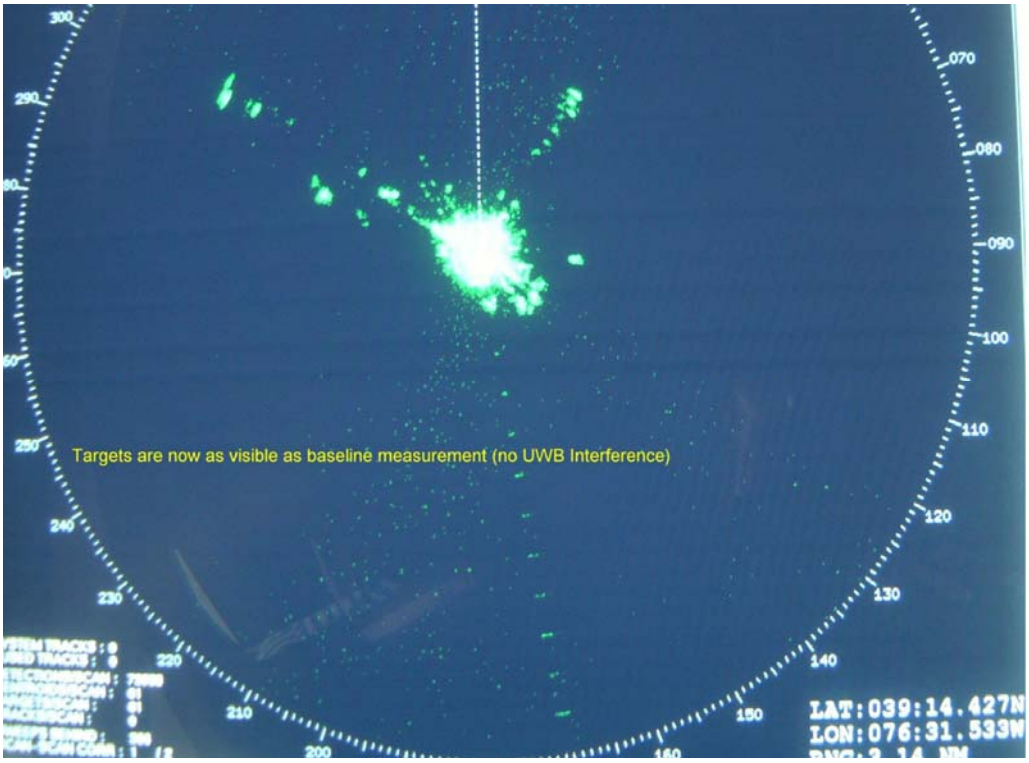

Figure 61. Radar A PPI display with 10-MHz prf UWB signal at -116 dBm/MHz (RMS detection).

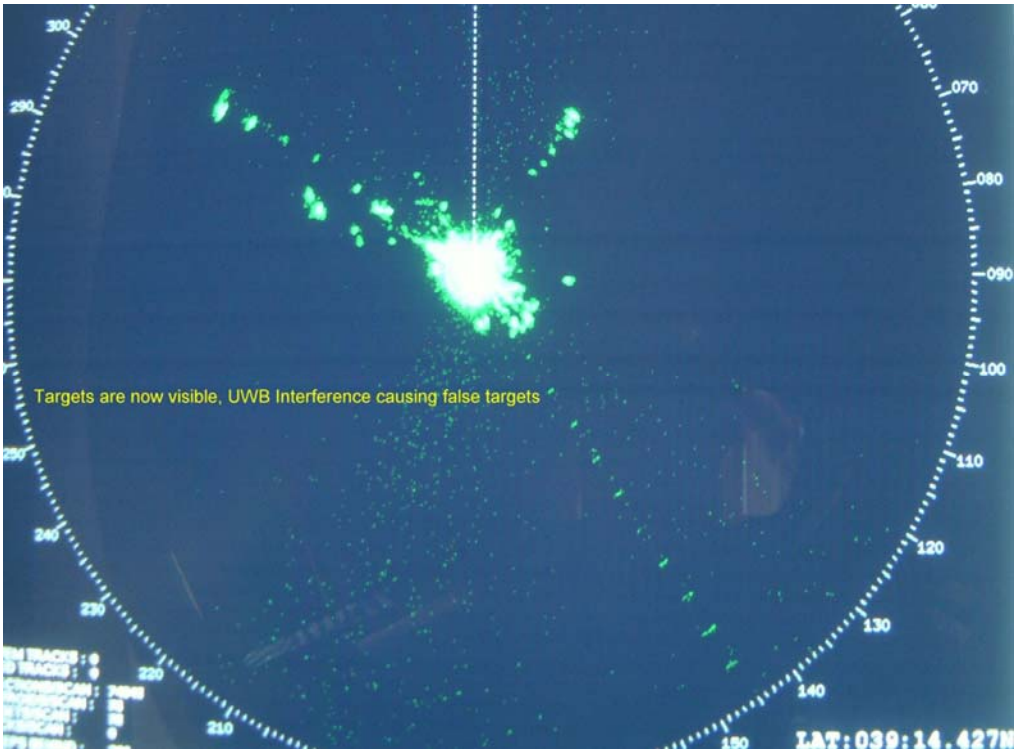

Figure 62. Radar A PPI display with 10-MHz prf UWB signal at -111 dBm/MHz (RMS detection).

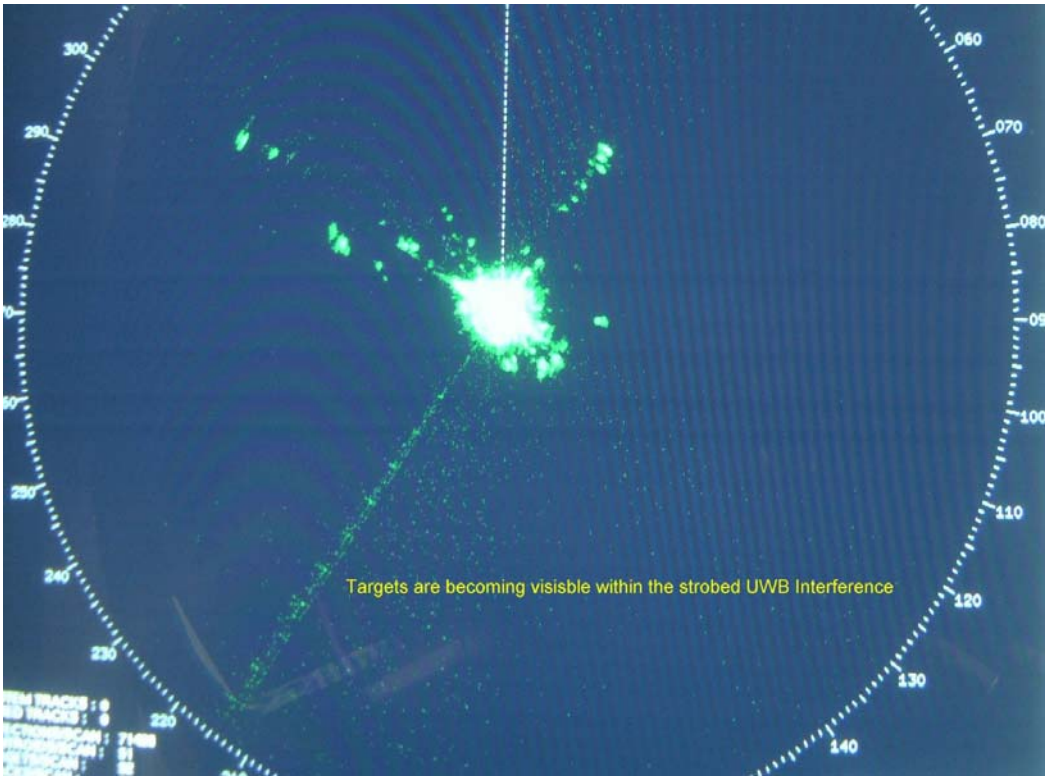

Figure 63. Radar A PPI display with 10-MHz prf UWB signal at -106 dBm/MHz (RMS detection).

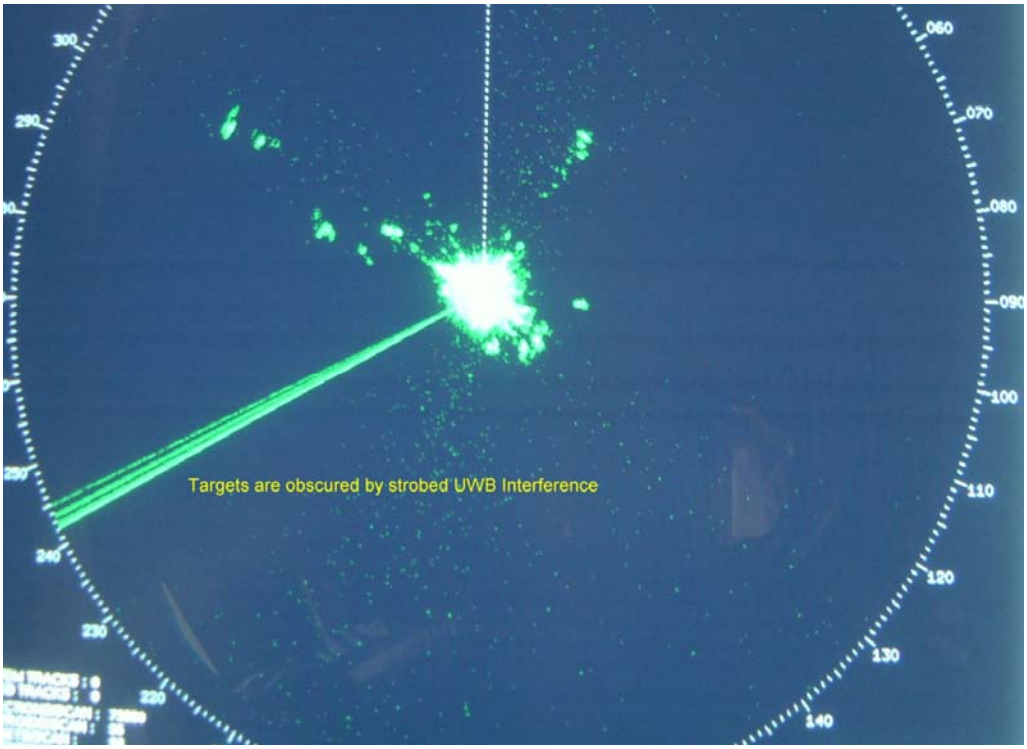

Figure 64. Radar A PPI display with 10-MHz prf UWB signal at -86 dBm/MHz (RMS detection).

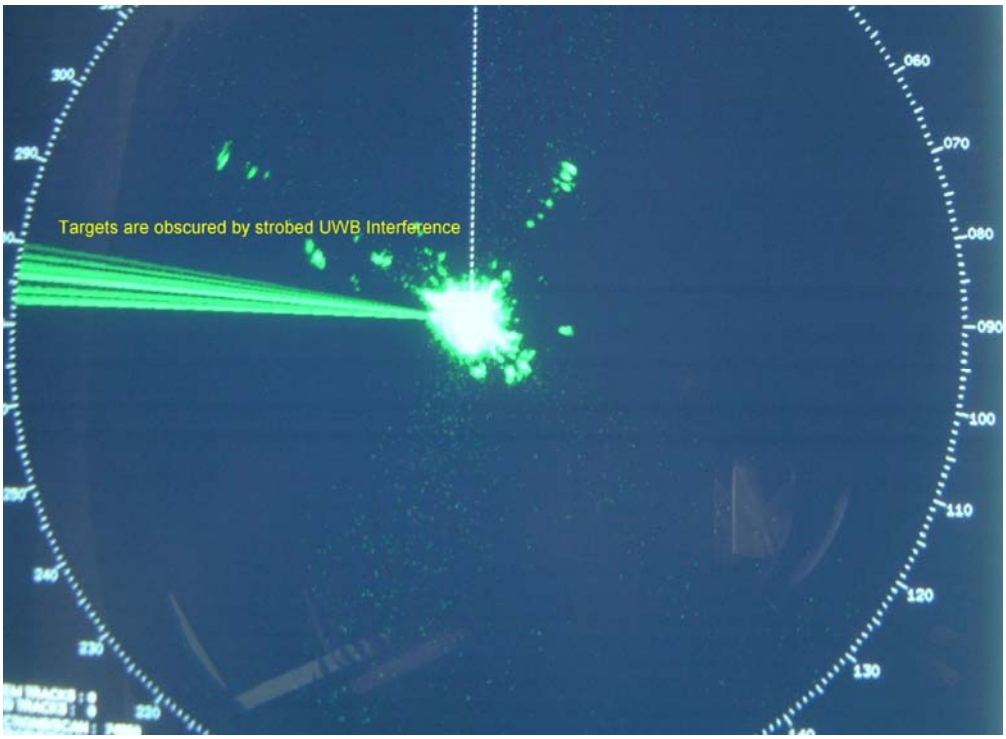

Figure 65. Radar A PPI display with 10-MHz prf UWB signal at -66 dBm/MHz (RMS detection).

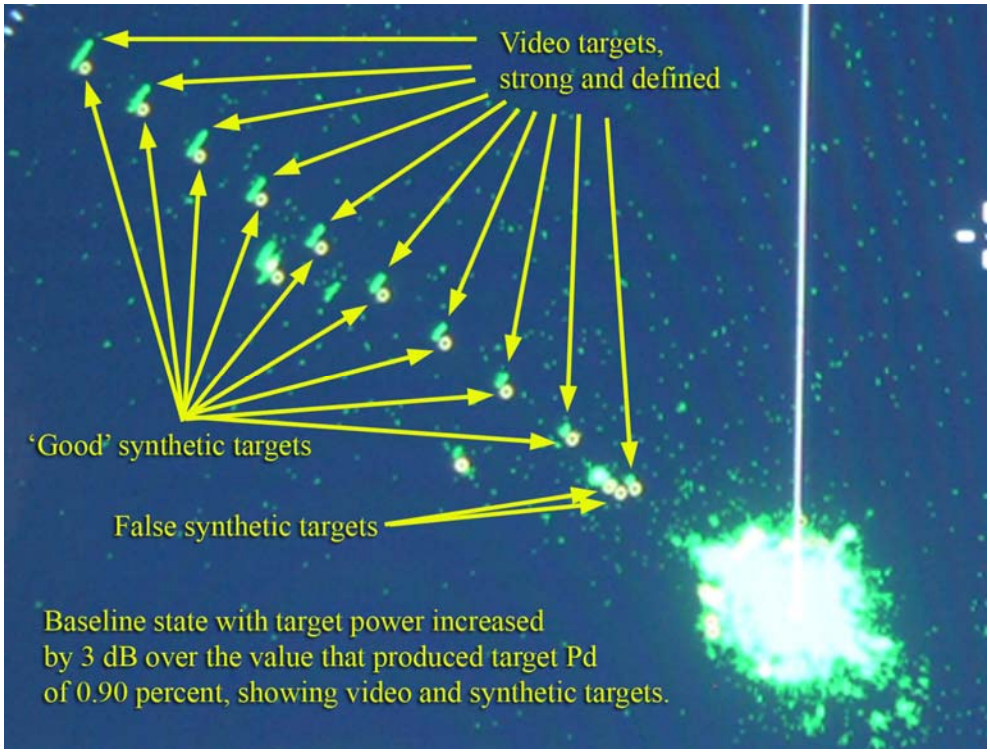

Figure 66. Radar A PPI display with high power video targets and synthetic targets, baseline state (no interference). Compare to Figure 67, which shows more false targets when UWB interference was injected.

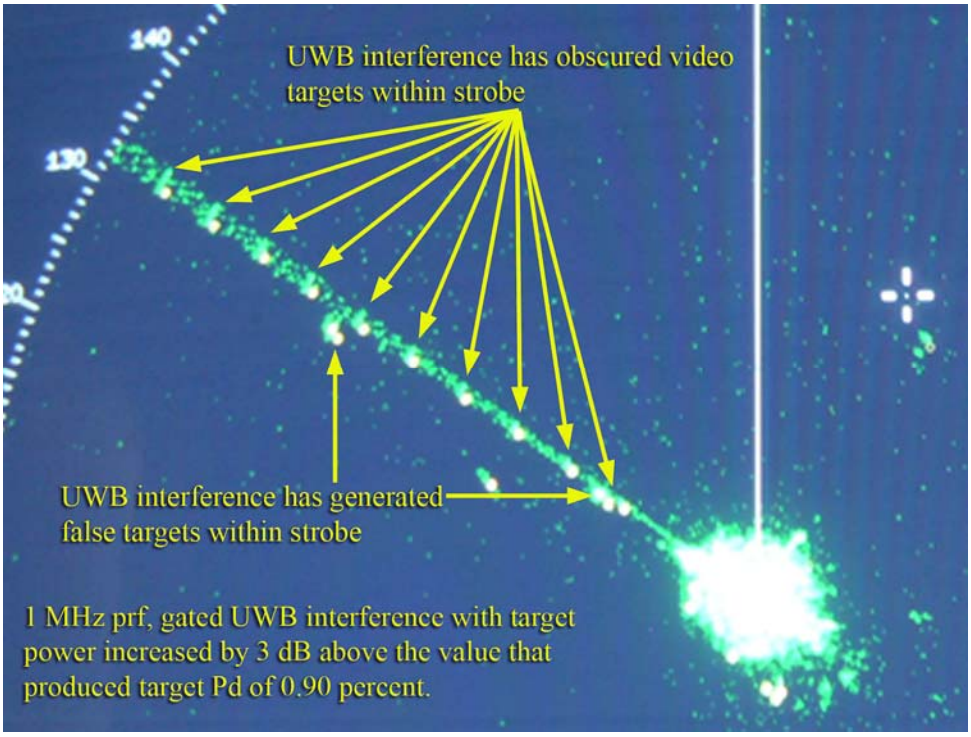

Figure 67. Radar A PPI display with 1 MHz UWB interference suppressing desired raw video targets and synthetic targets while generating false synthetic targets. (Compare to the baseline state of Figure 66.)

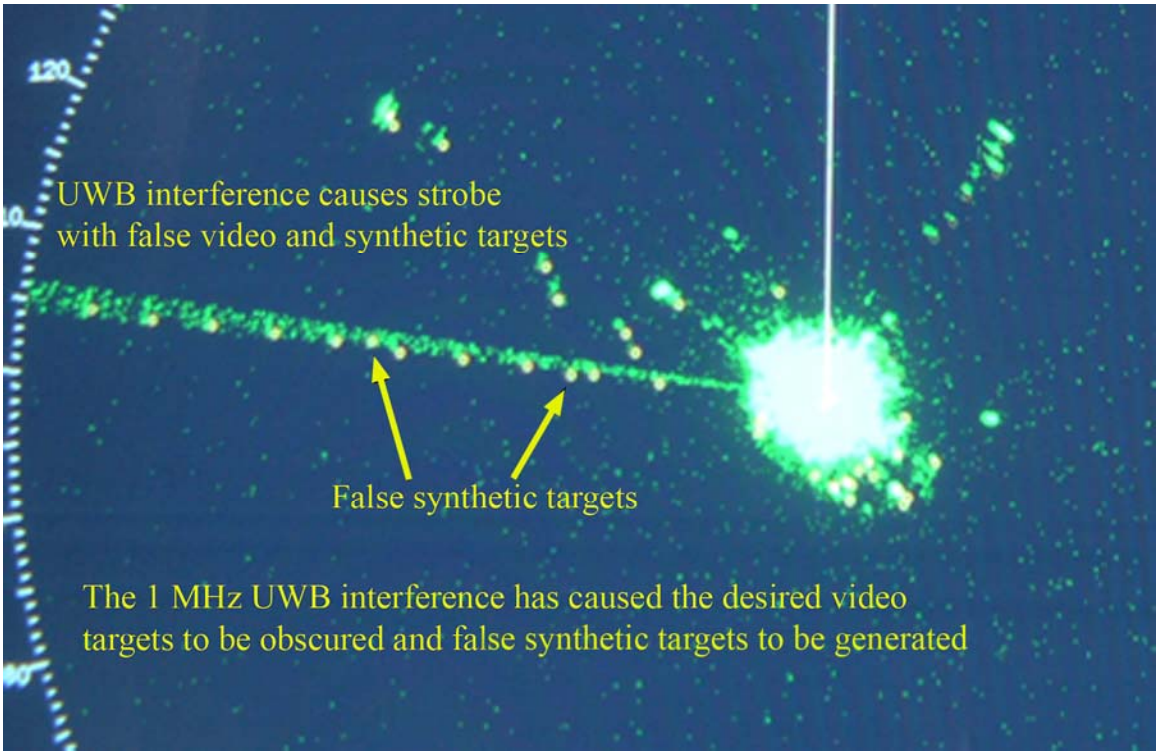

Figure 68. Radar A PPI display showing a loss of video targets and generation of false synthetic targets due to 1-MHz UWB interference.

7 INTERFERENCE MEASUREMENTS ON AN AIRBORNE METEOROLOGICAL RADAR

7.1 Introduction

This report describes the methodology and results of interference tests on a 9-GHz airborne weather radar. Interference waveforms were injected into the radar at its RF frequency and the effects of the interference were recorded as a function of *I/N* ratio in the radar receiver IF stage. Interference waveforms that were tested included: OFDM, unmodulated pulsed, chirped pulsed, phase-coded pulsed, and BPSK.

7.2 Characteristics of the Airborne Weather Radar

The pertinent technical characteristics of the airborne radar are shown in Table 29. The radar is widely utilized on large-capacity, multi-engine turboprop transport aircraft, and it may operate on large jet aircraft in the future. It has functions for identification of active precipitation and identification of wind shear. It has operational modes for short-range, medium-range, and long-range weather surveillance.

Table 29. Characteristics of the Airborne Weather Radar

Radar Characteristic	Value	
Radar Modes	Weather surveillance and wind shear alert	
Frequency Agility Range	9310-9410 MHz, spaced every 5 MHz	
Frequency Used for Testing	9335 MHz	
Transmitter Type	Solid state	
Transmitter Peak Power	10 kW (?)	
Pulse Modulations	Unmodulated pulses (short range) 5-Chip Barker Coded (medium range) 13-Chip Barker Coded (maximum range)	
	Minimum range	Maximum range
Pulse Repetition Rates	2000 pps	230 pps
Pulse Width Range	0.19 μs	234 μs
IF Bandwidth Range	5 MHz	52 kHz
Antenna Type	Gimbaled, flat-plate slotted array	
Antenna Gain	+32 dBi	
Antenna Sector Scan Angular Range	±15° (minimum), ±135° (maximum)	
Antenna Sector Scan Rate	60°/sec	
Antenna Beamwidth	2.7° horizontal, 4° vertical	
Radar Receiver Noise Figure	5 dB	
Radar Output	Color-coded display, with colors based on the strength of echo returns	

The radar normally operates with automatic frequency agility, hopping among twenty frequencies across 100 MHz of spectrum between 9310-9410 MHz. Available frequencies are spaced 5 MHz apart. During frequency-agility operations, the radar changes frequency from pulse to pulse. Frequencies are selected pseudo-randomly, with a uniform distribution. The frequency-hopping design is intended to minimize frequency-dependent effects in weather echo returns, as well as to enhance operational effectiveness in multi-radar environments. For the tests, the radar was operated in a single-frequency mode.

The radar transmitter generates RF pulses from a set of solid-state modules. The pulses are unmodulated in short-range operations, 5-chip Barker coded when the radar is operating at medium range, and 13-chip Barker coded when the radar is operating at long range.

The radar antenna is a flat-plate, slotted array that sector-scans on a mechanically gimbaled mount inside a radome on the nose of the aircraft. The elevation angle of the scanning (relative to horizontal) is manually controlled from the cockpit during flight.

The radar receiver is a conventional triple-stage heterodyne design in which the RF front-end LNA noise figure determines the noise figure of the entire receiver. The overall receiver noise figure is 5 dB. RF energy from the LNA is downconverted to the input frequency of the first IF stage, at 870 MHz. That signal is downconverted to the frequency of the second IF stage, at 90 MHz. The 90-MHz signals are processed through a quadrature modulator stage that produces *I-Q* outputs. Final downconversion brings the echo signals to baseband video between 0-50 MHz, where they undergo narrowband filtering to match operational pulse widths. Baseband video is detected and sampled with either an 8- or 11-bit A-D converter, depending upon the selected radar range scale. This radar utilizes a CFAR processor to reduce the effects of noise and clutter. Final IF bandwidths are adjusted automatically to match the radar pulse width (or sub-pulse width, in Barker-coded pulse modes). The portion of the radar IF that is significant for this report is shown schematically in Figure 69.

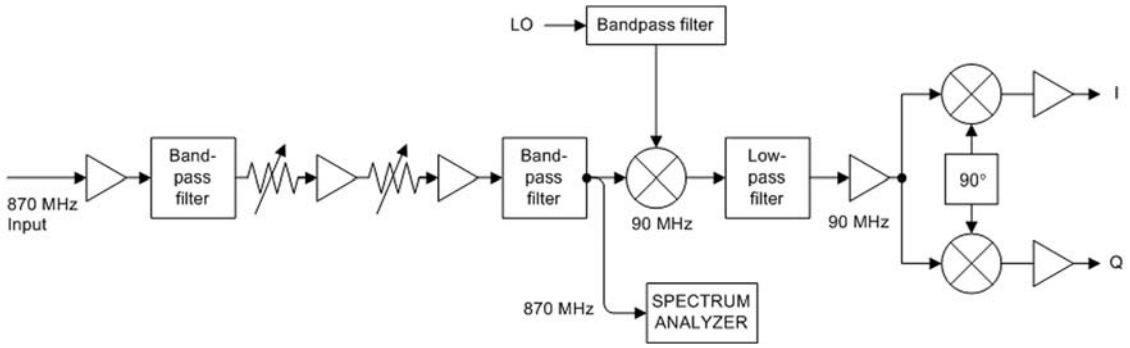

Figure 69. Block diagram of part of the airborne weather radar IF stage.

The radar video output is digitally processed into a color-coded, high resolution cockpit display. Colors correspond to the intensity of precipitation and wind shear ahead of the aircraft. An example of a weather surveillance display when the radar was operated in a receive-only mode, in which it was processing against only its internal noise, is shown in Figure 70. In this figure, as in the interference tests, the radar was operating in its 40 nm maximum range weather surveillance mode; the range rings are 10 nm apart.

The weather radar used in this study represents the current state-of-the art for this technology. Its hardware is highly integrated and modular, and its signal-processing software for echo returns is highly sophisticated. Its capabilities are believed to represent the best hardware and signal processing that are currently available in airborne platforms performing weather surveillance and wind shear detection missions.

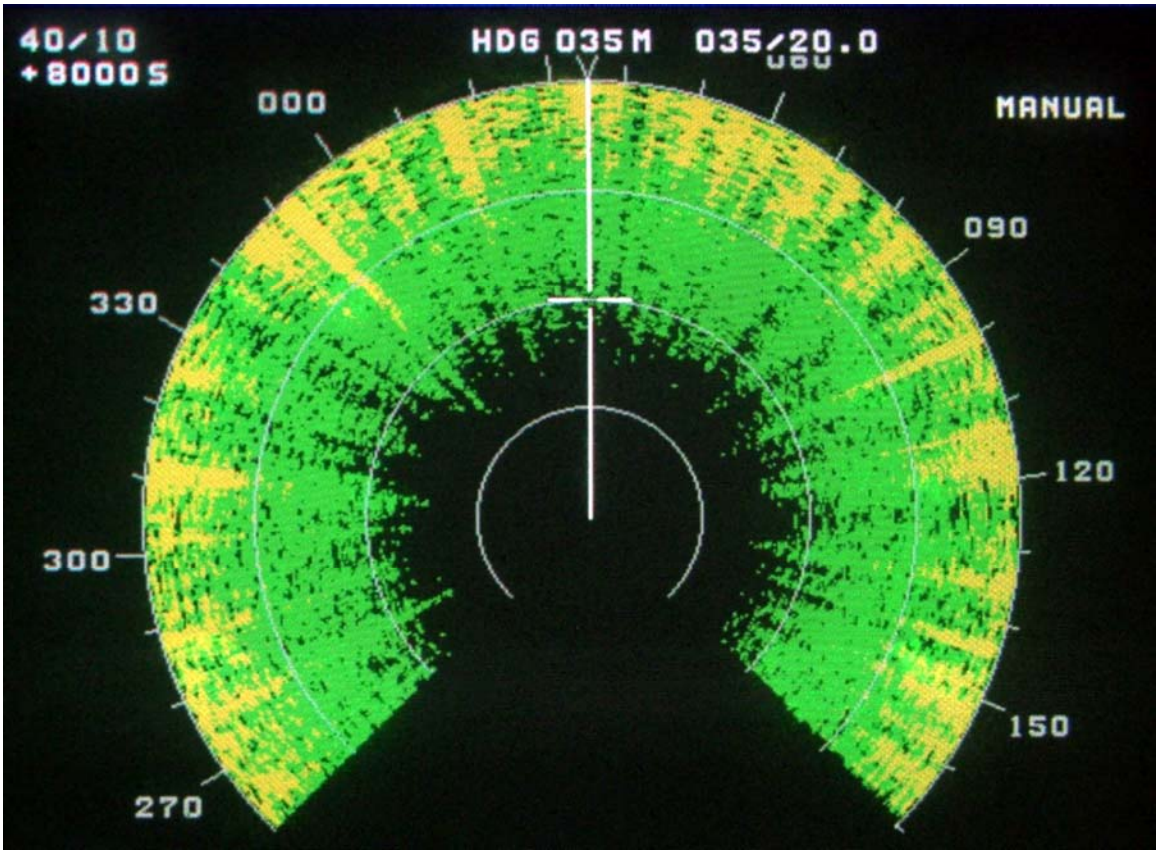

Figure 70. Example of the airborne weather radar display in the weather surveillance mode. There is no interference and the radar is running as receive-only. Green and yellow colors indicate that the receiver is processing only its internal noise.

7.3 Interference Measurement Protocol for the Airborne Weather Radar

The goal of the interference tests was to observe the effects of interference on a radar operational frequency as a function of both the type of interference and the interference-to-noise (*I/N*) ratio of the interference in the radar IF stage. Characteristics of the interference waveforms are listed in Table 30.

Table 30. Characteristics of Interference Waveforms for Airborne Weather Radar Tests

Interference waveform	Pulse width (μs)	Sub-pulse or scaled width (μs)	Pulse repetition rate (pps)	Bandwidth or chirp width (MHz)	Duty cycle (%)
Chirped 1	10	n/a	750	10	0.8
Chirped 2	10	n/a	750	50	0.8
Chirped 3	13.6/1.65	n/a	750	660/80	0.8
Phase coded 1	0.64	0.049	1600	1.56	0.1
Phase coded 2	20	1.54	1600	0.05	3.2
Unmod pulse 1	1	n/a	8000	1	0.8
Unmod pulse 2	1	n/a	19000	1	1.9
Unmod pulse 3	1	n/a	35000	1	3.5
BPSK 1	10	2	2000	400/80	0.4
BPSK 2	80	16	4500	400/80	7.2
BPSK 3	10	17.7	515	45/80	0.91
BPSK 4	10	1.7	5150	460/80	0.88
OFDM	Continuous*	n/a	n/a	20	100*

*The OFDM interference was continuous within the 45-ms beam-scanning interval of the radar antenna.

Since most airborne weather radars operate on single frequencies, the primary goal of the tests on this radar was to observe the effects of interference when it was likewise operated on a single frequency. Some additional interference tests were also performed when the radar was operating in its wideband, frequency-agility mode. For both of the radar modes (single-frequency and frequency agility), the protocol for injecting interference and observing its effects was the same. The interference injection arrangement is shown as a block diagram in Figure 71.

The entire radar transmitter/receiver system (including the antenna and all of the radar hardware except for the cockpit monitor display) was mounted at the top of a 20-meter high tower, the tower itself being located on the summit of the highest hill in the area. The radar transmitter was turned off, so that the radar operated in a receive-only mode. The maximum range was set to 40 nmi to eliminate the effect of STC. Processed data were displayed on a cockpit monitor. When no interference was injected, the radar showed only the effects of its internal noise on the cockpit display, as shown in Figure 70.

Interference waveforms were generated with a vector signal generator (VSG)[27] that had been programmed for the waveform characteristics of Table 30. The RF output of the VSG was routed via a hardline from the radar control room to a directional coupler at the radar antenna. Thus the interference energy was injected into the radar ahead of the first RF front-end LNA. The interference energy passed through the radar receiver RF front end, was mixed down and passed through the multi-stage IF (as described above), was quadrature-demodulated to generate *I-Q* outputs, and then passed through a digital signal processor. The processor output was routed to the cockpit display in the radar control room.

[27] A programmable Agilent VSG, model 8267C.

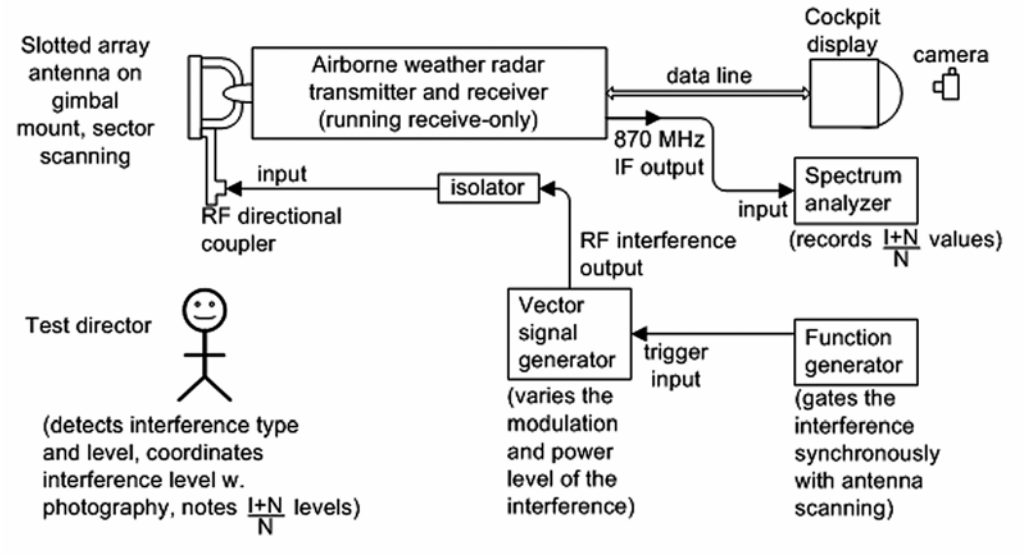

Figure 71. Block diagram of the airborne weather radar interference test setup.

Simultaneously with the observation of interference effects on the cockpit display, the *(I+N)/N* level was monitored on a spectrum analyzer connected to the first stage of the IF (tapped internally as depicted in Figure 1). Thus the effect of interference could be correlated directly with its measured *(I+N)/N* level.[28] An example of the spectrum analyzer data derived from the tap point in the radar IF stage is shown in Figure 72. The interference was gated on for 45-ms intervals, equal to the time required for the radar antenna beam to scan a single azimuth. This made the interference interval equal to the interval it would occupy if it were emitted by a point source in the antenna's far field.

During normal operations, the radar receiver gain automatically decreased from one complete sector scan (that is, a left-right plus a right-left antenna scan) to the next. Each change in receiver gain caused the *I/N* level to change by an equal number of decibels. The decrease from scan to scan was from one to two decibels. Thus, if the initial *I/N* level for an interference waveform was, e.g., +20 dB, that level would normally decrease from scan to scan to levels that would successively look like, e.g., +19 dB, +18 dB, +16 dB, +15 dB, +13 dB, etc. After a succession of about 12 of these decreases, (i.e., after about 12 complete sector scans), the radar automatically performed a complete recalibration of the receiver, the gain level reverted to its original, highest value, and the entire gain sequence was repeated.

[28] Subsequent to the tests, the measured *(I+N)/N* values were converted to the *I/N* values that are reported here.

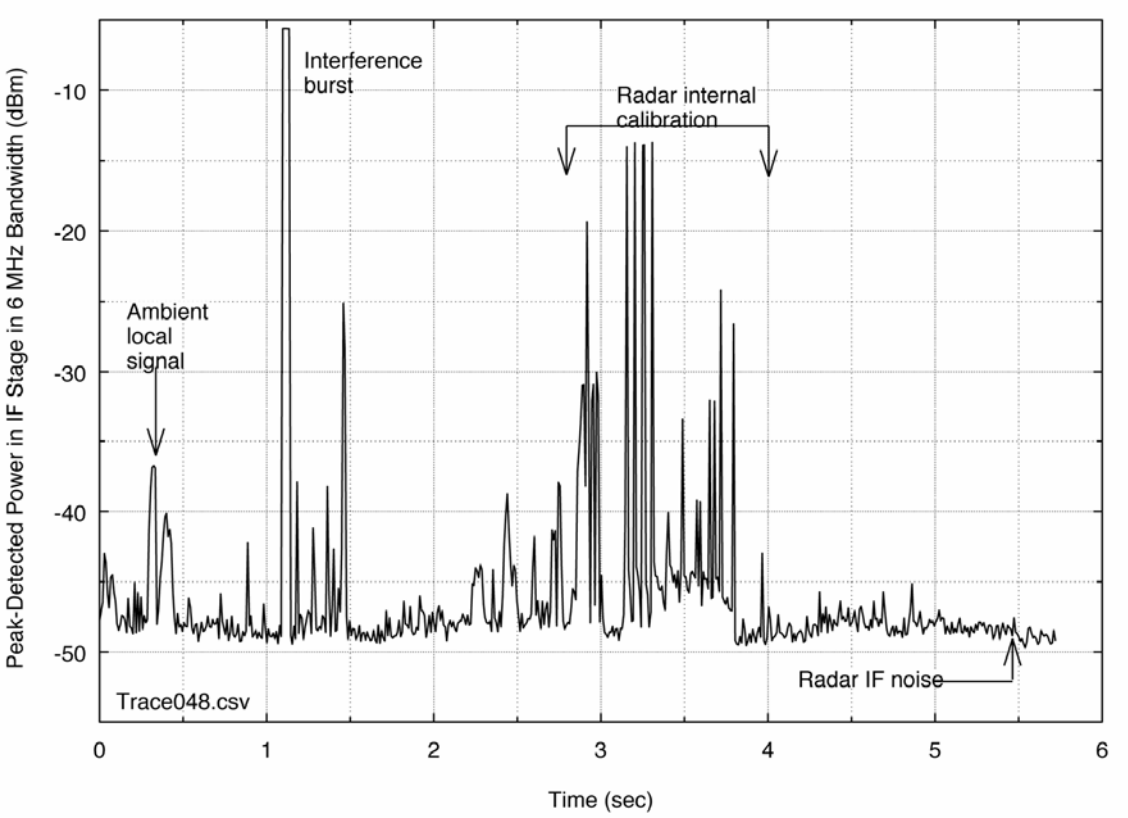

Figure 72. Interference burst as observed in the airborne radar IF stage. The trace is peak-detected, so the RMS level of the radar noise is 10 dB lower (relative to the amplitude of the interference burst) than shown here.

The test personnel used this built-in, gain-varying behavior of the radar to their advantage by generating a high *I/N* level from the VSG at the beginning of each radar gain sequence and then watching the decreasing effect of the interference on the cockpit display as the internal radar gain was automatically decreased from scan to scan. When no interference effects were observed on that display, the corresponding *I/N* level was noted. The VSG power output level was kept constant through each of the gain-variation sequences.

Because this type of radar does not process discrete targets, the criterion of probability of detection of targets is not applicable. Instead, its display was assessed qualitatively as a function of interference. The qualitative levels that were used were: strongly visible; marginally visible; barely visible; and no visible effect. Figures 73-75 show examples of the radar display when an interference effect was strong, marginal, and barely visible, respectively.

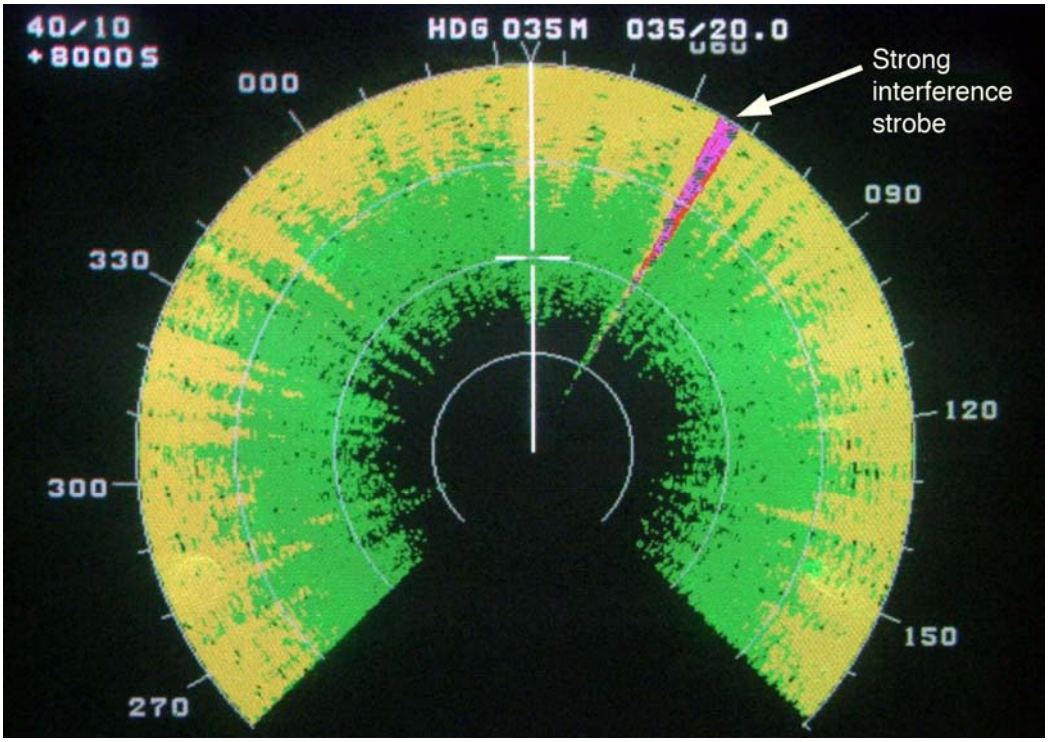

Figure 73. Example of a strongly visible interference strobe (caused by phase-coded waveform 2 at *I/N* = +60 dB).

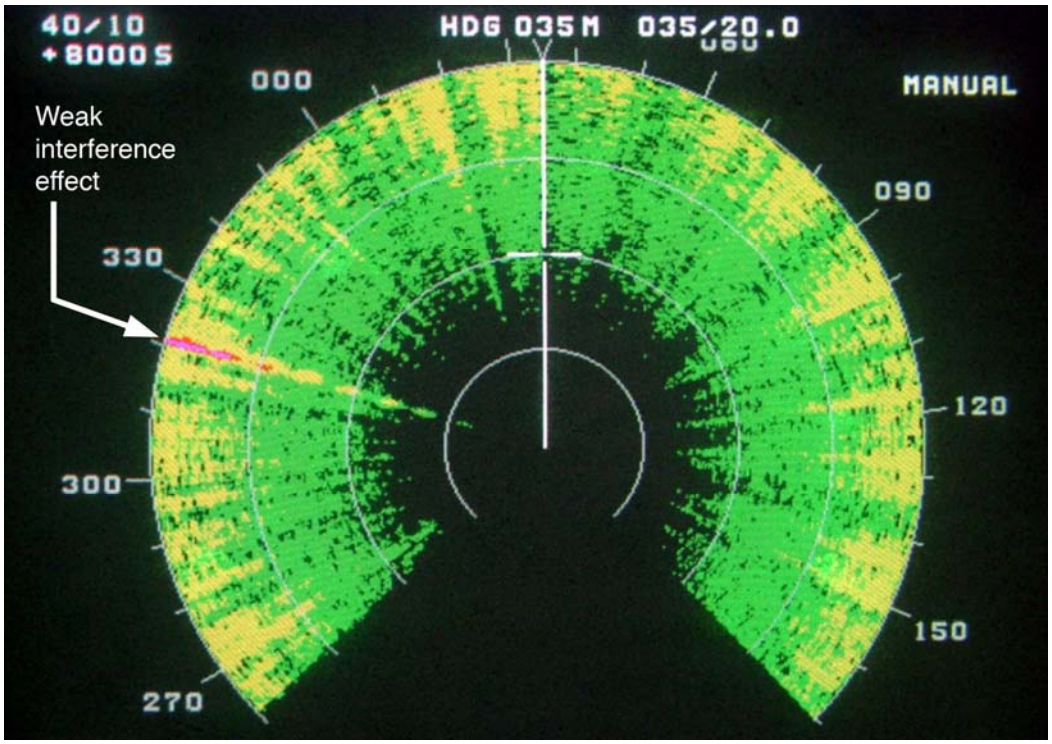

Figure 74. Example of a marginal interference strobe (caused by unmodulated pulse waveform 1 at *I/N* = +24 dB).

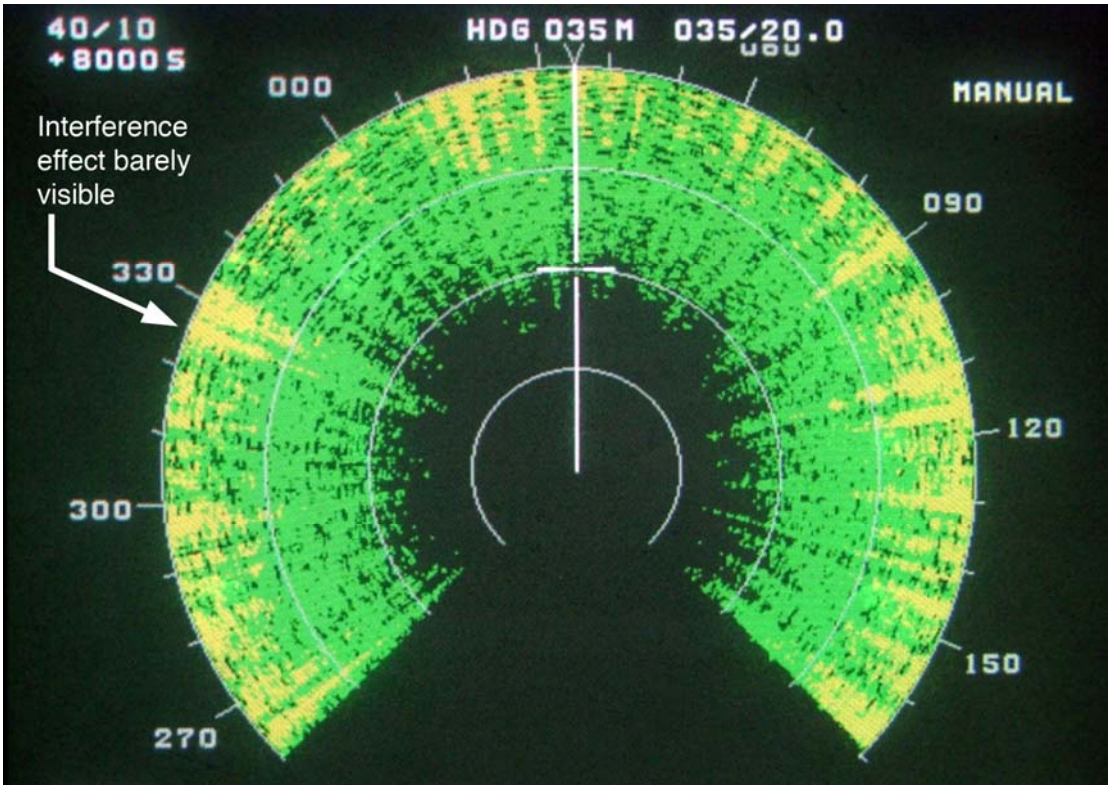

Figure 75. Example of barely visible interference (caused by unmodulated pulse waveform 1 at *I/N* = +20 dB.

7.4 Results of Interference Measurements on the Airborne Weather Radar

Results for the airborne weather radar in the single-frequency mode are summarized in Table 31. The results show that the chirp-pulsed waveforms, phase coded waveform 1, BPSK 1, BPSK 3, and BPSK 4 did not cause strobes on the radar's display at *I/N* ratios ranging from +43 to +63 dB. (Those power levels were the maximum that the test equipment could generate, the available maximum depending upon the modulation of each interference waveform.) BPSK 2 caused an effect at an *I/N* of +30 dB. The unmodulated pulsed waveforms 1 and 2 caused effects at *I/N* levels of +18-19 dB, and the unmodulated pulsed waveform 3 caused effects at an *I/N* of +25 dB.

In contrast, the airborne weather radar was affected at relatively low *I/N* levels by the OFDM signal. This result was not surprising due to that signal's high duty cycle. The OFDM signal was 20 MHz wide and continuous throughout a 45-ms dwell time. Therefore, it filled the entire IF filter with energy the entire time the waveform was gated on. The *I/N* had to be below -2 dB before the OFDM signal no longer affected the display.

Table 31. Results of Interference Tests on the Airborne Weather Radar*

Interference Signal Modulation	Peak-to-RMS *I/N*[29] (dB)	Interference Effect On Radar
Chirped 1	+63	No visible effect on display
Chirped 2	+52	No visible effect on display
Chirped 3	+43	No visible effect on display
Phase Coded 1	+47	No visible effect on display
Phase Coded 2	+60 +36 +30 +28 +25	Strongly visible strobes Strongly visible strobes Marginally visible strobes Barely visible strobes No visible effect on display
Unmodulated 1	+57 +22 +19	Visible strobes Marginally visible strobes No visible effect on display
Unmodulated 2	+57 +21 +18	Visible strobes Marginally visible strobes No visible effect on display
Unmodulated 3	+32 +29 +25	Visible strobes Marginally visible strobes No visible effect on display
BPSK 1	+44	No visible effect on display
BPSK 2	+52 +32 +30	Strongly visible strobes Marginally visible strobes No visible effect on display
BPSK 3	+54	No visible effect on display
BPSK 4	+43	No visible effect on display
OFDM	+33 -2 -6	Strongly visible strobes Marginally visible strobes No visible effect on display

* Where "no visible effect on display" is indicated, the corresponding *I/N* level indicated is the maximum power level that could be achieved with the test equipment.

Other than for OFDM, the airborne weather radar was affected at some level or another by the following interference waveforms: unmodulated pulsed 1, 2, and 3; BPSK 2; and phase coded 2. The threshold for these waveforms was from +21 dB to +32 dB. (In contrast, the OFDM interference threshold was from *I/N* = -6 dB to -2 dB.) All but one of these waveforms had duty cycles of 1.9% or greater, the sole exception being a duty cycle of 0.8% for unmodulated pulsed 1. This observed relationship between a duty cycle of about 1% or greater and the eventual occurrence of visible interference effects was consistent with the results of tests on other types of radars in this study.

[29] The *I/N* levels in this table have been corrected from measured *(I+N)/N* levels.

Figures 76-77 illustrate the contrast between the relatively robust radar performance at high *I/N* levels for signals with duty cycles of a few percent or less versus the relatively low threshold for the high duty cycle OFDM signal. Figure 76 shows the effect of OFDM interference at *I/N* levels of -2 dB and +16 dB, while Figure 77 shows the effect of the Phase 2 waveform at *I/N* levels of +28 dB and +45 dB. Comparison of these figures shows that the high duty cycle OFDM interference waveform caused effects that were quantitatively similar to those of the low duty cycle (3.2%) phase coded pulsed 2 waveform, but that there is a difference of about 30 dB between the *I/N* levels where the onset of interference effects begins for these two waveforms.

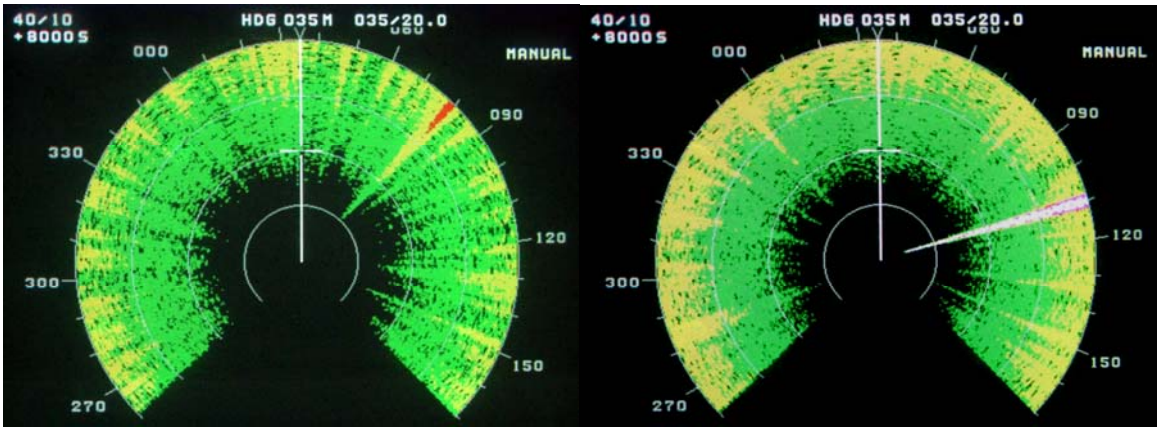

Figure 76. Barely visible (left) and strongly visible (right) strobes due to high duty cycle OFDM interference at *I/N* levels of -2 dB and +16 dB, respectively.

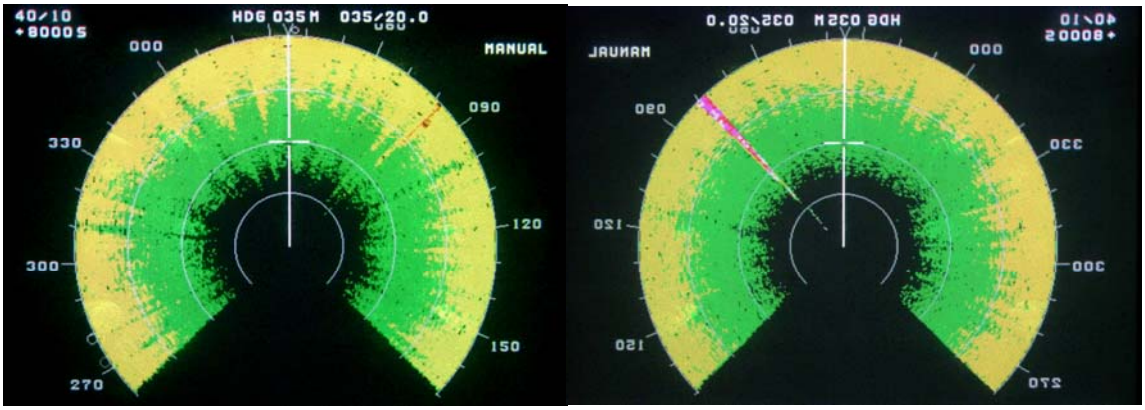

Figure 77. Barely visible (left) and strongly visible (right) strobes due to low duty cycle (3.2%), phase-coded pulsed waveform 2 interference at *I/N* levels of +28 dB and +45 dB, respectively. The effects are similar to those of Figure 76, but occur at *I/N* levels that are about 30 dB higher than the OFDM interference thresholds.

When the radar was operated in its frequency agility mode, all interference was mitigated. This was due to the radar design, in which the radar ceases operations on a frequency on which interference is detected; this behavior was observed during the tests. Interference would appear on the screen as it did for the single frequency case (e.g., the chirp-pulsed waveforms had no

effect at even the highest levels, while the OFDM signal had a strong effect at low levels). But as soon as one full sector-scan was completed, the receiver would stop hopping to the frequency (or frequencies) of the interference and the display would revert to its baseline appearance until the frequency of the interference was changed to match the radar's frequency.

7.5 Summary of Interference Effects for the Airborne Weather Radar

The airborne weather radar showed no effects from interference with the lowest duty cycles, on the order of 0.1%, at even the highest *I/N* levels that could be achieved, on the order of +50 dB to +60 dB. Interference waveforms with higher duty cycles, on the order of 1-3% duty cycles, caused effects to occur at *I/N* levels on the order of +21 dB to +32 dB. But for a communication-type signal (OFDM) with a nearly 100% duty cycle (within the 45 ms mainbeam dwell interval of the radar antenna scan), the *I/N* levels where interference effects were manifested for OFDM signals were substantially lower, between -6 dB to -2 dB.

These results are consistent with the results from other radars in this study. In general, radar receivers seem to perform robustly in the presence of signals such as those emitted by other radars (with duty cycles less than 1-3%), but are not robust in the presence of interference with high duty cycles (near 100%) such as are characteristic of communication signals.

8 SUMMARY OF INTERFERENCE EFFECTS ON RADARS

This report describes the results of wide-ranging interference measurements that have been performed on many representative radar receivers. The receiver types included long range air search radionavigation radars, a short range air search radionavigation radar, a fixed ground-based weather radar, an airborne weather radar, and several maritime radionavigation radars. Missions performed by these radars include en-route (long range) air traffic control and air defense; airport traffic control; weather surveillance and warning; and maritime navigation and surface search. The radars that have been tested operate in several microwave spectrum bands: 1200-1400 MHz; 2700-2900 MHz; 2900-3100 MHz; and 8500-10500 MHz. Five major results have been observed and documented; they are summarized here.

8.1 Radars are Vulnerable to the Effects of Communication Signal Interference

The results of interference tests with communication signal modulations are summarized in Table 32. Interference with communication-type modulations caused degradation in radar performance at *I/N* levels between -9 dB to -2 dB, well below the noise floor of each radar receiver. One radar lost targets at an *I/N* level of -10 dB, and *I/N* = -6 dB caused most of the radars to lose targets. Future improvements to meteorological radars are predicted to render them vulnerable at *I/N* levels as low as -14 dB.

Table 32. *I/N* Levels of Communication Signal Modulations at which Performance Decreased for All Radars Tested

Radar Tested	*I/N* Threshold for Decreased P_d
Long Range Air Search Radiolocation Radar 1 (installation 1)	-9 dB
Long Range Air Search Radiolocation Radar 1 (installation 2)	-9 dB
Long Range Air Search Radiolocation Radar 2	-6 dB
Short Range Air Search Radionavigation Radar	-9 dB
Fixed Ground-Based Meteorological Radar	-9 dB*
Maritime Radionavigation Radar A	-7 dB
Maritime Radionavigation Radar B	-10 dB
Maritime Radionavigation Radar C	-6 dB to -9 dB
Maritime Radionavigation Radar D	-9 dB
Maritime Radionavigation Radar E	-6 dB
Maritime Radionavigation Radar F	-6 dB
Airborne Meteorological Radar	Between -6 to -2 dB

* -14 dB is the predicted threshold for the upgraded version of the fixed meteorological radar.

8.2 Radars Perform Robustly in the Presence of Interference from Other Radars

In contrast to the effects of interference from communication signal modulations, pulsed interference at low duty cycles (less than about 1-3%) was tolerated at *I/N* ratios as high as +30 dB to +63 dB. The radar receivers that were tested performed robustly in the presence of signals transmitted by other radars.

8.3 Low-Level Interference Effects in Radar Receivers are Insidious

The loss of targets at low interference levels is insidious; there is no overt indication to radar operators or even to sophisticated radar software that losses are occurring. No dramatic indications such as flashing strobes on radar PPI screens are observed. This insidiousness can make low-level interference more dangerous than higher levels that will generate strobes and other obvious warning indications for operators or processing software.

Even when radars experience serious performance degradation due to low-level interference, it is very unlikely that such interference will be identifiable as such. It is therefore unlikely that such interference will ever result in reports to spectrum management authorities even when it causes loss of desired targets. Since low-level interference is not expected to be identified or to generate reports when it occurs, lack of such reports *cannot* be taken to mean that such interference does not occur.

8.4 Low-Level Interference Can Cause Loss of Radar Targets at Any Range

Interference can (and will) cause loss of targets at any distance from any radar station; loss of targets due to radio interference is not directly related to distance of targets from radar stations. When radar performance is reduced by some number of decibels, *X*, then all targets that were within *X* decibels of disappearing from coverage will be lost. Range from the radar is not a factor in this equation. Interference can cause loss of desired, large cross section targets (such as commercial airliners, oil tankers, and cargo ships) at long distances, as well as small cross section targets at close distances. Low-observable targets that could be lost include, for example, light aircraft; business jets; incoming missiles; missile warheads; floating debris including partially submerged (and extremely dangerous) shipping containers; life boats; kayaks, canoes, dinghies; periscopes; and swimmers in life jackets.

Because any radar target can potentially be lost at any distance in the presence of radio interference, radio interference does not translate directly into an equivalent radar range reduction. “Range reduction” should therefore *not* be used as a metric in discussions of adverse effects of interference on radars, unless such range reduction is qualified with a reference to a (unrealistic) condition of fixed, constant cross sections for all desired targets.

8.5 Radar Interference Waveforms and Test Reporting Should be Standardized

During radar interference measurements, the interference signals should be standardized to include: broadband noise; CW; impulse UWB (dithered and non-dithered); direct sequence UWB; multiband OFDM UWB; CDMA; TDMA; BPSK; QPSK; QAM; GMSK; OFDM; and pulsed signals (both linear FM-modulated (chirped) and unmodulated).

Plots of P_d versus *I/N* are a useful and effective method of displaying interference data and should be adopted as a standard for future radar interference measurements.

For pulsed signals, the parameters of pulse width and prf which comprise the duty cycle should be varied to determine the point at which interference effects transition from pulse-like to noise-like or CW-like. For linear-FM pulsed interference signals, the chirp rate and chirp bandwidth should be varied to observe the onset of the same effects.

9 REFERENCES

[1] F.H. Sanders and V.S. Lawrence, "Broadband spectrum survey at Denver, Colorado," NTIA Report 95-321, Sep. 1995.

[2] F.H. Sanders, B.J. Ramsey, and V.S. Lawrence, "Broadband spectrum survey at San Diego, California," NTIA Report 97-334, Dec. 1996.

[3] F.H. Sanders, B.J. Ramsey, and V.S. Lawrence, "Broadband spectrum survey at Los Angeles, California," NTIA Report 97-336, May 1997.

[4] F.H. Sanders, B.J. Ramsey, and V.S. Lawrence, "Broadband spectrum survey at San Francisco, California," NTIA Report 99-367, Jul. 1999.

[5] C.A. Filippi, R.L. Hinkle, K.B. Nebbia, B.J. Ramsey, and F.H. Sanders, "Accommodation of broadcast satellite (sound) and mobile satellite services in the 2300-2450 MHz band," NTIA Technical Memorandum TM-92-154, Jan. 1992.

[6] P.E. Gawthrop, F.H. Sanders, K.B. Nebbia, and J.J. Sell, "Radio spectrum measurements of individual microwave ovens, volume 1," NTIA Report 94-303-1, Mar. 1994.

[7] P.E. Gawthrop, F.H. Sanders, K.B. Nebbia, and J.J. Sell, "Radio spectrum measurements of individual microwave ovens, volume 2," NTIA Report 94-303-2, Mar. 1994.

[8] M.G. Biggs, F.H. Sanders, and B.J. Ramsey, "Measurement to characterize aggregate signal emissions in the 2400-2500 MHz frequency range," NTIA Report 95-323, Aug. 1995.

[9] M.I. Skolnik, *Introduction to Radar Systems*, 2nd ed., New York, NY: McGraw-Hill, 1980.

[10] M.I. Skolnik, ed., *Radar Handbook*, 2nd ed., New York, NY: McGraw-Hill, 1990.

[11] D.K. Barton, *Modern Radar System Analysis*, Norwood, MA: Artech House, 1988.

[12] P.A. Lynn, *Radar Systems*, New York, NY: Van Nostrand Reinhold, 1987.

[13] L.V. Blake, "Recent advancements in basic radar range calculation technique," pp. 49-59, in *Radars Vol. 2: The Radar Equation*, D.K. Barton, ed., Norwood, MA: Artech House, 1974.

[14] L.V. Blake, Summary of "A guide to basic pulse-radar maximum-range calculation," pp. 151-154, in *Radars Vol. 2: The Radar Equation*, D.K. Barton, ed., Norwood, MA: Artech House, 1974.

[15] D. Meyer and H. Mayer, *Radar Target Detection: Handbook of Theory and Practice*, New York: Academic Press, 1973.

[16] A. Paul, G. Hurt, T. Sullivan, G. Patrick, R. Sole, L. Brunson, C-W. Wang, B. Joiner, and E. Drocella, with Contributors S. Williams and G. Saam, "Interference protection criteria, Phase 1: Compilation from existing sources," NTIA Report 05-432, Oct. 2005.

[17] M.I. Skolnik, Editor-in-chief, *Radar Handbook*, 2nd ed., New York: McGraw-Hill, 1990.

[18] ITU-R Recommendation M.1372-1, "Efficient use of the radio spectrum by radar stations in the radiodetermination service," International Telecommunication Union, Radiocommunication Sector, 1998.

[19] S. Kingsley and S. Quegan, *Understanding Radar Systems*, London: McGraw-Hill, 1992.

[20] ITU-R Recommendation M.1464, "Characteristics of and protection criteria for radionavigation and meteorological radars operating in the frequency band 2700-2900 MHz," International Telecommunication Union, Radiocommunication Sector, 1998.

[21] R. Doviak, D. Zrnic, and D. Surmans, "Doppler Weather Radar," *Proceedings of the IEEE*, vol. 67, no. 11, Nov. 1979.

[22] ITU-R Recommendation M.1313, "Technical characteristics of maritime radionavigation radars," International Telecommunication Union, Radiocommunication Sector, 2000.

[23] L.K. Brunson, J.P. Camacho, W.M. Dolan, R.L. Hinkle, G.F. Hurt, M.J. Murray, F.A. Najmy, P.C. Roosa, Jr., and R.L. Sole, "Assessment of compatibility between ultrawideband devices and selected federal systems," NTIA Special Publication SP-01-43, Jan. 2001.

APPENDIX A: EXAMPLE INTERFERENCE REJECTION (IR) RESPONSES OF A MARITIME RADIONAVIGATION RADAR

The IR feature of radars is discussed at length in Section 1. IR is fundamentally a correlator function that operates on either a pulse-to-pulse basis (on either the repetition interval or the pulse width) or else on a scan-to-scan basis. For pulse correlation techniques, repetition intervals and pulse widths of return echoes that match the transmitter's nominal characteristics are allowed to pass through the correlator and are displayed, whereas other received pulses are rejected. IR only works against pulsed, asynchronous interference. It is not effective against high duty cycle interference, such as communication signals.

This appendix shows examples of the interference rejection performance in the presence of various types of pulsed interference inputs for maritime radionavigation Radar A. The radar characteristics are described in detail in Section 6.

In these tests, the interference was always pulsed, with a pulse width of 10 μs. But the duty cycle of the interference varied from one test to the next. The results shown here were obtained with duty cycles of 0.1%, 1%, and 5%, corresponding to prfs of 100 Hz, 1 kHz, and 5 kHz. For each duty cycle, the amplitude of the interference was gradually increased and the performance of the radar receiver was assessed by examining the PPI display with the IR function turned on versus turned off. "Gated" refers to the case where the interference is created on the azimuth of the targets, for the duration required for a radar mainbeam to sweep across stationary targets. "Ungated" means that the interference is generated for the duration of an entire 360-degree sweep of the radar beam.

IR was found to be an effective method for mitigating the effects of pulsed interference up to a duty cycle as high as 1-3%. The effectiveness of IR decreased for higher duty cycles. IR was found to be totally ineffective against high duty cycle interference such as communication signals.

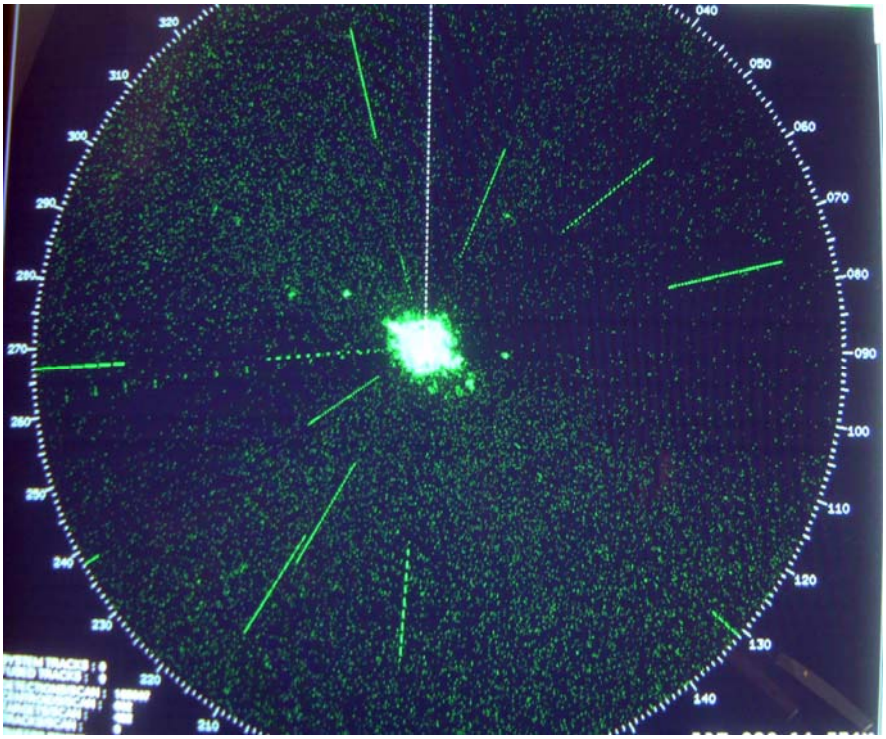

Figure A-1. +50 dB *I/N*, ungated,10 µs pw, 0.1% duty cycle, IR off.

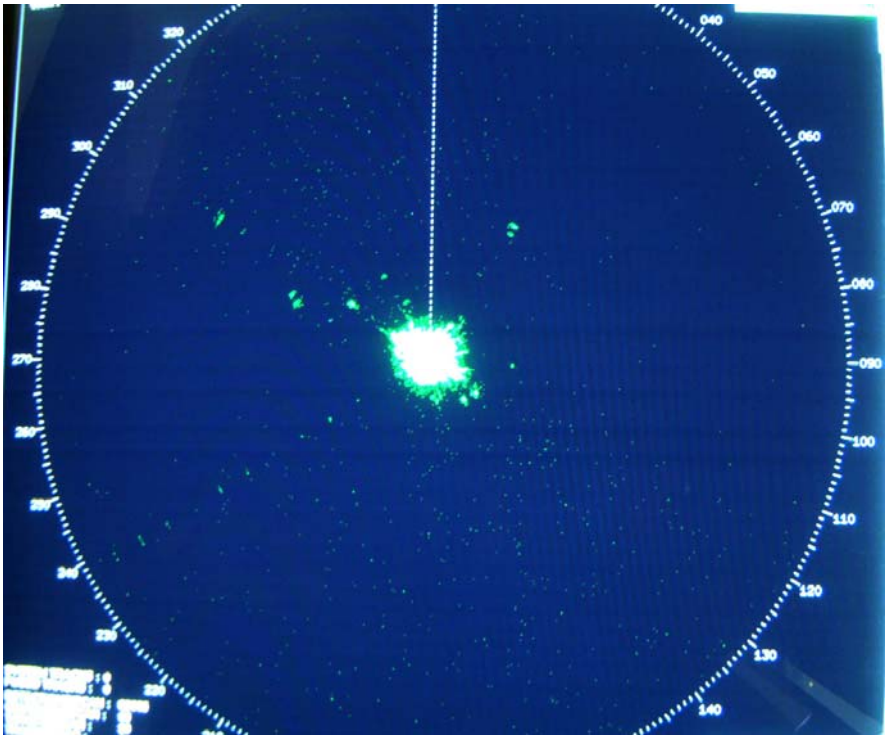

Figure A-2. +50 dB *I/N*, ungated, 10 µs pw, 0.1% duty cycle, IR on.

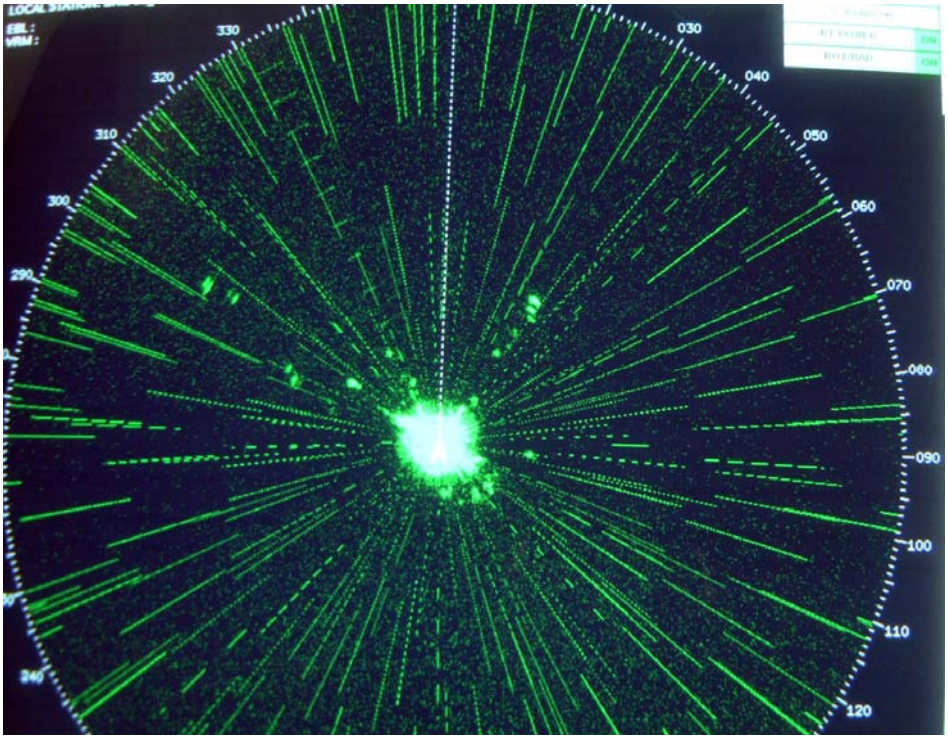

Figure A-3. +50 dB *I/N*, ungated, 10 µs pw, 1% duty cycle, IR off.

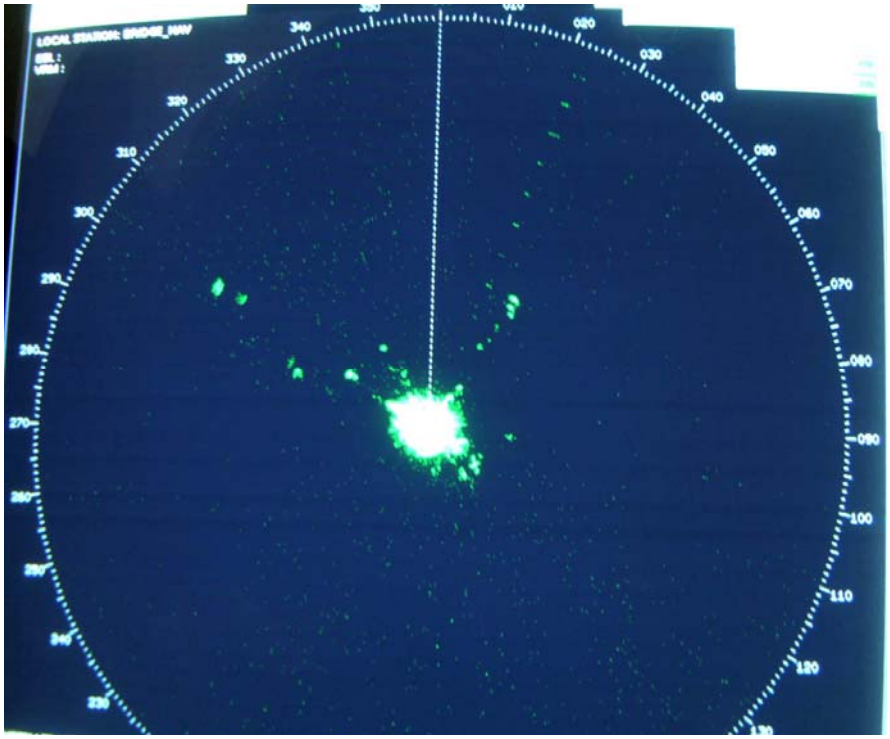

Figure A-4. +50 dB *I/N*, ungated, 10 µs pw, 1% duty cycle, IR on.

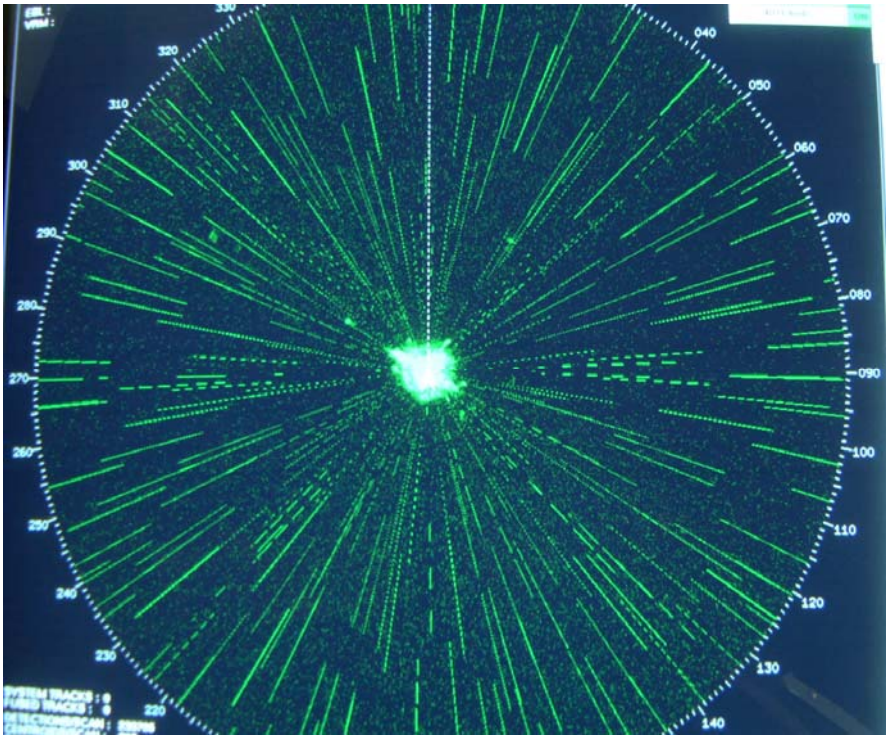

Figure A-5. +80 dB *I/N*, ungated, 10 µs pw, 1% duty cycle, IR off.

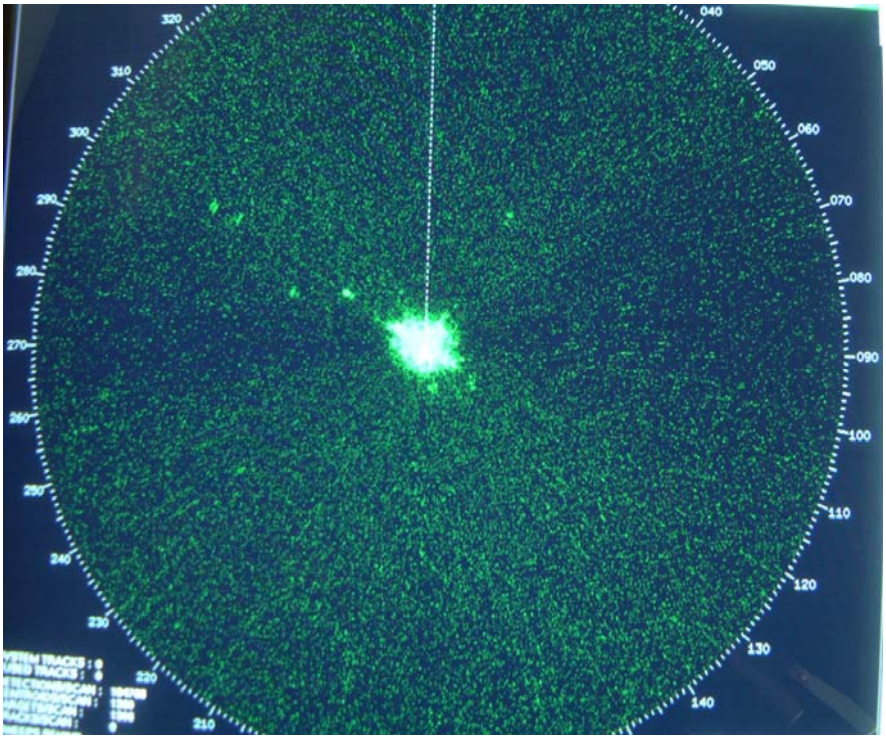

Figure A-6. +80 dB *I/N*, ungated, 10 µs pw, 1% duty cycle, IR on.

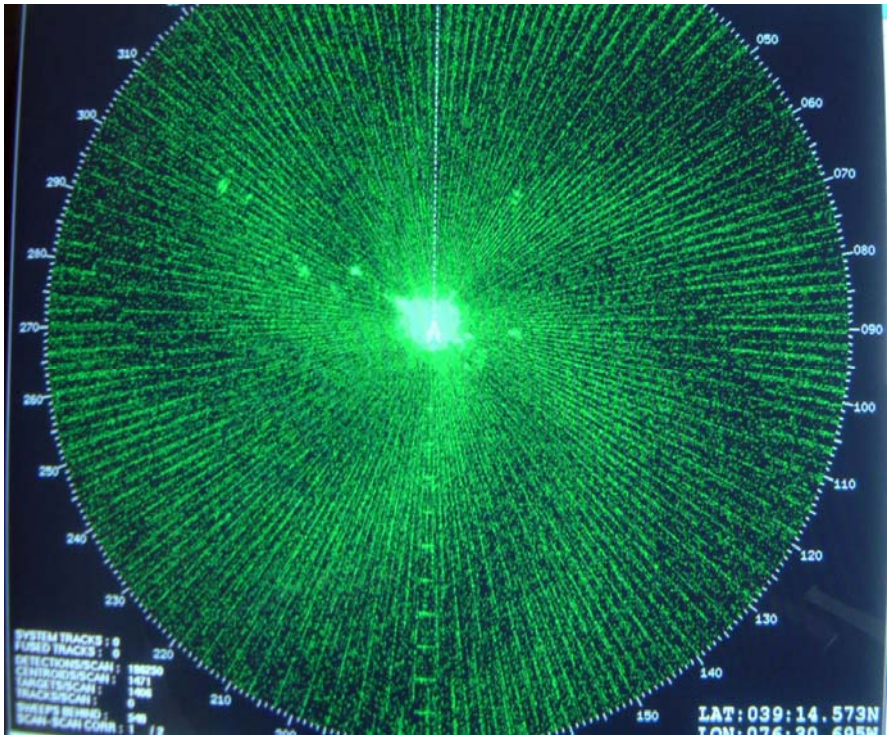

Figure A-7. +10 dB *I/N*, ungated, 10 µs pw, 5% duty cycle, IR off.

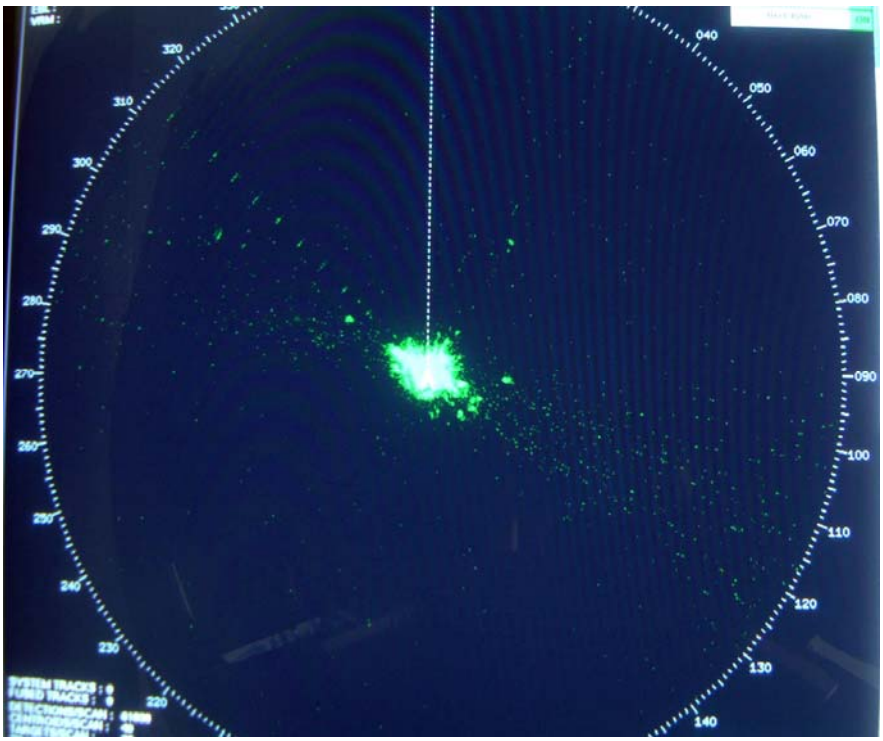

Figure A-8. +10 dB *I/N*, ungated, 10 µs pw, 5% duty cycle, IR on.

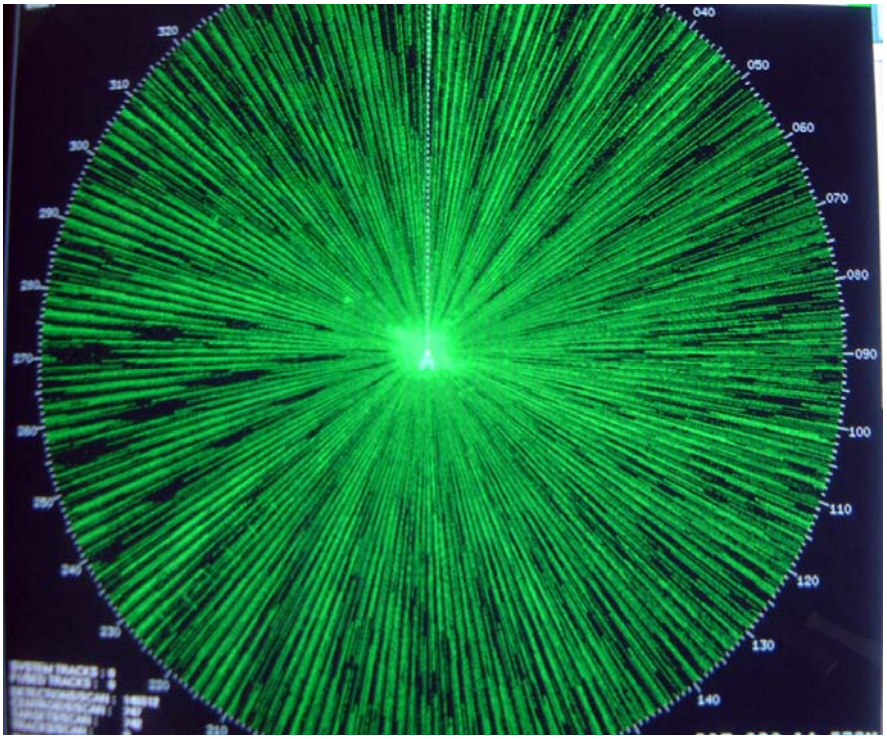

Figure A-9. +15 dB *I/N*, ungated, 10 µs pw, 5% duty cycle, IR off.

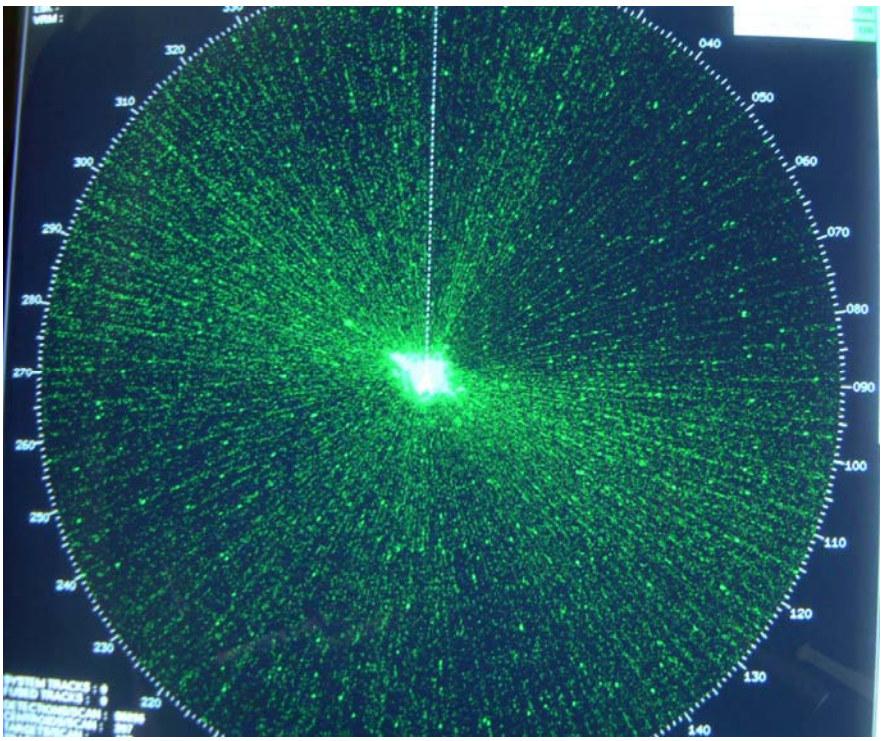

Figure A-10. +15 dB *I/N*, ungated, 10 µs pw, 5% duty cycle, IR on.

APPENDIX B: SELECTED INTERFERENCE EMISSION SPECTRA

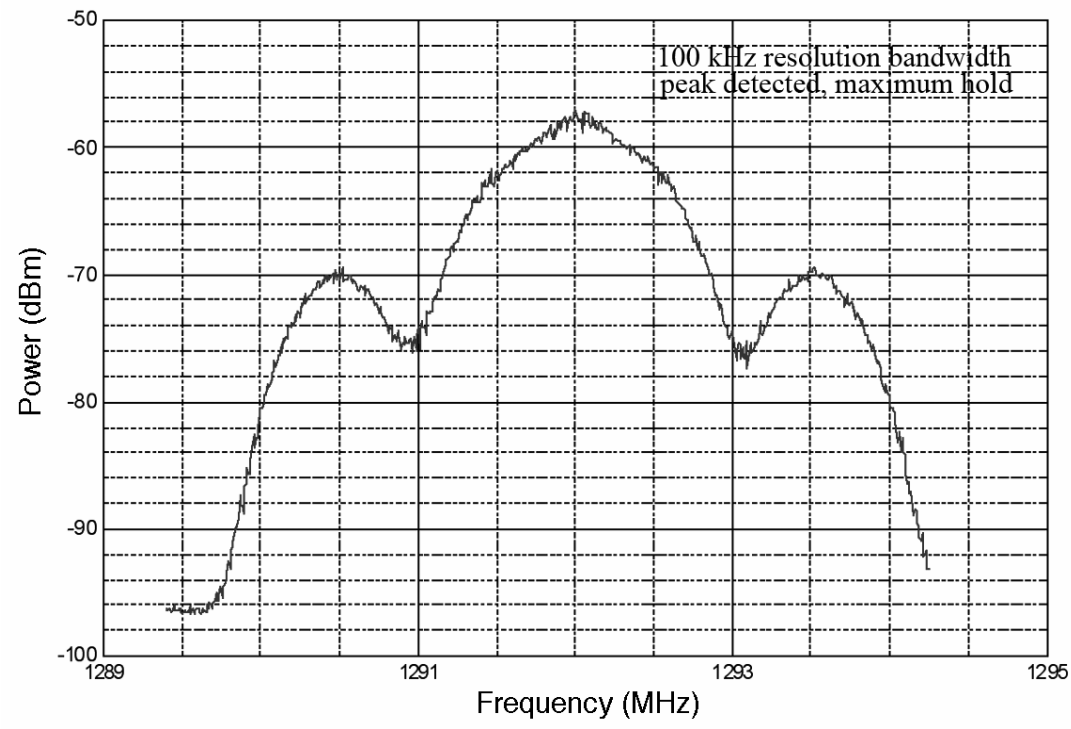

Figure B-1. 1.023 MBit/s BPSK interference signal spectrum.

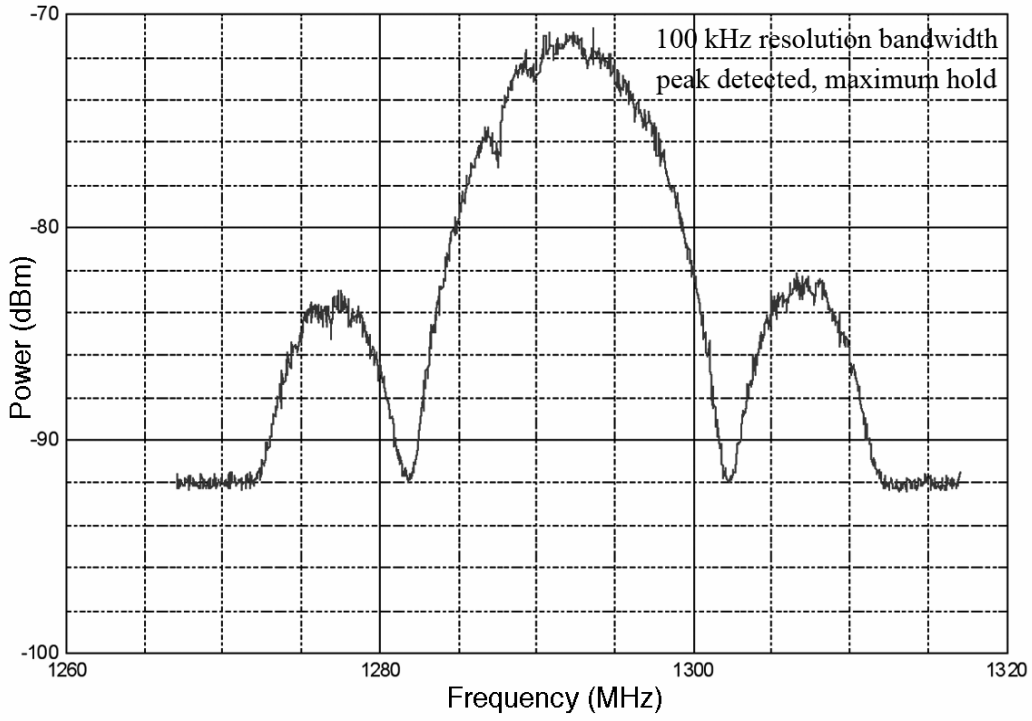

Figure B-2. 10 MBit/s BPSK interference signal spectrum.

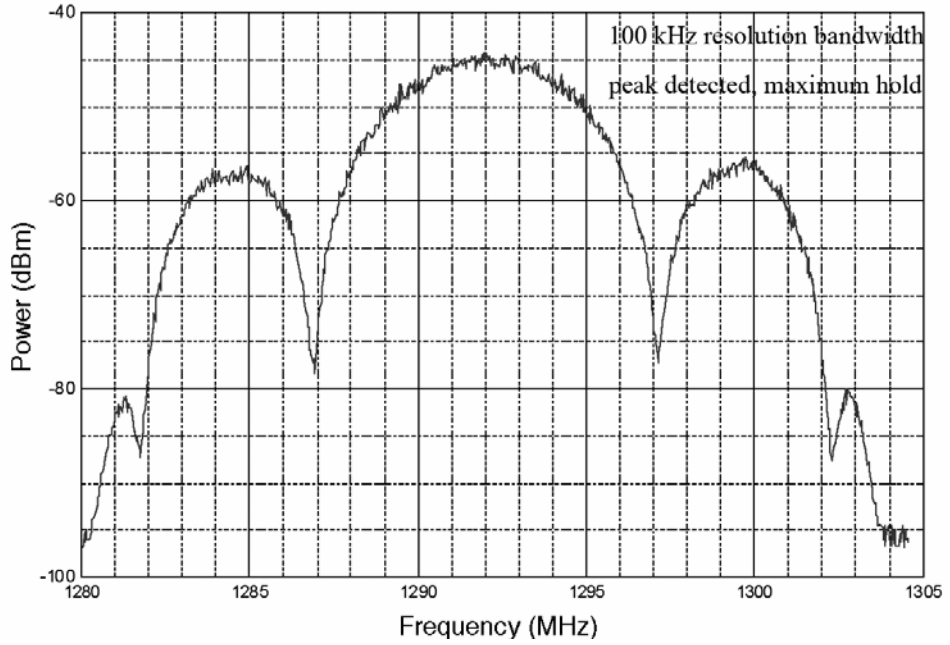

Figure B-3. 5 MBit/s BPSK interference signal spectrum.

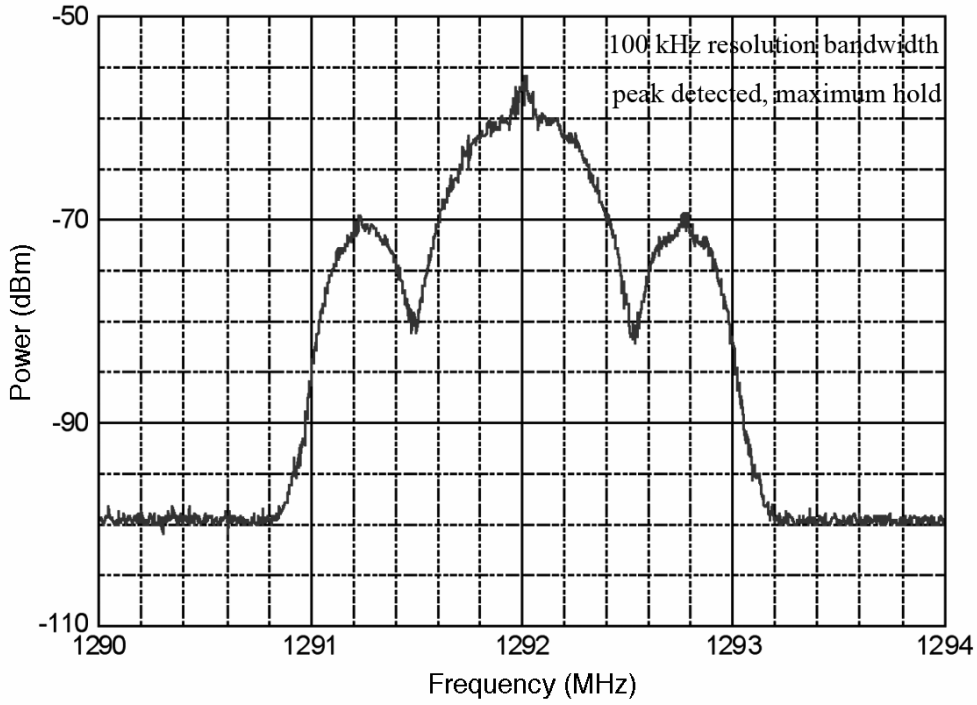

Figure B-4. 0.5 MBit/s BPSK interference signal spectrum.

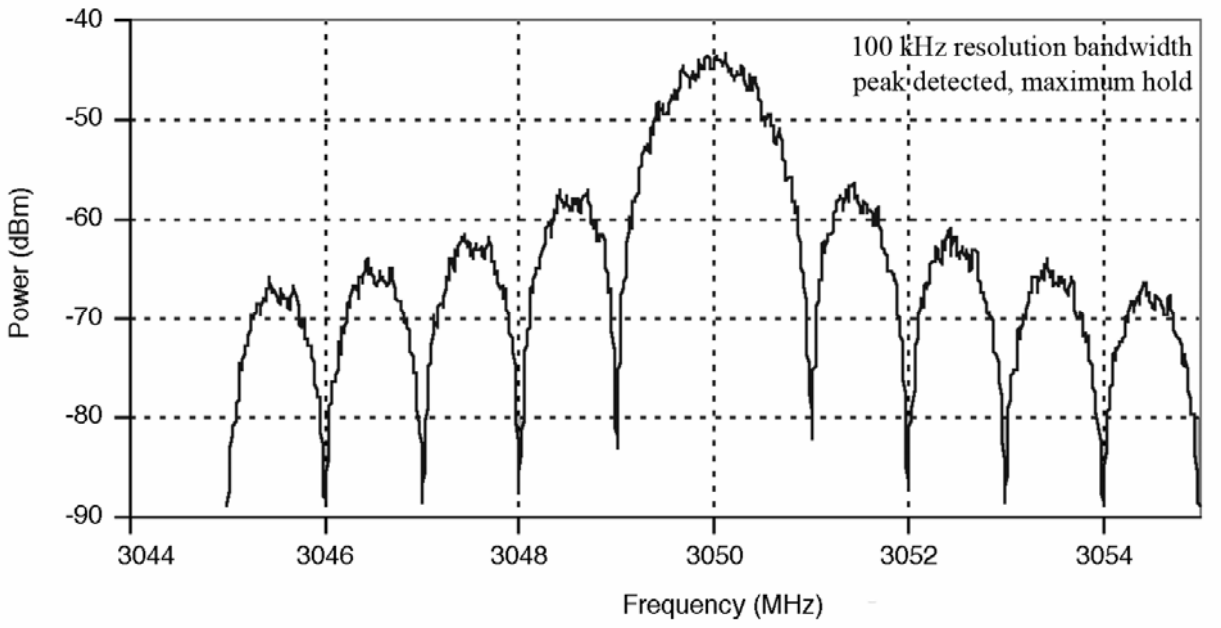

Figure B-5. 2 MBit/s QPSK interference signal spectrum.

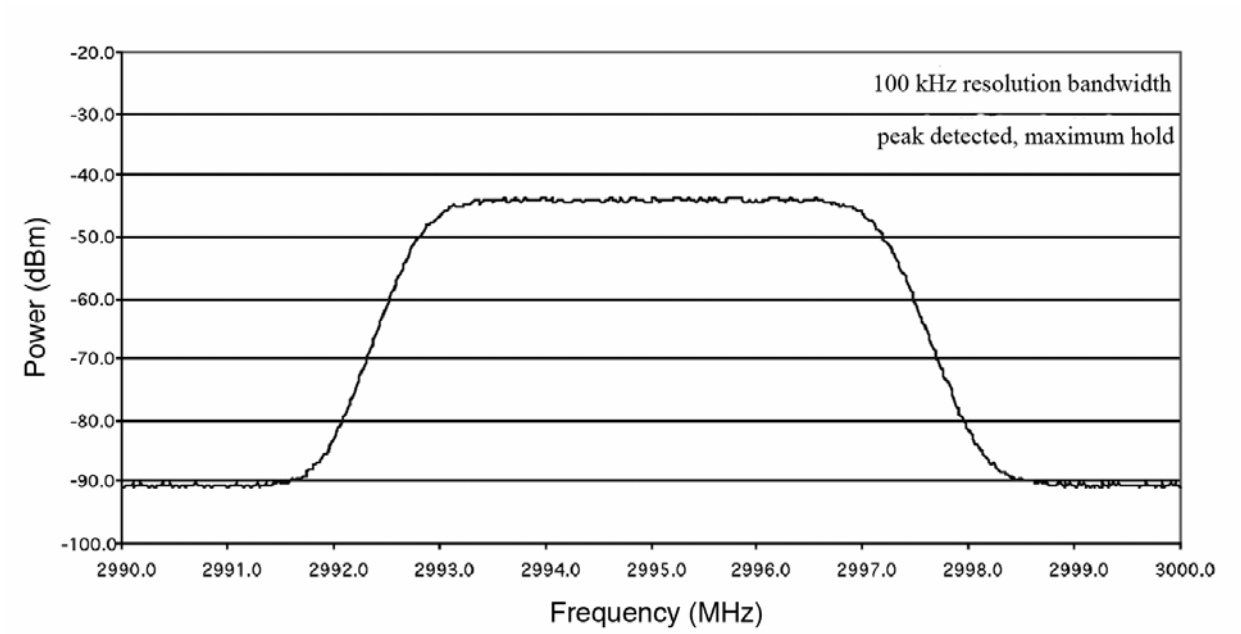

Figure B-6. W-CDMA interference signal spectrum.

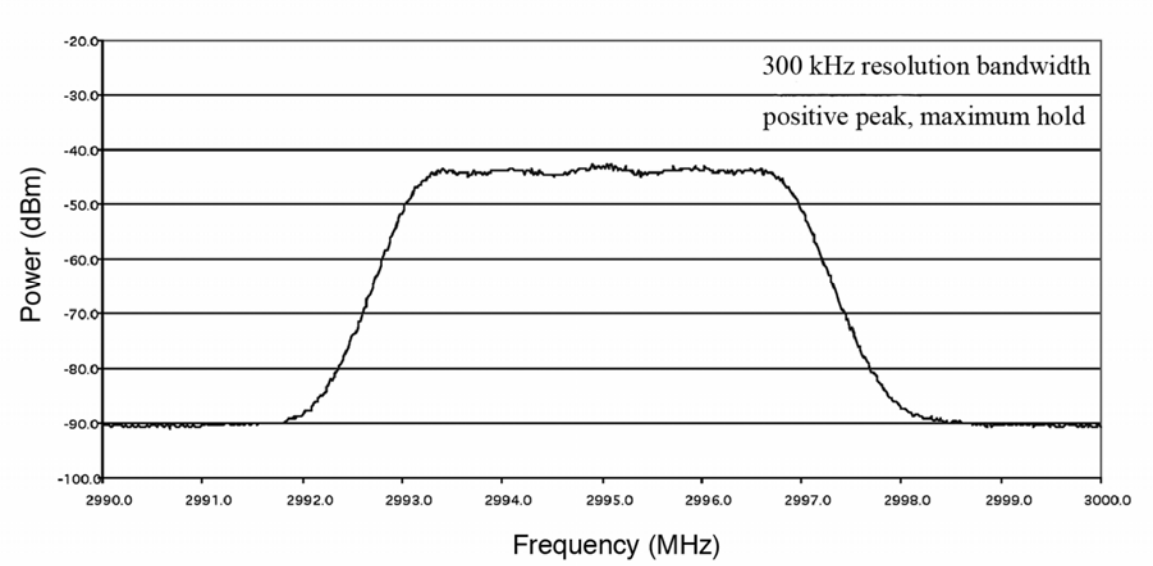

Figure B-7. CDMA-3X interference signal spectrum.

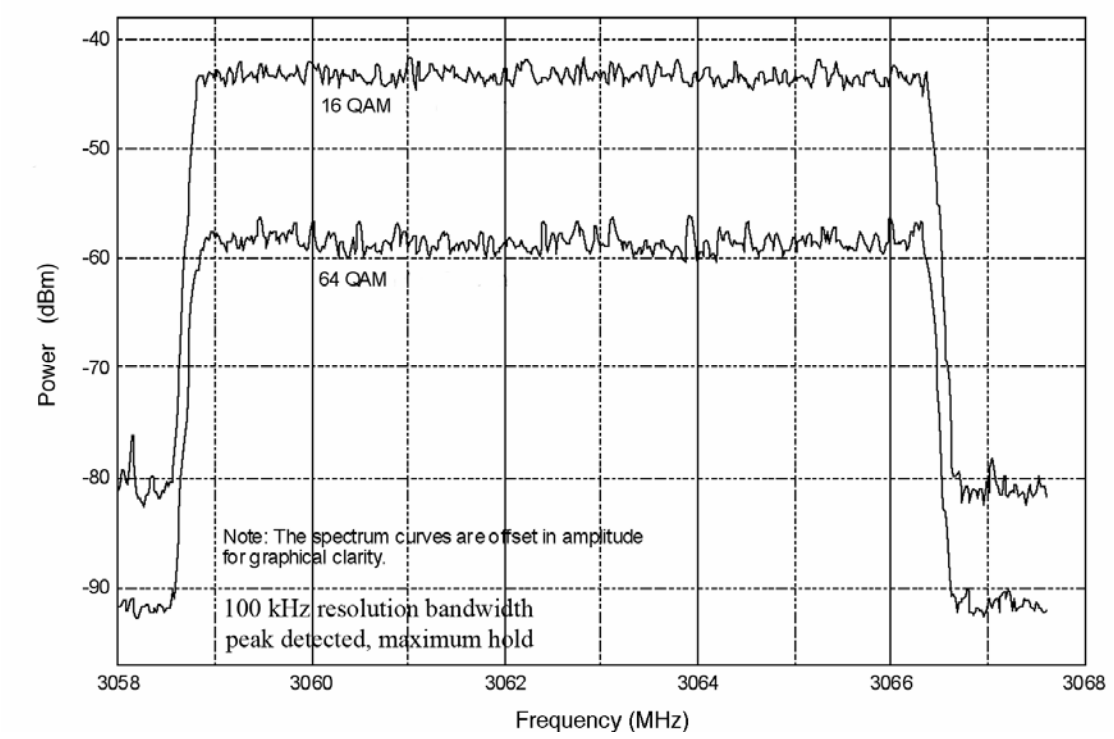

Figure B-8. QAM interference signal spectra for maritime radar tests.

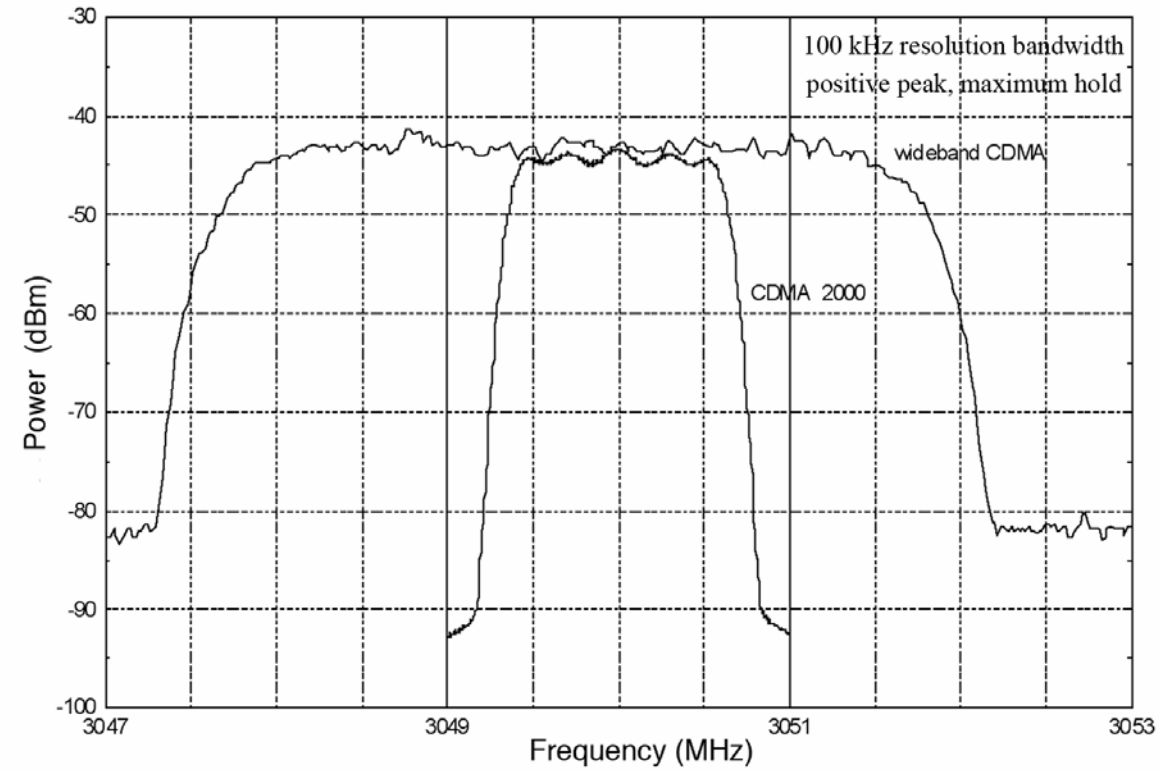

Figure B-9. CDMA interference spectra for maritime radar tests.

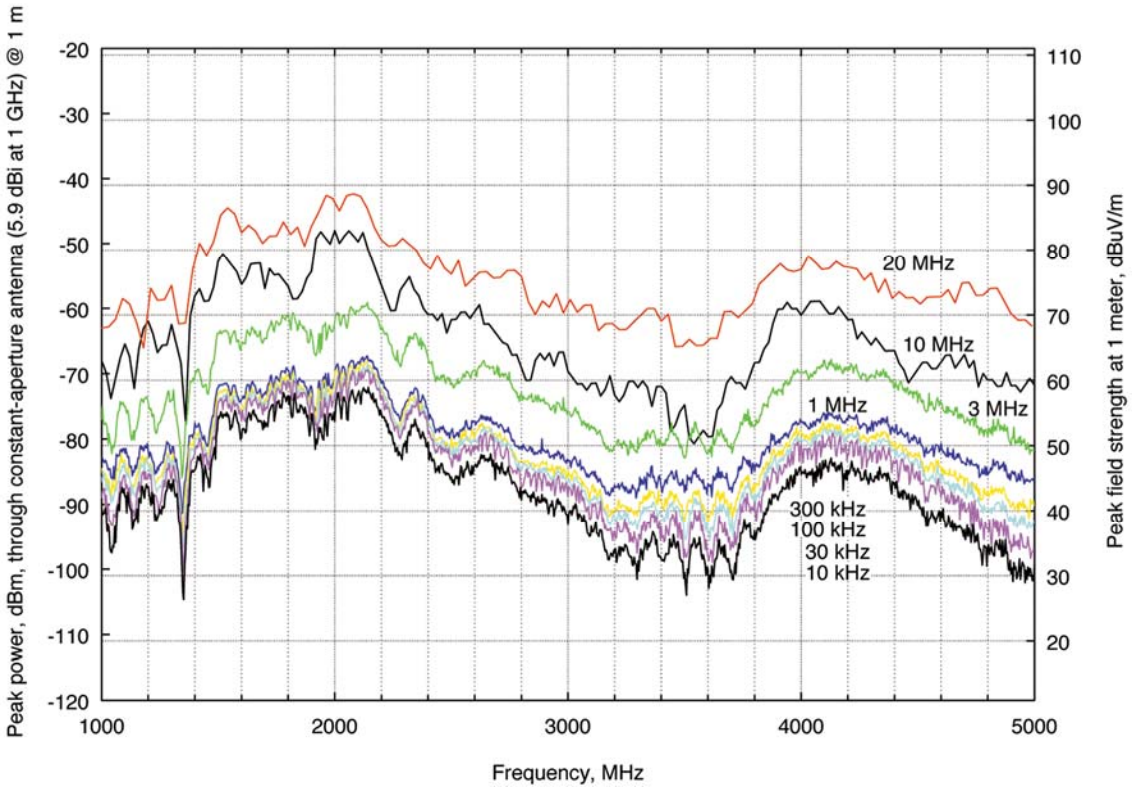

Figure B-10. UWB interference spectra as a function of receiver bandwidth.

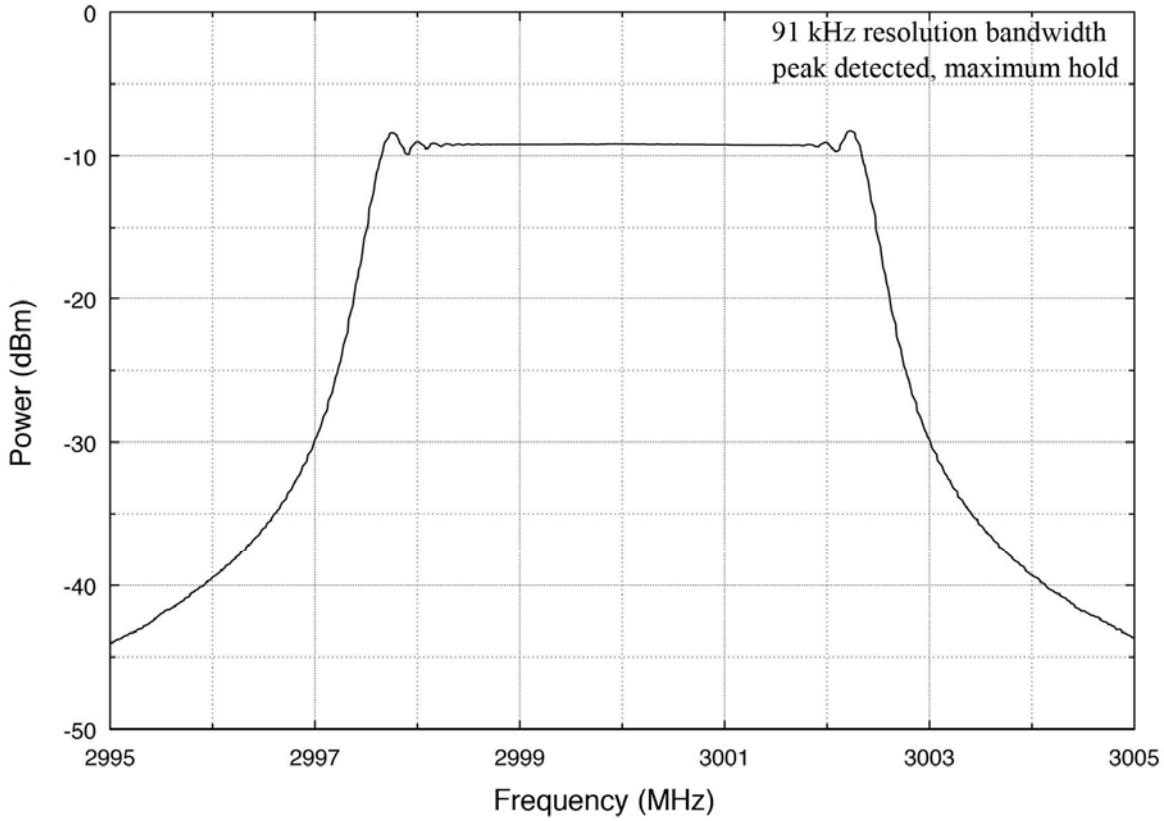

Figure B-11. Chirped-pulse interference spectrum. Chirp width was equal to about 5 MHz.

APPENDIX C: CALIBRATION OF UNDESIRED SIGNALS AND EXAMPLES OF RADAR IF SELECTIVITY CURVES

CW and interference signal calibrations on radars were performed as follows. An Agilent E-4440A spectrum analyzer, set in zero span mode and with the RMS detection selected, was connected to a radar channel IF output. A CW signal tuned to the radar operating frequency was then injected into the radar RF port and a level was found that produced an [*(I+N)/N)*] of 3 dB; equivalent to an *I/N* ratio of 0 dB. The undesired signal level was recorded, and identified to be equivalent to an *I/N* ratio of 0 dB. The process was repeated for channel B (if such a channel was present), and for each type of interference signal. Using the calibrated *I/N* ratio of 0 dB, the other *I/N* values were determined.

In addition, a CW signal was swept in frequency and the response of the IF circuitry of the radar receivers was measured for each channel and recorded with a spectrum analyzer. The 3-dB IF bandwidth of the radar receiver was determined in this way. Selected measurements of radar IF bandwidths are shown in the figures below, with names of the radars referring to the titles of the main text sections. The actual frequency of the IF outputs is usually around 32 MHz. However, in some cases (Figures C-1 and C-2) the frequency axes have been changed to show the corresponding RF frequencies of the radars.

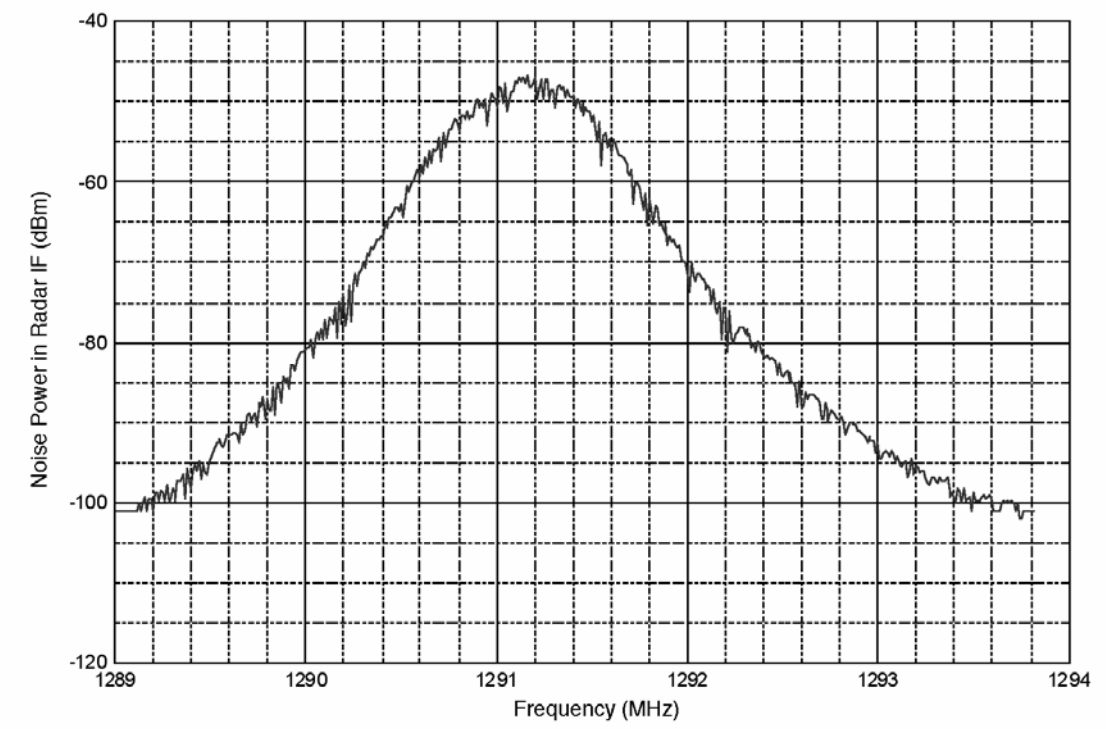

Figure C-1. Channel A IF response of Long Range L-Band Radar 1, referred back to RF frequencies. 100 kHz resolution bandwidth, peak detected, maximum-hold.

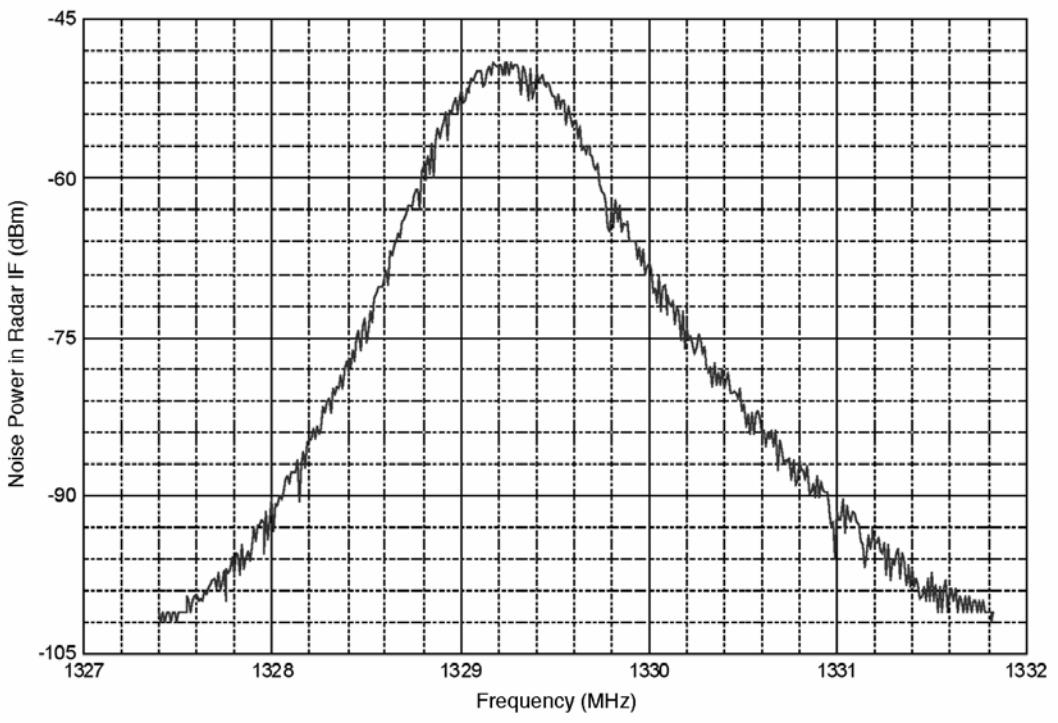

Figure C-2. Channel B IF response of Long Range L-Band Radar 1, referred back to RF frequencies. 100 kHz resolution bandwidth, peak detected, maximum-hold.

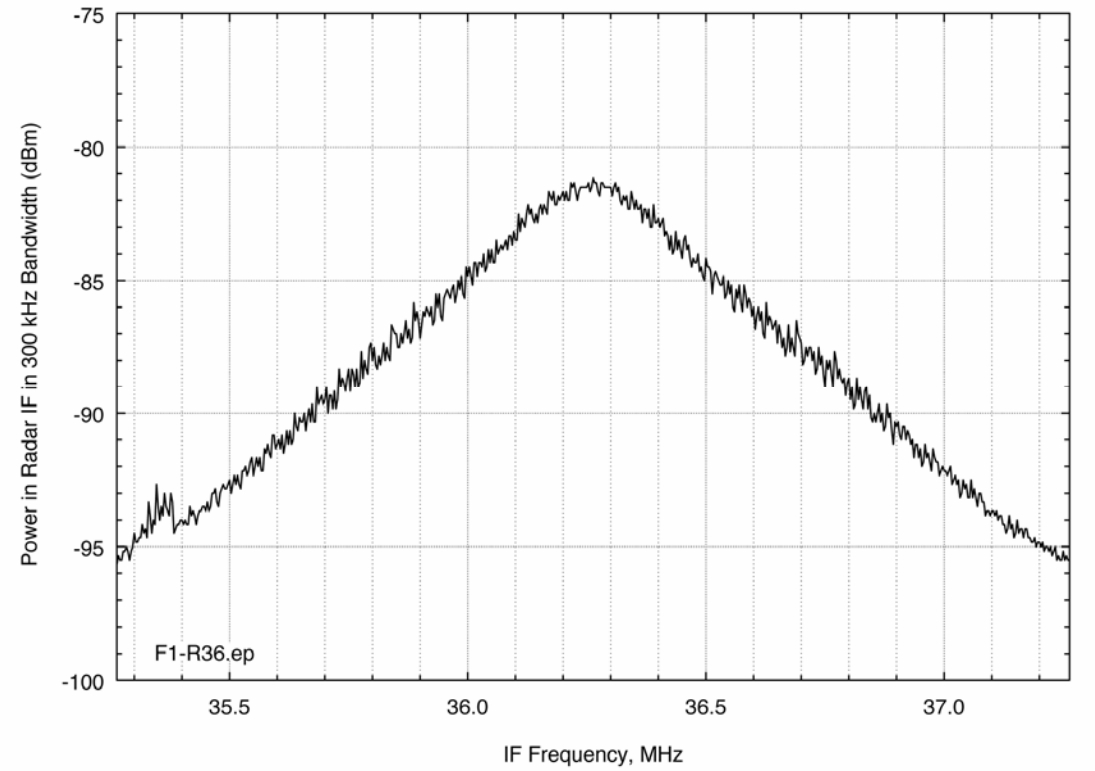

Figure C-3. IF response of one channel of Long Range Radar 2, centered at 36.25 MHz. 300 kHz resolution bandwidth, peak detected, maximum-hold.

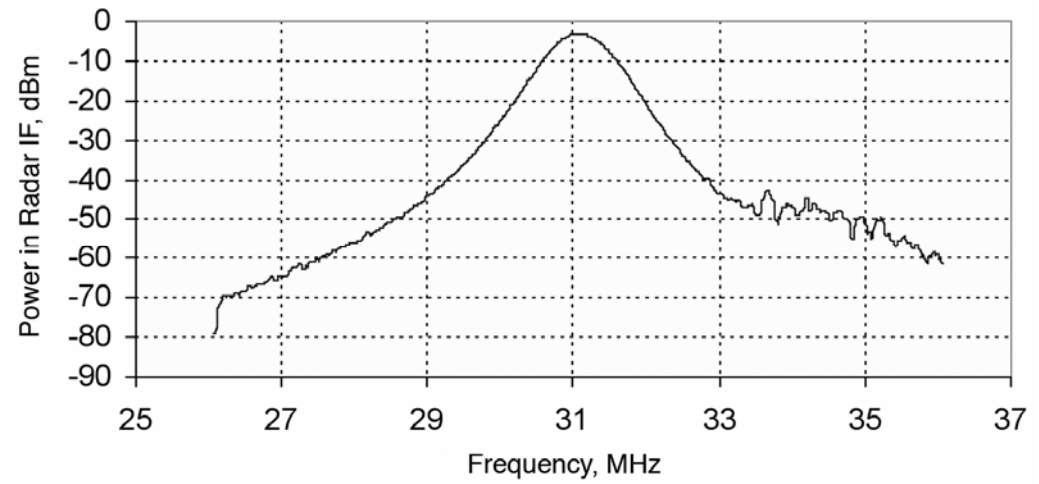

Figure C-4. IF response curve of the short-range air search radar, centered near 31 MHz. 100 kHz resolution bandwidth, peak detected, maximum-hold.

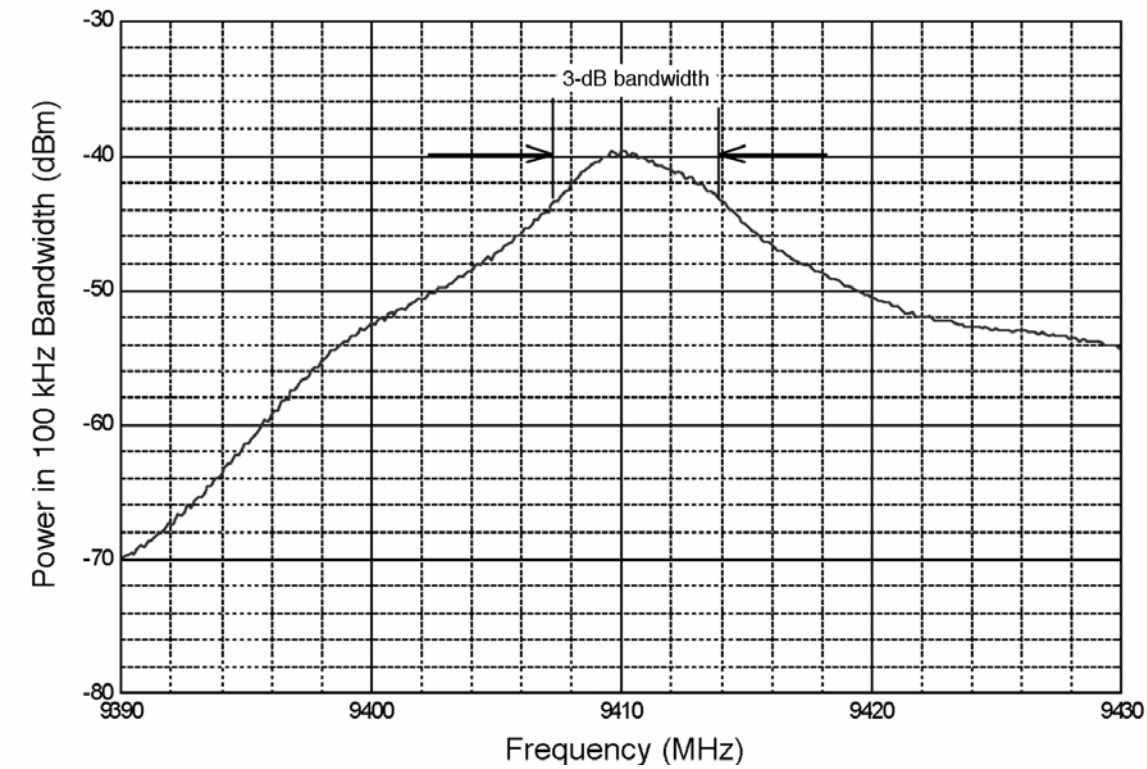

Figure C-5. IF response curve of a typical maritime radionavigation radar (Radar F). The IF frequencies are mapped to their RF equivalents. 100 kHz resolution bandwidth, peak detected, maximum-hold.

APPENDIX D: TEST RESULTS ILLUSTRATING THE EFFECTIVE DUTY CYCLE OF FM-PULSED WAVEFORMS IN A MARINE RADAR RECEIVER

The measurements in this appendix were performed with marine radionavigation Radar F described in the main body of the report. The chirped waveforms identified in Tables 18 and 21 were injected into the radar receiver to investigate how the signal's duty cycle and pulse width are altered through the receiver, changing from the RF pulse waveform that was originally transmitted to the form that is manifested in the radar's detector/processor.

Testing has shown that the effective duty cycle of the interfering waveform is a key element in the ability of a radar receiver to suppress interference effects from unwanted pulsed signals. The results of these tests show that the effective duty cycle of chirped pulsed interference is reduced inside the receiver as compared to the duty cycle that occurs at the radar receiver RF front end.

D.1 Background

The victim receiver's IF output response (amplitude and pulse width) to interference from chirped pulses is a function of the rate at which the chirped frequency sweeps through the victim radar receiver pass-band. This rate, called chirp rate (R_c), is given by: $R_c = (B_c/\tau)$, where R_c is the sweep rate (in megahertz per microsecond), B_c is the chirp frequency range (in megahertz) and τ is the pulse duration (in microseconds). Victim radar receivers should not respond to interference on frequencies outside the -20 dB pass-band of their IF circuitry, assuming that the amplitude of the interference is below the front-end overload threshold of the radar receiver RF front end.

D.2 Measurement Technique

The pulses were injected into the radar receiver at the nominal RF frequency of 9410 MHz at the LNA input. The receiver was not connected to its antenna, to ensure that no other signals could couple into the receiver during testing. A measurement point was identified on the IF circuit card, a spectrum analyzer was set to zero-span mode with a resolution bandwidth commensurate with the radar receiver, and then the analyzer was connected to the measurement point to monitor the response of the radar to the injected waveforms[30]. The radar was placed in stand-by mode so that the receiver was activated, but its transmitter was not generating pulses.

The radar receiver used a summing multistage logarithmic amplifier (Figure 3 in the main report). The IF test point that was used is located at the output of the third amplifier. A CW signal was swept in frequency from 9370 to 9450 MHz to determine the response of the receiver and to measure the receiver's IF bandwidth. The result is shown in Figure D-1. The 3-dB IF bandwidth of the radar was set to short pulse mode 1. This mode, which used a pulse width of 200 ns for a maximum range of 3 nautical miles, was measured at 6 MHz. A spurious receiver response was noted at 9381 MHz, 20 dB below the peak response at 9410 MHz.

[30] The spectrum analyzer was also used to measure and record the time waveform envelopes of the pulses at the fundamental RF frequency, prior to injection into the radar receiver.

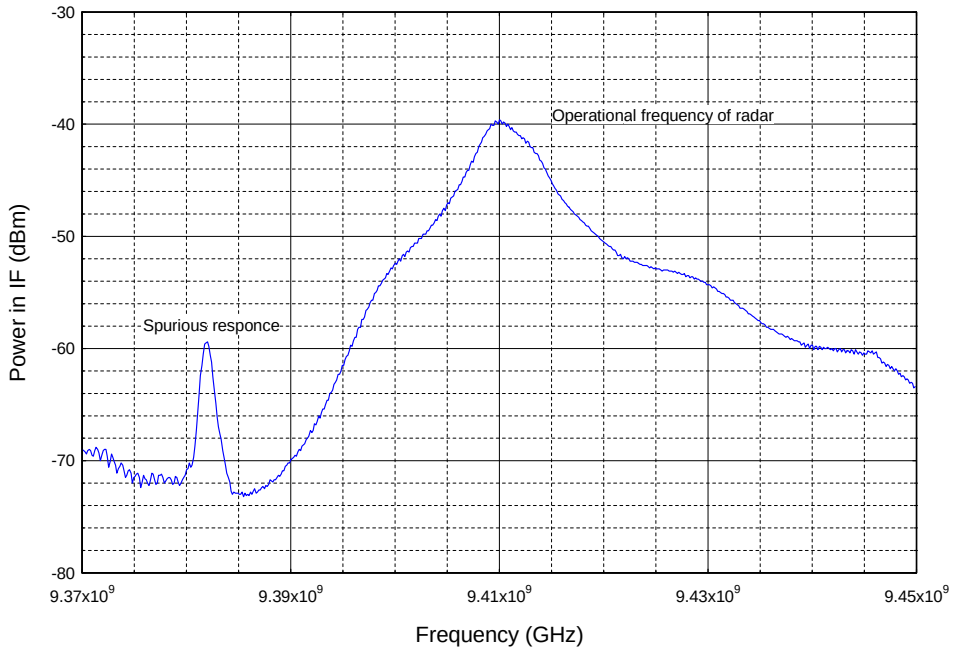

Figure D-1. Frequency response of the IF stage of marine Radar F to a CW input signal when the radar was in its short-pulse mode, shown as a function of the RF frequency of the CW input.

D.3 Results

The results of the measurements are shown in Figures D-2 through D-9. The figures show time waveforms of the pulses after they have passed through the receiver's LNA and IF circuitry. These are the waveforms that are sent into the receiver's processor and detector. For these measurements the -6 dB points are used to specify pulse widths. Figure D-2 shows that unmodulated 1-µs RF pulses (the baseline signal) were still 1-µs wide in the radar's IF bandwidth. However for the chirped pulsed signals, the widths of these pulses in the IF passband of the receiver were shorter than the ones that were transmitted at the RF level. Since the pulse repetition interval (pri) did not change, the effective duty cycle was consequently reduced.

Table D-1 summarizes the results of the differences in pulse width between the RF transmitted pulses and the pulses that are presented to the detector/processor of the radar receiver. The percent difference was calculated by dividing the received pulse width by the transmitted pulse width and then multiplying by 100.

D.4 Summary

Due to the chirping characteristics of the waveforms and the response of the radar receiver, the effective duty cycles and pulse widths of the waveforms at the radar's detector/processor input are *smaller* than those of the *transmitted* waveforms. The interference susceptibility tests have shown that a radar's robustness against the effects of pulsed interference is closely related to the duty cycle and pulse width of the interfering waveforms. As the effective duty cycles and pulse widths are lowered, radar receivers are able to better mitigate the effects of pulsed interference,

as the CFAR circuitry and other mitigation techniques outlined in ITU-R Recommendation M.1372 become more effective. Therefore, when assessing the compatibility of radionavigation radars and chirped pulsed waveforms, tests and measurements along with analyses should take such effects into account. As the data in this appendix demonstrate, the *effective* duty cycle and pulse width in radar receivers should be considered along with the *I/N* ratio when assessing the impact of chirped waveforms on radar receivers.

Table D-1. Characteristics of Chirp-Pulse Waveforms Injected into Marine Radar F

Waveform	**Transmitted Pulse width (μs)**	**Pulse width (μs) at detector-processor**	**Detector-processor pulse width divided by full pulse width**
Chirp 1	10	5.1	0.51
Chirp 2	10	1.0	0.10
Chirp 3	1.65	0.20	0.12
Chirp 4	2	0.20	0.10
Chirp 5	16	1.0	0.063
Chirp 6	17.7	1.2	0.068
Chirp 7	1.7	0.20	0.118

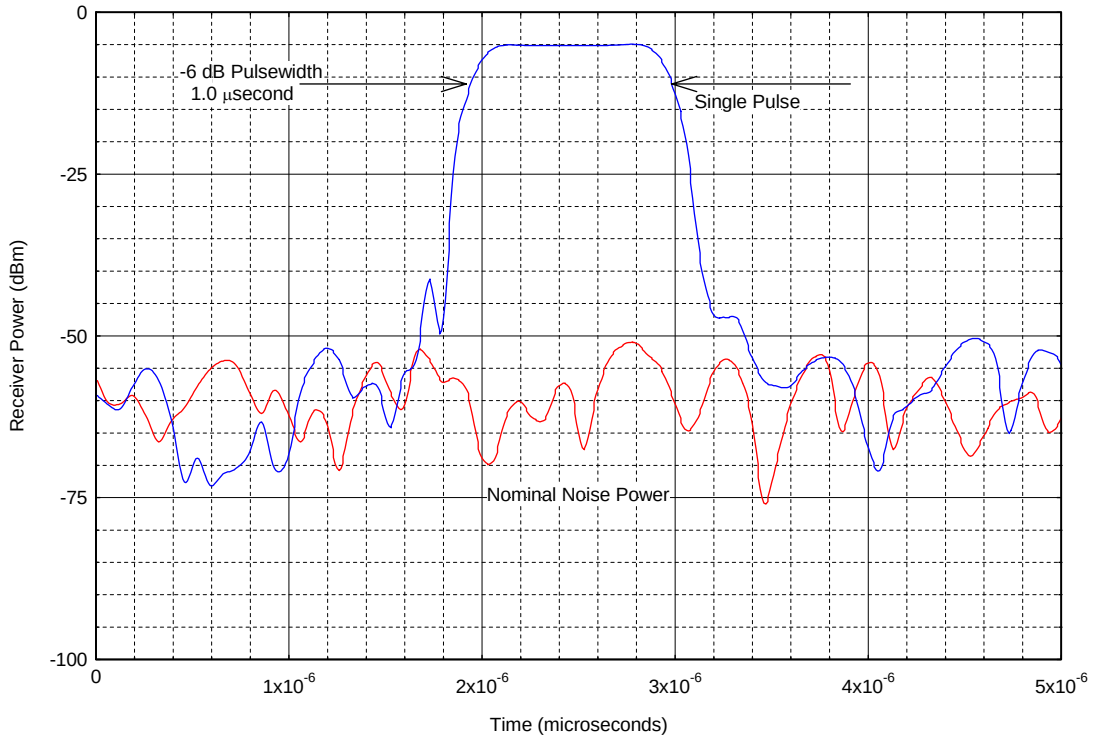

Figure D-2. 1-μs unmodulated pulse in marine Radar F receiver. Because the radar IF bandwidth is greater than 1 MHz, the pulse appears well-formed in the time domain.

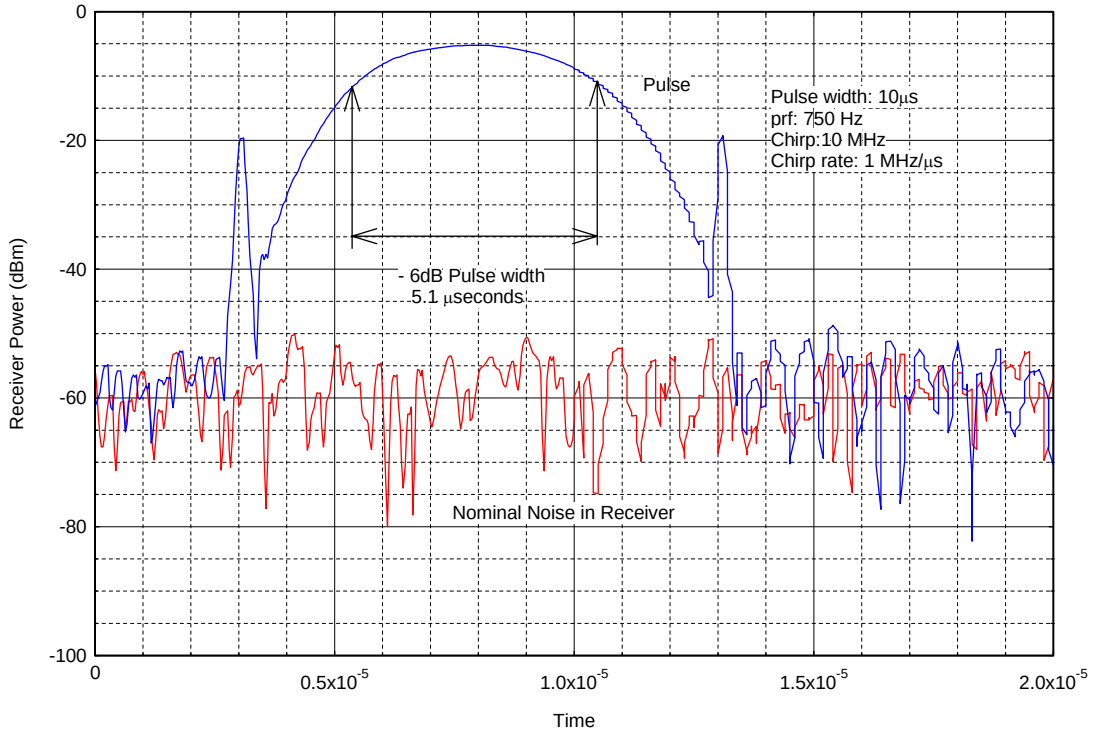

Figure D-3. Chirped waveform 1 in marine Radar F receiver. The time waveform is a result of the Radar IF bandwidth being less than the chirp bandwidth.

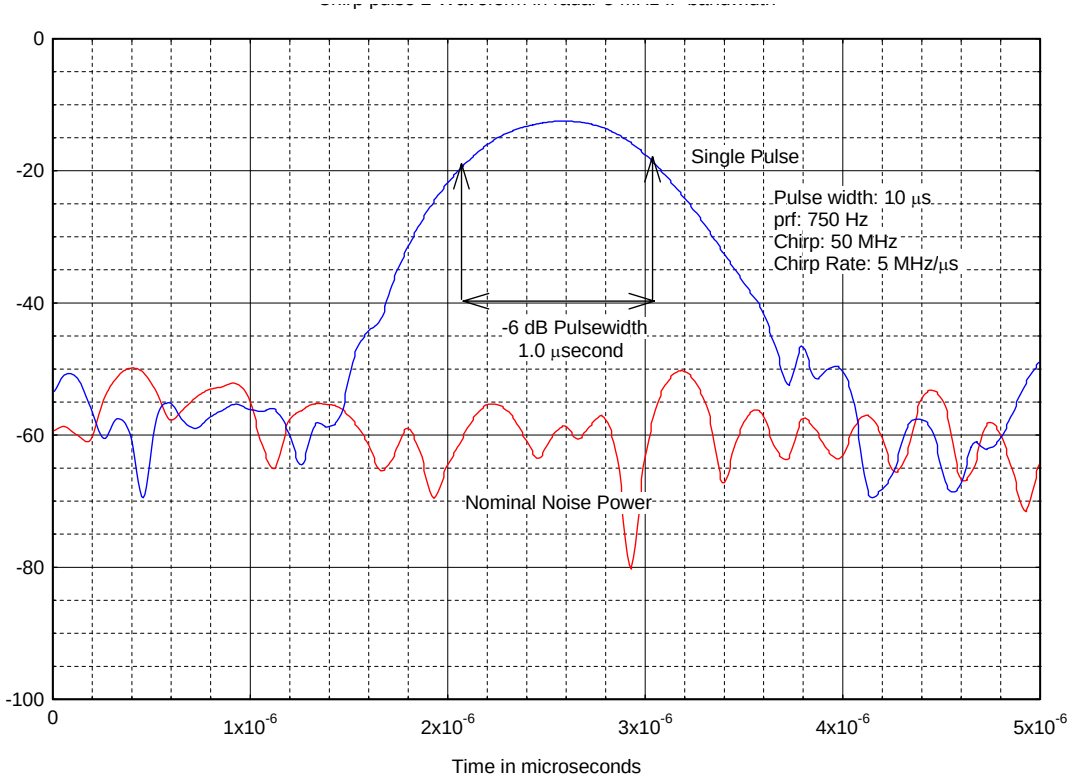

Figure D-4. Chirped waveform 2 in marine Radar F receiver.

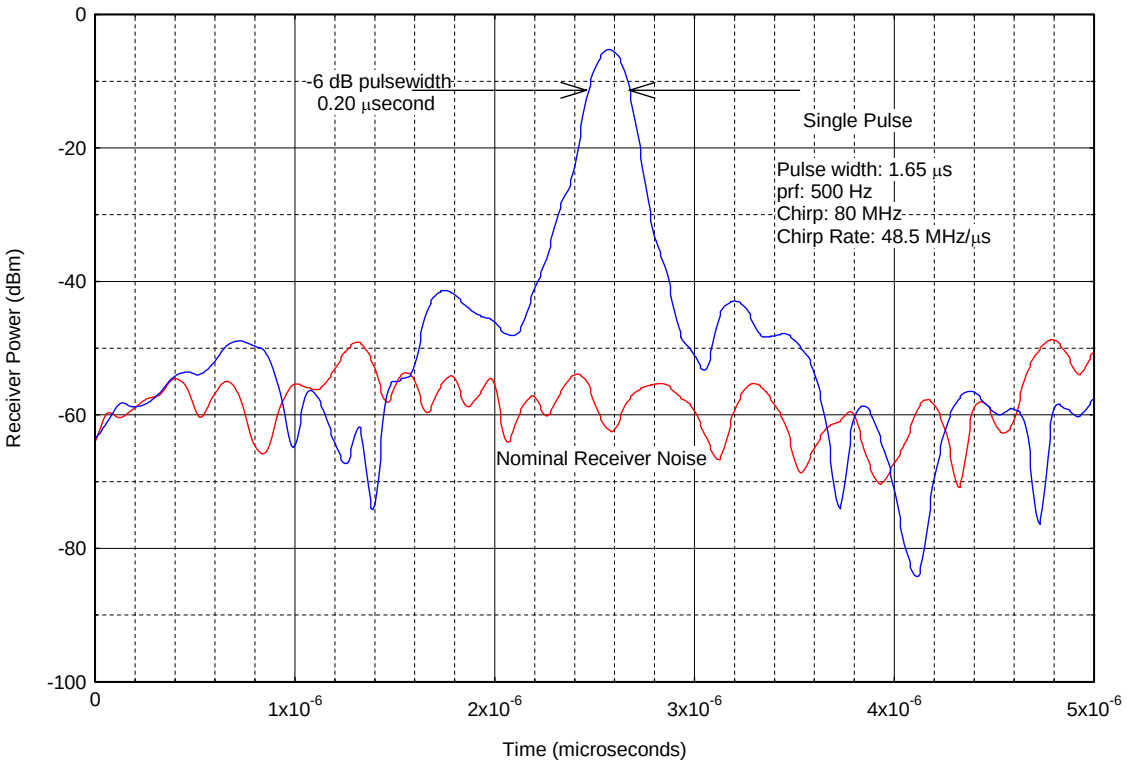

Figure D-5. Chirped waveform 3 in marine Radar F receiver.

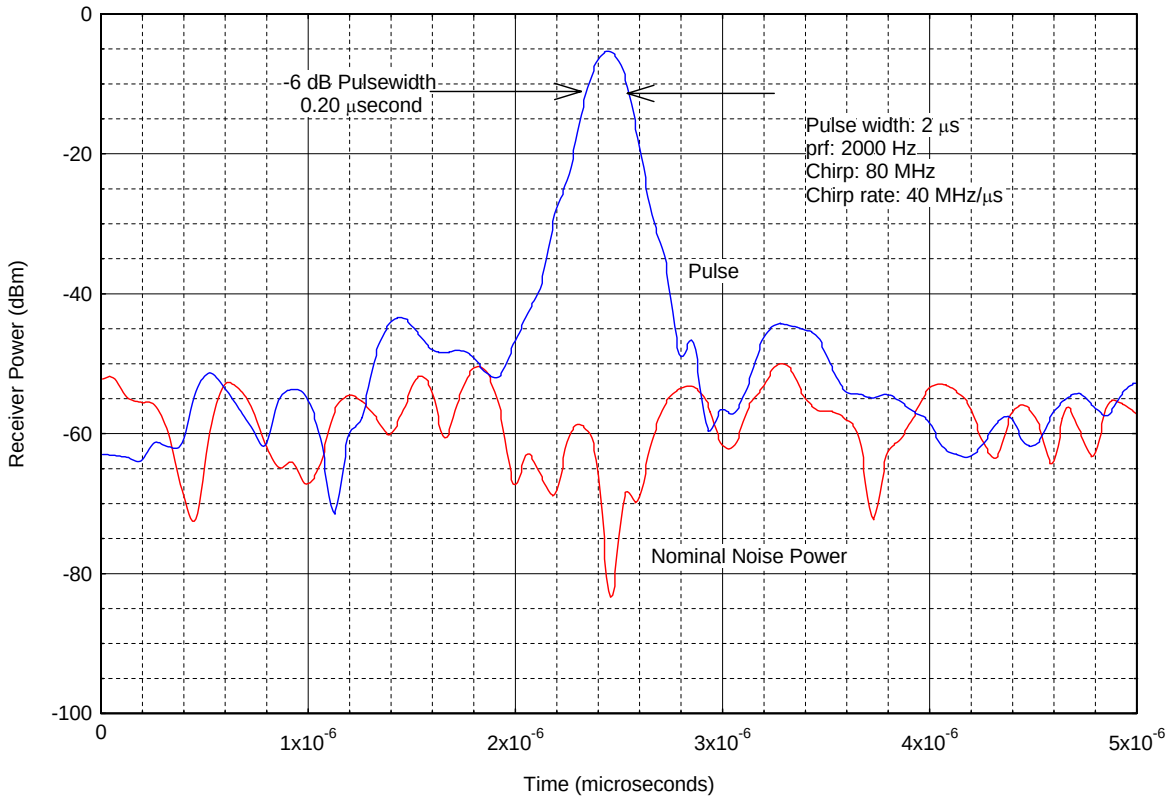

Figure D-6. Chirped waveform 4 in marine Radar F receiver.

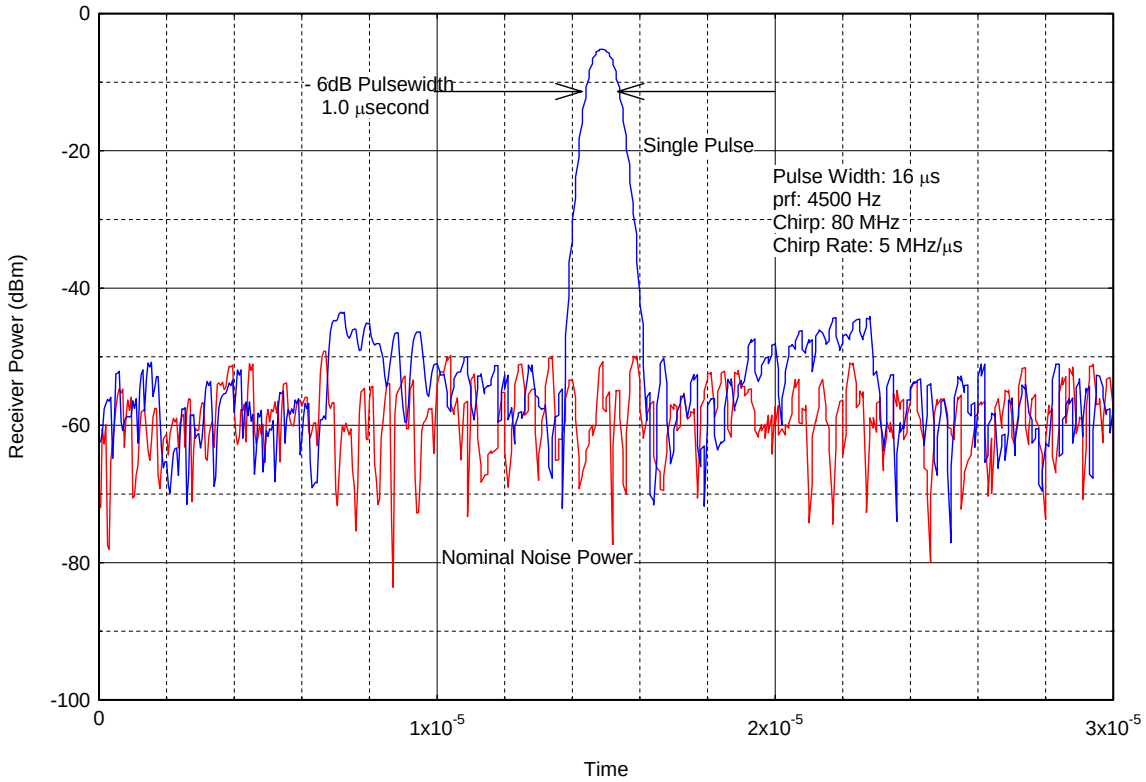

Figure D-7. Chirped waveform 5 in marine Radar F receiver.

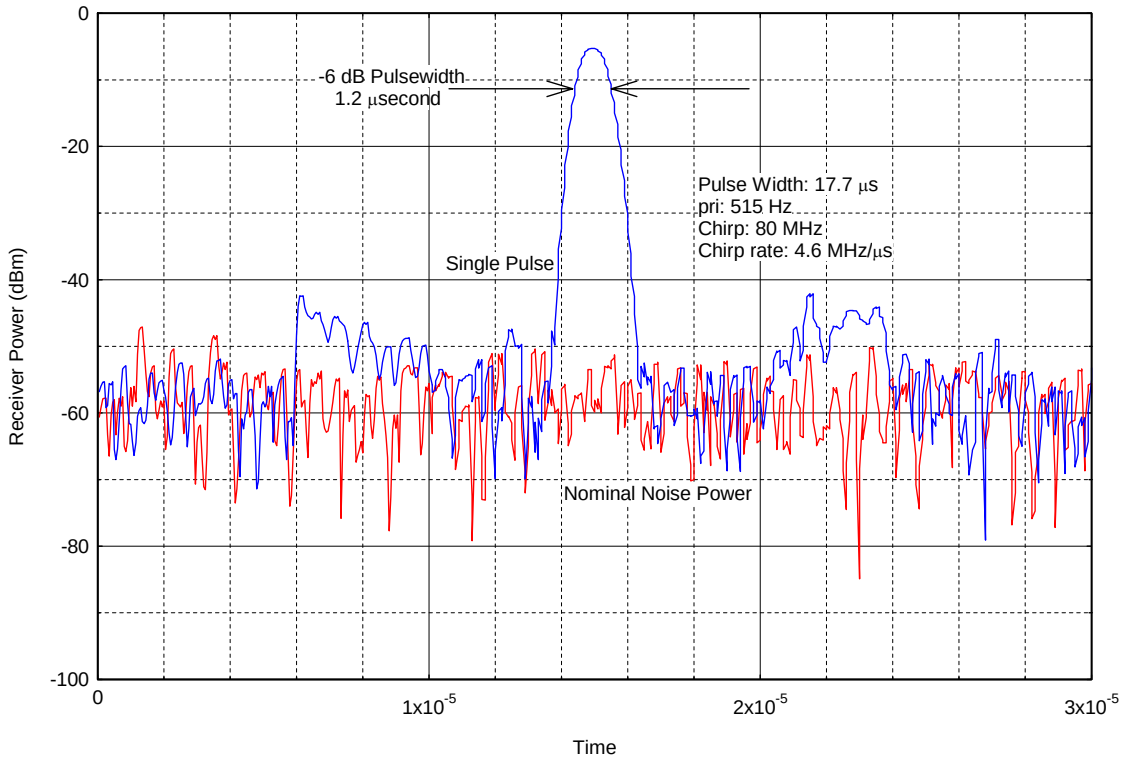

Figure D-8. Chirped waveform 6 in marine Radar F receiver.

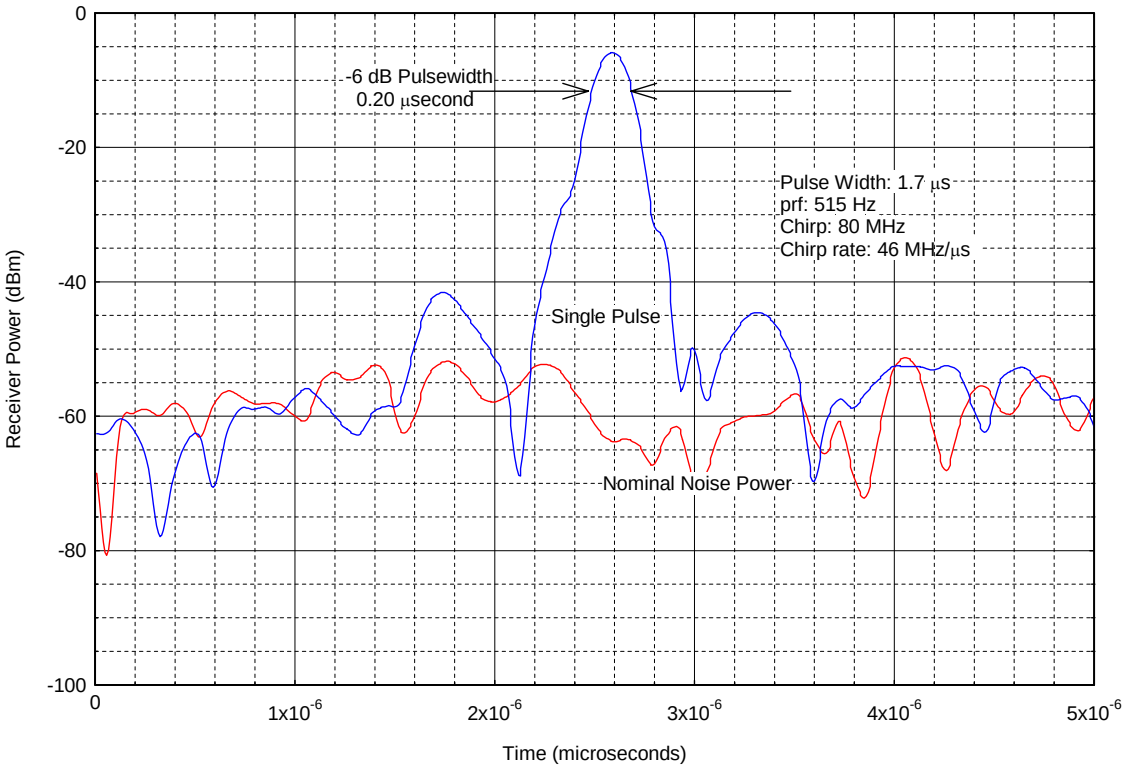

Figure D-9. Chirped waveform 7 in marine Radar F receiver.

FORM **NTIA-29** (4-80)

U.S. DEPARTMENT OF COMMERCE
NAT'L. TELECOMMUNICATIONS AND INFORMATION ADMINISTRATION

BIBLIOGRAPHIC DATA SHEET

1. PUBLICATION NO.	2. Government Accession No.	3. Recipient's Accession No.
TR-06-444		

4. TITLE AND SUBTITLE	5. Publication Date
Effects of RF Interference on Radar Receivers	September 2006
	6. Performing Organization Code: NTIA/ITS

7. AUTHOR(S)	9. Project/Task/Work Unit No.
Frank H. Sanders, Robert L. Sole, Brent L. Bedford, David Franc, and Timothy Pawlowitz	

8. PERFORMING ORGANIZATION NAME AND ADDRESS	10. Contract/Grant No.
NTIA/ITS.T U.S. Department of Commerce 325 Broadway Boulder, CO 80305	

11. Sponsoring Organization Name and Address	12. Type of Report and Period Covered

14. SUPPLEMENTARY NOTES

15. ABSTRACT (A 200-word or less factual summary of most significant information. If document includes a significant bibliography or literature survey, mention it here.)

This report describes the results of interference tests and measurements that have been performed on radar receivers that have various missions in several spectrum bands. Radar target losses have been measured under controlled conditions in the presence of radio frequency (RF) interference. Radar types that have been examined include short range and long range air traffic control; weather surveillance; and maritime navigation and surface search. Radar receivers experience loss of desired targets when interference from high duty cycle (more than about 1-3%) communication-type signals is as low as -10 dB to -6 dB relative to radar receiver inherent noise levels. Conversely, radars perform robustly in the presence of low duty cycle (less than 1-3%) signals such as those emitted by other radars. Target losses at low levels are insidious because they do not cause overt indications such as strobes on displays. Therefore operators are usually unaware that they are losing targets due to low-level interference. Interference can cause the loss of targets at any range. Low interference thresholds for communication-type signals, insidious behavior of target losses, and potential loss of targets at any range all combine to make low-level interference to radar receivers a very serious problem.

16. Key Words (Alphabetical order, separated by semicolons)

radar interference; radar interference vulnerability; radar performance degradation; radar target loss; radar target detection; RF interference; UWB interference effects

17. AVAILABILITY STATEMENT	18. Security Class. (This report)	20. Number of pages
UNLIMITED.		162
	19. Security Class. (This page)	21. Price:

NTIA FORMAL PUBLICATION SERIES

NTIA MONOGRAPH (MG)

A scholarly, professionally oriented publication dealing with state-of-the-art research or an authoritative treatment of a broad area. Expected to have long-lasting value.

NTIA SPECIAL PUBLICATION (SP)

Conference proceedings, bibliographies, selected speeches, course and instructional materials, directories, and major studies mandated by Congress.

NTIA REPORT (TR)

Important contributions to existing knowledge of less breadth than a monograph, such as results of completed projects and major activities. Subsets of this series include:

NTIA RESTRICTED REPORT (RR)

Contributions that are limited in distribution because of national security classification or Departmental constraints.

NTIA CONTRACTOR REPORT (CR)

Information generated under an NTIA contract or grant, written by the contractor, and considered an important contribution to existing knowledge.

JOINT NTIA/OTHER-AGENCY REPORT (JR)

This report receives both local NTIA and other agency review. Both agencies' logos and report series numbering appear on the cover.

NTIA SOFTWARE & DATA PRODUCTS (SD)

Software such as programs, test data, and sound/video files. This series can be used to transfer technology to U.S. industry.

NTIA HANDBOOK (HB)

Information pertaining to technical procedures, reference and data guides, and formal user's manuals that are expected to be pertinent for a long time.

NTIA TECHNICAL MEMORANDUM (TM)

Technical information typically of less breadth than an NTIA Report. The series includes data, preliminary project results, and information for a specific, limited audience.

For information about NTIA publications, contact the NTIA/ITS Technical Publications Office at 325 Broadway, Boulder, CO, 80305 Tel. (303) 497-3572 or e-mail info@its.bldrdoc.gov.

This report is for sale by the National Technical Information Service, 5285 Port Royal Road, Springfield, VA 22161,Tel. (800) 553-6847.